Formation of Polymer Coatings by Electropolymerization

by

Xiaoping Ling

A thesis
presented to the University of Waterloo
in fulfillment of the
thesis requirement for the degree of
Doctor of Philosophy

in

Chemical Engineering

Waterloo, Ontario, Canada 1998

The University of Waterloo requires the signatures of all persons using or photocopying this thesis. Please sign below, and give address and date.

ABSTRACT

Coatings of poly(2-vinylpyridine) have been formed successfully on various substrates in aqueous medium by electropolymerization of the 2-vinylpyridine monomer. The effects of various chemical and physical variables on the electropolymerization process have been studied. These include electrolyte pH, monomer concentration, operating temperature, methanol content in the electrolyte, electrolysis duration, and nature and concentration of the supporting electrolytes. The polymer coating formed was characterized by u.v.-visible, FT-IR and ^{1}H NMR spectroscopies. Polymer composition, glass transition temperature and the presence of certain impurities were examined using instrumental techniques. Coating adhesion, porosity, conductivity and corrosion resistance were also evaluated. Coating thickness and surface roughness distribution were measured quantitatively using confocal scanning laser microscopy.

The principal contributions of this research are the development of a successful method for the formation of poly(2-vinylpyridine) coatings via electropolymerization and the proposal of a mechanism for the process. When protonated in an acid aqueous electrolyte, 2-vinylpyridine can migrate and adsorb onto the cathodic surface during electrolysis. At a half-wave potential of –1.0 V (SCE) or more negative, the protonated 2-vinylpyridine molecules can be reduced to free-radicals which then combine with neutral formed 2-vinylpyridine molecules to form polymer chains. The polymer formed can still undergo protonation in the acidic aqueous electrolyte and be reduced at more negative electrode potentials to produce polymeric radicals. From these polymeric radicals, highly branched and crosslinked polymer chains are produced on the electrode surfaces. The value of electrolyte pH is critical to the

electropolymerization process and lies in a narrow range close to the *p*Ka value of the monomer so both protonated and neutral 2-vinylpyridine are present in sufficient amounts in the electrolyte.

Cyclic potential sweep electrolysis in the range from –0.7 to –2.5 V and at a scan rate of 30 mV/s was found to be suitable for 2-vinylpyridine electropolymerization on mild steel substrates. Monomer concentrations between 0.2 and 0.3 M 2-vinylpyridine were found to produce the best coatings. A suitable range of methanol content in the electrolyte was found to be between 10 to 25 *vol* %. An operating temperature between 20 and 40 °C was found to be most favourable for coating formation. Higher operating temperatures (> 40°C) tended to generate low molecular weight polymer, increasing the solubility of the coating polymer in the electrolyte and leading to a thin coating. The relative importance of these operating parameters decreased in the following order: monomer concentration > solution pH > methanol content in the electrolyte > operating temperature. Other operating parameters examined included electrolysis duration, which was found to affect the coating thickness proportionally during the first 2 hours, but had little effect on the coating thickness thereafter. NH_4ClO_4 was found to be the best supporting electrolyte for the coating formation, however, its concentration did not affect the process significantly.

Poly(2-vinylpyridine) coatings have also been formed successfully on various substrates, including zinc, lead, stainless steel, copper, brass and graphite. Other monomers have been tried to form homopolymer coatings partly to test the proposed process mechanism for 2-vinylpyridine electropolymerization. This research has resolved some of the experimental discrepancies previously reported in the literature. The results and conclusions from this work

should contribute significantly to the fundamental understanding of electropolymerization as well as to practical aspects of the process.

ACKNOWLEDGMENTS

I would like first to express my thanks and appreciation to my supervisors, Professors M. D. Pritzker, C. M. Burns and J. J. Byerley in the Department of Chemical Engineering for their advice, guidance, encouragement and support during the course of this work. I also would like to express my gratitude to the Graduate Review Committee of the Department of Chemical Engineering when I began my research project, especially Professor G. L. Rempel, former Department Chair, and Professor T. A. Duever, former Associate Chair for Graduate Studies and Research. I also express my thanks and appreciation to Professor D. Burns, Dean of the Faculty of Engineering, for his help and support throughout the course of this project.

Acknowledgment is extended to Dr. S. Damaskinos and Professor A. E. Dixon in the Department of Physics for the use of the confocal scanning laser microscope; to Dr. A. G. Brolo and Professor D. E. Irish in the Department of Chemistry for the use of the surface enhanced Raman scattering spectroscope; to Professor M. Tchir in the Department of Chemistry for his advice on polymer characterization with NMR spectroscopy; to Professor D. E. Matthews in the Department of Statistics & Actuarial Science for his consultation on experimental design; to Professor D. E. Brodie in the Department of Physics for his help on the polymer coating conductivity measurements; to Dr. N. McManus in the Department of Chemical Engineering for his help in polymer characterization; to Mr. R. Dickhout and the late Mr. R. Frankle in the Department of Chemical Engineering for their valuable advice and kindly assistance on this project; to my lab-mate and friend Mr. Dana F. Gourley for all the discussions (even though sometimes the discussion was not directly related to the thesis topic) and suggestions on my research.

This research has been supported by the Natural Sciences and Engineering Research Council of Canada (NSERC) and the Faculty of Engineering and Department of Chemical Engineering of the University of Waterloo.

To Jesus Christ, my Lord and my God!

TABLE OF CONTENTS

LIST OF TABLES

LIST OF FIGURES

CHAPTER 1

INTRODUCTION AND RESEARCH OBJECTIVES

1.1. Introduction

The formation of organic and polymer coatings on conducting substrates has always been of great interest. The coatings can be applied for purposes of surface decoration, optical activity alteration, heat and frictional resistance enhancement and corrosion protection (Leidheiser, 1979; Walter, 1986a and 1986b; Funke, 1987; Sekine et al., 1992; De Bruyne et al., 1995). Other important applications include improvement of interfacial/interlaminar shear strength and toughness of brittle composites (Subramanian and Jakubowski, 1978; MacCallum and MacKerron, 1982; Chang et al., 1987; Iroh et al., 1990 and 1991; Wimolkiatisak and Bell; Iroh et al., 1993a and 1993b; Liang et al., 1993; Iroh et al., 1994), as well as use in modified electrodes (Abruna et al., 1981; Murray, 1984a and 1984b; Hillman, 1987; Diaz, 1991), microelectronic devices and semiconductors (Belanger and Wrighton, 1987; Billingham and Calvert, 1989), matrices for incorporating electroactive groups at electrode surfaces (Oyama and Anson, 1979a, 1979b and 1980; Sharp et al., 1985), chemical sensors (Harsanyi, 1995) and polyelectrolytes (Tenenbaum, 1961; Oosawa, 1971; Nuyken, 1992).

Originally, organic and polymer coatings were applied manually or mechanically on substrates. However, manual or mechanical application of coatings had inherent disadvantages and gave rise to additional problems (Cooke et al., 1971). Currently, the

principal mode of organic and polymer coating formation for protection purposes is the application of paint formulations based on synthetic polymers, which are generally applied to the substrate by an electrophoretic deposition technique (Brewer, 1973). Electrophoresis was introduced industrially during the 1960's and is now used world-wide due to its many advantages (Levinson, 1972). It involves the deposition of a pre-formed ionizable polymer on a conducting substrate from polymer solutions or suspensions by electrophoretic means. The object is dipped into a tank of soluble polymer and a current is passed through the system. The polymer is attracted to the article and forms a coherent protective layer.

The electrophoretic technique requires that the polymer used in the process has good solubility, as well as a reasonable viscosity and mobility in the media. These requirements often limit the technique. In addition, the electrophoretic technique requires a very large amount of energy to deposit the coatings. Very high applied cell potentials of 200~500 volts are necessary for migration and deposition of the polymer. The combination of these high voltages and the appreciable currents leads to a large Joule heating of the electrolyte. Consequently, constant cooling and temperature control are required during operation. The resulting coatings must be subsequently cured at elevated temperatures (> 200°C). One frequent fault of coatings formed in this manner is the relatively poor adhesion to the metal surface. This arises because attachment stems primarily from the flocculation of polymer micelles at the substrate-liquid interface without any preceding interaction on a molecular scale between the polymer and the substrates (Mengoli, 1979).

Electropolymerization is quite different from electrophoretic deposition (Teng et al., 1977). In this technique, electrolysis is used to initiate the process with the monomer being polymerized *in situ* to a conducting surface. For this reason, the process is often referred to as electroinitiated polymerization. In contrast to the electrophoretic coating method, high potentials are not necessary for electropolymerization. It uses low molecular weight monomers that have higher solubility in the media, as well as more favourable viscosity and mobility than in the case of the electrophoresis process. Polymerization initiation can be directly controlled by electrolytic means. It also provides a possible method to control the propagation and termination processes. It is possible for the formed polymer to have a controlled molecular weight and molecular weight distribution and a predetermined yield (Wimolkiatisak and Bell, 1992). Chemical additives are not needed for initiation in this type of polymerization, leading to a purer polymer product containing no initiator fragments. This is a significant advantage for the polymer coating industries because initiator fragments are usually sites where degradation of the coatings first begins. Electropolymerization usually involves some specific interaction between the monomer and the electrode surface which leads to better coating adhesion (Mengoli et al., 1979a). In addition, due to the use of monomers for *in situ* polymerization on the substrates, the monomer solutions with a relatively low viscosity can wet the substrates more easily than do polymer solutions and therefore can permit polymerization within crevices of the substrates, locking the polymer chains firmly in place (Lee and Bell, 1995a; Zhang et al., 1996). A further advantage of the electropolymerization process is that the high temperature thermal curing process can often be avoided. Therefore, it is possible to obtain a polymer coating on a conducting substrate from low molecular weight precursors,

free from impurities in many cases by single electrochemical process (Garg et al., 1978). The process is usually operated under mild conditions and from a practical standpoint requires only simple industrial equipment similar to that used for electroplating.

Electropolymerization is a relatively new technique involving aspects of electrochemical engineering, polymer science, organic chemistry and coating/plating technology. The complexity and breadth of the subject have made it more difficult for systematic and comprehensive studies to be done. Most of the research so far has focused on producing coatings and measuring their polymer and film properties (Meverden and Hogen-Esch, 1983; Seery and Amis, 1991; Fell and Bohn, 1993; Yoshida et al., 1993; Hogen-Esch et al., 1995; Martin et al., 1996; Rafique et al., 1996). Relatively little research has been directed at elucidating the mechanisms operating in this method (Fleischmann et al., 1983; Mengoli et al., 1983; Iroh et al., 1991; Iroh et al., 1993a and 1993b; Lee and Bell, 1995a and 1995b; Zhang et al., 1996). This lack of understanding of the underlying mechanisms has contributed to poor quality coatings and poor reproducibility in some of the previously reported work (Murray, 1984a and 1984b; Troch-Nagels et al., 1992; De Bruyne et al., 1995).

Coating morphology analysis, including coating thickness and surface roughness measurements, is a very important aspect in the coating industry. Usually, various microscopic techniques (e.g., scanning electron microscopy, scanning tunneling microscopy, atomic force microscopy, etc.), are applied for qualitative measurement of coating topology. There has been a lack of suitable techniques for quantitative measurement of coating thickness, which may have led to errors in evaluating coating quality and to problems in applying the coatings.

1.2. Research Objectives

The primary objective of this project is to exploit and develop new electrochemical techniques for *in situ* synthesis of polymer coatings on conducting substrates in aqueous solutions. Poly(2-vinylpyridine) coating formation on mild steel substrates by electroreduction polymerization is chosen as the system upon which to base the investigation. Electropolymerizations involving other organic monomers and substrates are to be extensions of this work. Investigation of the effects of experimental parameters on coating quality is also a primary objective of the project. This is to be used to determine the relative importance of the operating parameters and the optimum combination of the operating parameters. Further details of the poly(2-vinylpyridine)–mild steel system will be studied and used to postulate a reaction mechanism for this electropolymerization process.

Polymer characterization is another important aspect of the research project. It can be used to confirm the formation of the desired polymeric materials and to help understand the mechanism of the electropolymerization process. The measurement of the composition and physical and chemical properties of the coatings, as well as quantitative analysis of coating morphology (e.g., coating thickness and coating surface roughness) are also very important aspects of the research objectives. Successful completion of the project is expected to contribute significantly to electropolymerization theory, as well as provide a basis for practical application of the technique.

CHAPTER 2

COATING FUNDAMENTALS

2.1. Coatings and Coating Formation

A satisfactory coating can be described as a continuous, highly adherent film of a uniform thickness over a substrate. There are many kinds of coatings having different characteristics depending on the application. The coating must be converted to a dense and tight solid membrane. The effectiveness of a particular coating is very much determined by the overall coating process. In the following section, various coating formation processes are presented and their advantages and disadvantages are discussed (Durney, 1984; Satas, 1991).

2.1.1. Coating Formation by Solvent Evaporation

Coating formation by solvent evaporation, which in principle should be the simplest method, is far from simple to apply in practice. The formation of a coating does not commence until the evaporation of the solvent reaches an advanced stage and the resin molecules are brought into such close proximity that their mutual attraction causes them to coalesce. Coating properties are influenced by the molecular arrangement or structure within the coating. A homogeneous, dense structure is promoted by a solvent that maintains maximum dispersion and mobility of the polymers during coating formation. If the solvent and polymer are not well mixed and the polymer mobility in the solvent is not

high enough, then resin precipitation may occur in the bulk solution and not on the substrate. The attraction between the polymer molecules not only is limited to coatings produced from solution, but also is the basis of all coatings, as well as the force that binds the molecules together.

If the solvent evaporates too rapidly when the coating is applied, the resin will tend to dry before it contacts the surface and overspraying will result. Fast-evaporating solvents also eliminate any possibility of brushing. Alternatively, solvents that evaporate too slowly will cause very slow coating formation. Slow evaporation generally produces sticky coatings with solvent being retained in the coating for a long period of time, making the coating less water and chemically resistant. In order to obtain a strong, smooth and continuous resin coating, it is usually necessary to use a combination of solvents, which include *active solvents*, *latent solvents* and *diluents*. The *active solvents* are those which easily dissolve the resin and are primarily responsible for solvation. The *latent solvents* are less active, but still act as solvents, while the *diluents* are materials which tend to soften the resin, but will not actively dissolve it. The aim in mixing solvents is to provide for uniform evaporation. The different solvents evaporate at different rates. The active solvent is usually the last solvent to leave the film, creating the conditions whereby the resin molecules orient themselves to form a smooth, clear, continuous film. One distinct advantage of the solvent evaporation method is that coating formation is fast and takes place in a single stage since the resin is a long-chain oligomer prior to solvation. Because these coatings are permanently soluble in their own solvents, these coatings are generally easier to repair and maintain than thermosetting or conversion coatings. However, it is not practical to use these coatings in any medium containing their own solvents. Moreover, it

is often more difficult to apply these coatings than conversion coatings, whether done by air-spraying or by brushing.

2.1.2. Coating Formation by Change-of-Phase

Change-of-phase (or hot-melt) is a technique in which the resin is converted, usually by heat, from a solid to a liquid and then back to a solid. The principal materials used in this process are asphalt and coal tars. The liquid resin can readily be applied to a substrate by *daubing*, a process of brushing a material on a surface while it remains in a liquid state. For the interior of pipes, the hot-melt materials are often applied by centrifugal force. The common method of external application involves applying several pipe-wraps onto the liquid resin as the pipe revolves.

The hot-melt technique is effective whenever a basic resin can be converted (melted) to a liquid or semi-liquid form. Since no solvent or volatile material is involved, 100% of the resin material is applied to the surface. Thick coatings are easily formed from the hot-melt materials and, when applied properly, the hot-melt materials should have no difficulty in settling on the surface of the substrate. However in practice, the liquid resin may cool rapidly at the substrate/resin interface, resulting in poor adhesion. The formation of a good coating also depends on the condition of the substrate surface, the control of the resin and substrate temperature, as well as the ambient humidity. It may also be difficult to apply a coating to an already coated surface.

2.1.3. Coating Formation by Oxidation

The formation of coatings by oxidation primarily evolves from drying oils which are natural materials of vegetable or fish origin, i.e., compounds of one molecule of glycerin and three molecules of long-chain fatty acids. The oils are applied in relatively thin films and are allowed to stay in place until they have reacted with oxygen in the atmosphere long enough to become hard and dry. Oxidation of an oil can isomerize, polymerize and cleave the carbon-carbon chain, as well as form oxidation products. The steps involved in this type of film-formation include 1) an induction period in which little visible change in physical or chemical properties of the oil occurs while antioxidants present in the film are being destroyed; 2) an increase in oxygen uptake and formation of hydroperoxides and conjugates; 3) the autocatalytic decomposition of the hydroperoxides to form free radicals; 4) the start of polymerization and cleavage reactions. Oxygen absorption reaches a maximum rate at about the time the film forms and then oxygen continues to be absorbed, but at a much lower rate.

Drying oils and oil-modified coatings can be applied very easily by either brushing or air spraying. Oil-based materials can wet substrate surfaces very easily to form sufficiently flexible coatings. These coatings generally have good weather durability and can provide protection for a number of years. On the other hand, they are not highly protective due to the relatively high water vapour transfer rate. The lack of resistance to alkali is another major deficiency of oil-based coatings, precluding application to any alkaline surface. Also, most oil-based coatings become brittle with aging.

2.1.4. Coating Formation by Polymerization

Polymerization is a reaction in which large molecules are created from many small monomers. Normally, it is a process which must be controlled carefully under strict conditions. Previously, it was not considered to be applicable to the *in situ* formation of coatings. The few examples of coating formation by polymerization actually entailed cross-linking processes. Recently, successful film formation by electropolymerization has been reported and will be discussed in detail later.

Polymerization by cross-linking broadly includes many types of baked coatings such as those used on appliance surfaces. The polymerization takes place between a monomer and one or more different types of polymers to produce the cross-linked polymer coating. In this case, a rigid, three-dimensional molecular structure is created *in situ* to form a film which is insoluble in its own solvents and is not softened appreciably by heat. Cross-linked coatings are generally harder and more protective than oxidation conversion coatings due to greater chemical, water and solvent resistance.

2.1.5. Coating Formation by Coalescence

Coalescence of polymeric particles is an important basis for coating techniques (Wicks et al., 1992). In this case, the polymer is not in solution but rather present as a dispersion of insoluble polymer particles. After application and loss of the volatile components, the particles coalesce to a continuous film. Latex is the most common application of this technique. Because the viscosity of the dispersion is independent of the molecular weight of the polymer and depends primarily on the volume fraction of the internal phase and the packing fraction of the particles, it is possible for the system to have

low viscosity, with relatively high solids content of high molecular weight polymers. The high molecular weight polymers provide sufficient strength in the films for many applications without the need for cross-linking.

When applying the coalescence technique for film formation, the operation must be conducted at a temperature higher than the glass transition temperature (T_g) of the polymeric materials. This allows polymer molecules in the latex particles to be free to diffuse into neighboring particles so that the individual particles disappear in the coalesced film. Usually, it is necessary to emulsify a plasticizer into the latex to reduce the T_g of the latex polymer in order to permit film formation at a lower temperature. Unfortunately, this may introduce some impurities into the film and reduce the resistance of the coating to degradation.

Sol-gel technology is another example of coating formation by coalescence. It originally was a method of fabrication of high quality ceramics and glasses. It involves the dispersion of colloidal particles in a liquid to form a *sol* and then the destabilization of the *sol* to produce a *gel*. The principles and applications of sol-gel technology have been recently collected by Klein (1994). In recent years, this technique has been extended to the fabrication of films and fibers. Since the chemical reactants for sol-gel processing can be purified conveniently by distillation and crystallization, films of high purity can be fabricated by sol-gel processing. Chemicals used in film formation by sol-gel processing are dissolved in a liquid to form a solution. Since all the starting materials are mixed at the molecular level in the solution, a highly homogeneous film can be expected. The pores in properly dried gels are often extremely small since the components of a homogeneous gel are intimately mixed. This allows lower processing temperatures to be used for sol-gel-

derived ceramics. This can be important in compositions which undergo undesired phase transitions or have volatile components, or which exist in structures which undergo undesired diffusion or compositional changes at higher temperature. Another advantage of sol-gel processing is that, because of the solution form of the raw materials, trace elements can be easily introduced into the solution by adding the elements in the form of organometallic compounds or soluble organic or inorganic salts. Such trace elements can be important in adjusting the microstructure or in improving the properties of films. The viscosity, surface tension and concentration of the polymeric solution can be easily adjusted. Large-area films of desired composition and thickness can be easily formed on a substrate of complex geometry. The methods of application of the film, including dipping, spinning, spraying or even painting, can be easily tailored to any specific requirement. Films formed by the sol-gel technique usually have to be thermally cured under high temperature (up to 1200°C). Severe shrinkage and collapse of the films often occur during the pyrolysis.

2.1.6. Inorganic Coating Formation

Usually, inorganic coatings refer to zinc and silicate coatings from either a water or solvent base. The formation of a coating from zinc and inorganic or organic silicates involves a class of reactions different from what takes place in the case of organic films. While the molecules of organic films are primarily made up of carbon atoms combined into long-chain linear polymers or cross-linked polymers, the basic building blocks of inorganic coatings are silica, oxygen and zinc. In liquid form, they contain relatively small molecules of metallic silicates or organic silicates. These essentially monomeric materials are cross-

linked into a silica-oxygen-zinc structure. This occurs through a chain of rather complex chemical reactions, some of which take place rather rapidly while others proceed slowly.

There are essentially three steps in the formation of inorganic coatings: 1) the concentration of the silicates in the coating by evaporation of solvent after the coating has been applied to the surface; 2) the ionization of the zinc which initiates the reaction of the zinc ion with the silicate molecule to form a zinc silicate polymer; 3) the completion of the film reaction over a long period of time by continued formation of zinc ions, which react to increase the size of the zinc silicate polymer and cross-link it into a very insoluble, resistant, three-dimensional structure. The principal method of application for inorganic coatings is by spraying. Curing is a crucial requirement for this method.

2.2. Coating Adhesion

Adhesion is a critical factor in the evaluation of coatings (Fowkes et al., 1981; Vakula and Pritykin, 1991; Wicks et al., 1992) and determines whether the coating is merely a thin sheet of material lying on the substrate or an integral part of the substrate. Three types of adhesive bonds are identified, namely chemical, polar and mechanical bonds, depending on the characteristics of the substrate and coating. Chemical adhesion, which is created by a chemical reaction between the coating and the substrate, is undoubtedly the strongest bond. Polar adhesion is considered secondary valence bonding where the adhesion occurs by way of secondary attractions between the resin molecules and the substrate surface microstructure. The adhesion strength is proportional to the sixth power of the intermolecular distance, but does not become effective until this distance is

under 5 Å (Federation of Societies for Coating Technology, 1978). Most of the adhesion of organic coatings is of the polar or secondary valence type: the resin molecules are attracted to the substrate and result in a coating. If the coating formation process is accomplished by a series of *in situ* chemical reactions on the substrate, the resin molecules can react directly with the metallic species at the substrate. In this way, a primary valence bond (i.e., chemical bond) between the resin coating and the substrate can form, thereby increasing the coating adhesion. Coating formation by electropolymerization belongs in this category since the monomers are polymerized *in situ* on the substrates.

Mechanical adhesion is the type of adhesion associated with surface roughness resulting in anchor patterns. An anchor pattern is the surface roughness formed by peaks and valleys on the substrate. These can vary over a relatively wide range of depths. However, most important is the density of hills and valleys which enhance the adhesion by an increase in surface area and actual roughness. Some coatings which are not strongly bonded or are thick require good surface roughness and a deep anchor pattern to obtain adequate adhesion. Most high-performance coatings obtain adequate adhesion with an anchor pattern between 1 to 2 μm in depth. Such a surface roughness substantially increases the surface area over which the coating has an opportunity to bond (Snogren, 1974).

CHAPTER 3

THEORY

3.1. Chemistry of Vinylpyridine and its Polymerization

3.1.1. The Structure and Properties of the Monomer

Vinylpyridine is structurally similar to styrene, but is based on the pyridine ring rather than the benzene ring. Although three kinds of vinylpyridines exist (as shown below), the commercially important ones are 2- and 4-vinylpyridine, and most of the vinylpyridine derivatives are synthesized from these two compounds.

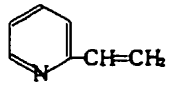

2-(vinylpyridine)

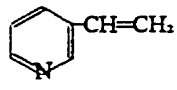

3-(vinylpyridine)

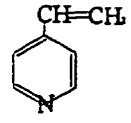

4-(vinylpyridine)

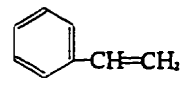

styrene

Vinylpyridine is weakly basic. The nitrogen atom in the pyridine ring is electronegative, which results in the attached double-bond being polarized. It is soluble in common organic solvents and slightly soluble in water. Some important physical properties of vinylpyridines are shown in Table 3.1. Vinylpyridines have a distinct and intense odour and show narcotic effects on rats and mice after administration via ingestion or inhalation. The compounds also cause irritation of the skin and mucous membranes. The toxicity of 4-vinylpyridine is approximately twofold higher than 2-vinylpyridine and is classified as a highly toxic material. Its safe exposure level in a workplace is 0.5 mg/m^3 (Khan, 1989). As a result of their high tendency to polymerize, vinylpyridines must be

stabilized for storage and transportation.

Vinylpyridines are generally prepared by dehydrogenation of the corresponding alkylpyridine or by dehydration of hydroxyalkylpyridine (Khan, 1989). Because of the presence of the nitrogen atom in the pyridine ring, vinylpyridines can undergo a large number of chemical reactions, e.g., oxidation, hydrogenation, bromination, dimerization, etc. (Giam, 1961; Tomcufcik and Starker, 1961). The electronegative nitrogen atom can attract positive ions, making the whole molecule positively charged and, therefore, attracted to the negative pole in an electric field. Although most of the pyridine derivatives can participate in both anodic oxidation and cathodic reduction reactions, only cathodic reduction reaction has been reported (Toomey, 1984). More information on 2-vinylpyridine is available in the literature (Wall et al., 1951; Petro and Smyth, 1957; Luskin, 1974; Nuyken, 1992).

Table 3.1. Important physical properties of vinylpyridines (from Perrin, 1965; Khan, 1989; Nuyken, 1992)

Type of Monomer	b.p. (°C)	d_4^{20}	n_D^2	*p*Ka	Solubility in water (g/L)
2-Vinylpyridine	79-82 *	0.9985	1.5495	4.92	4.92
4-Vinylpyridine	65 ‡	0.9800	1.5499	5.50	5.62

* under 736.6 mm Hg; ‡ under 381 mm Hg.

3.1.2. Polymerization and Polymer Properties

As a vinyl derivative with the electron-withdrawing pyridine group attached to the double-bond, vinylpyridine is susceptible to free radical and anionic polymerization. The

polyvinylpyridines have similar properties to polystyrenes, but require a higher temperature for moulding. Due to the need for large amounts of synthetic rubber during World War II, polyvinylpyridines were needed to replace polystyrenes. This gave strong impetus to the study of the polymerization and copolymerization of vinylpyridines.

Typical vinylpyridine polymerization processes include 1) radical polymerization with 2-methyl-5-vinylpyridine, initiated by potassium persulfate in the presence of anionic emulsifiers such as sodium lauryl sulfate and sodium laureate (Crescenti et al., 1965), and with 4-vinylpyridine initiated by potassium persulfate and sodium palmitate (Katchalsky et al., 1957), and 2) anionic polymerization with 2- or 4-vinylpyridine initiated by *n*-butyllithium (Matsuzaki et al., 1977), 2-ethylpyridyllithium (Hogen-Esch and Jenkins, 1981), dibenzylmagnesium (Soum and Foutanille, 1980) or cumylbarium (Tang and Francois, 1983). No attempt at cationic polymerization has been reported (Nuyken, 1992). The polymerization process is complicated by side reactions of the initiators with polar-substitutes. The fraction of the initiators producing growing chains is, therefore, low. Side reactions of the growing centres may also occur, particularly at higher temperatures. The rate of polymerization is low, especially for 2-vinylpyridine, mostly due to steric effects and the effect of high-temperature side reactions. Electrochemically initiated vinylpyridine polymerization, which can overcome some of these shortcomings, was introduced in the early 1950s (Parravano, 1951). One example of this is the electrochemical anionic polymerization of 4-vinylpyridine reported by Bhadani and Parravano (1970). A more detailed review of this area will be presented in a later section.

Poly(2-vinylpyridine) is water soluble as a basic salt in the presence of 31% or more of the equivalent amount of hydrogen iodide. Wall et al. (1951) studied the electrical

properties of poly(2-vinylpyridine) and measured a number of quantities, including the transference number of the polyion, the number of equivalents of polymer transported per faraday, the fraction of iodide ions associated with the polyanions and the overall degree of ionization of the polymer. They also found that when hydrogen ions were added, the polymer accumulated a positive charge and the polycation migrated toward the cathode. Vinylpyridine polymers have been used as carriers in oxidation and reduction reactions. The presence of the tertiary nitrogen makes the polymers a convenient starting point for the preparation of cationic polyelectrolytes. They are also very important in applications such as polymeric reagents and in electrical applications. The presence of the weakly basic nitrogen in the ring makes vinylpyridine polymers useful in flocculation and adsorption of metal ions for such applications as waste water treatment (Funt, 1991). Recently, Sekine et al. (1992) reported that poly(2-vinylpyridine) coatings formed by electropolymerization provided superior corrosion protection. More detailed discussion of their findings will be given later.

3.2. Principles of Electropolymerization

3.2.1. Electrochemical Techniques for Electropolymerization

3.2.1.1. Linear Sweep Voltammetry

Linear sweep voltammetry is a popular technique for electrochemical studies. It has proven useful in obtaining information about complicated electrode reactions (Bockris and Reddy, 1970; Noel and Vasu, 1990; Newman, 1991). It is performed by applying a triangular potential wave to the working electrode with respect to a reference electrode.

Considerable information can be obtained from a qualitative inspection of the obtained *i-v* diagram (voltammogram). It can indicate the half-wave potential of the concerned reactions, the diffusion limiting current (or the peak current) of the particular system, the reversibility of the reactions and the possible occurrence of a sequence of electron transfer steps. Analytical expressions relating peak current and peak potential have been derived for a number of simple systems. Many of these are given by Bard and Faulkner (1980).

In application of voltammetry to electropolymerization, it has been found that sometimes more than one current wave appears along the anodic or cathodic potential sweeps of the voltammograms. Some recent examples include the electropolymerizations of ferrocene and cobaltocene electrode films (Nishihara et al., 1987), acrylamide (Hacioglu et al., 1989), maleic anhydride in an acetonitrile-dimethylformamide mixture (Akbulut and Hacioglu, 1991) and of allylphenylether in acetonitrile (Sen et al., 1995). These multi-waved voltammograms indicate that at least one other electron transfer reaction is occurring after oxidation or reduction of the monomer. This phenomenon has not attracted enough attention.

3.2.1.2. Chronoamperometric Electrolysis

Chronoamperometric electrolysis (also called potentiostatic electrolysis) is conducted with a three-electrode system. The potential between the working and reference electrodes is maintained by a potentiostat (Bard and Faulkner, 1980). An electronic feedback circuit continually compares and controls the working electrode potential with respect to the reference electrode. Several factors should be considered in choosing the appropriate electrolysis potential, including the threshold reaction potential

determined by voltammetry, the potential at which interfering reactions may occur and the desired rate of the electrochemical reaction. Analytical expressions relating current and potential for some typical chronoamperometric systems are available in the literature (Bard and Faulkner, 1980).

3.2.1.3. Galvanostatic Electrolysis

Galvanostatic electrolysis (also called constant current electrolysis) is carried out by applying a constant current between the working and auxiliary electrodes using a galvanostat. Only a simple, two-electrode configuration is required for galvanostatic electrolysis. Analytical expressions relating potential and current for some simple systems are available in the literature (Bard and Faulkner, 1980). The galvanostat ensures a constant current density and thus a controlled rate of the electrochemical reaction. The Faradaic efficiency can be calculated directly for this type of electrolysis. The total charge passed can be calculated directly since the product of current and time can be obtained without having to do a separate measurement. However, as the reaction proceeds, the potential on the working electrode may change, new electrochemical processes may occur at different potentials and a change in the composition or character of the product may result.

3.2.1.4. Cyclic Potential Sweep Electrolysis

Cyclic potential sweep (CPS) electrolysis is an extension of the chronoamperometric method. In this technique, the potential is cyclically scanned between fixed limits. If the rate of mass transport to the electrode is insufficient to maintain a

steady concentration of reactants during regular potentiostatic electrolysis, some undesirable effects may be produced. The morphology of the formed coating may change and secondary reactions may be favoured. CPS electrolysis is a method of interrupting or modifying the pattern of imposed potentials to minimize these effects. Cycling the potential of the system provides an opportunity for mass transport to minimize concentration polarization and provides a lower average current density for the process (Funt, 1991). A lower current density can reduce the possibility of secondary reactions and lead to more uniform coatings. The use of CPS to conduct electropolymerization has been reported (Abruna et al., 1981; Nishihara et al., 1987; Ohno et al., 1990). Its special features for studying electropolymerization have been summarized by Funt (1991).

3.2.1.5. Current Reversal Electrolysis

Current reversal electrolysis is a galvanostatic technique in which a series of current pulses (with different current values) are applied to the electrolytic system. It permits good control of the initiation, propagation and termination steps in polymerization and consequently produces a polymer with controlled molecular weight and molecular weight distribution, as well as predetermined yield (Ogumi et al., 1976; Mano and Calafate, 1983; Ruckenstein and Park, 1991; Dujardin et al., 1986; Garcia-Camarero; 1990; Funt et al., 1986). Such a method is particularly appropriate for a polymerization process in which chain termination does not occur readily (e.g., ionic polymerization). Current reversal can be used to form polymer coatings at both electrodes and to minimize the effects of concentration polarization due to the depletion of reactions at the electrode (Funt, 1991). This last effect is useful in all deposition processes for producing uniform

and compact coatings. An example of this kind of technique is pulse plating. Some good review papers are available (Devaraj et al., 1990). Current reversal electrolysis can also be used in electropolymerization to study accurately the lifetime of the chain radical (Bhadani and Kundu, 1984; Iroh and Labes, 1992).

3.2.1.6. Constant Cell-Potential Electrolysis

Constant cell-potential electrolysis is carried out by applying a constant potential between the working and auxiliary electrodes using a power source. Only a simple, two-electrode configuration is required for this operation. However, no information of any individual electrode potential can be obtained during the electrolysis. As the reaction proceeds, although the cell potential is kept constant, the potential on the working electrode may change, and new electrochemical processes may occur at the working electrode and a change in the composition or character of the product may result. This technique is popularly applied in manufacturing processes of well-studied systems in the electrochemical industry. It has been applied for electropolymerization as well (Teng et al., 1977; Sekine et al., 1992).

3.2.2. Electroinitiation and Polymerization

Electropolymerization is a process in which an initiator is generated *in situ* by an electrochemical reaction. It is different from an electrochemical synthesis since the amount of monomer polymerized is not in a stoichiometric ratio with the amount of electrical charge passed. The ways in which an electrochemical system can be employed to perform a polymerization process can be classified according to the mechanisms of the

polymerization process: a) free radical polymerization, b) anionic polymerization; c) cationic polymerization and secondary groups: d) organometallic species-induced co-ordination polymerization and e) group-transfer polymerization (Funt, 1991). The initiators of polymerization can include the monomer molecules, supporting electrolyte ions, solvent molecules, some impurities in the system or any species deliberately added to the electrolyte (Dey and Rudd, 1974; Akbulut et al., 1975; Subramanian and Jakubowski, 1978; MacCallum and MacKerron, 1982; Lee and Bell, 1995a). Sometimes, it is difficult to distinguish between these possibilities until the role played by every species present in the electrolyte is carefully investigated and a detailed mechanism of the process is thoroughly understood (Funt, 1991; Odian, 1991; Rosen, 1993; Ling et al., 1997).

3.2.2.1. Free Radical Polymerization

Free radical initiation was the first recognized electropolymerization reaction (Wilson, 1949). The free radical initiators can be generated irreversibly at the cathode by reduction of hydrogen ions adsorbed on the electrode surface from an aqueous solution

$$(H_3O^+)_{ad} + e^- \rightarrow H_2O + (H^\bullet)_{ad} \qquad (3.1)$$

or by reduction of protonated monomer species adsorbed on the cathode surface

$$(M\text{-}H^+)_{ad} + e^- \xrightarrow{k_1} (HM^\bullet)_{ad} \qquad (3.2)$$

Since the radicals are normally adsorbed on the electrode surface, they are presented in the above equations with the subscript *ad*. However, this subscript will be omitted from the remainder of this work for the purpose of simplicity.

Sometimes when conditions allow, a free radical initiator can also be generated by activation of a redox catalyst

$$Fe^{3+} + e^- \rightarrow Fe^{2+} \quad (3.3)$$

$$Fe^{2+} + H_2O_2 \rightarrow Fe^{3+} + {}^{\bullet}OH + {}^{-}OH \quad (3.4)$$

or by direct reduction of a peroxy compound

$$R_2O_2 + e^- \rightarrow RO^{\bullet} + RO^- \quad (3.5)$$

Free radical initiators can also be generated at the anode by oxidation reactions, e.g., anodic dissolution in the presence of peroxy compounds

$$Fe \rightarrow Fe^{2+} + 2e^- \quad (3.6)$$

$$Fe^{2+} + H_2O_2 \rightarrow Fe^{3+} + {}^{\bullet}OH + {}^{-}OH \quad (3.7)$$

or by the Kolbe reaction

$$CH_3COO^- \rightarrow CH_3^{\bullet} + CO_2 + e^- \quad (3.8)$$

Considering the initiation process in which a monomer molecule is directly involved (reaction 3.2), the initiation rate v can be expressed in terms of the current (Shapoval and Gorodyskii, 1973):

$$v = \frac{i}{nF} = k_1[M - H^+][H^+]e^{-\alpha n f \eta} \quad (3.9)$$

where i is the initiation current density, n is the electron transfer number and often equals 1 in an electropolymerization process, F is the Faraday constant, α is the transfer coefficient, η is the electrode overpotential, and f is a combination of Faraday constant, molar gas constant and operating temperature (= F/RT).

The $(HM^{\bullet})_{ad}$ radicals may immediately react in one of three ways:

1) recombination with each other at the electrode surface:

$$HM^{\bullet} + {}^{\bullet}MH \xrightarrow{k_3} HM\text{-}MH \quad (3.10)$$

at a rate of

$$v_1 = k_2[HM^\bullet]^2 \tag{3.11}$$

2) combination with the generated hydrogen radicals ($H^\bullet$) at the electrode surface:

$$HM^\bullet + H^\bullet \xrightarrow{k_3} MH_2 \tag{3.12}$$

at a rate of

$$v_2 = k_3[HM^\bullet][H^\bullet] \tag{3.13}$$

The consequence of the reactions (3.10) and (3.12) is the so-called *cage effect*.

3) reaction with a neutral monomer to initiate the polymerization

$$HM^\bullet + M \xrightarrow{k_4} HM\text{-}M^\bullet \tag{3.14}$$

at a rate of

$$v_3 = k_4[HM^\bullet][M] \tag{3.15}$$

Thus, the actual polymerization rate depends on the rates of reactions (3.2) and (3.14), which in turn are determined by the overpotential η, the monomer concentration *[M]* and the active radical concentration *[HM•]*. The yield, Γ, of the polymer can then be written, provisionally, as the ratio of the rate of reaction (3.14) to the sum of the rates of the parallel reactions (3.10), (3.12) and (3.14):

$$\Gamma = \frac{v_3}{v_1 + v_2 + v_3} \tag{3.16}$$

$$= \frac{k_4[HM^\bullet][M]}{k_2[HM^\bullet]^2 + k_3[HM^\bullet][H^\bullet] + k_4[HM^\bullet][M]} \tag{3.17}$$

$$= \frac{k_4[M]}{k_2[HM^\bullet]+k_3[H^\bullet]+k_4[M]} \tag{3.18}$$

Equation (3.18) indicates that for an electroreduction polymerization (ERP) process, the polymer yield decreases as the free radical concentrations increase, while the yield increases with a rising monomer concentration. For an electrooxidation polymerization (EOP) process, a corresponding relationship can be obtained with a similar analysis.

Researchers originally believed that only a small amount of electricity was required to initiate the polymerization in an electropolymerization process. The polymerization would then proceed continuously. However, the actual processes are more complicated, at least in a free radical-initiated electropolymerization process. The strong cage effect (e.g., reactions 3.10 and 3.12) would consume a large amount of free radicals generated and cause a very low initiation efficiency, especially for an electropolymerization coating formation process when the reactions occur in the close vicinity of the electrode surface. Therefore, a much larger amount of electricity (than the theoretically calculated amount) has to be provided continuously for electrolysis throughout the electropolymerization. In addition, some side reactions (e.g., hydrogen evolution and/or substrate oxidation) may also occur on the electrode surface and contribute to the process current. Chain transfer reactions may occur in the process and affect the process kinetics. Almost anything may act as a chain-transfer agent under the appropriate conditions, including the initiators, supporting electrolytes, solvent molecules, monomers and inactive polymer chains. The effect of dissolved oxygen in the electrolyte is another complicating factor for an electropolymerization process. It can affect a process either as an initiator or an inhibitor/retarder, or as both at the same time. On the other hand, the post-polymerization

after the cessation of current flow can influence the yield of a electropolymerization in a different way, i.e., producing more polymer products with less electricity consumption (Ogumi et al., 1976; Funt, 1991; Iroh and Labes, 1992). Last but not least, a coating formation process is different from bulk polymerization. In a coating formation process, some portion of the formed polymer deposits on the electrode surface while another portion may not remain on the surface but dissolve in or precipitate out of the electrolyte. This will surely cause an error in estimation of the yield of polymer products on the basis of a weight change measurement of the coating samples. Due to the complexity of an electropolymerization process and the lack of knowledge of its detailed mechanism, the significance of any theoretical analysis of the process kinetics using the above equations (3.1 to 3.18) is limited from a quantitative point of view, although it can still be instructive from a qualitative point of view.

3.2.2.2. Anionic Polymerization

The cathodic reduction of a supporting electrolyte followed by the interaction with monomer molecules or the direct electrochemical reduction of the monomer molecules can form anionic radicals and lead to the initiation of anionic polymerization (Morton 1983; Fetters, 1984). In this type of polymerization, each electron transferred at the electrode produces a single chain. The chain can grow on electrodes or desorb from the electrode surfaces (due to the repulsion from the negatively charged electrodes) and propagate in the bulk solution. Each chain grows until the monomer is exhausted in the medium, leaving behind a living chain-end. This chain can react further with additional monomer or

with a new monomer added to the reaction medium, unless some terminator in the medium reacts with the chain and ends the process.

If the electron affinity of the cation of the supporting electrolyte is greater than that of the monomer, the cation will be reduced first at the cathode. The reduced species may react with the monomer to form species capable of initiating anionic polymerization:

$$S^+ + e^- \Leftrightarrow S \tag{3.19}$$

$$S + M \Leftrightarrow S^+ + M^{-\bullet} \tag{3.20}$$

where *S* denotes the supporting electrolyte and *M* is the neutral monomer. The anionic radicals can combine with each other to form a di-anionic diradical:

$$M^{-\bullet} + M^{-\bullet} \xrightarrow{k_3} {}^{\bullet-}M{-}M^{-\bullet} \tag{3.21}$$

which can combine with a neutral monomer to form a trimer:

$${}^{\bullet-}M{-}M^{-\bullet} + M \xrightarrow{k_4} {}^{\bullet-}M{-}M{-}M^{-\bullet} \tag{3.22}$$

and so on. The rates of the various stages in the process are

$$v_1 = k_1[S^+]e^{(-\alpha nf\eta)} - k_2[S]e^{(1-\alpha)nf\eta} \tag{3.23}$$

$$v_2 = k_3[S][M] - k_4[S^+][M^-] \tag{3.24}$$

$$v_3 = k_5[M^{-\bullet}]^2 \tag{3.25}$$

The rate of the electrode reaction depends on the cathodic overpotential and very little on the concentration of the supporting electrolyte since S^+ is regenerated through interaction with the monomer (reaction 3.20). The efficiency of initiation, which may be measured by the forward rate constant k_3 of the reaction (3.20), is determined by the difference in electron affinity between *S* and *M*. This quantity is constant for each *S*-*M* pair.

If the half-wave potential for reduction of S^+ is more negative than that of the monomer, electropolymerization will be initiated by direct reduction of the monomer molecule to the anion radical

$$M + e^- \Leftrightarrow M^{-\bullet} \tag{3.26}$$

that can then undergo initiation and propagation via reactions (3.21) and (3.22). The rate of the electrochemical reaction

$$v_4 = k_7[M]e^{(-\alpha n f \eta)} - k_8[M^{-\bullet}]e^{(1-\alpha)nf\eta} \tag{3.27}$$

is proportional to the monomer concentration and depends strongly on the cathodic overpotential η, assuming that k_8 is small. The rate of dimerization of the anionic radicals via reaction (3.25) is limited by the rate of anion radical formation and by Coulombic repulsion. The rate of reaction (3.22) which represents polymer chain growth is given as

$$v_5 = k_6[^{\bullet-}M—M^{-\bullet}][M] \tag{3.28}$$

and is determined by the initiating dianion and the monomer concentration.

The actual kinetics of an electropolymerization process is much more complicated than the above description. For example, an anionic process prefers an aprotic medium and requires stringent material purity, in particular exclusion of proton-donating impurities during the course of the reaction. A small amount of proton-donating impurities (e.g., moisture) can affect the process kinetics significantly. The anion radicals, especially the di-anion radicals, are very likely repelled by the cathode surface. This might prevent a polymer coating from forming even if polymerization occurs. On the other hand, under such conditions, a remarkable degree of control over the rate of reaction and the product composition can be exercised. Combined with proper electrochemical techniques, polymers with a controlled molecular weight and molecular weight distribution and

predetermined yield can be produced. Therefore, an accurate process kinetic description now still depends on the experimental results. No reliable theoretical description is available yet.

3.2.2.3. Cationic Polymerization

The electrochemical oxidation at the anode produces active cation radicals that can initiate polymerization. The oxidation of a supporting electrolyte containing anions such as BF_4^- or ClO_4^-, can form radicals such as $BF_3^{\bullet}$ or $ClO_4^{\bullet}$, which are common initiators of cationic polymerization. The suggested mechanism of cationic initiation involves anodic oxidation of a supporting electrolyte anion (e.g., oxidation of ClO_4^- to form a $ClO_4^{\bullet}$ radical)

$$ClO_4^- \xrightarrow{k_1} ClO_4^{\bullet} + e^- \tag{3.29}$$

and then the interaction between the radical and the monomer on the electrode surface to form the carbonium radical $M^{+\bullet}$

$$ClO_4^{\bullet} + M \xrightarrow{k_2} ClO_4^- + M^{+\bullet} \tag{3.30}$$

The rate of such an initiation process is given by the following expressions

$$v_1 = k_1[ClO_4^-]\, e^{(1-\alpha)nf\eta} \tag{3.31}$$

$$v_2 = k_2[ClO_4^{\bullet}][M] \tag{3.32}$$

In the steady state, the overall rate of polymerization is determined by the rate of the electrode reaction, v_1, which varies exponentially with the electrode overpotential. It also depends on the monomer concentration and the concentration of perchlorate ion, which can be regenerated by reaction (3.30).

A second possibility can occur if the anodic oxidation of the monomer takes place at a less positive electrode potential than that required for reaction (3.29). In this case, direct anodic oxidation of a monomer molecule

$$M \xrightarrow{k_3} M^{+\bullet} + e^- \tag{3.33}$$

can take place. Its rate

$$v_3 = k_3[M]\, e^{(1-\alpha)nf\eta} \tag{3.34}$$

depends on the monomer concentration and the electrode overpotential.

Although the possibility of the electroinitiation of cationic polymerization has been demonstrated and explained theoretically, it has been observed in only a few cases with monomers having electron-rich substitutes adjacent to the double-bond (Breitenbach and Srna, 1962). The actual kinetics of a cationic polymerization process is generally much more complicated than that described above. It is strongly affected by the ionic environment of the reaction system, similar to that in anionic polymerization. Rates of polymerization differ considerably in various solvents. Differences in the nature of the electrode substrates also affect the rate of processes. Chain transfer may become a dominating process when conditions are appropriate, and limit polymer chain growth and thus, the molecular weight of the product.

3.2.2.4. 2-Vinylpyridine Polymerization

The presence of electronegative nitrogen and the attachment of a double-bond at the *o*-position of the pyridine ring introduces unique and complicating factors to 2-vinylpyridine polymerization. Chemically initiated 2-vinylpyridine polymerization can proceed by either a free radical mechanism or an anionic mechanism (Leonard, 1971). For

3.2.3. Reaction Medium

In an electropolymerization system, the reaction medium always includes a solvent, supporting electrolytes and electrodes. Each of these components has a strong influence on the polymerization mechanism and product quality.

3.2.3.1. Solvent

The choice of solvent influences many aspects of the electropolymerization process. Mutual solubility of the monomer and supporting electrolyte is the basic requirement for an appropriate solvent. In addition, the solubility of the polymer coating must be considered. A maximum solubility difference between the chosen monomer and the corresponding polymer is often preferred. The solvent should not favour the dissolution of the coating over its formation. The solvent must be chemically compatible with the polymerization reaction, e.g., proton-donating solvents must be avoided for anionic polymerization and proton-accepting solvents must be avoided for cathodic polymerization. Solvents such as CCl_4 that are prone to chain transfer should not be used if high molecular weights are desired. Solvents also influence the morphology of polymer chains, polymer coating thickness and uniformity. Some solvents favour chain extension, while others enhance the intrachain attraction, and therefore, produce a polymer with a tightly coiled structure. Moreover, it is important for the solvent to remain stable during an electropolymerization process. Solvent dissociation by reduction or oxidation reactions before the desired electroinitiation reaction occurs should be avoided.

Water is always found to be a good solvent for obtaining polymer coatings. More recently, the awareness of the environmental problems associated with disposing of

organic solvents has promoted the investigation of systems requiring little or no organic solvent. Besides its practical advantages with respect to cost and environmental concerns, water has a high surface tension and can enhance physical adsorption of the dissolved monomers on electrode surfaces. This favours the formation of coatings with good adhesion to substrates. The addition of alcohol to water is sometimes necessary to enhance the solubility of the monomers while maintaining a low solubility for its corresponding polymer. Methanol is particularly suitable for this purpose. It normally has a good affinity with monomers and incompatibility with the corresponding polymers. At the same time, methanol is unlikely to affect the adsorption of the monomers on the electrode surface significantly due to its relatively low ability to adsorb. The water/methanol ratio will affect the properties of the synthesized polymers. An increase in the amount of methanol will lead to coatings consisting of higher molecular weight chains. Some good research reports of the effects of solvent/water ratio of the electrolyte on the polymer coating formation by electropolymerization are available (Liang et al., 1993; Iroh et al., 1993a and 1993b; Lee and Bell, 1995b). Although it is possible for an electropolymerization process to be carried out by a free radical or an ionic mechanism, the use of water as the primary reaction medium likely limits the polymerization to a free radical mechanism (Iroh et al., 1991; Iroh et al., 1994).

3.2.3.2. Supporting Electrolyte

Basically, a supporting electrolyte serves to increase the conductivity of the electrolyte by providing a relatively high ionic concentration. A relatively high concentration of the supporting electrolyte can swamp the effects of migration of minor

species to the electrodes. Consequently, in a quiescent solution, diffusion to the electrodes becomes the only significant means of mass transport for species present in small amounts. It also allows the interpretation of electroanalytical data easier by simplifying the mass transport equations (Bard and Faulkner, 1980). In the area of electropolymerization, it has also been found that supporting electrolytes are sometimes directly involved in the electroinitiation process (Shapoval and Gorodyskii, 1973; Funt, 1991). It has even been reported that no detectable polymerization can occur in the absence of a supporting electrolyte (Garg et al., 1978).

In electropolymerization, the solubility of the supporting electrolyte and the range of potential over which the supporting electrolyte is stable emerge as the major criteria for the selection of the supporting electrolyte. KCl is one of the most commonly used supporting electrolytes, although the Cl^- ions may sometimes cause problems such as generating Cl_2 on the anode surface or complexing with cations in the solutions. From this point of view, the relatively large ions (e.g., perchlorate anion and ammonium cation) are stable over a wider range of electrode potential and are unlikely to cause complexation. Tetraalkylammonium perchlorate is often used in relatively non-polar systems (Funt, 1991). It not only increases the conductivity of the electrolytic solutions, but also increases the hydrogen overpotential by adsorbing on the electrode surfaces and forming so-called chicken-fat electrode.

3.2.3.3. Substrate

The basic requirement for a substrate in an electropolymerization process is that it should not react with the solvent or the solute species. It is also important for the

substrate not to undergo reduction or oxidation reactions before or during the electrolysis. The electrode potential at which electropolymerization takes place varies depending on the electrode material. This is different for an EOP process and an ERP process. For an EOP process, the concern is that the metal substrate may be oxidized, suggesting that noble metal is a preferred candidate. The anodic limit of metal substrates in aqueous systems increases in the following order (Subramanian, 1979)

$$Zn \rightarrow Fe \rightarrow Ni \rightarrow Pb \rightarrow Ag \rightarrow Pd \rightarrow Pt \rightarrow Au$$

For an ERP process, oxidation of the metal is not a problem, but hydrogen evolution at the cathode becomes a concern. Generally, more electronegative metals are easier to coat. Also, metal substrates having a higher hydrogen overpotential can be coated more easily. This is probably due to the adsorbed hydrogen obstructing the formation of a polymer coating. The cathodic limit of the metal substrates in aqueous solutions, considering their hydrogen overpotential, increases in the following order (Subramanian, 1979)

$$Pd \rightarrow Au \rightarrow Pt \rightarrow Ni \rightarrow Fe \rightarrow Cu \rightarrow Sn \rightarrow Pb \rightarrow Zn \rightarrow Hg$$

The morphology of an electrode surface can also influence the coating formation process: porous surfaces may be coated more easily than smooth ones, apparently because of the greater surface reactivity of porous surfaces.

CHAPTER 4

ELECTROPOLYMERIZATION — LITERATURE REVIEW

4.1. Electropolymerization

Electropolymerization has been observed for quite some time in the practice of organic electrochemistry. In 1939, Wilson pointed out that reduction by alkali metals occurred in the same way as reduction at a cathode surface and consequently suggested that electrochemical initiation of polymerization was possible. Ten years later, Dineen et al. (1949) and Wilson (1949) observed that unsaturated compounds underwent hydrogenation with great difficulty at a mercury cathode in acid medium, whereas they were rapidly polymerized. However, the use of electrochemically generated radicals to initiate polymerization is a rather recent innovation (Mengoli and Tidswell, 1975).

Some important advantages of electropolymerization were recognized at the beginning of its development (Shapoval and Gorodyskii, 1973). Since the species responsible for initiating polymerization are formed through an electrochemical reaction, the rate of initiation can be controlled easily by varying electrochemical parameters such as applied current density or potential. Electropolymerization processes can often be carried out under mild conditions and the polymers produced will not contain initiator fragments which can cause degradation of the polymer coating. Electrochemical initiation may also influence polymer chain growth, for instance in the orientation of molecules (stereoregulation) (Fettes, 1967; Tomilov, 1968).

In the early work on electropolymerization, attention was focused on the polymerization processes that performed in the bulk solutions (Funt, 1968; Yamazaki et al., 1968). During the electropolymerization, however, it was often noticed that some polymer films formed on the electrode surfaces, which were considered to be undesirable side reactions. These films changed the electrode potentials in an erratic manner and made it difficult to study the process mechanisms. This started the research into the characteristics of electrochemically deposited polymers on metal surfaces. This was found to be a very complicated research area, given different monomers, reaction circumstances and the variety of electrode materials. Although it was claimed that any electronically conducting materials (metallic or non-metallic) could be coated, only noble metals, such as platinum (Akbulut et al., 1975), silver (Fleischmann et al., 1983; Mengoli et al., 1983), and gold (Desbene-Monvernay et al., 1978) were often used as substrates. Sometimes, substrates with high hydrogen overpotential, e.g., zinc and lead (Pistoia et al., 1976) and graphite (Subramanian and Jakubowski, 1978; MacCallum and MacKerron, 1982; Iroh et al., 1994) were also used. Recently, the attention given to materials has moved toward iron and its alloys with the research directed at producing coatings for long term protection (Mengoli et al., 1991; Musiani et al., 1993).

A large number of experiments have involved non-aqueous systems with various additives as supporting electrolytes. The most often used organic solvents include N,N-dimethylformamide (DMF), dimethyl sulfoxide (DMSO) and acetonitrile (AN) (Mengoli and Tidswell, 1975; Abruna et al., 1981), while the most popular supporting electrolyte was tetraalkylammonium perchlorate (Funt, 1991). Recently, aqueous systems have become more attractive for electropolymerization investigations (Pistoia et al., 1978;

Mengoli et al., 1991; Lee and Bell, 1995a; Zhang et al., 1996) due to the increasing environmental concern and the fire hazard associated with organic solvents, as well as the economic advantage of aqueous systems.

The number of monomers exploitable for electropolymerization in aqueous systems is restricted, first of all, by the solubility of the monomers in an aqueous solution. In order to increase the monomer solubility in the solvents, it was suggested (Mengoli and Musiani, 1987) that some organic solvents (e.g., alcohols) be added to the aqueous solution. This was found to produce polymer coatings with more insoluble fractions (i.e., the higher molecular weight fractions). However, it was pointed out (Subramanian, 1979) that because the alcohol in the solvent increased the polymer solubility in the medium, the rate of formation of the polymer coating must be greater than its rate of dissolution. Whenever a polymer of relatively high solubility was formed, only thin films were produced on the substrates. On the other hand, it was reported that the more soluble the polymer was in the electrolyte, the more likely the coatings were to be powdery or spongy (Mengoli et al., 1979a and 1980).

During electropolymerization of polymer coatings by controlled-potential techniques, it was often found that the current decreased quickly after the onset of the electrolysis (Mengoli and Musiani, 1987; Sekine et al., 1992). However, the current did not decrease all the way to zero, but remained at a low level steadily for the rest of the process. Some researchers (Subramanian, 1979; Mengoli and Musiani, 1994) suggested that this occurred because the coating formed was swollen with the electrolyte or the coating was in the form of a gel. Therefore, it would remain electrically conducting to some extent and allow electropolymerization to continue. Some research has been done

(Iroh et al., 1993a and 1993b; Lee and Bell, 1995b) in studying the mass transfer phenomena through polymer coatings on electrode surfaces using some fundamental electrochemistry relationships (Bard and Faulkner, 1980).

4.2. Electrooxidation and Electroreduction Polymerization

Electropolymerization can be classified according to the relevant electrode dynamic characteristics. If the process occurs at an anode, it is called electrooxidation polymerization (EOP); if it occurs at a cathode, it is called electroreduction polymerization (ERP). Due to the uniqueness of the two electrode processes, the applied techniques and operating conditions are distinct. EOP has received much more attention than ERP in the previous research. It was even concluded that electropolymerization leading to polymer deposition on an electrode was based largely on the anodic oxidation of aromatic compounds. An extensive review of electropolymerization film formation was published by Adamcova and Dempirova (1989). However, some information needs to be updated.

4.2.1. Electrooxidation Polymerization

The most significant EOP studies thus far have dealt with the electropolymerization of phenol and its derivatives on steel substrates. As simple and cheap monomers, phenol and its derivatives can be electropolymerized, form strongly reticulated polymer films on metal substrates, and provide a coherent and robust barrier against corrosion. The first patent in this area was granted to McKinney and Fugassi in 1960 for their work in both the molten state and the aqueous state with minor amounts of

non-aqueous solvents. In 1967, another patent was granted to General Electric (Borman, 1967) for the electropolymerization of phenols in water/organic solvent mixtures. Although experimental results were not particularly promising in the early stage, interest was sustained in *in situ* electropolymerization of phenols for corrosion protection for a number of reasons. This was due to simplicity and flexibility of the experimental apparatus, versatility with respect to the substrate to be coated, promising physical properties of the coatings and the possibility of coating inaccessible areas.

Since the late 1970's, systematic and extensive studies were carried out on phenol electropolymerization for metal protection (Mengoli and Musiani, 1987, 1994). Various electrochemical techniques (e.g., cyclic potential sweep, potentiostatic and galvanostatic) have been employed to form quality coatings and to elucidate the process mechanism as well. Various solvent-electrolyte combinations have been tested, including molten, non-aqueous solutions, alkaline aqueous solutions, alkaline alcoholic solutions, hydroalcoholic solutions containing amines and acidic solutions. In molten and non-aqueous solutions (McKinney and Fugassi, 1960), very high voltages were required and uneven polymer growth at the metal surface was observed. In using aqueous alkaline solutions, thin (several μm thick) and powdery coatings were obtained and the current efficiency was found to be low. The ratio of monomer to alkali was found to be a critical parameter in this case. In alkaline alcoholic solutions using sodium hydroxide (Borman, 1967), adherent and homogeneous coatings were obtained, but they could not effectively resist penetration by corrosive agents due to their extreme thinness (maximum 1 μm). However, when aliphatic amine (Mengoli et al., 1980) or ammonia (Mengoli et al., 1990) was used instead of hydroxide (the hydroalcoholic solutions), it was found that the polymer coating

thickness could be increased to 15 ~ 20 μm, considered as an optimal coating thickness for corrosion protection. *In situ* spectroscopic evidence obtained by surface enhanced Raman scattering (SERS) (Fleischmann et al., 1983; Mengoli et al., 1983) showed that allylamine displaced most hydroxide and phenoxide ions from the electrode surface, thus preventing the formation of a compact layer by oxidation. In addition, the growing polymer layer remained quite hydrophilic, permeable to the monomer approaching the electrodes and sufficiently conducting. Oxalic acidic solutions were also tested as possible media for electropolymerization of phenols (Mengoli and Musiani, 1986a). A two-layer coating was formed by anodizing mild steel in oxalic acid-phenol mixtures, with an underlying ferrous oxalate layer being stabilized by the polyoxyphenylene formed on top of it. It was also found (Mengoli and Musiani, 1986b) that the coating characteristics could be modified by adding sodium silicate to improve adhesion and sodium sulfite to promote the growth of thicker coatings. Recently, the technique was applied to form protective coatings on phosphated mild steel and phosphated galvanized steel (Musiani et al., 1993). Improved corrosion protection was also achieved by increasing the molecular weight of the coating material after electropolymerization through thermal curing when the selected monomer contained a functional group (e.g., an allyl-group) which can be thermally activated (Mengoli et al., 1981).

Besides phenol and its derivatives, some other organic compounds were also studied for polymer coating formation by electropolymerization. Polypyrrole films were prepared in deoxygenated acetonitrile with tetraethylammonium tetrafluoroborate (Et_4NBF_4) as the supporting electrolyte (Diaz and Kanazawa, 1983). The polymer was synthesized potentiostatically at a voltage of 0.8 V *vs.* standard calomel electrode (SCE).

The thickness of the film obtained was < 0.5 μm, but thick films (up to 200 μm) were formed by galvanostatic electrolysis. A scheme for electrooxidation polymerization of pyrrole was proposed (Adamcova and Dempirov, 1989). Polymer film formation by co-polymerizing pyrrole with other organic compounds such as phenol and furan, was also reported (Narmann et al., 1983). The films formed showed good strength, electrical conductivity, and thermal stability. Organic and inorganic species were also inserted into polypyrrole films to improve properties. For example, electrodeposition of platinum particles in a polypyrrole film was reported to decrease the ohmic resistance significantly (Vork et al., 1987; Chandler and Pletcher, 1986).

4.2.2. Electroreduction Polymerization

Research has been performed on ERP processes. Methyl methacrylate was polymerized at a mercury electrode in acidic aqueous solutions (Shelepin and Fedorova, 1964). The cathode compartment was separated from the anode compartment by a closed tap. Since polymerization could only occur when monomer was in contact with air, it was suggested that the polymerization is associated with reduction of impurities of a peroxide nature in the system or their decomposition products. Another electropolymerization of methyl methacrylate in an aqueous sulfuric acid solution in a two-compartment cell was reported later (Pistoia et al., 1976). Polymerization from acrylonitrile/acrylic acid mixtures has been conducted using a three-compartment cell separated by two sintered glass disks (Teng et al., 1977). Some fundamental results concerning the relationship between polymerization voltage and coating thickness and appearance were obtained. Acrolein was reduced on metallic surfaces to form polyacrolein films in DMF, with

benzyltrimethylammonium perchlorate (BTMAP) as the supporting electrolyte (Desbene-Monvernay et al., 1978). Acrylonitrile and methacrylonitrile were polymerized cathodically under various electrolysis conditions (Tidswell and Mortimer, 1981a and 1981b). Polymer films have also been prepared by cathodic polymerization of halogenated xylenes at an iron electrode in a non-aqueous electrolytic solution (Ohno et al., 1990). Lee and Bell (1995a and 1995b) formed polymer coatings derived from the monomers such as acrylamide, acrylonitrile, and N,N'-methylenebisacrylamide on an aluminum alloy cathode at room temperature with persulfate as initiator for the electropolymerization. A three-compartment galvanostatic cell with stainless steel counter electrodes was used for the process. The electropolymerization was performed with the galvanostatic method. The initiation reaction was confirmed to occur by a free radical mechanism by carrying out the process in the presence of benzoquinone, a well-known free-radical inhibitor. Zhang et al. (1996) formed poly(styrene-co-4-carbonxyphenyl maleimide) coatings onto steel with the similar experimental set-up. Maleic anhydride was electrochemically polymerized in acetonitrile-dimethylformamide mixture with tetra-butylammonium tetrafluoroborate as supporting electrolyte (Akbulut and Hacioglu, 1991). The synthesis was accomplished by utilizing a controlled potential electrolysis technique. A brown paramagnetic polymer coating was formed on the platinum electrodes. ESR and FT-IR were applied to characterize the polymer coatings. A process mechanism was proposed. However, it appeared that certain basic concepts of electrochemistry (e.g., the diffusion current density in voltammetry) were incorrect and the polymerization process was not explained clearly.

Hydrogen evolution is often the greatest restriction for an ERP coating formation process. It may sometimes even completely prevent the formation of the coating, not to

mention causing a low current efficiency. However, this problem can be prevented when materials with high hydrogen overpotential are used as cathodes. A typical material of this kind is graphite. Considerable electropolymerization research has been carried out using graphite and some significant results have been obtained. Graphite fibers are commercially used for the manufacture of composites due to their mechanical performances and by analogy to glass fiber technology. Coating these graphite fiber composites with a layer of polymer film formed by *in situ* electropolymerization can enhance the interlaminar shear strength of the graphite fiber. Subramanian and Jakubowski (1978) galvanically polymerized polyacrylamide coatings on graphite fibers in aqueous solutions. MacCallum and MacKerron (1982) electropolymerized various monomers, including vinyl polymer and some cyclic functional groups. It was demonstrated that the effect of electropolymerization on the interfacial properties of the resulting composite was manifested by variations of the measured interlaminar shear and impact strengths of the specimens. It was concluded that the electrochemically formed interlayer contributed to one or more of the toughening mechanisms that are available to fiber reinforced composites. The potential value of interface modification by electrochemical polymerization was clearly indicated.

Zhang et al. (1987) co-polymerized acrylonitrile and methyl acrylate onto graphite fibers using the electrochemical method. The coatings were relatively uniform and their modules could be systematically varied by controlling the monomer ratio in the electrolyte solution. The glass transition temperature and molecular weight of the co-polymer were measured. Monomer reactivity ratios based on free radical kinetics were determined from cyclic voltammetry data. A hydrogen radical initiation mechanism was suggested for the

process. Iroh et al. (1990) studied the galvanostatic co-polymerization of 3-carboxyphenyl maleimide and styrene onto graphite fibers in a sulfuric aqueous solution. The process occurred rapidly and the rate increased with the increase of the monomer concentrations and current density. Besides the polymer coatings formed on the graphite fiber surface, some polymer was also found to form in the solution. Iroh et al. (1991) reported experimental results of electropolymerization of polyacrylamide on graphite fibers using a similar experimental set-up and operating conditions. The rate of electropolymerization was obtained from the slope of the linear region of the curve for polymer weight gain as a function of electropolymerization time. It was found to depend on the initial monomer concentration, sulfuric acid concentration, and current density raised to the powers of 1.67, 0.02, 0.54, respectively. Iroh et al. (1993a) reported the results of mechanism studies of co-polymerization of 3-carboxyphenyl maleimide and styrene onto graphite fibers in a sulfuric aqueous solution by electropolymerization. Cyclic voltammetric analysis results suggested radical initiation of polymerization via the reduction of the 3-carboxyphenyl maleimide. Hydroquinone and 2,2-diphenylpicrylhydrazyl (DPPH) were added to test for a free-radical mechanism and a radical chain electropolymerization mechanism was strongly suggested. Kinetic analysis showed a first- and ½ -order dependence of the rate of chain growth on the initial monomer concentration and initiator concentration, respectively. A subsequent study on poly(N,N'dimethyl acrylamide) coating formation on graphite fiber in an aqueous sulfuric acid solution also suggested a free-radical polymerization mechanism for this system. A hydrogen initiation mechanism was suggested for the process (Iroh et al., 1993b). Liang et al. (1993) co-polymerized 2- and 4-carboxyphenyl methacrylamide with either methyl methacrylate or N-phenylmaleimide on graphite fibers

by electropolymerization. It was found that a higher solvent/water ratio helped to increase polymer weight gain by increasing the solvent swelling and increasing the diffusion coefficient of the active species.

The ERP process of most interest to this work is the electropolymerization of poly(2-vinylpyridine) (Sekine et al., 1992; De Bruyne et al., 1995; Ling et al., 1998a and 1998c). Due to the presence of the nitrogen atom in the pyridine ring, it is possible for a variety of reactions to occur with a vinylpyridine molecule. Polyvinylpyridines are particularly important for use as polyelectrolytes and polymeric reagents in electrical applications. Furthermore, they may form metal-organic complexes at the basic nitrogen moiety (Khan, 1989; Nuyken, 1992). Initially, fundamental studies were carried out to understand the basic electrolytic properties of poly(2-vinylpyridine). For example, Wall et al. (1951) studied the ionization of 2-vinylpyridine in hydroiodic acid solution to form a polymeric electrolyte. Anderson et al. (1965) studied its electrolytic properties by carrying out electropolymerization at a mercury cathode in a concentrated solution of 2-vinylpyridine in 67% aqueous tetraethylammonium *p*-toluenesulfonate. Sekine et al. (1992) tried to form protective coatings on mild steel by both EOP and ERP processes with numerous monomers, based on aniline, phenol, normal vinyl and heterocyclic vinyl type monomers. Several electrolytic media, including aqueous and non-aqueous solutions, were also tested using various electrochemical techniques, e.g., cyclic potential sweep, potentiostat, galvanostat, and constant cell-potential. Poly(2-vinylpyridine) coating was formed in a methanol/water solution with ammonium perchlorate as the supporting electrolyte. The corrosion resistance of the coating was measured by the ac impedance technique and it was concluded that poly(2-vinylpyridine) coating formed in a constant

cell-potential system had the best corrosion resistance among all the tested polymer coatings. However, Troch-Nagels et al. (1992) and De Bruyne et al. (1995) found it was difficult to repeat the reported result due to the intense hydrogen evolution on the steel cathode surfaces. They could only form poly(2-vinylpyridine) coatings on zinc substrates which are known for their high hydrogen overpotential. The process was quite fast (within a period of 0.5 to 20 minutes) and produced a coating that was insulating and had a high corrosion resistance, tested by salt spray and polarization techniques. Based on the gravimetric measurements and the hypothesis of one electron reduction per monomer, Bruyne et al. estimated the coating to be as thick as 90.6 μm. No thermal curing was necessary when the process was carried out at an elevated temperature (40 to 60°C).

Interesting research was also carried out on 4-vinylpyridine electropolymerization (Bhadani and Parravano, 1970). The process, identified as electrochemical anionic polymerization, was done in pyridine with sodium tetraphenylboron as supporting electrolyte. Platinum electrodes were used for both anode and cathode. The electrolysis was performed galvanostatically. Polymer was found to form in the liquid phase of the cathodic compartment exclusively, where a yellow to red-orange solution developed during the electrolysis. The extent of the reaction was very sensitive to the experimental conditions and a small amount of impurities such as air or moisture could terminate the polymerization immediately. During the voltammetric study, two reduction waves were observed at –2.15 and –2.4 V, respectively. The former potential was assigned to 4-vinylpyridine monomer reduction reaction and the latter one was assigned to the reduction of pyridine or $NaBPh_4$. The formed polymer was soluble in CH_3OH, CH_3Cl and DMF, but insoluble in H_2O and THF. C_6H_6 and $C_6H_5CH_3$ were found to swell the polymer. Three

possible modes of initiation were proposed: 1) direct electron transfer to monomer; 2) electron transfer to monomer from Na metal deposited on the cathode; 3) initiation by pyridyl radical anions formed by reduction of pyridine.

4.2.3. Comparison of EOP and ERP

A comparison of EOP and ERP processes shows that each has its own distinctive characteristics. Film formation by the EOP process is often accompanied by oxidation of the metal substrates. Metal oxide layers accumulate on the metal substrates, leading to porous and thin polymer films. Therefore, noble metals are often used as substrates for most EOP studies. No such oxidation occurs in the ERP process so more compact and thicker films are expected. However, when ERP processes are processed in an aqueous medium, there is always the possibility of hydrogen evolution occurring along with the coating formation, leading to a porous and irregular coating, not to mention a low current efficiency. That is why very often ERP processes are carried out on materials with high hydrogen overpotential (e.g., zinc, lead, etc.). For materials which do not have a high hydrogen overpotential, intense hydrogen evolution is often the main reason for the failure of coating formation by ERP. As mentioned previously, much less research has been done on the ERP processes. No comprehensive mechanism has been proposed. In view of the promising results with poly(2-vinylpyridine) in protective coating formation, a more thorough study of the system is warranted.

4.3. Polymer Coating Morphology Analysis

Coating morphology is one of the important factors in evaluating the quality of polymer coatings, especially coating uniformity and thickness which greatly influence the performance properties. Minute flaws (i.e., pits, craters and pores) in the coatings will also affect properties such as conductivity, permeability and corrosion resistance. Thus, it is necessary to evaluate the morphology of the polymer coatings formed. A convenient and reliable method for non-destructive analysis which can provide a detailed evaluation of the morphology of the coating such as its roughness and thickness, is essential in selecting a suitable synthesis technique for producing the coatings.

Quantitative measurement of coating thickness and qualitative observations of the morphology of the coating have conventionally been carried out by separate techniques. The former is usually accomplished by estimating the weight increase of a coated sample (gravimetry), while the latter is commonly done by various microscopic techniques, namely, scanning electron microscopy (SEM) or scanning tunneling microscopy (STM). Other techniques such as magnetic induction, eddy current, radioisotope backscattering, resistivity measurement and X-ray fluorescence have also been applied occasionally for evaluating polymer coatings. A number of recent publications describing the applications of these methods for evaluating coating morphology are available in the literature (Sheard and Somekh, 1988; Yang et al., 1988; Haworth and Robinson, 1991; Lewis and Bush, 1991; Solov'ev, 1991; Roessiger and Raffelsberger, 1992; Edneral, 1993; Silkin and Ponomarev, 1993; Latter, 1994; Montgomery, 1994; Reilly, 1994; Hong et al., 1995).Due to the complexity of the polymer coating properties (e.g., conductivity, uniformity,

fluorescence and other optical and thermal properties) and the intrinsic limitations of these various techniques, the application of these methods is often restricted. For example, the magnetic induction method can only be used for steel substrates; the eddy current technique requires that the substrate and the coating have sufficiently different electrical conductivities; the radioisotope backscattering technique requires the atomic numbers of the coating and substrate materials to be significantly different; the X-ray fluorescence technique is limited since many synthesized polymers contain fluorescein; and the resistivity measurement method can be applied only to insulating coatings and can be influenced by many factors concurrently (e.g., coating composition and uniformity, the presence of coating defects, adhesion between the coating and the substrate and variations in the geometry of the substrate and in the preparation of the surface). An independent calibration curve is often needed for each individual case.

In this work, we have applied confocal scanning laser microscopy (CSLM) as a new non-destructive method to analyze the topography and the morphology of a polymer coating. The technique is fast and easy to operate. It can provide high resolution images of the coating surface as well as quantitative measurement of the surface roughness and the coating thickness. Although our application is on poly(2-vinylpyridine) coatings formed on mild steel substrates by *in situ* electropolymerization, the technique should be feasible for a wide range of coating/substrate systems, as long as the coating examined is not completely opaque. In this and the following chapter, the principles and history of the development of CSLM are presented as well as a detailed description of its application to poly(2-vinylpyridine) coatings formed by electropolymerization. A brief assessment of some popularly used microscopic techniques for morphological analysis is first given.

4.3.1. Popular Techniques for Morphological Analysis

There are a number of techniques for investigating the morphology of surfaces. However, as mentioned previously, the techniques for surface profile evaluation and quantitative coating thickness and roughness measurements are often separated. Gravimetry is the most widely used technique for the measurement of coating thickness, while SEM and STM are the most popularly used methods for the observation of surface morphology.

4.3.1.1. Gravimetry

Gravimetry involves determining the mass change of a sample as a result of coating formation. In the case of coatings formed electrochemically, it is usually done either by directly recording the sample weight changes before and after coating formation (Mengoli and Tidswell, 1975; Teng et al., 1977; Mengoli and Musiani, 1987; Sekine et al., 1992; Musiani et al., 1993) or by measuring the total amount of charge passed in the process and calculating the coating mass using basic electrochemical relations such as Faraday's Law (Denisevich et al., 1982; McCarley et al., 1990; Mengoli et al., 1990; Taj et al., 1993; De Bruyne et al., 1995). When only a thin coating is formed, the coating weight is normally very small compared to the weight of the substrate which can lead to a significant relative error in the estimate of the coating weight. Another major problem with the second approach stems from the fact that only the initiation step during electropolymerization involves electron transfer, whereas the propagation and termination steps do not (Funt, 1991). In addition, it is known that some side electrochemical reactions (e.g., hydrogen evolution and metal substrate oxidation (Mengoli and Musiani, 1994; Ling et al., 1998a))

usually accompany the electropolymerization, making charge transfer more difficult to interpret. The determination of the coating thickness from the coating weight is also subject to additional error since it is necessary to have an accurate value of the actual coating density which is usually unknown (Mengoli and Musiani, 1986; Odian, et al., 1991; Taj et al., 1993).

4.3.1.2. Scanning Electron Microscopy (SEM)

Although SEM has been widely used to examine polymer coatings (Wang et al., 1989; McCarley et al., 1990; Ohno et al., 1990; Arapapavinasam, 1993; Musiani et al., 1993; De Bruyne et al., 1995), it has several limitations. Frequently, organic coatings must be coated with gold or other conductive materials (Teng et al., 1977; Ohsaka et al., 1987; Kunimura et al., 1988). Experimental conditions, such as high vacuum and beam heating, may alter or damage the coating surface. Furthermore, quantitative data such as coating thickness cannot be obtained by STM.

4.3.1.3. Scanning Tunneling Microscopy (STM)

The principles and the applications of STM have been described in recent publications (Guntherodt and Wiesendanger, 1992; Wiesendanger and Guntherodt, 1992; Bockris and Khan, 1993; Wiesendanger and Guntherodt, 1993; DiNardo, 1994). STM has found increasing use for both metal and polymer thin films (Heben et al., 1989; Everson and Helms, 1991; Ngo et al., 1993; Song et al., 1993). Because the tunneling current is very sensitive to the distance between the substrate and the probe, STM is not well suited for

large areas or rough surfaces. Similar to SEM, quantitative data such as coating thickness and surface roughness distribution cannot be obtained by STM.

4.3.2. Confocal Scanning Laser Microscopy

Confocal scanning laser microscopy (CSLM) offers the distinct advantage of eliminating defocused images rather than creating a blur of those images as in standard microscopy. The intensity of the CSLM image drops sharply as the image is defocused, whereas the intensity does not change with a standard microscope. Therefore, the plane which is in focus can be observed without interference from layers above or below. This property allows imaging of structures with height differences comparable to the wavelength of the laser beam, thus permitting quantitative measurements of surface roughness. Its defocusing characteristic also permits optical cross-sectioning of a non-opaque specimen and can distinguish between coating and substrate. This allows the quantitative measurement of coating thickness. CSLM images tend to have sharper edges and stronger contrast than images obtained with a standard microscope. The technique is convenient to operate, can perform scans rapidly and does not damage the specimen. There are no strict requirements on the coating and substrate materials in order for CSLM to image the surface topography. Measurement of coating thickness, however, does require that the coating be translucent to some extent.

The principle of confocal microscopy was first described by Young and Roberts (1951). The details of this type of imaging were first described by Minsky (1961). Davidovits and Egger (1969) were the first to develop a working laser-based confocal microscope. Wilson and Sheppard (1984) and Wilson (1990) have provided a detailed analysis of this technique.

Dixon et al. (1991a) developed a transmitted-light and reflected-light scanning stage microscope, which uses the same confocal detector for both reflected and transmitted light. The transmitted beam is re-injected into the optical path of the microscope parallel to the reflected beam. The microscope forms images both in transmission through the top and bottom of the specimen as well as in reflection from the top and bottom of the specimen. The various beams are separated by placing a half-wave plate and a polarizer in the transmission arm of the microscope and a second polarizer in the detection arm of the microscope. This has the advantage of imaging large area samples with very high resolution. Recently, the first practical scanning beam confocal transmission microscope was described, along with new applications in transmission (Dixon et al., 1991b). This device has all the advantages of a scanning stage microscope in addition to producing a high resolution image (512 × 512 pixel and 256 grey levels) in less than two seconds. Because the contrast mechanisms for these images are different, the reflection and transmission images contain complementary information. The optical slicing property of the confocal microscope is used to obtain single confocal slice images both in transmission and reflection. The modified confocal scanning beam laser microscope developed by Dixon et al. has been used to measure the surface roughness of a copper deposit (Ling et al., 1995). In this study, CSLM is used to measure quantitatively the uniformity and thickness of the polymer coated. Some of the research results from this analysis have recently been published (Ling et al., 1998b).

4.4. Polymer Characterization

Polymer characterization is important for confirming the formation of the polymeric materials and investigating their properties. It can also be used to study the structure of polymeric materials and be helpful in understanding the process mechanism. The techniques for polymer characterization used in this project are briefly reviewed below.

4.4.1. Ultraviolet and Visible Spectroscopy

Ultraviolet and visible spectroscopy is used to examine materials qualitatively, providing information regarding the structure, formula and stability of the materials (Shugar and Dean, 1989). Absorption spectra are produced when ions or molecules absorb electromagnetic radiation in the ultraviolet or visible regions. The absorption of energy is a result of displacing an outer electron in the molecule. The spectrum is a function of the whole structure of a substance and the information obtained should be used in conjunction with other evidence to confirm the identity of a compound. Since molar absorptivity values frequently exceed 10,000 L mol^{-1} cm^{-1}, dilute solutions can be used. This technique has been used for characterization of poly(2-vinylpyridine) formed by bulk polymerization (Foster, 1969; Phillips et al., 1970) and by electropolymerization (Sekine et al., 1992; De Bruyne et al., 1995).

4.4.2. Fourier Transform Infrared (FT-IR) Spectroscopy

Infrared spectroscopy has long been recognized as a powerful tool for the characterization of polymers (Koenig et al., 1994). It is based on the absorption of radiation in the infrared frequency range due to the molecular vibrations of the functional groups contained in the polymer chain. Prior to FT-IR, infrared spectroscopy was carried out using a dispersive instrument utilizing prisms or gratings to disperse the infrared radiation geometrically. Using a scanning mechanism, the dispersed radiation was passed over a slit system which isolated the frequency range falling on the detector. This technique is highly limited in sensitivity because most of the radiation transmitted through a sample as a function of frequency does not fall on the open slits. The FT-IR provides speed and sensitivity due to the use of a *Michelson interferometer* consisting of two mirrors and a beam splitter. The beam splitter transmits half of all incident radiation from a source to a moving mirror and reflects half to a stationary mirror. Radiation reflected by the sample is reflected by the two mirrors to the beam splitter where the amplitudes of the waves are combined either destructively or constructively to form an interferogram as seen by the detector. By means of algorithms, the interferogram is Fourier-transformed into the frequency spectrum. This technique has several distinct advantages over conventional dispersive techniques. It can scan the infrared spectrum constantly throughout its optical range in fractions of a second at moderate resolution. It can measure all wavelengths simultaneously with a high signal-to-noise ratio. The interferometer has no slit or grating. As a result, its energy throughput is high. FT-IR has been applied to characterize poly(2-vinylpyridine) formed by electropolymerization (De Bruyne et al., 1995).

4.4.3. Nuclear Magnetic Resonance (NMR) Spectroscopy

Nuclear magnetic resonance (NMR) spectroscopy is a powerful method for elucidating chemical structures. The basic principle of this technique is that the nuclei of certain isotopes have an intrinsic spinning motion around their axes which generates a magnetic moment along the axis of spin. The simultaneous application of a strong external magnetic field and the radiation from a second and weaker radio-frequency source to the nuclei results in transitions between energy states of the nuclear spin. Absorption occurs when these nuclei undergo transition from one alignment in the applied field to an opposite one. The energy needed to excite these transitions can be measured. Nuclei with zero electric quadrupole moment give the best resolved spectra, which include ^{1}H, ^{13}C, ^{19}F, ^{29}Si and ^{31}P. The result is often the delineation of complete sequences of groups or arrangements of atoms in the molecule. Quantitative analysis is available by integration of areas under the absorption peaks and the peak of the internal standard.

Abundant information of NMR analysis for poly(2-vinylpyridine) is available in the literature (Natta et al., 1961; Matsuzaki and Sugimoto, 1967; Weill and Hermann, 1967; Hogen-Esch and Jenkins, 1981; Khan and Hogen-Esch, 1983). Matsuzaki et al. (1976 and 1977) reported their stereoregularity studies of polyvinylpyridines with ^{1}H and ^{13}C NMR. The deuterated and nondeuterated polyvinylpyridines were synthesized by radical polymerization and by anionic polymerization. The results showed that the polyvinylpyridines formed by either radical and anionic polymerization were atactic. Yin and Hogen-Esch (1994) synthesized poly(2-vinylpyridine)-b-poly(t-butylmethacrylate) and studied its stereoregularity with ^{1}H NMR. No report has been published on an NMR study of polyvinylpyridines formed by electropolymerization.

4.5. Reaction Mechanism Studies of Electropolymerization

4.5.1. Inhibition Study of Polymerization

The addition of free-radical inhibitors is a commonly used technique for determining whether a free-radical mechanism is occurring. In the presence of certain inhibitors and radical scavengers, free-radical polymerization can be completely stopped while ionic polymerization should not be affected. The inhibitors act by reacting with the initiating and propagating radicals and converting them either to nonradical species or radicals with too low reactivity to undergo propagation. The commonly used inhibitors include quinones (such as benzoquinone and chloranil) and 2,2-diphenyl-1-picrylhydrazyl (DPPH). Research regarding the use of inhibitors to study the mechanisms of radical polymerization in various systems has been reported (Yassin and Rizk, 1978a and 1978b; Kamachi et al., 1977, 1978, 1979a and 1979b). An example is the dilatometric study of the behaviour of some inhibitors in the polymerization of liquid vinyl acetate (Bartlett and Kwart, 1950). The behaviour of DPPH, hydroquinone, dinitrodurene, nitrobenzene, p-nitrotoluene, iodine and *o*-, *m*- and *p*-dinitrobenzenes as inhibitors of the peroxide-induced polymerization of vinyl acetate was studied kinetically by the dilatometric method. Information about the rate of initiation, the order and relative speed of the chain-terminating step and the number of chains stopped by a terminating molecule was obtained by analyzing the relevant results. Another example of an inhibition study was done by Iroh and his colleagues (1993a) on co-polymerizing 3-carboxyphenyl maleimide and styrene onto graphite fibers in aqueous solutions. Hydroquinone and DPPH were used in a cyclic voltammetric analysis to confirm the free-radical mechanism of the electropolymerization

process. The results suggested radical initiation of polymerization via the reduction of the 3-carboxyphenyl maleimide.

4.5.2. Surface Enhanced Raman Scattering Spectroscopy

Raman spectroscopy is used to determine molecular structures and compositions of organic and inorganic materials. It can span the entire vibrational spectrum with one instrument. When an intense beam of monochromatic light impinges on a material, most collisions are elastic with the frequency of the scattered light being the same as that of the original light (so-called *Rayleigh scattering*). Another type of scattering that can occur simultaneously with the Rayleigh scattering is known as the *Raman effect*. It arises when the change in the vibrational mode of a molecular bond resulting from a beam of intense monochromatic radiation causes a change in the molecular polarizability.

Surface enhanced Raman scattering (SERS) was first recognized about two decades ago (Jeanmaire and Van Duyne, 1977; Albrecht and Creighton, 1977). It was noticed that the Raman scattering intensity of a molecule adsorbed on the surfaces of certain metals (e.g., Au, Ag and Cu) could be remarkably enhanced (up to 10^6 times). This gives SERS a much higher sensitivity compared to ordinary Raman scattering. Furthermore, this enhancement occurs only for species at the metal surface. SERS is therefore ideal for study of adsorption of organic compounds at metal surfaces. However, the technique is restricted by the necessity of creating a rough surface prior to irradiation and of only using certain metals in order for enhancement to occur (Seki, 1986). Nevertheless, SERS has been found to be powerful in examining chemical and physical phenomena associated with adsorption at metal/solution interfaces (Chang and Furtak,

1982; Brandt, 1985; Brolo et al., 1997). Its applications range from electrochemical studies such as corrosion processes (Gui and Devine, 1994; Odziemkowski et al., 1994), film growth (Missono et al., 1994) and self-assembled monolayers (Matsuda et al., 1995) to medical applications (Nabiev et al., 1994) and trace analysis (Gouveia et al., 1994; Rodger et al., 1996). Some comprehensive reviews of this technique are also available (Pemberton, 1991; Pettinger, 1992).

Pyridine and its derivatives were the first substances investigated by SERS (Fleischmann et al., 1974). In addition to a large amount of research concerning simple organic compounds, some of the research has been concerned with the adsorption of macromolecules at metal surfaces (Diaz et al., 1979; Kaneto et al., 1983). In some cases, investigators had difficulties in using SERS to gain a clear understanding of macromolecular adsorption on metal surfaces (Lee and Meisel, 1983; Kobayashi and Imai, 1985). In other cases, very useful information was obtained (Lippert and Brandt, 1988; Garrell and Beer, 1988 and 1989; Tashiro et al., 1990; Mostefai et al., 1996). Certain research problems in electropolymerization processes were solved by SERS technique (Fleischmann et al., 1983). However, most of the previous SERS work has dealt with either micromolecular or macromolecular adsorption on metal surfaces instead of *in situ* polymerization of monomers at metal surfaces as investigated in this research.

CHAPTER 5

EXPERIMENTAL DESIGN AND PROCEDURE

5.1. Reagents and Experimental Apparatus

5.1.1. Reagents

2-vinylpyridine (Aldrich Chemical Company) was purified to remove the inhibitor (0.1 *wt.* % *p-tert*-butylcatechol) by distillation at 70°C under vacuum (100 kPa Hg). All other chemicals were analytical grade and used without further purification. The solvent was normally a water/methanol mixture with volume ratio of 8:2. The normal supporting electrolyte was 0.05 M NH_4ClO_4. Various amounts of $HClO_4$ or NH_4OH were added to the electrolyte to adjust the solution pH as required. When another chemical was used as the supporting electrolyte, the corresponding acid with the same cation was used to adjust the solution pH. All solutions were prepared with ultra-pure water (Millipore® ultra-pure water system) and a total solution volume of 60 mL was used in each electropolymerization experiment.

5.1.2. Electrodes and Electrolytic Cell

A three-electrode system was used to carry out the electropolymerization in a 100-mL electrolytic cell open to the atmosphere. For the polymer coating formation, the working electrode was usually a mild steel coupon (SAE 1018-1020, C: 0.20%, Mn:

0.60%, P: 0.04% maximum, S: 0.05% maximum) with an active surface area of 5.5 cm^2, while the counter electrode was a platinum wire. The reference electrode was a standard calomel electrode (SCE, Aldrich Chemical Company) and all the potentials reported in this project are referred to the SCE scale. The working electrode was cleaned ultrasonically first in a soap solution for 30 minutes and then polished with SiC-type abrasive paper (up to 1200 grade). Degreasing was carried out with trichloroethylene for 2 minutes, followed by a washing with soap solution to remove the grease and trichloroethylene, a rinsing with a large amount of deionized water and finally a rinsing with ultra-pure water. The prepared metal samples were stored in a desiccator until needed. The platinum wire was cleaned by immersion in the Electrode-Cleaner® solution (Fisher Scientific, containing 500 mL 2-(iso)-propanol, 500 mL ethyl ether, 250 mL concentrated hydrochloric acid and 250 mL water) for 2 minutes and then rinsed with tap water and ultra-pure water.

A copper electrode was used when investigating the process mechanism with SERS spectroscopy. This electrode was a copper disk with a diameter of 3 mm, while the counter and reference electrodes remained the same as before. Before using the copper electrodes for the SERS investigation, they were roughened *ex situ* electrochemically by applying several oxidation-reduction cycles between −1.0 and 1.0 V at 30 mV/s in 0.1 M KCl solution for achieving the optimum SERS spectra (Brandt, 1985; Beer et al., 1989). When other electrode materials were examined for polymer coating formation by electropolymerization, the surface areas were kept the same at 5.5 cm^2 and the same procedure for preparation of the working electrode was applied as mentioned above.

5.1.3. Experimental Apparatus

An EG&G potentiostat/galvanostat (EG&G Princeton Applied Research, Potentiostat/Galvanostat, Model 273) was used to control the electrochemical processes during electropolymerization. During electrolysis, the electrode potential or current was monitored as a function of time on a computer screen and the potential or current data were recorded on the data logging computer (JPC 386SX). The working electrode was placed in the middle of the electrolytic cell, and the platinum coil counter electrode was located against the internal wall of the cell. The SCE reference electrode was positioned close to the working electrode. Experiments were normally carried out at 20°C with magnetic stirring maintained throughout the electrolysis. A schematic of the experimental apparatus is shown in Fig. 5.1.

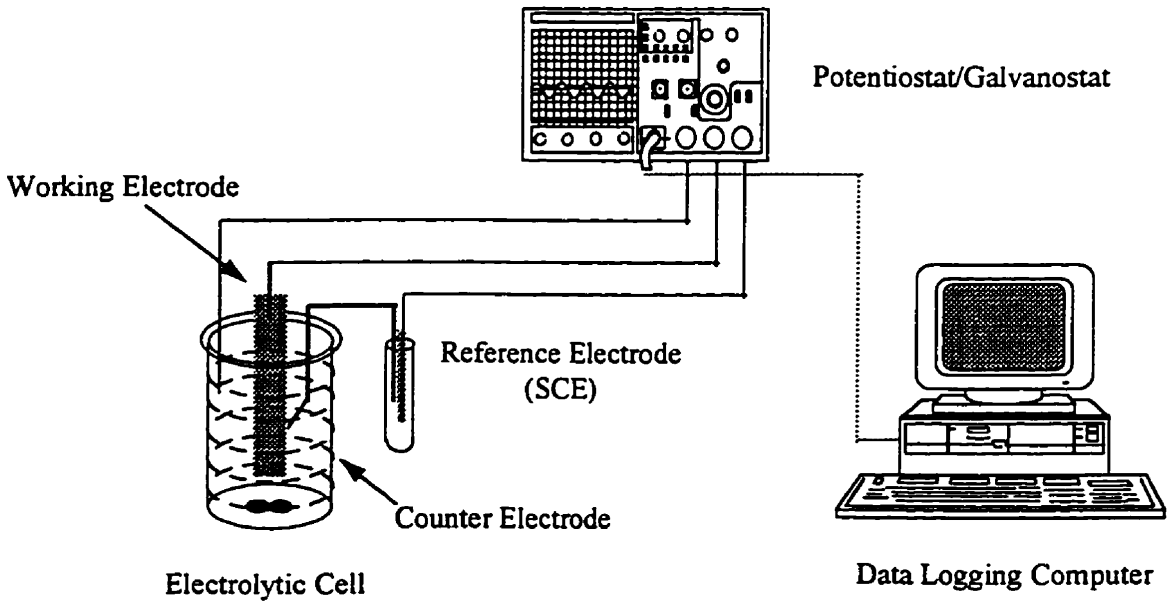

Fig. 5.1. Experimental apparatus for *in situ* electropolymerization of poly(2-vinylpyridine) coatings on mild steel substrates from aqueous solutions.

5.2. Electropolymerization for Coating Formation

5.2.1. Preliminary Experiments: Linear Sweep Voltammetry Studies

The purposes of these preliminary experiments were to study the basic electrochemical properties of the 2-vinylpyridine aqueous system and assess the feasibility of electropolymerizing poly(2-vinylpyridine) coatings on mild steel substrates. Information on parameters such as half-wave potential ($E_{1/2}$) for reduction or oxidation of the monomer, supporting electrolytes and solvents was expected. Any side reaction can be indicated by the results of the voltammetry studies. Some basic operating conditions (e.g., supporting electrolyte, solution pH, and potential sweep range and rate, etc.) were adjusted until polymer coatings with acceptable quality were obtained.

5.2.2. Studies of Various Electrochemical Techniques

The purpose of these experiments was to determine the most suitable electrochemical technique for electropolymerization. These electrochemical methods considered included chronoamperometric electrolysis, improved chronoamperometric electrolysis, galvanostatic electrolysis, cyclic potential sweep (CPS) electrolysis and constant cell-potential electrolysis.

5.2.3. Single Parameter Studies

In order to obtain a good understanding of the effects of the operating parameters on electropolymerization, single parameter studies were carried out. In every series of

experiments, one operating parameter was varied over a certain range while the other parameters were kept constant at certain values. The parameters and the range over which they were studied are listed in Table 5.1. The values of the constant parameters are also listed in the table. These values were obtained from initial fractional-factorial by designed experiments described in the next section. It is important to emphasize the need to maintain these parameters at appropriate values, or otherwise, the experimental results may be misleading.

5.2.4. Statistical Studies

Statistically designed experiments were carried out to investigate interactions between the operating parameters. The chosen statistical technique was the *orthogonal fractional* factorial (*OFF*) design, also called *optimum operating condition search design* (McLean and Anderson, 1984; Dey, 1985). From the results of these designed experiments, the relative importance of the operating parameters can be obtained as well as the optimum combination of the operating parameters for the electropolymerization process. The operating parameters studied by the OFF designed experiments and the levels of the variances of these parameters are listed in Table 5.2. The results from the single parameter studies were used to choose the parameters for these experiments. A standard 4-parameter and 3-level OFF design is shown in Table 5.3

Table 5.1. Parameters and their ranges tested in the single parameter experiments.

Operating parameter	Normal value ‡	Range tested
2-Vinylpyridine Concentration (M)	0.25	0.01 ~ 0.4
Methanol Concentration in the Solvent (vol. %)	20	1 ~ 40
Operating Temperature (°C)	20	10 ~ 70
Supporting Electrolyte (NH_4ClO_4) Concentration (M)	0.05	0.01 ~ 0.2
Electrolysis Duration	2 hrs	15 min. ~ 10 hrs
Electrode Surface Area (cm^2)	5.5	0.07 ~ 100
Solution pH	4.8	1 ~ 10
Potential Range for Sweep Electrolysis (V)	−0.7 ~ −2.5	−0.7 ~ −4
Potential Scan Rate for Sweep Electrolysis (mV/s)	30	5 ~ 100

‡ In a single parameter experiment when one operating parameter is varied over a certain range, the remaining parameters are kept constant at their *normal value*.

Table 5.2. Some important operating parameters and their 3-level ranges studied

	(A) Operating temperature (°C)	(B) Monomer concentration (mol/L)	(C) Methanol concentration (*vol.* %)	(D) Solution pH
I	20	0.15	5	4.5
II	30	0.25	15	5.0
III	40	0.35	25	5.5

Table 5.3. 4-Parameter, 3-Level standard orthogonal fractional factorial design

Code of Parameters †	(A)	(B)	(C)	(D)	Experimental
Number of Experiment					Results ‡
1	I	I	I	I	t_1
2	I	II	II	II	t_2
3	I	III	III	III	t_3
4	II	I	II	III	t_4
5	II	II	III	I	t_5
6	II	III	I	II	t_6
7	III	I	III	II	t_7
8	III	II	I	III	t_8
9	III	III	II	I	t_9

† Preceding Table 5.2 gives the code of the parameters and the meaning of *A*, *B*, *C* and *D* designations.

‡ A comprehensive evaluation of the quality of the formed polymer coatings, including coating thickness and surface roughness distribution.

The obtained results can be used to calculate the optimum level of the operating parameters by calculating the relevant OFF averages with the equations below:

$$\overline{A_I} = \frac{t_1 + t_2 + t_3}{3} \tag{5.1}$$

$$\overline{A_{II}} = \frac{t_4 + t_5 + t_6}{3} \tag{5.2}$$

$$\overline{A_{III}} = \frac{t_7 + t_8 + t_9}{3} \tag{5.3}$$

$$\overline{B_I} = \frac{t_1 + t_4 + t_7}{3} \tag{5.4}$$

$$\overline{B_{II}} = \frac{t_2 + t_5 + t_8}{3} \tag{5.5}$$

$$\overline{B_{III}} = \frac{t_3 + t_6 + t_9}{3} \tag{5.6}$$

$$\overline{C_I} = \frac{t_1 + t_6 + t_8}{3} \tag{5.7}$$

$$\overline{C_{II}} = \frac{t_2 + t_4 + t_9}{3} \tag{5.8}$$

$$\overline{C_{III}} = \frac{t_3 + t_5 + t_7}{3} \tag{5.9}$$

$$\overline{D_I} = \frac{t_1 + t_5 + t_9}{3} \tag{5.10}$$

$$\overline{D_{II}} = \frac{t_2 + t_6 + t_7}{3} \tag{5.11}$$

$$\overline{D_{III}} = \frac{t_3 + t_4 + t_8}{3} \tag{5.12}$$

The maximum differences of the averages of the same fractional factors can also be calculated to reveal the relative importance of the various operating parameters

$$R_i = \overline{Max_i} - \overline{Min_i} \qquad \text{i = A, B, C and D} \qquad (5.13)$$

5.2.5. Post-Treatments of the Coated Samples

After the electropolymerization process, the coated samples were rinsed with deionized water and dried in vacuum (VWR 1410) for 24 hours to remove solvents and remaining monomer retained inside the coating. Thermal curing was done optionally at ~120°C for 30 minutes to complete the polymerization. The cured coating samples were compared with the uncured samples to assess the effects of thermal curing. The coated samples were weighed to estimate coating thickness and density.

5.2.6. Poly(2-Vinylpyridine) Formation by Bulk Polymerization

For comparative purposes, poly(2-vinylpyridine) was also formed at room temperature by bulk polymerization with 1 *wt* % benzoyl peroxide (Aldrich) as free radical initiator (Chohan et al., 1992). The polymer was precipitated by pouring the reaction solution into hexane (BDH). The crude polymer was then purified by dissolving in tetrahydrofuran (BDH) and precipitating again with hexane. The polymer was finally dried under vacuum at room temperature.

5.3. Polymer Characterization

5.3.1. Ultraviolet and Visible Spectroscopy

The ultraviolet and visible spectroscopic study was carried out with a Beckman® DU 600 Spectrophotometer in a wavelength range of 190 to 1100 nm. Coatings obtained before and after thermal curing were dissolved in methanol for the test. Although the solubility of the polymer coating in methanol was low, enough could be dissolved for purposes of the analysis. Pure methanol was used as the reference for the spectra. Monomer and polymer formed by bulk polymerization were also examined and their spectra were compared with that of the polymer coating obtained by electropolymerization.

5.3.2. FT-IR Spectroscopy

The FT-IR spectroscopic study was carried out with a Nicolet® 520 FT-IR Spectrometer in a wavelength range of 250 to 4000 cm^{-1}. The polymer coatings were removed from the metal substrates and mixed with pre-dried KBr powder to make small discs for the FT-IR test. Coated samples obtained before and after thermal treatment were examined to investigate the effects of thermal curing on the polymer coatings. The resulting spectra were compared with the standard poly(2-vinylpyridine) spectra available in the literature (Pouchert, 1981).

5.3.3. ^{1}H NMR Spectroscopy

The NMR spectroscopic study was carried out with a 250 MHz Bruker® NMR (Am-250, Bruker Spectrospin). The polymer coating was dissolved in dimethyl-$_{d6}$ sulfoxide (DMSO-$_{d6}$) to make up 10 ppm solutions for the ^{1}H NMR tests. The resulting spectra were compared with the standard poly(2-vinylpyridine) spectra in the literature (Pouchert and Behnke, 1993).

5.4. Polymer Coating Property Measurements

5.4.1. Chemical Composition Measurement

The chemical compositions (i.e., C, H and N ratio) of the polymer coatings were measured by isotope mass spectrometry (EA208 Carlo Erba® Elemental Analyzer). Polymer samples were removed from the metal substrates and combusted in He/O_2 at 1030°C, followed by separation with a Porapak® type Q GC column (Mesh 50-80). Peak heights of CO_2, N_2 and H_2O were measured and converted to C, N and H ratio. Coatings both before and after thermal curing were examined.

5.4.2. Glass Transition Temperature Measurement

The polymer coatings were removed from the metal substrate and analyzed using differential scanning calorimetry (DSC 2920, TA Instruments) to determine its glass transition temperature (T_g). The measurement was carried out in the temperature range of 25 to 125°C at a heating rate of 10°C/min. under the protection of helium. Indium metal was used for calibration.

5.4.3. Inorganic Impurity Measurement

Inorganic impurities, especially metal ions such as iron and manganese from metal substrates, were measured by a Direct Current Plasma spectrophotometer (ARL SS-7 DCP, Fisons®). Since the metal impurities might be in the form of inorganic ions or metal-organic complexes, the test was performed in both organic and aqueous media. For measurement in the organic system, the polymer was dissolved in DMSO and then diluted with DCP base oil (Spex® base oil 20). For the aqueous system measurement, the polymer was first dissolved in dimethyl formamide (DMF) and then dried in the air by solvent evaporation. The dry polymer sample was then dissolved in 5 N HCl solution for the DCP study. Any Fe^{3+} in the HCl was removed by passage through an ion exchange column packed with Amberlite IRA-400 (Dorfner, 1972).

5.4.4. Conductivity Measurement

The electronic conductivity of the poly(2-vinylpyridine) coating on the metal substrate was measured with a high precision Electrometer/Multimeter (Keithley 619) equipped with a four-point differential probe (Keithley 3000 series). The resistance measurement was made by moving the probes over the coating surface and reading the coating conductivity directly from the Electrometer.

5.4.5. Corrosion Resistance Measurement

The corrosion resistance of the coated metal samples was evaluated by polarization studies (Walter, 1986b). A coated sample was immersed in a test solution (3% NaCl solution) for 3 hours under ambient conditions. A polarization curve was then

obtained by polarizing the coated sample from the open-circuit potential (E_{ocp}) in the cathodic direction and then in the anodic direction. The resulting voltammogram was then compared with the voltammogram of a bare metal sample. The improvement of the corrosion resistance of the sample was determined by the change of the corrosion current and corrosion potential (Fowkes et al., 1981; Funke, 1987).

5.4.6. Adhesion Measurement

The adhesion characteristics of the polymer coating were investigated using a cross hatching technique (ASTM, 1993). The surface of a coated metal sample was scored several times in parallel directions on the surface with a sharp knife and then scored similarly on the surface perpendicularly to the previous scoring lines. A PVC tape was pressed on the scratched coating surface and pulled off to qualitatively evaluate the strength of adhesion.

5.4.7. Porosity Measurement

The compactness of the polymer coating was evaluated by a copper cementation technique used by De Bruyne et al. (1995). A coated sample was first immersed in a 0.1M $CuSO_4$ (BDH) solution for 30 seconds to allow copper to cement out on any uncoated portion of the mild steel substrate. Since the cemented copper has a much stronger contrast than the polymer coating, quantitative image analysis can be done to evaluate the ratio of the area of the copper deposit to that of the polymer coating over the surface.

5.4.8. Coating Weight Increase and Coating Density Estimation

The mass of the polymer coating formed was measured by comparing the sample weight before and after the electropolymerization. Good sensitivity was possible since the accuracy of the sample weight was on the order of 0.1 mg, while the masses of the polymer coatings and metal samples were about 10 mg and 10 g, respectively. The polymer coating mass was combined with the coating thickness measured by CSLM to determine its density.

5.5. Coating Morphology Analysis

Analysis of coating morphology including coating roughness distribution, coating uniformity and coating thickness is a very important factor in evaluating coating quality. Confocal scanning laser microscopy (CSLM) was applied in this project for this purpose. A Model-325P UNIPHASE® He-Ne Laser (1 mW, with wavelength of 632.8 nm) was employed as the illumination for surface scanning. The optical diagram, experimental apparatus and detailed operating parameters have been published elsewhere (Dixon et al., 1991a and 1991b, Ling et al., 1995). The surface scan of the coating was carried out over surface areas from 200 × 200 μm to 4 × 4 mm. The corresponding resolutions vary from 0.4 to 7 μm, respectively.

The whole procedure was continually observed on a monitor during a scanning process. It involved first focusing the laser beam just above the coating surface so that no distinct image of any part of the surface appeared on the monitor. Then the focus of the laser beam was slowly lowered onto the surface and the locations of the points on the surface of the

focal plane were observed. Eventually, the laser beam passed through the entire surface slice by slice and focused within the bulk of the coating so that all the distinctive images disappeared from the monitor. The intensity of the reflected images at each surface location was automatically measured throughout this scanning process by an on-line computer system. The number of images taken and the depth over which the laser beam was focused were predetermined and set according to the roughness and thickness of the coating. By combining the entire set of intensity images, a map of the maximum intensities across the whole surface was obtained. A quantitative measure of the coating surface roughness was made by combining this map with further image processing.

Because the poly(2-vinylpyridine) coating is not completely opaque, the laser beam could penetrate the entire coating and focus on the surface of the metal substrate. Following the same procedure as described above, a maximum intensity image of the metal substrate was obtained without interference from the adhering coating layer. From these maximum intensity images and the corresponding depths, it was possible to obtain surface depth profiles and to reconstruct 3-D topographic images of the scanned surfaces, which have the advantage of providing a better stereoscopic expression of the particular surfaces.

Since the reflected light only has high intensity at the air/coating and coating/substrate interfaces and essentially zero intensity within the voids, coating and substrate, a profile of the coating thickness along a line could be obtained by performing a cross-sectioning scan of the laser beam over the line. This method gave direct visualization of the thickness and uniformity of the coating. The coating thickness at any given point or the average value over a particular distance could be determined by measuring the light intensity as a function of depth into the sample at the given location. By repeating this process at a number of points along the line, the

variation of thickness along the line could be determined. This allowed flaws in the coating as small as the image resolution to be detected. Flaws as small as this are difficult to detect with a standard microscope.

By applying the double reflection and transmission characteristics of the modified CSLM and scanning over a relatively large surface area, information on the surface roughness distribution over the entire surface could be obtained over a wide range of areas. The largest surface area scanned in this project was 4 mm × 4 mm.

5.6. Process Mechanism Studies

5.6.1. Inhibition Study

The radical inhibitors *p*-benzoquinone and 2,2-diphenyl-1-picrylhydrazyl (DPPH) were used to determine whether electropolymerization of 2-vinylpyridine occurs by a free-radical mechanism. Very low concentrations of the inhibitors were added (10^{-3} M) for the tests. The inhibitors were dissolved in the electrolyte before the electrolysis, while the other operating conditions remained unchanged as before for a typical coating formation process (i.e., 0.25 M 2-vinylpyridine in 20% methanol aqueous solution with 0.05 M NH_4ClO_4 as supporting electrolyte and solution pH of 4.8, adjusted with $HClO_4$). The weight change of the working electrode before and after the electropolymerization was recorded and compared with that from a similar electrolysis process without inhibitors. The electrolysis current change during the electrolysis was recorded and compared with that obtained without inhibitors.

5.6.2. Surface Enhanced Raman Scattering Spectroscopy Study

Raman spectra were obtained with a Ramascope 1000 (Renishaw) system. A Melles Griot He-Ne laser (17 mW, with wavelength of 362.8 nm) equipped with a holographic notch filter was employed as the source of illumination. A computer (Pentium 167, JPC) was used to record spectral data. To study the protonation of 2-vinylpyridine molecules in aqueous solutions of different solution pH without electrolysis, ordinary Raman scattering spectroscopy was used. The Raman spectrum of neat 2-vinylpyridine monomer was also obtained for comparison. The adsorption of 2-vinylpyridine species on a copper electrode surface was studied by surface enhanced Raman scattering (SERS) spectroscopy. SERS was also applied to study the adsorption of 2-vinylpyridine species on the copper electrode surface *in situ* during electropolymerization at different electrode potentials. To achieve optimum SERS spectra, 3-mm diameter pure copper (>99.99) disks were used as the working electrode. The copper electrode was *ex situ* electrochemically roughened by applying several oxidation-reduction cycles between −1.0 and 1.0 V at 30 mV/s in 0.1 M KCl solution before use (Brandt, 1985; Beer et al., 1989). The cathodic compartment and anodic compartment of the electrolytic cell were separated by a sintered glass membrane. Details of the electrolytic cell are given in the relevant literature (Brolo et al., 1997). The electropolymerization process in these experiments was carried out potentiostatically. Nitrogen gas was used to purge the dissolved oxygen from the electrolyte in the cathodic compartment prior to the electrolysis and was continuously sparged throughout the process.

5.6.3. Extended Voltammetry Study

This extended voltammetry study of the process mechanism was carried out with a polymer modified electrode. The electrode was a mild steel coupon pre-coated with poly(2-vinylpyridine) using the electropolymerization process described before. This pre-coated electrode increased the hydrogen overpotential remarkably and thereby allowed the voltammetric scan to be extended to a much more negative potential. Concurrently, the electrolysis current was suppressed significantly by the presence of the high resistance polymer coating. Many unique characteristics of the electrolytic system can be observed by using such modified electrodes (Murray 1984a and 1984b). Other operating parameters were similar to other in the ordinary voltammetry studies described in the previous section. To provide insight into the mechanism of coating formation, electrolysis of the pre-coated electrode was also conducted in an electrolyte containing dissolved poly(2-vinylpyridine), pre-formed by bulk polymerization process without any monomer present.

5.7. Other Studies

5.7.1. Poly(2-Vinylpyridine) Coating Formation on Various Substrates

After the studies of poly(2-vinylpyridine) coating formation on mild steel substrates, other materials were applied for the coating formation. The substrates included aluminum, brass, copper, graphite, lead, stainless steel and zinc. The operating parameters were kept unchanged. The results were compared to those obtained with a mild steel substrate to determine the effects of the nature of the substrates on poly(2-vinylpyridine) coating formation by electropolymerization.

5.7.2. Polymer Coating Formation from Different Monomers

Other monomers were also employed to form polymer coatings on various substrates via electropolymerization. The studies still focused on ERP processes in aqueous systems. The monomers to be examined, together with their *Q-e* values (Greenley, 1984), monomer *p*Ka values (Perrin, 1965) and relevant references, are listed in Table 5.4. An important purpose of this part of the experiments was to generalize the conclusions from the process mechanism study concerned with poly(2-vinylpyridine) coatings.

Table 5.4. Monomers for polymer coating formation by electropolymerization (from Greenley, 1984 and Perrin, 1965).

Type of monomer	*Q* value	*e* value	*p*Ka value of monomer	Reference
2-Vinylpyridine	1.41	–0.42	4.92	Sekine et al., 1992; De Bruyne et al., 1995
4-Vinylpyridine	2.47	0.84	5.62	Bhadani and Parravano, 1970; Sekine et al., 1992
1-Vinylimidazole	0.11	–0.68	7.5	Sekine et al., 1992
Acrylonitrile	0.48	1.23	—	Sekine et al., 1992; Teng et al., 1977
Methacrylonitrile	0.86	0.68	—	Mengoli et al., 1991
Methyl methacrylate	0.78	0.40	—	Shelepin and Fedorova, 1964; Pistoia and Voso, 1976
Acrylamide	0.23	0.54	—	Sobiesky and Zerner, 1969
Aniline	—	—	4.6	Venugopal et al., 1995

CHAPTER 6

RESULTS AND DISCUSSION — PART ONE: ELECTROPOLYMERIZATION COATING FORMATION

Although it has been reported that some unsaturated compounds can self-initiate and form polymer coatings on mild steel substrates in acidic media (Pistoia et al., 1976; Mengoli et al., 1979a, 1979b and 1991, Zhang and Bell, 1997), this does not occur in the case of 2-vinylpyridine polymerization. Preliminary experiments were carried out by immersing various metal (including mild steel) samples in the 2-vinylpyridine electrolytes for various time periods (from 0.5 to 48 hours) with no current flow. No polymer coating was found to form on the substrates. The mild steel samples were oxidized in the acidic solution which resulted in the formation of some black oxides on the surfaces. It is concluded that current flow through the cell is necessary to initiate the 2-vinylpyridine polymerization.

6.1. Electrolyte Preparation

When the electrolytes are first mixed, i.e., 0.05 M NH_4ClO_4 in 10% methanol aqueous solution, the solution pH is ~5.5. When the desired amount of 2-vinylpyridine monomer is added to the above electrolyte, the solution pH increases to ~7.5 due to its weakly basic monomer. The electrolyte appears clear and no noticeable heat generation is

observed during the above mixing. Solution agitation is necessary for the monomer to dissolve.

6.2. Linear Sweep Voltammetry Studies

Preliminary voltammetric experiments were carried out in the potential range of 3.0 to –3.0 V with various potential scan rates. The voltammograms showed that oxygen evolution is the only anodic reaction in the system. Since this project focused on electroreduction reaction at cathode surfaces, the following discussion of the voltammetry results is confined to the cathodic portion of the voltammogram.

When no 2-vinylpyridine monomer is added to the electrolyte (i.e., only 0.05 M NH_4ClO_4 in 10% methanol aqueous solution), the electrolyte begins to dissociate cathodically at about –0.40 V. Considerable hydrogen evolution is observed at the mild steel cathode. This voltammogram is shown in Fig. 6.1a. When 0.25 M 2-vinylpyridine is added to the above electrolyte, hydrogen evolution is still very prominent and the voltammogram shows no reduction wave of 2-vinylpyridine. However, when the solution pH is decreased from the original 7.5 to ~5 (with concentrated $HClO_4$), hydrogen evolution is found to be delayed and suppressed significantly (Fig. 6.1b). A distinct reduction wave is observed before the onset of the large current rise due to hydrogen evolution. The $E_{1/2}$ of this new wave is about –1.0 V.

After a linear potential scan between –0.7 and –2.5 V at 30 mV/s, some white or light yellow solids are observed on the cathode surface. When the voltammetry scan is

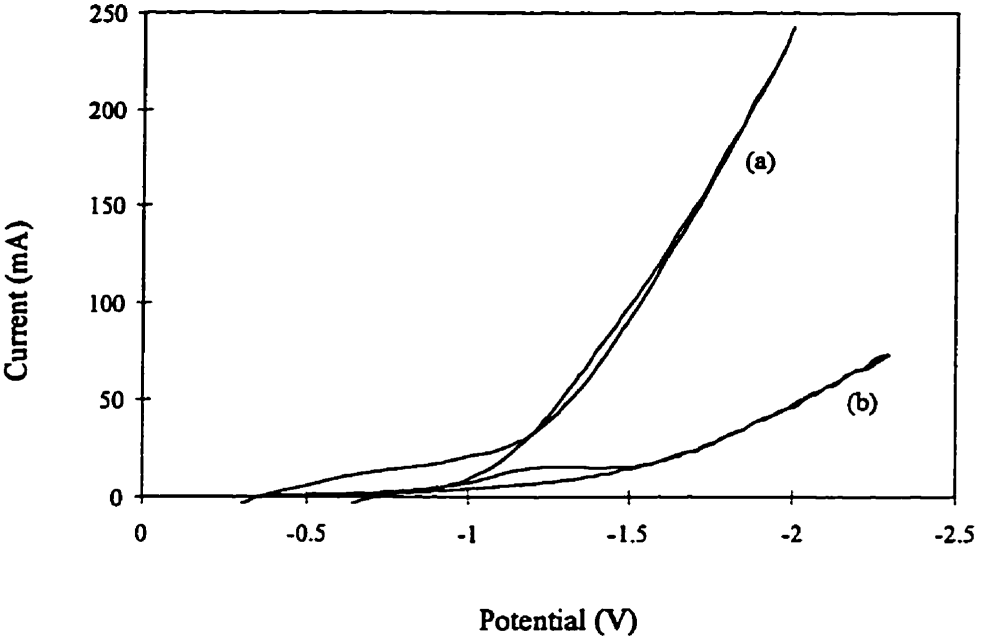

Fig. 6.1. Typical voltammograms of 0.05 M NH_4ClO_4 in 10% methanol aqueous solution. (a) Without 2-vinylpyridine and solution pH = 7.5. (b) With 0.25 M 2-vinylpyridine and solution pH = 4.8; Potential scan rate = 30 mV/s.

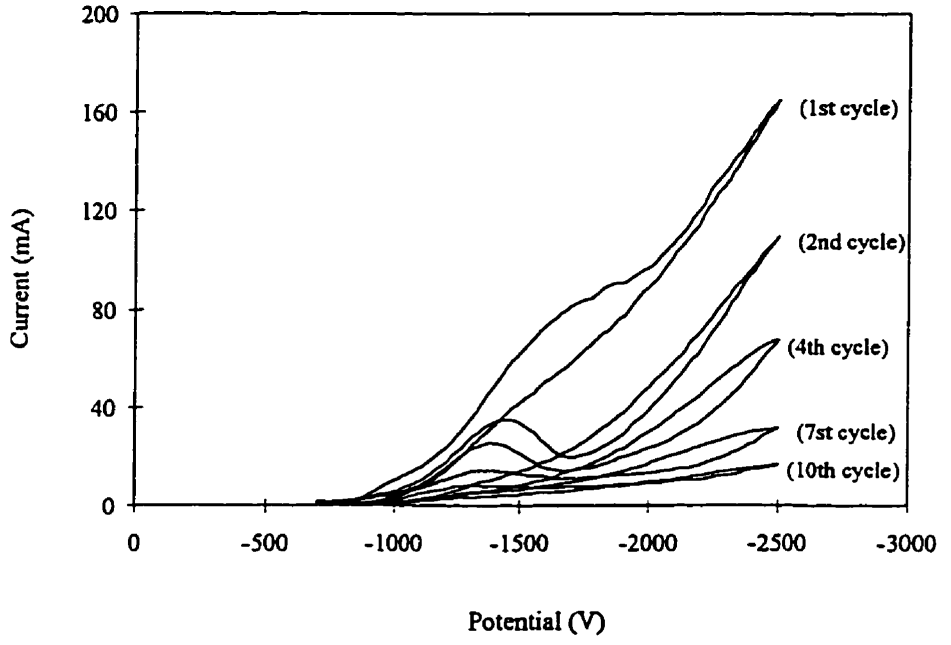

Fig. 6.2. The decrease of the electrolysis current in a cyclic voltammetric electrolysis of 2-vinylpyridine electrolyte. The operating conditions are the same as those in Fig. 6.1b.

carried out repeatedly, the current response of the process is found to decrease rapidly, Within 10 cycles, the current has dropped to about 10% of its initial value, indicating that some highly resistant film has formed on the electrode surface (Fig. 6.2).

The experimental results indicate that 2-vinylpyridine can be reduced at the cathode prior to hydrogen reduction at the appropriate pH. An organic deposit forms on the cathodic surface very rapidly after the reduction of the monomer. The deposit appears to have low conductivity and causes a dramatic decrease in electrolytic current. It also displays a high hydrogen overpotential and therefore delays and suppresses the hydrogen evolution on the cathode surface. Solution pH is found to have a marked effect on the process. This suggests that the formation of the organic deposit on the cathodic surface occurs as the consequence of monomer reduction rather than hydrogen reduction, which has often been proposed as the initiation step of certain electropolymerization processes (Shapoval and Gorodyskii, 1973; Subramanian and Jakubowski, 1978; MacCallum and MacKerron, 1982; Iroh et al., 1991; Iroh et al., 1993a and 1993b). More evidence for this suggestion will be given later in the discussion of the impact of electrolyte pH on the electropolymerization. A detailed discussion of the process mechanism will be given in Chapter 10.

6.3. Coating Formation Using Various Electrochemical Methods

6.3.1. Chronoamperometric Electrolysis

In this technique, the electrode potential of the working electrode is kept at a fixed value during electropolymerization. Operating conditions for the chronoamperometric

electrolysis (e.g., the constant cathodic potential for the electrolysis) are based on the findings from the above voltammetry studies. A typical chronoamperometric electrolysis is carried out at a constant potential of −1.3 V for 2 hours. Coating formation can be observed during the electrolysis by the gradual change in colour of the electrode surface from silver-gray to yellow. Hydrogen bubbles are formed on the cathode surface during the electrolysis. The hydrogen bubbles form evenly over the electrode surface, which then expand and coalesce and finally detach from the electrode surface. The films are found to contain some small craters with dimensions from a few micrometers to 1 millimeter (Fig. 6.3). These craters are the result of hydrogen bubbles on the electrode surfaces during the coating formation. However, the coating images from CSLM (Fig. 6.3) show that the bases of these crates do not extend to the metal substrate. The colour of the electrolyte slowly changes during the electrolysis from clear to light yellow.

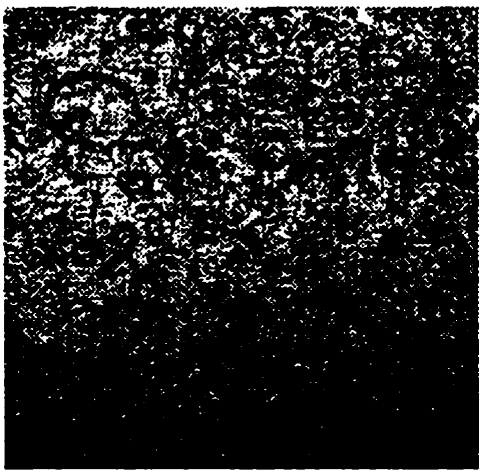

Fig. 6.3. Coating surface morphology from CSLM in a 4 mm × 4 mm scanning area, after a two-hour chronoamperometric electrolysis at −1.3 V. The electrolyte is 0.25 M 2-vinylpyridine in 10% methanol aqueous solution with 0.05 M NH_4ClO_4 as supporting electrolyte at a solution pH of 4.8, adjusted with $HClO_4$.

It is also found that the electrolysis current drops abruptly after the onset of the electrolysis. In about 5 minutes, the electrolysis current drops to about 10% of the initial current (Fig. 6.4a). However, when electrolysis is carried out at the same potential in the electrolyte without the monomer, no current drop is observed (Fig. 6.4b). The relevant current signal is noisy due to the evolution of hydrogen bubbles. This is identical to the results in the voltammetry studies and supports the earlier conclusion that the current drop is the result of the formation of a highly resistant coating on the electrode surface.

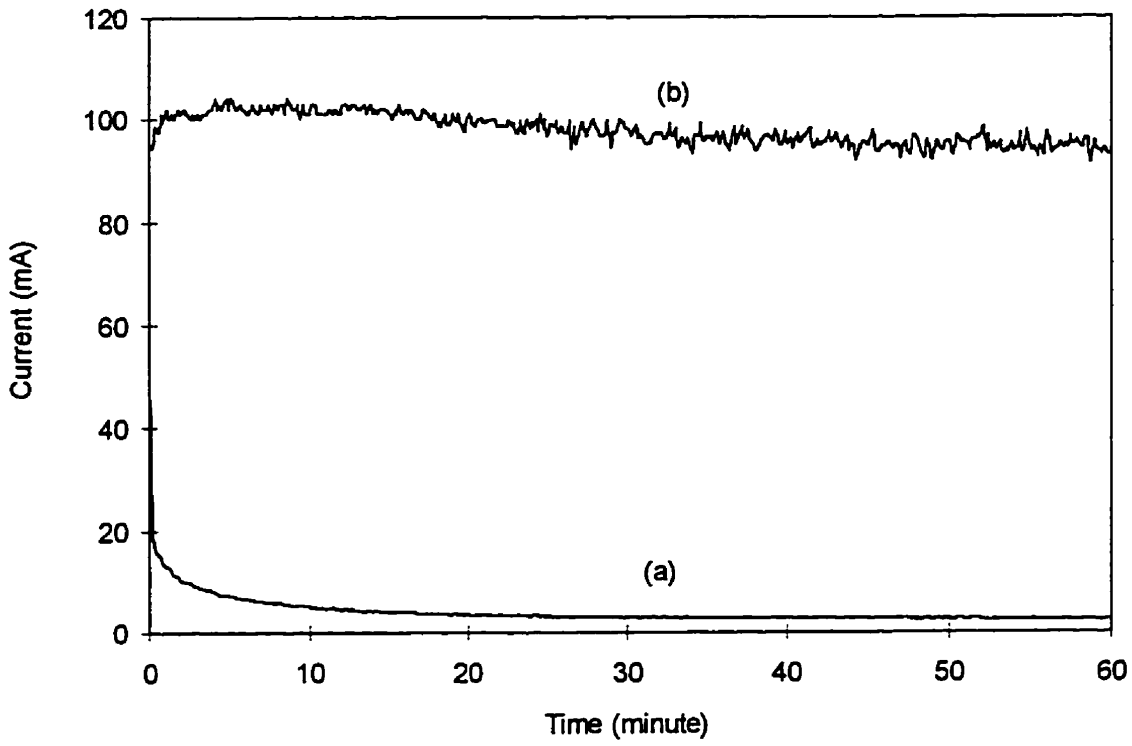

Fig. 6.4. Current *vs.* time diagram during chronoamperometric electrolysis at a constant cathodic potential of −1.3 V, with solution of a) 0.25 M 2-vinylpyridine and b) no monomer present. The other operating conditions are the same as described in Fig. 6.3.

Although the current drops rapidly after the onset of the electrolysis, it does not fall to zero. Instead, it reaches a relatively steady value in about 15 minutes and maintains

that value for the rest of the process. During this steady current period, the polymerization process continues at the electrode surface. This is indicated from the change of colour of the coating and the increase in sample weight. The reason for this steady current is not completely clear yet. It may be the consequence of several reduction reactions in the system. For example, it may be partially due to hydrogen reduction during the electrolysis. It may be caused by the fact that the formed coating is somewhat porous due to the nature of the coating or due to the hydrogen evolution during the coating formation. The growing polymer coating may be a solvent-swollen ionically conducting gel, that may allow rather easy transport of hydrogen ions, monomers and oligomers, and thus permit electron transfer leading to hydrogen evolution and electropolymerization at the metal/coating interface (Mengoli and Musiani, 1994; Liang et al., 1993; Lee and Bell, 1995a and 1995b). More discussion about this phenomenon will be provided later when the process mechanism is proposed.

Different values of cathodic potentials were used for the chronoamperometric electrolysis. If the cathodic potential is too negative (≤ -1.5 V), excessive hydrogen evolution occurs. This disrupts film formation, leading to a thin and irregular coating with small clumps over the electrode surface. As expected, less hydrogen is generated at less negative cathodic potentials, but the formed coatings are extremely thin. When the electrolysis is carried out at an electrode potential less negative than -1.0 V, no visible coating forms on the electrode surface after two hours of electrolysis. However, the electrolysis current also decreases quickly after the onset of the electrolysis. The substrate looks purple and blue. When the working electrode potential is less negative than -0.8 V, the electrolysis current remains at a lower but constant level during the course of

electrolysis. The current response of the process looks similar to that in Fig. 6.4b. After two hours of electrolysis at such a electrode potential (< –0.8 V), no change can be observed on the substrate. The current appears to be due primarily to hydrogen reduction. It appears that a condition may exist which promotes the first mono-molecular layer of polymer molecules to form and be adsorbed on the electrode surface which significantly alters the electrochemical properties of the electrodes. This explanation is consistent with the principle of polymer-modified electrodes (Murray, 1984a and 1984b; Diaz, 1991). In our case, this first adsorbed monomolecular layer increases the electrical resistance and hydrogen overpotential of the working electrode. It is known that when the working electrode potential is slightly less negative than the $E_{1/2}$, the monomer reduction reaction can still occur but at a much slower rate. However, when the working electrode potential is significantly more positive than the $E_{1/2}$, no monomer reduction would occur. This may explain why the polymer film can still form on the substrate at a working electrode potential between –1.0 V and –0.8 V although the polymer film formed may be only a mono-molecular layer, while no polymer film forms on the electrode surface when the potential is above –0.8 V. This also supports the earlier conclusion that the polymerization is initiated by formation of monomer radicals rather than hydrogen radicals.

6.3.2. Modified Chronoamperometric Electrolysis

Various attempts were made to minimize the hydrogen evolution and improve the coating quality during chronoamperometric electrolysis. These included varying the extent of solution agitation and mechanically removing the gas bubbles from the electrode surface

during electrolysis. No significant improvement is found in either case. Although polishing the coupon very smoothly with alumina (0.05 micron, Grinder-Polisher Motopol 8) prior to electrolysis reduces the extent of hydrogen evolution, it also causes the polymer coating to be poorly adherent to the substrate. Considering the difficulties of applying this method to large and complex-shaped substrates, no further effort was made in this direction.

An interesting idea of applying a *varying-potential chronoamperometric electrolysis* to restrict hydrogen evolution and increase the coating thickness emerged from the practice of ordinary chronoamperometric electrolysis. The ordinary chronoamperometric electrolysis was modified by first applying a constant cathodic potential (e.g., −1.3 V) for a certain time and then gradually decreasing the potential to a lower value (e.g., −0.7 V) over a certain period. During the first (more negative potential) stage, a large amount of coating formed on the electrode surface. However, due to the intense hydrogen evolution, the coating is non-uniform. During the second stage when the potential is gradually reduced, the evolution of hydrogen subsides significantly and the coating formation process, although reduced as well, appears to occur primarily on the thinner recesses within the craters. Consequently, the craters are filled by the polymer, thereby making the coating more uniform. The potential waveform and the resulting current response are shown in Fig. 6.5. Some CSLM images of coated samples formed by the above improved chronoamperometric electrolysis are shown in Fig. 6.6. Some results of this section have recently been published (Ling et al., 1998a).

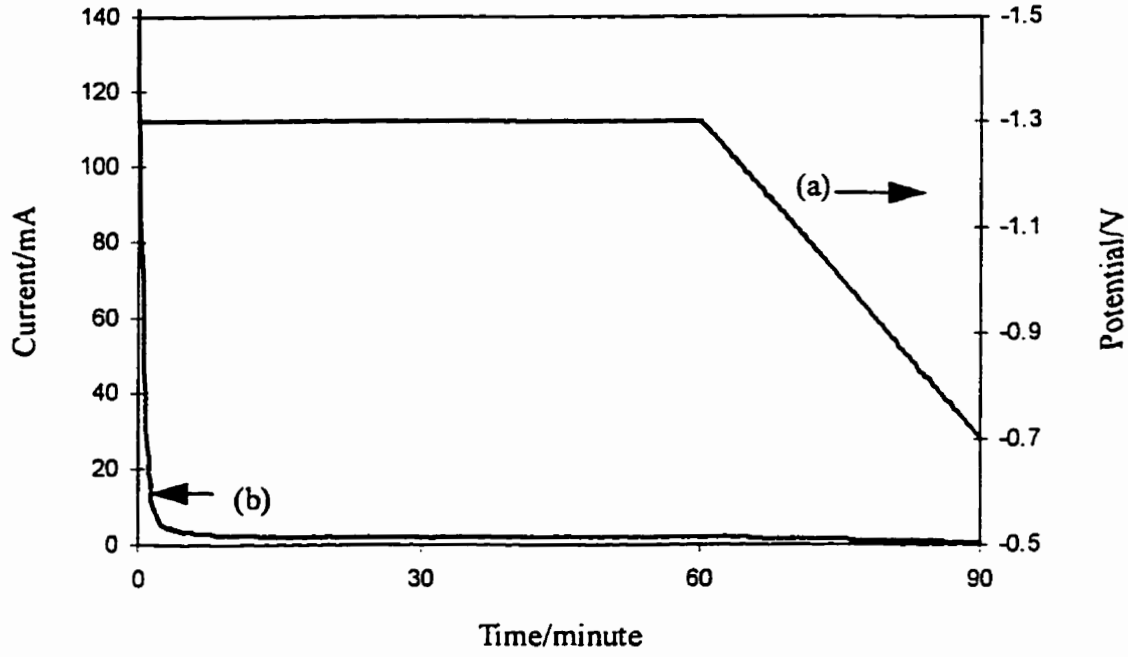

Fig. 6.5. The potential waveform *vs.* time (a) and resulting current response *vs.* time (b) diagram from a modified chronoamperometric electrolytic process. The electrolyte and other experimental conditions are the same as those in Fig. 6.3.

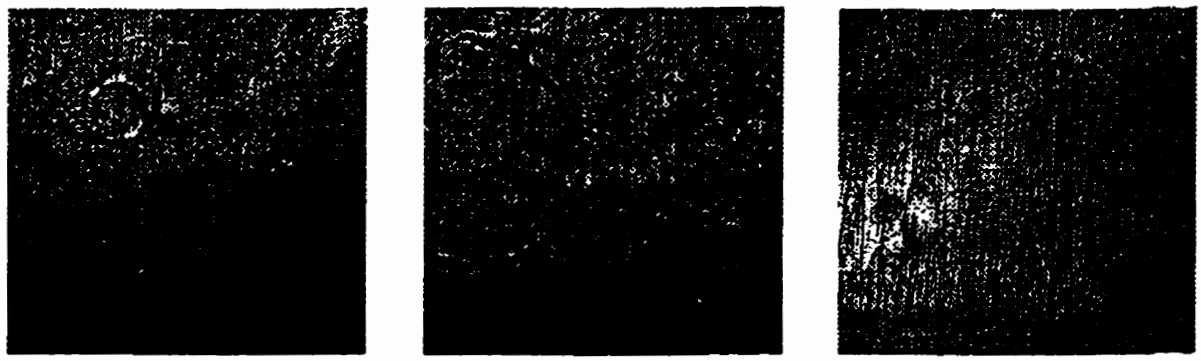

(a) (b) (c)

Fig. 6.6. The morphologies of coatings produced by the electrolytic process described in Fig. 6.5. CSLM images of partially filled pits at different magnification: (a) 4 mm × 4 mm, (b) 1 mm × 1 mm and (c) 200 μm × 200 μm.

6.3.3. Galvanostatic Electrolysis

Attempts to use galvanostatic electrolysis as an effective method for electropolymerization coating formation met with little success. The electrolysis was carried out at 10 to 100 mA/cm^2 for 10 minutes to 2 hours. The primary problem associated with this method is the difficulty in choosing a suitable constant current for the electrolysis. This information should be obtainable from a voltammetry study of the system. However, since the current decreases dramatically during the process due to the high resistance of the coating formed, it is impracticable to choose one value suitable for the whole electrolysis process. A high current causes intense hydrogen evolution, while a low current leads to very little coating formation. As the coating resistance increases rapidly along with the formation of the polymer films in a galvanostatic process, the electrode potentials increase rapidly as well. This leads to a very intense hydrogen evolution on the electrode surface. Such a phenomenon has been reported in the other electropolymerization processes carried out via galvanostatic electrolysis (Everson and Helms, 1991; Liang et al., 1993a and 1993b). The ineffectiveness of this method for electropolymerization coating formation is not unexpected. In an electropolymerization process, the electron transfer process is mostly involved in the initiation (or radical generation) step and so the current is not an essential critical factor in the process unless radical generation is rate limiting. On the other hand, an appropriate electrode potential is more important for the electrolysis process in order to control electrode processes and prevent side reactions. Therefore, the potentiostatic technique is preferred to the galvanostatic technique. Similar results have been concluded for other electropolymerization systems (Ohno et al., 1990; Mengoli and Musiani, 1994)

6.3.4. Constant Cell-Potential Electrolysis

This method differs from chronoamperometry in that the cell potential rather than the working electrode potential is kept constant during electrolysis. However, the use of constant cell-potential technique was also found to be unsuccessful in our study. The electrolysis was carried out at constant cell-potential of 3 to 10 V for 10 minutes to 2 hours. The basic problem in applying this technique is that the working electrode potential floats during the electrolysis, while the cell-potential is kept constant using a power supply (Hewlett Packard 6263B DC Power Supply). This is due to the dramatic increase in system resistance as the coating forms. The lack of control of the working electrode potential causes difficulty in controlling coating formation and leads to non-reproducible results. Sometimes some film can be forming, while at other cases only intense hydrogen evolution is observed. In addition, when applying this method for electropolymerization research, no fundamental information related to the electrode process is available and thus this technique is not useful for exploratory research. A potentiostatic method such as chronoamperometry is more effective since the working electrode potential is always kept controlled by the potentiostat and the current response is always being monitored. When the current changes, it is the counter electrode potential that floats in order to maintain the working electrode potential at the desired value (Bard and Faulkner, 1980).

6.3.5. Cyclic Potential Sweep (CPS) Electrolysis

6.3.5.1. Characteristics of CPS Electrolysis

CPS electrolysis is the extension of linear sweep voltammetry. It involves the application of repeated cathodic or anodic potential scans during electrolysis. The cathodic potential sweep range used in this study was normally between –0.7 and –2.5 V with a scan rate of 30 mV/s. The current *vs.* time (i~t) diagram of such a CPS process is shown in Fig. 6.7. During a CPS electrolysis it is found that the first current peak is very high and subsequent peaks shrink rapidly thereafter. The second current peak is usually 1/5 or 1/10 of the height of the first peak. After about three or four potential sweeps, the current peak height reaches a relatively constant value and remains at that approximate value through the rest of the process. This result is similar to the previous finding from the chronoamperometric study. The I-t diagram of a CPS process is composed of a series of repeating voltammograms. They provide important information about the system during the electrolysis, such as changes in the shapes of the voltammograms. From the enlarged partial I-t diagram (Fig. 6.8), it is clear that the current drops rapidly at the beginning of electrolysis (Fig. 6.8a) and reaches a relative steady condition where the system gives a similar response from one cycle period to the next (Fig. 6.8b). It also shows how the shapes of the voltammograms change gradually during this relative steady process (Fig. 6.8c). Thick and uniform coatings are formed by CPS electrolysis, and a coating image is shown in Fig. 6.9.

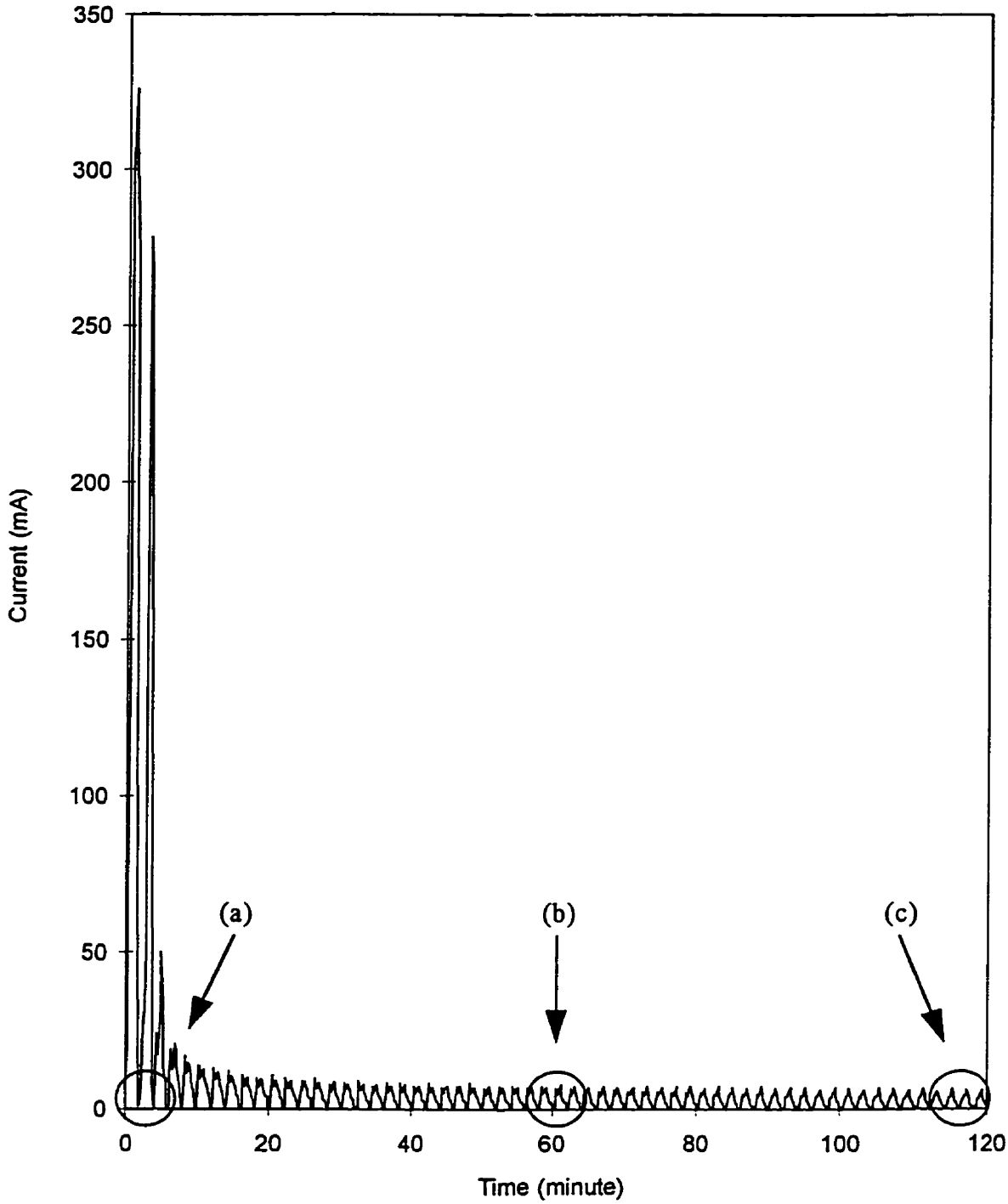

Fig. 6.7. A typical I-t diagram of a CPS electrolysis. The cathodic potential sweep range is between –0.7 and –2.5 V and the scan rate is 30 mV/s. The electrolyte and other experimental conditions are the same as those described in Fig. 6.3. (a), (b) and (c) are the three parts enlarged and shown in Fig. 6.8.

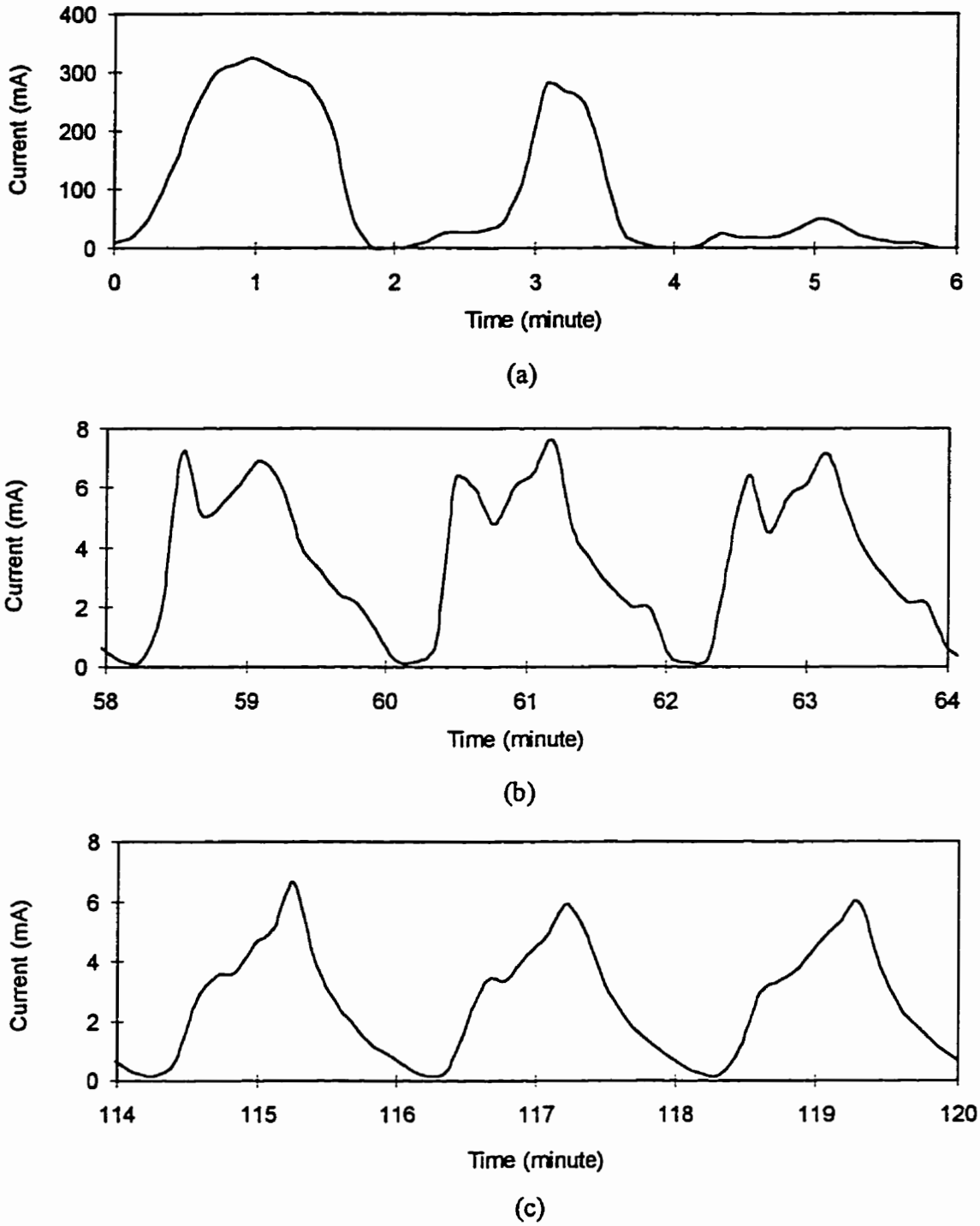

Fig. 6.8. The enlarged partial I-t diagram of the CPS process shown in Fig. 6.7. (a), (b) and (c) are from the beginning, the middle and the end of the I-t diagram, respectively.

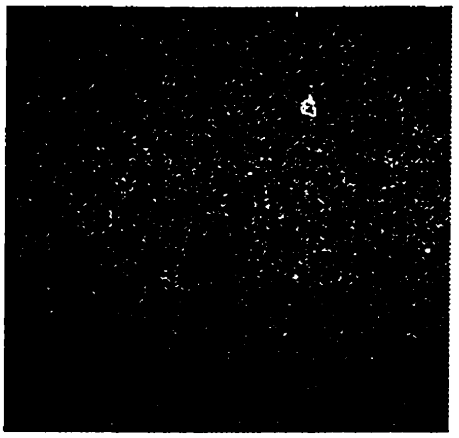

Fig. 6.9. Coating surface morphology from CSLM in a 1 mm × 1 mm scanning area, after a two-hour CPS electrolysis between –0.7 and –2.5 V at a scan rate of 30 mV/s. The other experimental conditions are described in Fig. 6.7.

A brief comparison of the results obtained using the different electrochemical techniques is summarized in Table 6.1. It is found that CPS produces the best quality coatings, i.e., the most uniform coatings with various thickness, and therefore, is the most suitable technique for electropolymerization of 2-vinylpyridine. With the application of a potential sweep during electrolysis, the working electrode potential is never maintained at a highly negative value for a long time. Therefore, initiator is not being generated throughout the entire process as will likely happen during chronoamperometry. Once the working electrode is held at a highly negative potential for a short period to generate enough initiators, it is changed to a value close to the system open circuit potential (E_{opc}) where no current passes through the electrodes and no electrode reaction occurs. During this period, the generated initiator species have the time to combine with the monomer molecules and propagate polymer chains. By reducing the time that the working electrode is at a very cathodic potential, hydrogen evolution and the formation of craters are kept to a minimum.

Table 6.1. Summary of different electrochemical techniques for coating formation.

Different electrochemical techniques	Result
Chronoamperometry (or Potentiostatic)	Intense hydrogen evolution (at high potential) or thin coating (at low potential)
Improved Chronoamperometry	The hydrogen pits in the coating are refilled to a certain degree, and uniform coating formed
Galvanostatic	Difficulties in choosing a proper constant current. Intense hydrogen evolution and no coating generation
Constant Cell-Potential	Floating electrode potentials and poor experimental reproducibility
Cyclic Potential Sweep	Thick and uniform coating formed

6.3.5.2. The Effect of the Potential Range of a CPS Electrolysis

The effect of the range of the working electrode potential during a CPS electrolysis has been studied by adjusting one limit while keeping the other limit constant. The other operating parameters are kept constant, as mentioned previously. The resulting I-t diagrams for these experiments are shown in Figs. 6.10 and 6.11. The experimental results and some simple descriptions are summarized in Tables 6.2 and 6.3.

When the potential sweeps are performed between –0.7 and –2.5 V (Fig. 6.10a), thick and uniform coatings are formed on the substrates. When the cathodic limit is increased to –2.2 V, a similar quality of coatings is obtained. The only difference between these two processes can be observed from the I-t diagrams (Fig. 6.10b). During the potential sweep between –0.7 and –2.2 V (Fig. 6.10b), the current of the process drops rapidly after the first cycle of potential sweep. In the case of the sweep from –0.7 V to

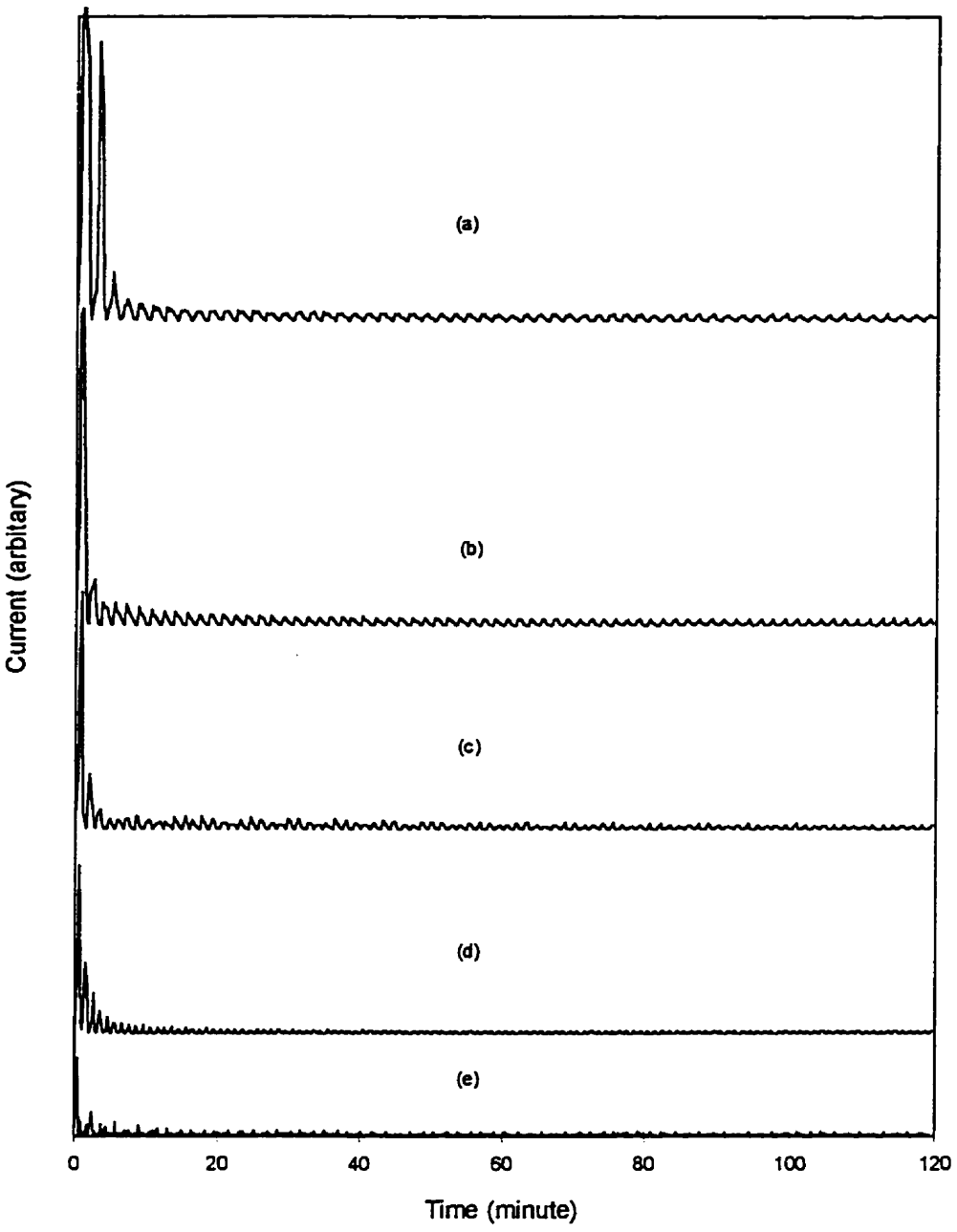

Fig. 6.10. The effect of the range of the working electrode potential during CPS electrolysis on the electropolymerization I-t diagrams. The explanation legend (a) to (e) is given in Table 6.2.

Table 6.2. Effect of the range of the working electrode potential of CPS electrolysis on coating formation. The other experimental conditions are the same as those described in Fig. 6.7. The relevant I-t diagrams are shown in Fig. 6.10.

Legend in Fig. 6.10	Anodic limit (V)	Cathodic limit (V)	Coating weight (mg)	Result
(a)	−0.7	−2.5	5.6	Thick and uniform coating
(b)	−0.7	−2.2	5.7	Thick and uniform coating
(c)	−0.7	−1.9	3.3	Thin and non-uniform film
(d)	−0.7	−1.6	1.6	Very thin and irregular film
(e)	−0.7	−1.3	0.3	No visible coating formed

−2.5 V (Fig. 6.10a), the current remains high after the first few cycles of potential sweep. A possible explanation is that hydrogen evolution is more intense in the case of the more negative cathodic limit. Consequently, it would take a longer time for the coating to build up to a point where its resistance begins to slow down the process. It is also worth noting that the amount of coating ultimately formed in the above two cases is virtually identical.

When the cathodic limit is increased further, the coating formation process is affected adversely. Hydrogen evolution becomes more intense and the coating formed become thin and non-uniform. Eventually, no visible coating can be observed when the cathodic limit reaches −1.3 V. From the I-t diagrams (Figs. 6.10c to 6.10e), it is observed that the current decrease with time becomes more gradual as the cathodic limit rises. This again suggests H_2 evolution becomes increasingly important at the same time.

For the experiments in which the cathodic limit is fixed at −2.2 V while the anodic limit varies, it is found that good quality coatings form when the anodic limit is ≥ −1.0 V. The corresponding I-t diagrams (Figs. 6.11c and 6.11d) show a rapid drop in the system

current and are quite similar to Fig. 6.10b, which also corresponds to a good coating. When the anodic limit is too negative (< −1.0 V), poor coatings are formed. The coatings are not only thin and non-uniform, but also porous and poorly adherent to the substrates. The I-t curves (Figs. 6.11a and 6.11b) show abnormal shapes. At the beginning of the processes, the currents decrease slowly due to the improper range of the potential sweep, indicating that the amount and quality of coatings being formed on the electrode surfaces are lower. After about 30 minutes of electrolysis, the currents start to increase quickly, indicating that the rates of coating formation are lower than that of coating detachment due to the effect of hydrogen evolution and/or coating dissolution. Hydrogen evolution at the cathode becomes very strong, leading to porous and poorly adhering coatings.

Table 6.3. Effect of the range of the working electrode potential of CPS electrolysis on coating formation. The other experimental conditions are the same as those described in Table 6.2. The relevant I-t diagrams are shown in Fig. 6.11.

Legend in Fig. 6.11	**Anodic limit (V)**	**Cathodic limit (V)**	**Coating weight (mg)**	**Result**
(a)	−1.6	−2.2	1.7	Thin and irregular coating, porous and poorly adherent to the substrate
(b)	−1.3	−2.2	1.4	Thin and irregular coating, porous and poorly adherent to the substrate
(c)	−1.0	−2.2	6.6	Thick and uniform coating
(d)	−0.7	−2.2	5.7	Thick and uniform coating

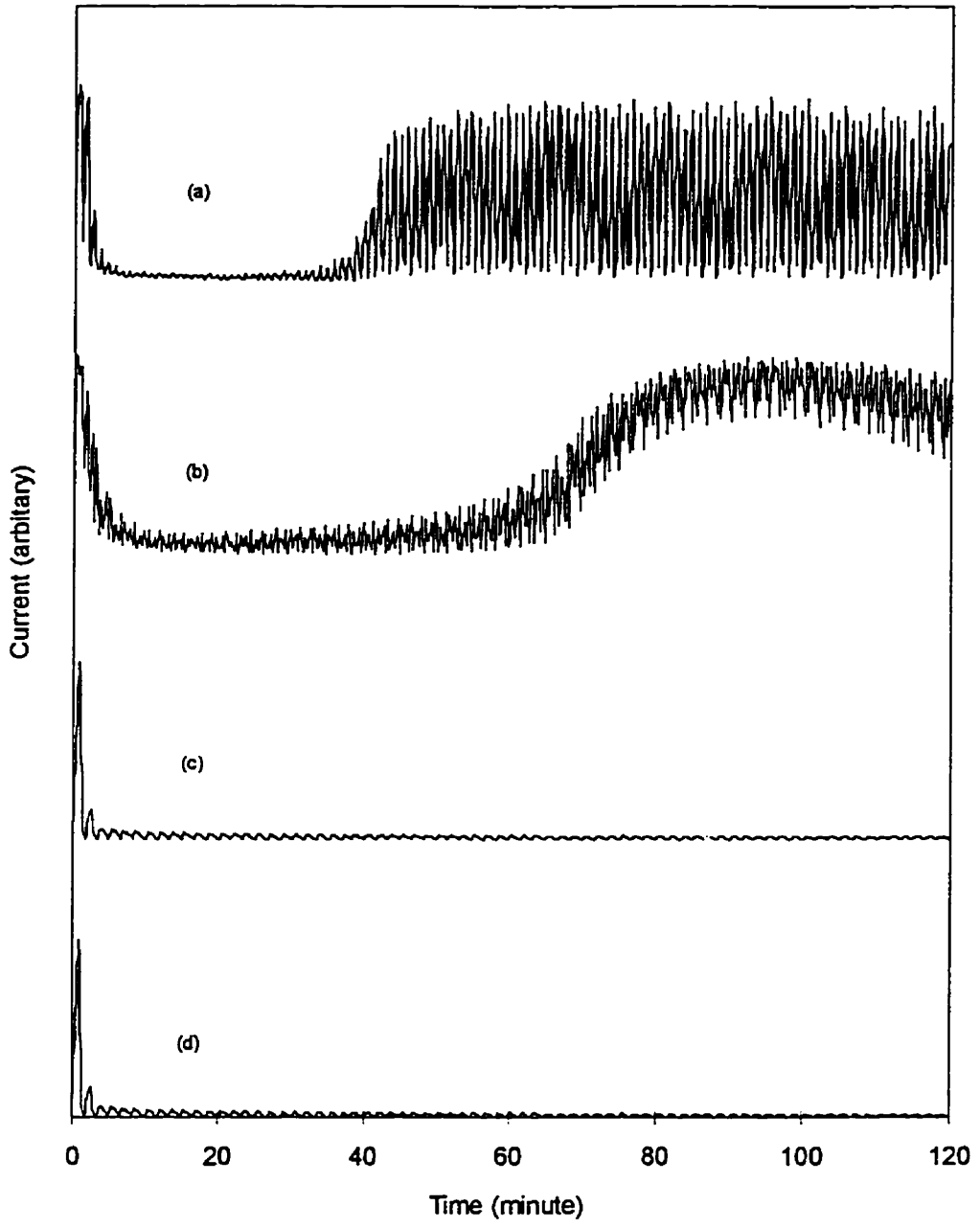

Fig. 6.11. The effect of the range of the working electrode potential during CPS electrolysis on the electropolymerization I-t diagrams. The explanation legend (a) to (e) is given in Table 6.3.

6.3.5.3. The Effect of the Potential Scan Rate of a CPS Electrolysis

When the CPS electrolyses are performed at different potential sweep rates in the range between –1.0 and –2.2 V, interesting results are obtained. If potential sweep rates are between 10 and 50 mV/s, an acceptable quality of coatings is produced. The I-t diagrams show rapid current decrease after the onset of the electrolysis (Figs. 6.12 b to 6.12d). At a high potential sweep rate (i.e., 100 mV/s), several cycles of electrolysis are required before a decrease in system current to a relatively stable value is obtained (Fig. 6.12a). This can be explained by the fact that the high sweep rate shortens the polymer growing time (the period when no or very low current flows through the electrodes) and makes it difficult for the coating to accumulate on the substrate. The coating is relatively thin and non-uniform. On the other hand, at a low potential sweep rate (i.e., 5 mV/s), the coating is also non-uniform and poorly adherent even though it is relatively thick. The relevant I-t diagram (Fig. 6.12e) is abnormal. The current decreases slowly at the beginning of the process and increases after about 40 minutes of electrolysis. Although there is now a longer continuous period for both the highly cathodic and open-circuit stages of the process, the initiation reaction (at cathodic potential with high current) and the propagation reaction (near the open-circuit potential with very low current) do not coincide much in time. Therefore, they cannot cooperate effectively for the polymerization and coating formation.

The above experimental results demonstrate that a proper combination of the potential sweep range and rate is very important for a successful electropolymerization coating formation process by the CPS technique. The selection of the values of the various

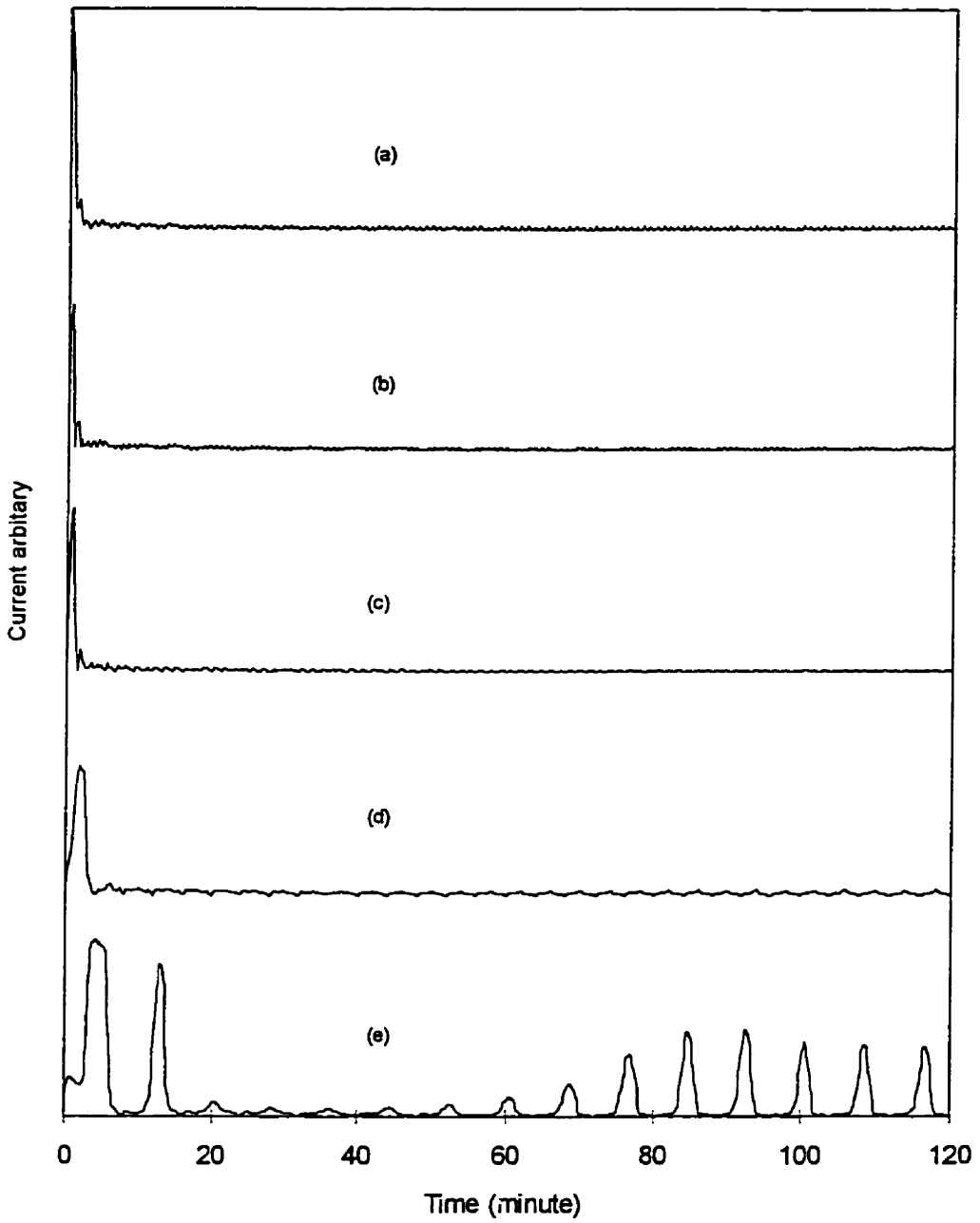

Fig. 6.12. The effect of the potential sweep rate during CPS electrolysis on the electropolymerization I-t diagrams. The explanation legend (a) to (e) is given in Table 6.4.

Table 6.4. Effect of the rate of potential sweep on coating formation (in the potential range of −1.0 to −2.2 V). The relevant I-t diagrams are shown in Fig. 6.12.

Legend in Fig. 6.12	Potential sweep rate (mV/s)	Coating weight (mg)	Result
(a)	100	4.9	Non-uniform coating
(b)	50	6.2	Thick and uniform coating
(c)	30	6.6	Thick and uniform coating
(d)	10	6.7	Thick and uniform coating
(e)	5	5.2	Even though coating is not very thin, it is non-uniform and poorly adherent

parameters is still empirical. Future research into developing a quantitative model would be useful for obtaining a better understanding of the interaction between these parameters.

6.4. Poly(2-Vinylpyridine) Formation by Free Radical Bulk Polymerization

For comparative purposes, poly(2-vinylpyridine) is also formed at room temperature by bulk polymerization with 1 *wt.* % benzoyl peroxide as free radical initiator. The colour of the reaction solution changed gradually from clear to light yellow during the polymerization. The formed polymer appears white after being purified repeatedly with hexane and THF and is soluble in methanol, THF and chloroform. Polymer products from processes under elevated temperatures (e.g., 40 and 70°C) usually have a dark brown colour. At a higher temperature when the rate of polymerization is too high, the molecular weight of the polymer products become low and the polymer products adopt a brown

colour characteristic of 2-vinylpyridine oligomer (De Bruyne et al., 1995). Auto-acceleration is evident at the end of the polymerization from the increase of the viscosity of the reaction solution.

Poly(2-vinylpyridine) formed by bulk polymerization has also been used to form coatings on mild steel substrates by the solvent evaporation technique. 4 grams of polymer are first dissolved in 20 mL THF and then the solvent allowed to evaporate partially until the viscosity of the polymer solution is suitable for coating formation. A mild steel coupon, similar to the ones used in the electropolymerization, are then dipped into the polymer solution for coating formation and then dried in air. The formed coatings are colourless and very smooth. After thermal curing at ~120°C for 30 minutes, the colour of the coating becomes brown and some cracks show in the coating surface. It is hard to control the coating uniformity and coating thickness. Sometimes air bubbles form in coatings during solvent evaporation process. The coatings are hard, but the adhesion of the coating on the substrate is not as good as that of the coatings formed by electropolymerization. A piece of coating can be scratched off the substrate relatively easily.

CHAPTER 7

RESULTS AND DISCUSSION — PART TWO: EFFECT OF OPERATING CONDITIONS

7.1. Effect of Solution pH

As mentioned previously, solution pH is a critical variable in the electropolymerization process. To study this, a series of voltammograms was obtained for a 0.25 M 2-vinylpyridine solution at various pH values. The cathodic portions of these voltammograms are shown in Fig. 7.1. The curves have been deliberately shifted along the horizontal axis to avoid any overlap. The anodic parts which show only the current rise for oxygen evolution are omitted. Before the addition of $HClO_4$ or NH_4OH to the 0.25 M 2-vinylpyridine solution to adjust pH, the electrolyte initially has a pH of 7.5. At this pH value, very intense hydrogen evolution occurs during the voltammetric experiments. No other current wave can be observed in the voltammogram. When the solution pH is increased by adding NH_4OH, a similar wave characteristic is observed. However, when the solution pH is reduced to about 5 using $HClO_4$, a significant cathodic shift of the starting potential for hydrogen evolution is observed and a new current plateau with a $E_{1/2}$ of about −1.0 V appears. When the solution pH is reduced further, the shape of the voltammograms shows no essential change. While the $E_{1/2}$ for the plateau remains at about −1.0 V, the current rise for hydrogen evolution shifts slightly in the positive direction. This may be due to the higher concentration of hydrogen ions in the solution at the lower pH.

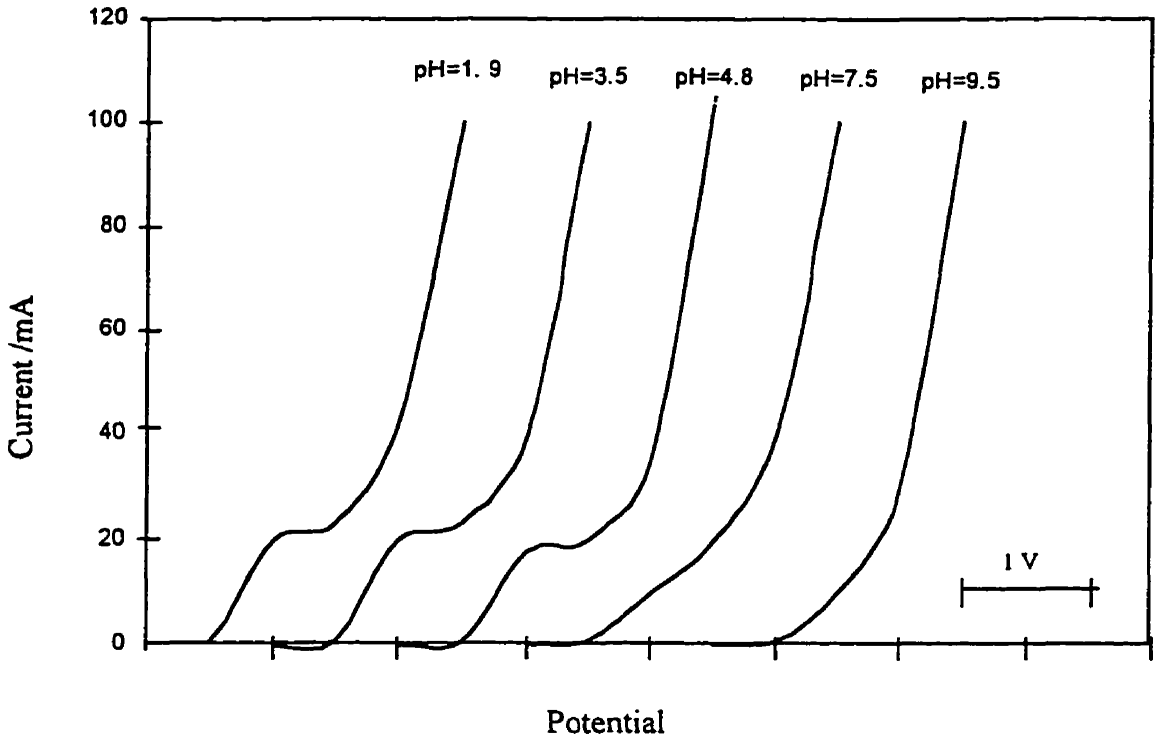

Fig. 7.1. The effect of solution pH on the shape of the voltammograms obtained in 0.25 M 2-vinylpyridine solution. Potential scan is between –0.7 V and –2.0 V and scan rate is 30 mV/s. The curves have been shifted along the potential axis to avoid any overlap.

Solution pH does influence the coating formation process significantly. After a one-hour chronoamperometric electrolysis at a constant cathodic potential of –1.3 V, a CSLM image of the coated sample morphology shows only scattered deposits on the electrode surface from a solution of pH 7.5 (Fig. 7.2b). At higher values of pH, even less deposit is formed (Fig. 7.2c). Only when the solution pH is reduced to about 5 does a uniform coating form on the electrode surface (Fig. 7.2a). However, further reduction in pH to below 4 results in hydrogen evolution at more positive potentials and very little deposit forms on the substrates. When the pH is lower than 2, no visible film formation can be observed. During the electrolysis, the solution pH remains unchanged. The experimental results are summarized in Table 7.1.

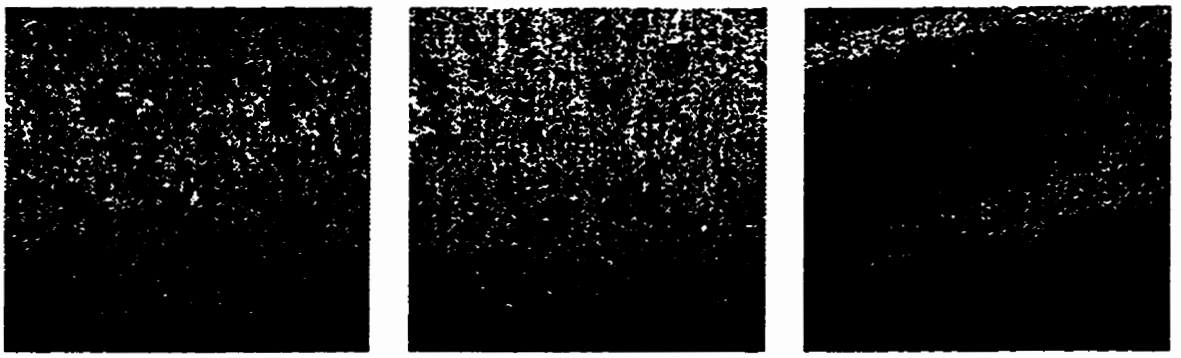

(a) (b) (c)

Fig. 7.2. The effect of solution pH on coating morphologies (4 mm × 4 mm scanning CSLM areas), after a one-hour chronoamperometric electrolysis at a constant potential of −1.3 V. (a) pH = 4.8: coating is uniform although small pits can be seen; (b) pH = 7.5: coating is scattered and irregular; (c) pH = 9.5: very thin and irregular coating.

During the chronoamperometric electrolysis (at −1.3 V) at various values of pH, the system current is found to decrease rapidly after the onset of the electrolysis (Fig. 7.3). Interestingly, even when very little or no visible film forms on the substrate surface at low pH (e.g., pH value of 1.9), the current still decreases very rapidly with time. On the other hand, at high pH the coating quality is poor, while the current drops off less sharply. The reason for this behaviour may be that extremely thin but very compact films have formed on the substrates even when the coating is poor. These experimental results are also summarized in Table 7.1.

When electrolyte pH > 7.5 or < 3.5, intense hydrogen evolution occurs, indicating that a large amount of hydrogen radicals have been generated at the cathode surface:

at low pH: $$2H_3O^+ + 2e^- \rightarrow 2H_2O + 2H^\bullet \rightarrow 2H_2O + H_2 \quad (7.1)$$

at high pH: $$2H_2O + 2e^- \rightarrow 2OH^- + 2H^\bullet \rightarrow 2OH^- + H_2 \quad (7.2)$$

Table 7.1. Summary of the experimental results of the effect of solution pH on coating formation from a one-hour chronoamperometric electrolysis at a constant cathodic potential of −1.3 V (0.25 M 2-vinylpyridine in 20% methanol aqueous solution with 0.05 M NH_4ClO_4 as supporting electrolyte at 20°C).

Solution pH	$E_{1/2}$ (V†)	Coating weight ± 0.3 (mg)	Current change in chronoamperometric electrolysis ‡	Coating morphology
1.9	−1.15	0	Current decreases quickly; reaches a final value of 1.35 mA/cm^2	No visible film
3.5	−1.15	0.5	Current decreases quickly; reaches a final value of 0.82 mA/cm^2	Very little visible film
4.8	−1.20	3.5	Current decreases quickly; reaches a final value of 0.45 mA/cm^2	thin film with small cracks and little clumps.
7.5	----	1.8	Current decreases quickly; reaches a final value of 0.91/cm^2	Scattered and irregular film
9.5	----	1.1	Current decreases quickly; reaches a final value of 1.64 mA/cm^2	Very thin and irregular film

† The $E_{1/2}$ corresponds to the half-wave potential for 2-vinylpyridine reduction reaction.

‡ Duration of experiments was one hour.

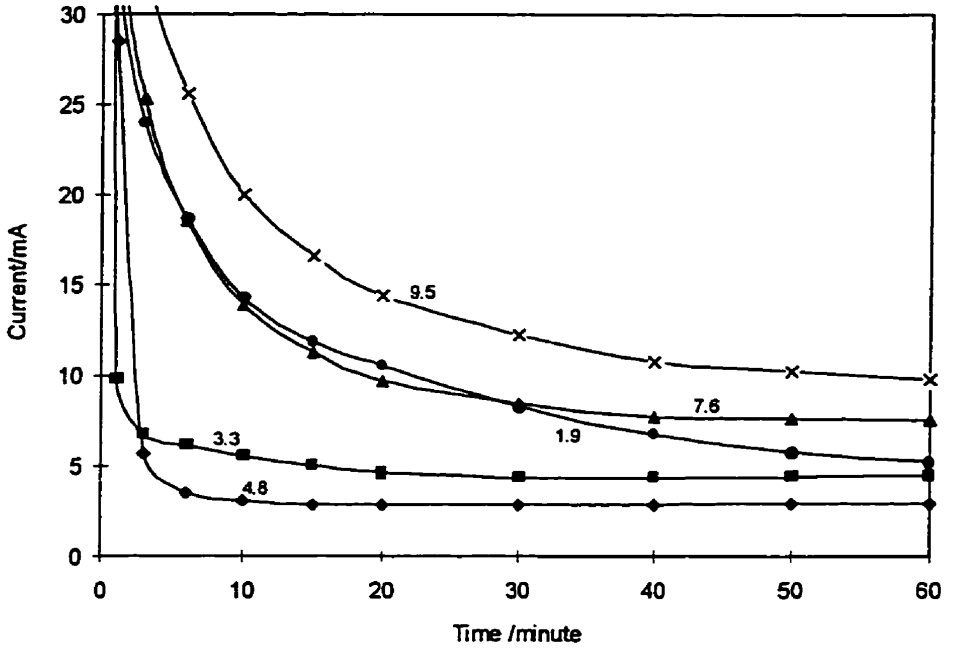

Fig. 7.3. The effect of solution pH on cathodic current during chronoamperometric electrolysis in a 0.25 M 2-vinylpyridine solution at constant potential of −1.3 V in 20% methanol aqueous solution with 0.05 M NH_4ClO_4 as supporting electrolyte. pH: (—●—) 1.9, (—■—) 3.3, (—◆—) 4.8, (—▲—) 7.5, (—×—) 9.5.

However, very thin polymer coatings, sometimes even no visible coating, can be observed on the electrode surfaces. This indicates that hydrogen radicals do not contribute to the initiation of polymerization. The initiation of the polymerization would involve the reduction of monomer molecules, indicated by the reduction wave at about −1.0 V on the voltammograms (Fig. 7.1). This conclusion is consistent with the one obtained before in linear sweep voltammetry studies (Section 6.2.). Obviously, electrolyte pH has a major effect on the electropolymerization process. The effect of pH on the shape of the voltammograms would seem to relate directly to the mechanism of the electropolymerization process. More detailed

discussion of this issue and the mechanism of process initiation reactions will be provided later in Chapter 10.

7.2. Effect of Methanol Concentration in Electrolyte

From the single parameter experiments, it is found that methanol content in the electrolyte plays an important role in the coating formation process. At low methanol content (e.g., 1 to 5 %), the solubility of 2-vinylpyridine in water is not high enough to make a 0.25 M 2-vinylpyridine solution without adding concentrated $HClO_4$ to lower the pH. As the solution pH is reduced, a portion of the 2-vinylpyridine molecules (I) is protonated to form 2-vinylpyridinium ions which are soluble in water. Detailed discussion of this issue will be presented later along with the results from Raman scattering spectroscopy. The 2-vinylpyridinium ions can be represented by a variety of canonical forms, such as II and III, etc.

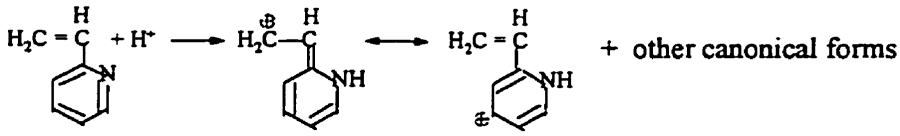

(7.3)

(I) (II) (III)

When the methanol content is low (e.g., 5%), the polymer formed during electrolysis has a low solubility in the electrolyte. Therefore, the coating starts to form rapidly after the onset of the electrolysis. However, since the coating formation process may be so rapid, the coating is non-uniform. The low molecular weight content in the coating is high which causes the coating to have poor solidification characteristics. Moreover, the coating does not adhere to the substrate very well and some actually falls off the electrode in small pieces. Some of

these pieces re-contact the electrode and form little lumps on the substrate. As the methanol content increases above 10%, the monomer and polymer become more soluble in the solvent. This increases the higher molecular weight polymer component in the film and yields a more solidified coating. Thick and uniform coatings start to form under these conditions. However, when the methanol content in the solvent is higher than 30%, the formed coating becomes thin but still uniform. Hydrogen evolution becomes more intense during coating formation, especially at the beginning of the process. The polymer now is more soluble in the electrolyte that a larger portion of it re-dissolves, particularly the low molecular weight component formed at the beginning of the process. Whatever coating is present is not capable of suppressing hydrogen evolution. The results of these experiments on the effect of methanol content are summarized in Table 7.2.

Table 7.2. Summary of the effect of methanol content in the electrolyte on the polymer coating formation by two-hour CPS processes. The electrolyte is 0.25 M 2-vinylpyridine with 0.05 M NH_4ClO_4 as supporting electrolyte and solution pH of 4.8, adjusted by $HClO_4$. The potential sweep is between –0.7 and –2.5 V at 30 mV/s.

Methanol concentration (*vol. %*)	**Coating weight ± 0.3** (mg)	**Comments**
1	2.9	Thin and non-uniform coating
5	4.1	Thin and non-uniform coating
10	6.5	Thin but uniform coating.
15	8.5	Thick and uniform coating
20	7.9	Thick and uniform coating
25	6.4	Thick and uniform coating
30	4.8	Thin but uniform coating
40	2.3	Thin but uniform coating

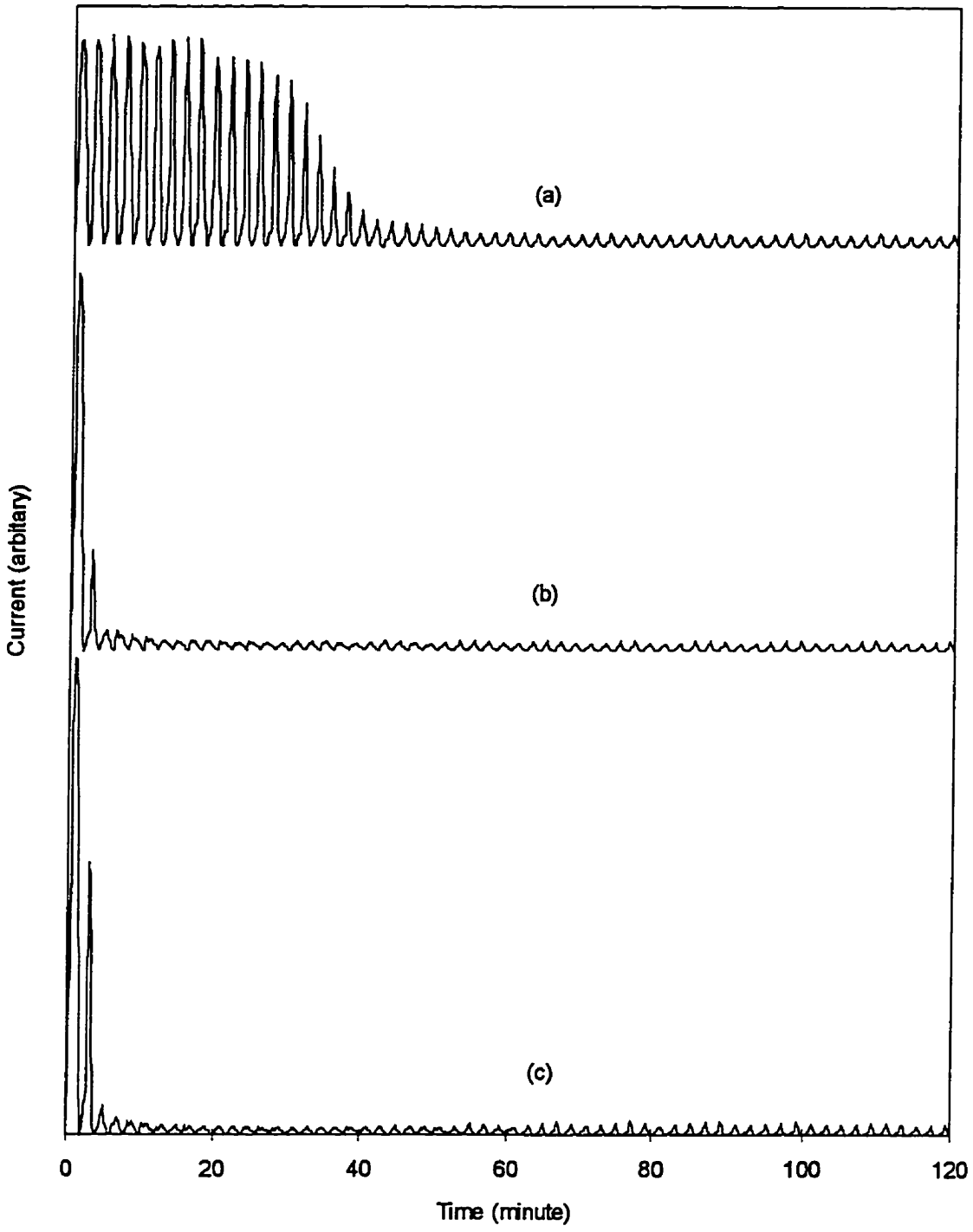

Fig. 7.4. The effect of methanol content in the electrolyte on the I-t diagrams obtained during CPS electrolysis of poly(2-vinylpyridine) coatings. The methanol contents (by volume) in the electrolyte are (a) 40 %, (b) 20 % and (c) 5 %. Same experimental conditions as described in Table 7.2.

The I-t diagrams of the CPS processes (Fig. 7.4) support the above explanations. With a low or intermediate methanol content (≤ 20%), the system current drops rapidly after the onset of the electrolysis, indicating that a resistant film forms on the electrode surface rapidly. When the methanol content is high (≥ 30%), the current only starts to decrease gradually after the first half-hour of electrolysis. This indicates that during the first half hour, virtually no film is formed on the electrode surface. However, the detailed voltammograms show that monomer reduction reaction still take place during this period. Apparently, the reduction product must be dissolving in the electrolyte as quickly as it forms.

The effect of solvent on polymer coating formation appears very complex. A solvent with an appropriate combination of components assists the stretching of the polymer coils, which is helpful for the formation of a thick, coherent and uniform coating. More research in this area is warranted.

7.3. Effect of Operating Temperature

Temperature was found to play an interesting role in the electropolymerization process. When the electrolysis is operated at 20°C (0.25 M 2-vinylpyridine in 20% methanol aqueous solution with 0.05 M NH_4ClO_4 as supporting electrolyte and solution pH of 4.8 adjusted with $HClO_4$), a thick and uniform yellow coating is obtained. During a two-hour CPS electrolysis (between –0.7 and –2.5 V at a scan rate of 30 mV/s), the electrolyte gradually becomes yellow as well. When the operating temperature is higher than 20°C, the coatings become thicker and the coating colour changes more quickly. Presumably, this is due to the increase in polymerization rate with rise in temperature. When the operating temperature is over 40°C, the

coating weight increase begins to slow as the temperature rises. This observation is consistent with the fact that the rate of polymerization increases as the temperature rises but when the temperature is too high the molecular weight of the polymer would be expected to decrease. The low molecular weight polymer has a higher solubility in the hot solvent than the high molecular weight polymer in the cooler solvent. Since the lower molecular weight portions would preferentially dissolve, this would leave behind enough of higher molecular weight components, resulting in very coherent and uniform coatings. The yellow colour of the electrolyte may be due to the presence of relatively low molecular weight polymer in the solution (Tien and Hogen-Esch, 1976; Jenkins et al., 1979; Mathis and Hogen-Esch 1982; Meverden and Hogen-Esch, 1983; De Bruyne et al., 1995). More discussion about this aspect will be presented later.

Support for the above explanation is found from the experimental result obtained at a lower electrolysis temperature. At 10°C, more coating forms on the substrate than at 20°C. Although polymerization occurs at a slower rate at the lower temperature, the resulting polymer has a higher molecular weight and therefore a heavier coating on the substrate. Moreover, the formed coating is found to have a much lighter colour than the ones produced at higher temperature, while the solution colour is much lighter as well. A yellow colour is normally characteristic of a lower molecular weight 2-vinylpyridine oligomer whereas a light or no colour is typically associated with a higher molecular weight polymer. The I-t diagrams of the CPS processes (Fig. 7.5) also support the above explanations. At higher temperature (e.g., 70°C), the electrolysis current through the whole process is higher than that at the lower temperature (Fig. 7.5c), indicating a higher rate of electropolymerization. At lower temperature (10°C), the drop of the current is relatively gradual at the beginning (Fig. 7.5a), indicating that

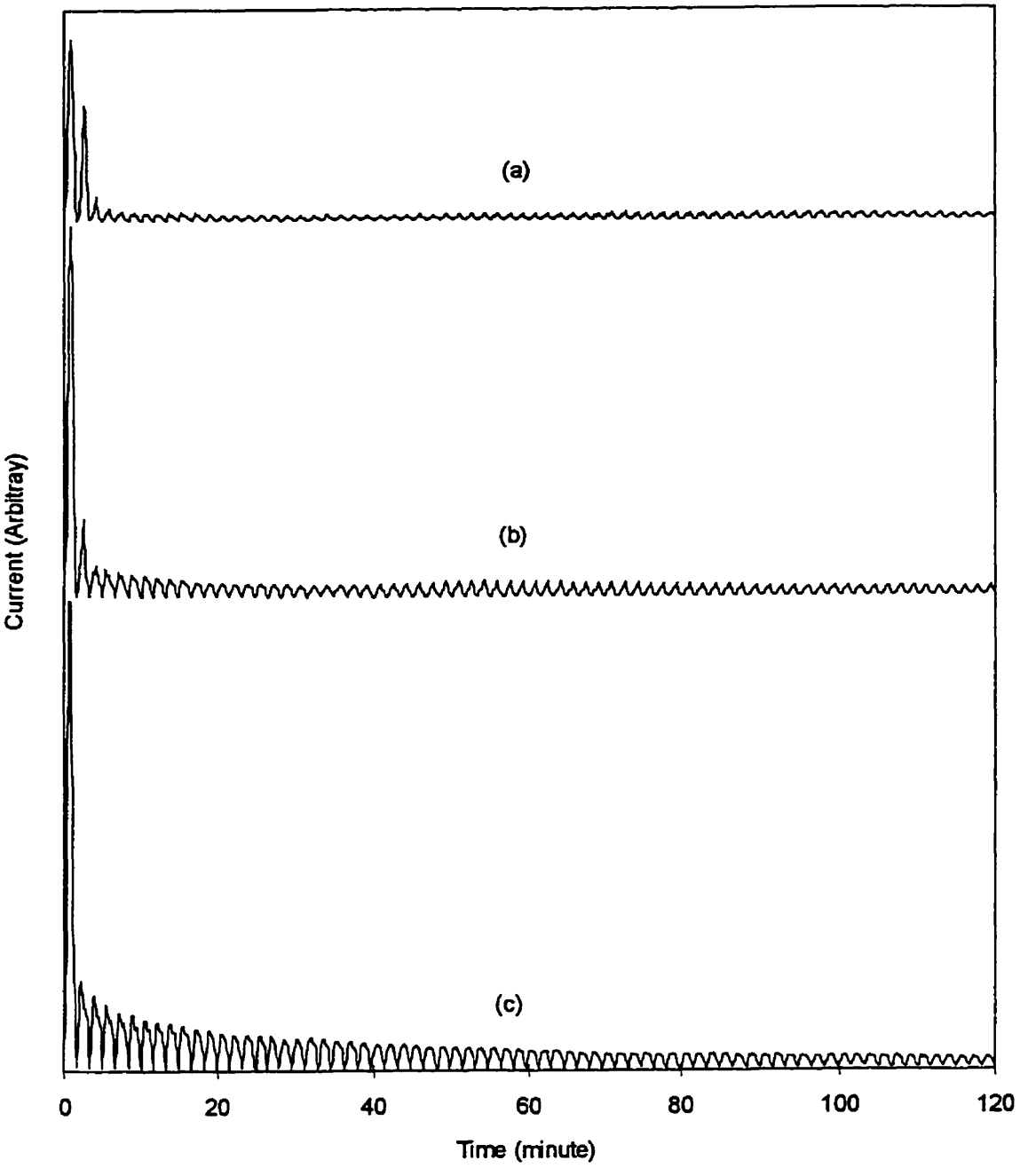

Fig. 7.5. The effect of operating temperature on I-t diagrams obtained during CPS electrolysis (between –0.7 and –2.5 V at 30 mV/s) of poly(2-vinylpyridine) coatings. The electrolyte was 0.25 M 2-vinylpyridine in 20% methanol aqueous solution with 0.05 M NH_4ClO_4 as supporting electrolyte and solution pH of 4.8 adjusted with $HClO_4$. The operating temperatures are (a) 10°C, (b) 40 °C and (c) 70 °C.

less coatings is formed on the electrode surface due to the slower rate of the electropolymerization. Taken together, the results on the effect of temperature suggest that increasing temperature promotes the formation of a thinner, low molecular weight coating that nonetheless can still be protective if the other conditions are favourable. The experimental results on the effect of temperature are summarized in Table 7.3.

Table 7.3. Summary of the experimental results on the effect of operating temperature on the electropolymerization. The experimental results are the same as described in Fig. 7.5.

Operating temperature (°C)	Coating weight (mg)	Comments
10	8.2	Thick and uniform coating with lighter yellow colour
20	7.9	Thick and uniform coating with yellow colour
30	8.2	Thick and uniform coating with yellow colour
40	8.5	Thick and uniform coating with yellow colour
50	7.3	Uniform coating with darker yellow colour
60	6.5	Very uniform coating with darker yellow colour
70	6.2	Very uniform coating with dark yellow colour

7.4. Effect of Monomer Concentration

These experiments are operated at 20°C using different amounts of monomer dissolved in 20% methanol aqueous solution with 0.05 M NH_4ClO_4 as supporting electrolyte and solution pH of 4.8 adjusted with $HClO_4$. The CPS are carried out between –0.7 and –2.5 V at a scan rate of 30 mV/s. It is found that the $E_{1/2}$ of 2-vinylpyridine reduction at different monomer concentrations are shifted only slightly. When the monomer concentration is low (< 0.15 M), intense hydrogen evolution is observed at the cathode surface. Consequently, the

formed coatings are thin and irregular. Presumably, there is not enough monomer in the electrolyte to compete with hydrogen for coverage of the electrode surface. As the monomer concentration increases, the electrode surface coverage by the monomer increases so that hydrogen evolution is suppressed. Meanwhile, the polymerization rate increases with the increase of monomer concentration, and therefore, thicker and uniform coatings are obtained. However, when the monomer concentration is too high (> 0.3 M), it is difficult to dissolve all of the monomer in the electrolyte. The coatings are found to be unevenly distributed on the electrode surfaces and are poorly solidified. Sometimes the polymeric material appears in a semi-fluid state on the substrate. This phenomenon is similar to the case when the solvent has a very low methanol content.

When the monomer concentration is very high, the polymerization occurs very rapidly and the resulting polymer would be expected to have low molecular weight. A low molecular weight polymer has a higher solubility in the solvent and solidifies with difficulty. The I-t diagrams (Fig. 7.6) of the CPS processes support the above explanations. At low monomer concentration (e.g., 0.1 M), the electrolysis current does not decrease for the first hour (Fig. 7.5a), indicating very little coating forms on the electrode surface. At high monomer concentration (e.g., 0.35 M), the drop of the current is very rapid and the current is much higher than that at low monomer concentration (Fig. 7.5c), indicating a rapid formation of polymer coating on the electrode surface. The experimental results are summarized in Table 7.4. What should be emphasized here is that a heavier coating alone does not necessarily indicate a good quality of coating. Coating uniformity should always be taken into account in coating quality evaluations.

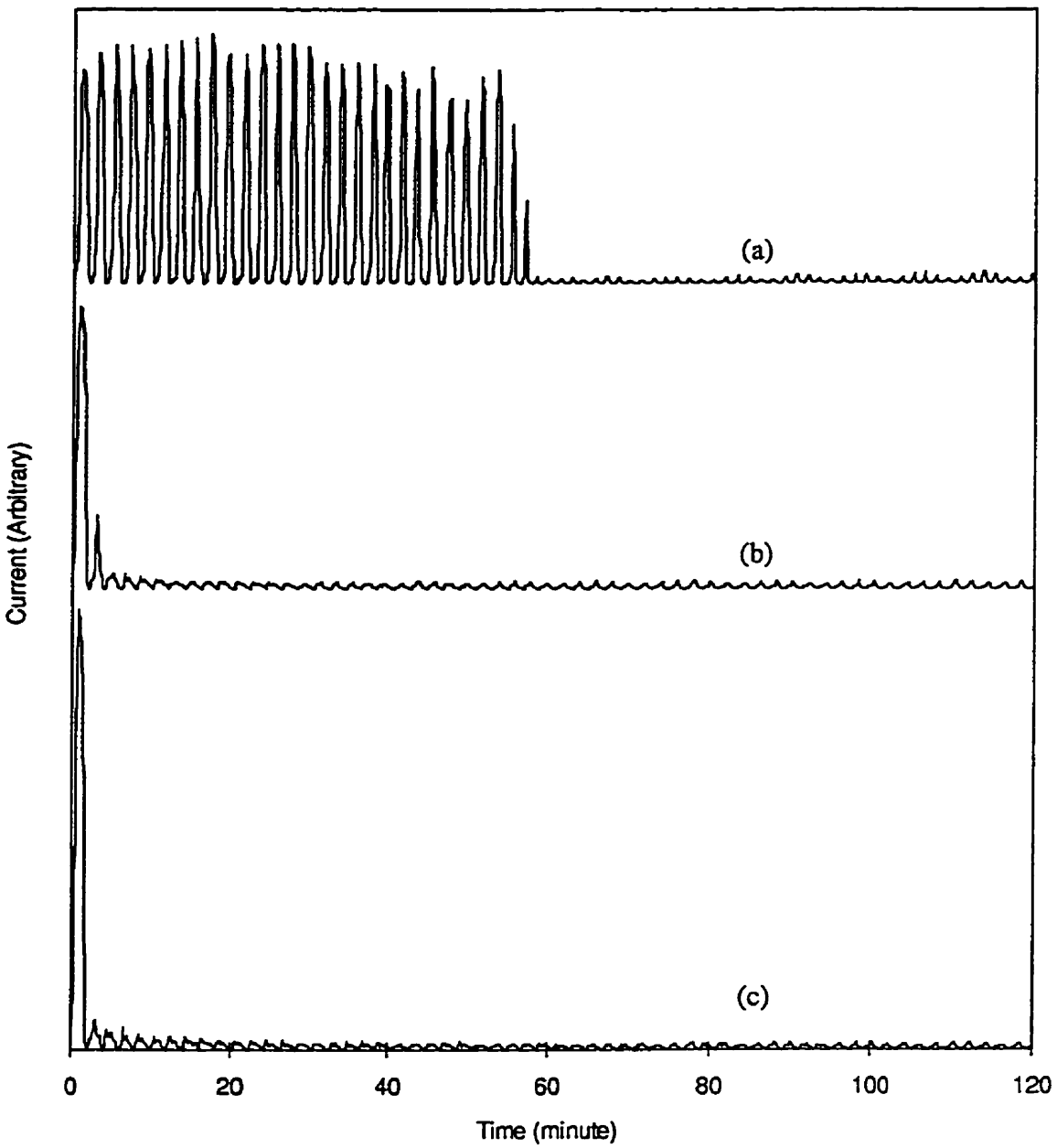

Fig. 7.6. The effect of monomer concentration on I-t diagrams obtained during CPS electrolysis (between –0.7 and –2.5 V at 30 mV/s) of poly(2-vinylpyridine) coatings. The electrolyte is 20°C in 20% methanol aqueous solution with 0.05 M NH_4ClO_4 as supporting electrolyte and solution pH of 4.8 adjusted with $HClO_4$. The monomer concentrations are (a) 0.1 M, (b) 0.25 M and (c) 0.35 M.

Table 7.4. Effect of monomer concentration on the electropolymerization process during two-hour CPS electrolysis.

2-Vinylpyridine concentration (M)	Coating weight (mg)	Comment
0.10	1.2	Extremely thin coating with intense H_2 evolution
0.15	2.2	Thin but uniform coating with intense H_2 evolution
0.20	3.2	Thick and uniform coating
0.25	3.4	Thick and uniform coating
0.30	11.3	Thick but non-uniform coating, the coating is sticky
0.35	13.8	Unevenly distributed coating, the polymer appeared to be able to flow on the electrode surface

7.5. Effect of Electrolysis Duration

The effects of CPS electrolysis duration on the electropolymerization process have been studied for time periods between 15 minutes to 10 hours. Although visible polymer deposit can be observed on the cathodic surface after the first cycle of the potential sweep (i.e., in 2 minutes), coatings of good quality cannot be obtained in shorter than one hour of CPS electrolysis. When electrolysis is carried out for only 20 minutes, coating formation is evident on the electrode surface, but not very uniform. Further electrolysis not only increases the thickness of the coating, but also makes it more uniform. At the beginning of the electrolysis, the electrode surface is fresh and the electrolysis occurs over a large surface area. The electrolysis current is high, providing a large amount of initiator in a short period resulting in rapid polymerization. At the same time, hydrogen evolution is very intense during this stage. While the polymer coating is forming rapidly on the electrode surface, the hydrogen evolution

interferes greatly and causes the polymer coating to be unevenly distributed. However, once the electrode surface becomes completely covered with the polymer coating (although it is still uneven) after enough electrolysis, hydrogen evolution is greatly suppressed. During the remaining electrolysis, coating formation occurs preferentially on the more thinly coated areas that have lower resistance and consequently becomes increasingly more level as it thickens.

When the electrolysis duration is over a certain period (i.e., 2 hours), the coating thickness stops increasing, and even decreases slightly. In this period, the electrolysis current does not drop to zero and the electropolymerization, i.e., the monomer reduction reaction which contributes to the electrolysis current, and the initiation, propagation and termination reactions, still carry on, but at a lower rate. Meanwhile, some of the formed poly(2-vinylpyridine) dissolves in the solvent. An equilibrium between coating formation and dissolution is eventually reached and the coating thickness reaches a constant value. The experimental results are summarized in Table 7.5.

Table 7.5. Effect of electrolysis duration on the electropolymerization.

Electrolysis Duration (minute)	**Coating weight (mg)**	**Comment**
20	2.2	Thin coating and not evenly distributed
30	3.9	Thin coating and not very uniform
60	5.0	Thicker and more uniform coating
90	7.0	Uniform coating
120	7.9	Thick and uniform coating
180	7.5	Thick and uniform coating
270	6.9	Thick and uniform coating
300	7.0	Thick and uniform coating
600	6.8	Thick and uniform coating

7.6. Effect of Supporting Electrolytes

7.6.1. Effect of the Nature of Supporting Electrolytes

Different inorganic compounds have been tested as supporting electrolytes for the electropolymerization, including NH_4ClO_4, $KClO_4$, KCl, NH_4Cl, $(NH_4)_2SO_4$, NH_4NO_3, $(NH_4)_3PO_4$ and H_3PO_4. The monomer (0.25 M) is dissolved in 10% methanol aqueous solvent with different supporting electrolytes. The acid corresponding to each supporting electrolyte has been used to adjust the solution pH to 4.8. The voltammograms obtained using different supporting electrolytes are quite similar. The $E_{1/2}$ of 2-vinylpyridine reduction in the different supporting electrolytes shift only slightly. The electropolymerization are performed by chronoamperometric electrolysis at −1.3 V for two hours. When NH_4ClO_4 is used as the supporting electrolyte with $HClO_4$ to adjust solution pH, thick and uniform coatings are obtained. The coating is very hard with excellent adhesion to the substrate. However, coatings from $KClO_4$-$HClO_4$ electrolytes are thinner than that those from NH_4ClO_4-$HClO_4$ electrolytes although the other operating conditions are the same. This is considered, at least partially, the consequence of the intramolecular solvation of alkali metal ions by the nitrogen atom of the penultimate pyridine ring. The intramolecular coordination results in the formation of a conformationally constrained multi-membered ring (Smid, 1969).

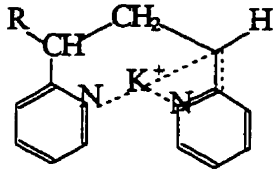

The strong intramolecular interaction between the alkali metal ion and the monomer molecule makes it less favourable for 2-vinylpyridine polymerization. Therefore, when $KClO_4$ replaces

NH_4ClO_4 as the supporting electrolyte, a thinner coating is obtained.

When NH_4Cl is used as the supporting electrolyte with HCl to adjust the solution pH, less coating is formed than with NH_4ClO_4. The coating is also relatively loose and powdery. This may be due to chlorine generation at the anode, which was detected in and around the electrolytic cell, (the chloride oxidation wave in the voltammogram overlaps with the oxygen evolution wave and therefore cannot be used as clear evidence of chlorine generation)

$$2Cl^- - 2e \rightarrow Cl_2 \tag{7.4}$$

The generated chlorine and its derivatives (e.g., ClO^-) can dissolve in the electrolyte, diffuse to the cathode surface and react with the living polymers or the cathodically generated initiators

$$Cl_2 + 2M^{\bullet} + 2e \rightarrow 2Cl^- + 2M \tag{7.5}$$

$$2ClO^- + 4H^+ + 2M^{\bullet} + 2e \rightarrow Cl_2 + 2M + 2H_2O \tag{7.6}$$

On the other hand, it is interesting that no hydrogen bubbles appear on the cathode surface during the electrolysis. The residual current is higher (up to 4–5 times) than that in the NH_4ClO_4 situation. An even thinner coating is obtained with KCl as supporting electrolyte due to the presence of the alkali metal ion in the electrolyte. An explanation to account for the loose and powdery coating formation is not available yet. When $(NH_4)_2SO_4$, NH_4NO_3 or $(NH_4)_3PO_4$ is used as supporting electrolyte with H_2SO_4, HNO_3 or H_3PO_4 to adjust the solution pH, respectively, similarly loose and powdery coatings to those obtained with chloride supporting electrolytes are obtained. No hydrogen bubbles are observed during these experiments.

When $HClO_4$ alone is used as the supporting electrolyte and for pH adjustment, good coatings similar to those from the NH_4ClO_4 solutions are obtained. Hydrogen bubbles are also observed during electropolymerization. Although ClO_4^- ions do not apparently inhibit hydrogen evolution, they are related somehow to the formation of good coatings. This implies

that either hydrogen evolution may not always be detrimental to coating formation, or that ClO_4^- ions may be involved in the polymer coating formation and adhesion process on the substrate. Further information related to these observations is not yet available. The experimental results on the effects of the different supporting electrolytes are summarized in Table 7.6. Some images of coatings from different supporting electrolytes are shown in Fig. 7.7. Comparing with the coating images from NH_4ClO_4-$HClO_4$ electrolytes (Figs. 6.6 and 6.9), it is clear that coatings from supporting electrolytes except NH_4ClO_4 are more powdery and granular. It is obvious from the above results that the function of the supporting electrolyte in 2-vinylpyridine electropolymerization is beyond that of simply enhancing the electrolytic conductivity. Both cations and anions affect the coating formation process and influence the coating adhesion on the substrates. More investigation should be carried out in this area in an effort to further understand the mechanism.

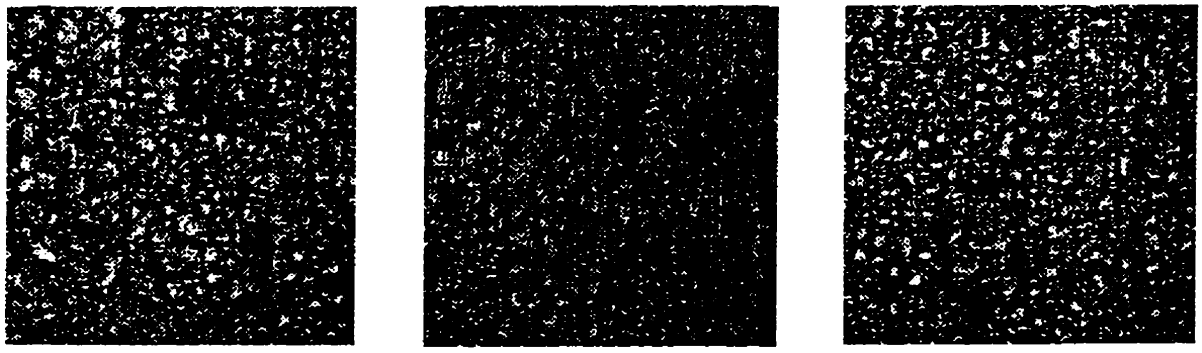

(a) (b) (c)

Fig. 7.7. CSLM images (200 μm × 200 μm) of poly(2-vinylpyridine) coatings from different supporting electrolytes (0.05 M) after a two-hour chronoamperometric electrolysis at a constant potential of −1.3 V. (a) from NH_4Cl-HCl electrolytes; (b) from $(NH_4)_2SO_4$-H_2SO_4 electrolytes; (c) from NH_4NO_3-HNO_3 electrolytes.

Table 7.6. Effect of different supporting electrolytes on the electropolymerization process during a two-hour chronoamperometric electrolysis at −1.3 V in 0.25 M 2-vinylpyridine solutions at pH 4.8.

Type of supporting electrolyte	Specific conductivity (S/m)	Residual current (mA/cm^2)	Hydrogen evolution observation	Coating weight (mg)	Comment
NH_4ClO_4	1.4735	0.52	visible	5.2	Thick, uniform and glassy coating, with hydrogen evolution observed during the electrolysis
$KClO_4$	1.2799	0.54	visible	4.3	Uniform and glassy coating with hydrogen evolution observed during the electrolysis
NH_4Cl	1.3751	1.33	non-visible	2.2	Thin and uniform but powdery coating, with no hydrogen evolution observed during the electrolysis
KCl	1.5020	1.89	non-visible	1.8	Thin and uniform but powdery coating, with no hydrogen evolution observed during the electrolysis
$(NH_4)_2SO_4$	1.5972	1.17	non-visible	3.6	Uniform but powdery coating, with no hydrogen evolution observed during the electrolysis
NH_4NO_3	1.4124	1.46	non-visible	3.1	Uniform but powdery coating, with no hydrogen evolution observed during the electrolysis
$(NH_4)_2SO_4$	1.3031	1.25	non-visible	3.5	Uniform but powdery coating, with no hydrogen evolution observed during the electrolysis
$HClO_4$	1.0366	0.57	non-visible	5.7	Thick, uniform and glassy coating, with hydrogen evolution observed during the electrolysis

7.6.2. Effect of NH_4ClO_4 Concentration on Electropolymerization Process

From the results of the above experiments on the effects of different supporting electrolytes on the electropolymerization, NH_4ClO_4 is selected as the normal supporting electrolyte for the remainder of this project. Different concentrations of NH_4ClO_4 have been used to test their effects on the electropolymerization process. The half-wave potential for 2-vinylpyridine reduction is found to be virtually unaffected by the NH_4ClO_4 concentration. Furthermore, the coatings obtained are very similar in their uniformity and thickness. NH_4ClO_4 does not appear to have a significant effect on electropolymerization above the lowest concentration of 0.01 M tested, as shown in Table 7.7.

Table 7.7. Effect of NH_4ClO_4 concentration on the electropolymerization process coatings formed during a two-hour CPS electrolysis.

NH_4ClO_4 concentration (M)	Specific conductivity (S/m)	Coating weight (mg)
0.01	0.9715	8.7
0.05	1.4735	7.9
0.1	2.0079	7.9
0.2	2.3145	6.4
0.35	3.1435	6.8
0.5	4.0954	7.1

7.7. Effect of Dissolved Oxygen

The effect of dissolved oxygen in the electrolyte on the electropolymerization process has been studied using a specifically designed electrolytic cell in which the anodic and cathodic compartments are separated by a sintered glass membrane. The same electrolyte as used in other experiments, i.e., 0.25 M 2-vinylpyridine solution in 20% methanol aqueous with NH_4ClO_4 as supporting electrolyte and solution pH of 4.8, adjusted with concentrated $HClO_4$, is used in both compartments. The cathodic compartment is purged with nitrogen for 30 minutes before conducting the electrolysis and is sparged with nitrogen gas throughout the electrolysis. The electropolymerization is performed by 2 hours CPS electrolysis between –0.7 and –2.5 V with scan rate of 30 mV/s. The coatings obtained are thinner and have a lighter (yellow) colour than those produced when no steps are taken to eliminate dissolved oxygen. Meanwhile, the electrolyte has less colour change during the process. In a two-hour CPS electrolysis, 5.5 mg coating is obtained, (*cf.* 7.9 mg coating from a two-hour CPS electrolyte with dissolved oxygen in the electrolyte).

Although it is often stated in the literature (Bhanu and Kishore, 1991; Odian, 1991) that dissolved oxygen plays meaningful roles of both initiator and inhibitor in a polymerization process, the situation may be different for an electropolymerization process. In an electropolymerization process, the process of initiator generation is an electrochemical reaction, often involving monomer reduction or oxidation reactions at the electrode surface. Therefore, the rate of the initiation reaction often depends on the applied electrode potential or the electrolysis current passing through the cell. For free radical polymerization, excess of radicals are generated in a short period when the electrode potential is highly cathodic. These

radicals may participate in the initiation reaction or react with one another or with a living polymer chain to terminate the polymerization. In other words, the electrochemically generated radicals may function as both initiators and inhibitors. In addition, the other electrode reactions (e.g., the hydrogen reduction in our case) can generate radicals to initiate or terminate the polymerization as well. Therefore, even if the dissolved oxygen does play some role in initiation or inhibition, its effects may be swamped by those of the electrochemically generated radicals.

7.8. Statistical Studies of Some Important Parameters

After the studies of the effects of single parameters on the electropolymerization process, some important parameters have been selected for the further study so as to evaluate their relative importance to the process. The following parameters have been selected on the basis of the single parameter experiments: operating temperature, monomer concentration, methanol content in the electrolyte and the solution pH (see Table 5.1). A series of 4-factor 3-level orthogonal fractional factorial designed experiments have been carried out. The effects of the parameters on the coating weight and morphology are summarized in Table 7.8. Using statistical analysis as mentioned in Chapter 5, some interesting results have been found and are reported in Tables 7.9 and 7.10. The relative importance of the parameters in the selected ranges to the electropolymerization process is found to decrease in the following order: monomer concentration (factor B) > solution pH (factor D) > methanol content (factor C) > temperature (factor A).

With a closer look at Table 7.9, we find that $\overline{A_I}$, $\overline{A_{II}}$ and $\overline{A_{III}}$ are close to each other and relatively evenly distributed, indicating that the effects of operating temperature over the

range of 20 to 40°C do not change much. Although A_{III} (40°C) appears to the best operating temperature, A_I (20°C) is recommended due to convenience and the fact that the temperature is not a strongly acting variable of the process. $\overline{B_I}$ is the smallest value in the entire series of experiments and therefore the situation of a low monomer concentration should always be avoided. Although high monomer concentration (B_{III}) increases the coating weight the most, it leads to uneven and poorly solidified coatings. Consequently, an intermediate concentration of 0.25 M 2-vinylpyridine (B_{II}) is suggested as the optimum level for the monomer concentration. $\overline{C_I}$ and $\overline{C_{II}}$ are very close to each other and are much higher than $\overline{C_{III}}$, indicating that the suitable methanol content should be between 5 to 15 vol %. Moreover, considering the difficulty of monomer dissolution in a low methanol-content solvent, C_{II} (15 *vol.* %) is suggested for use in future work. $\overline{D_I}$, $\overline{D_{II}}$ and $\overline{D_{III}}$ are well separated, indicating that the solution pH value can still affect the electropolymerization process significantly even in the small range from 4.4 to 5.5. D_{II} (pH 5) is certainly the most appropriate solution pH value for the electropolymerization. Therefore, a combination of the best operating conditions for the electropolymerization is A_I, B_{II}, C_{II} and D_{II}, i.e., operating temperature: 20°C; monomer concentration: 0.25 M; methanol content in the electrolyte: 15 *vol.* %; solution pH: 5.0. The consistency between these conclusions and the previous single-parameters is readily apparent.

Table 7.8. Results from the orthogonal fractional factorial designed experiments of a two-hour CPS electrolysis in $NH4ClO_4$ (0.05 M) -$HClO_4$ electrolyte.

Experimental parameters number of experiment	(A) Operating temperature (°C)	(B) Monomer concentration (M)	(C) Methanol concentration (%)	(D) Solution pH	Coating weight (mg)	Comment
1	I	I	I	I	1.6	Extremely thin however uniform coating
2	I	II	II	II	10.8	Thick and uniform coating
3	I	III	III	III	6.4	Uniform coating
4	II	I	II	III	1.6	Extremely thin however uniform coating
5	II	II	III	I	6.1	Uniform coating
6	II	III	I	II	18.5	Thick but non-uniform coating, not solidified
7	III	I	III	II	3.7	Thin but uniform coating
8	III	II	I	III	9.2	Thick and uniform coating
9	III	III	II	I	16.4	Thick but non-uniform coating, not solidified

Table 7.9. Fractional factorial averages calculated from data in Table 7.8.

$\overline{A_I}$	$\overline{A_{II}}$	$\overline{A_{III}}$	$\overline{B_I}$	$\overline{B_{II}}$	$\overline{B_{III}}$	$\overline{C_I}$	$\overline{C_{II}}$	$\overline{C_{III}}$	$\overline{D_I}$	$\overline{D_{II}}$	$\overline{D_{III}}$
6.27	8.73	9.77	2.30	8.70	13.77	9.77	9.60	5.40	8.03	11.00	5.73

Table 7.10. The maximum differences of the fractional factorial averages calculated from data in Table 7.9.

R_A	R_B	R_C	R_D
3.50	11.74	4.34	5.27

CHAPTER 8

RESULTS AND DISCUSSION — PART THREE: POLYMER CHARACTERIZATION AND COATING PROPERTY MEASUREMENT

8.1. Polymer Characterization

8.1.1. U.V.–Visible Spectroscopy Characterization

Since the poly(2-vinylpyridine) coatings are slightly soluble in methanol, enough polymer could be dissolved from a coated electrode for analysis by u.v.-visible spectroscopy. The polymer coating was obtained from a typical electropolymerization process. The electrolytes were 0.25 M 2-vinylpyridine in 20% methanol aqueous solution with 0.05 M NH_4ClO_4 as supporting electrolyte and solution pH of 4.8, adjusted with concentrated $HClO_4$. The electropolymerization was carried out at 20°C through a two-hour CPS electrolysis between –0.7 and –2.5 V at 30 mV/s. The u.v.-visible spectra of 2-vinylpyridine monomer and poly(2-vinylpyridine) in methanol solution are shown in Fig. 8.1. Although the scans have been carried out over a wide range of wavelengths between 190 to 1100 nm, Fig. 8.1 shows only the lower wavelength portion since the high wavelength section is primarily flat with no characteristic peak. The spectrum of the monomer (Fig. 8.1a) shows two peaks at 233 and 278 nm based on vinyl (π–π^* electron transformation) and pyridine groups (B absorption band of aromatic π–π^* electron

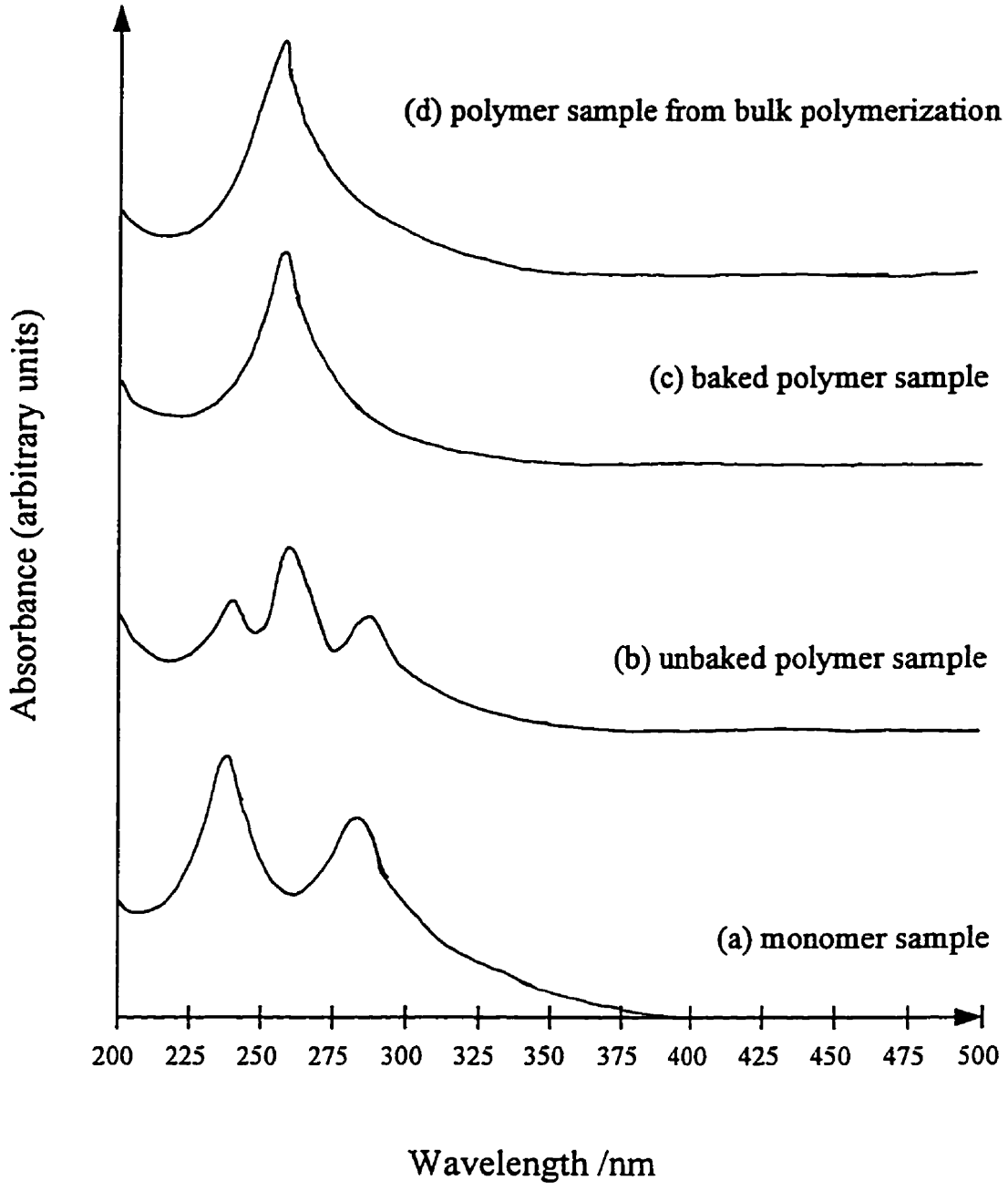

Fig. 8.1. u.v.-visible spectrum of poly(2-vinylpyridine) formed by electropolymerization. The electrolyte is 0.25 M 2-vinylpyridine in 20% methanol aqueous solution with 0.05 M NH_4ClO_4 as supporting electrolyte and solution and solution pH of 4.8, adjusted with $HClO_4$. The electropolymerization is carried out via a two-hour CPS electrolysis between –0.7 and –2.5 V at 30 mV/s.

transformation), respectively (Phillips et al., 1970). In the spectrum of uncured poly(2-vinylpyridine) formed by electropolymerization (Fig. 8.1b), the absorbances at these two peaks decrease and a new peak at 268 nm appears. This new peak at 268 nm is consistent with a poly(2-vinylpyridine) structure (Silverstein et al., 1981). After curing the above polymer sample at 120°C for 30 minutes or vacuum drying for 24 hours, the two peaks at 233 and 278 nm completely disappear. Only the 268 nm peak remains in the spectrum (Fig. 8.1c). For comparison, a poly(2-vinylpyridine) sample from bulk polymerization with benzoyl peroxide as initiator is examined by u.v.-visible spectroscopy. This spectrum (Fig. 8.1d) is found to be identical with the spectrum of the post-treated poly(2-vinylpyridine) sample formed by electropolymerization (Fig. 8.1c). This experiment suggests that poly(2-vinylpyridine) is being formed by the electropolymerization process and that there is not likely to be any other organic by-product formed by the electropolymerization. The poly(2-vinylpyridine) coating possibly has some unreacted monomer trapped in its network. Thus, the characteristic peaks for the monomer (233 and 278 nm) appear in the spectrum of the unbaked polymer (Fig. 8.1b). After thermal curing, the trapped monomer molecules are polymerized and these peaks disappear from the spectrum (Fig. 8.1c).

8.1.2. FT-IR Spectroscopy Characterization

A typical poly(2-vinylpyridine) coating formed under the conditions described previously has been examined by FT-IR spectroscopy. The resulting spectrum (Fig. 8.2) was compared with a standard poly(2-vinylpyridine) IR spectrum (Hummel, 1978) and a good agreement has been found. The only difference from the standard spectrum is the appearance of a strong peak at 1100 cm^{-1} which apparently does not match any of the

poly(2-vinylpyridine) characteristic peaks. However, the peak at 1100 cm^{-1} is normally assigned as a characteristic peak for ClO_4^- (Nakamoto, 1963), which of course is present in our electropolymerization system as the supporting electrolyte. In previous studies when ClO_4^- was used as supporting electrolyte for electropolymerization, this peak at 1100 nm was always observed from the FT-IR spectra of the relevant polymer products and assigned to ClO_4^- without any proof (McCarley et al., 1990; Huang et al., 1995; Sen et al., 1995). However, no investigation has ever been carried out to confirm directly this aspect. To confirm this hypothesis, a poly(2-vinylpyridine) coating sample, produced by the same electropolymerization process except with NH_4NO_3 as the supporting electrolyte and HNO_3 to adjust the solution pH, was examined by FT-IR spectroscopy. While most of this spectrum is identical with the one in Fig. 8.2, the strong peak at 1100 cm^{-1} does not appear. Instead, another strong peak at 1350 cm^{-1} is present in this new spectrum, which is normally assigned to NO_3^- (Nakamoto, 1963). This result indicates that ClO_4^- is indeed present in the coating. What should be emphasized is that the ClO_4^- ions are believed to be only physically trapped in the polymer network and no bond likely exists between the ClO_4^- ions and the organic compounds. An IR spectrum of poly(2-vinylpyridinium perchlorate) is available in the literature (Hummel, 1978), which has distinct differences from the spectrum of poly(2-vinylpyridine) formed by bulk polymerization or the spectrum of poly(2-vinylpyridine) formed by electropolymerization with ClO_4^- ions trapped in the structure (Fig. 8.2). More information about this aspect will be given later in the Raman spectroscopic studies.

The good correspondence of Fig. 8.2 to the published poly(2-vinylpyridine) IR spectrum also indicates that no organic by-product forms during the electropolymerization process. However, the spectral positions of the vinyl double-bond and the aromatic double-bond overlap in the wavelength range of 1400 to 1600 nm and therefore the 2-vinylpyridine spectrum is very similar to the one for poly(2-vinylpyridine). Therefore, one must be careful in concluding that polymerization has occurred on the basis of the FT-IR spectra alone. In addition to the results from u.v.-visible spectroscopy, further evidence of polymerization is found from the results of the NMR analysis.

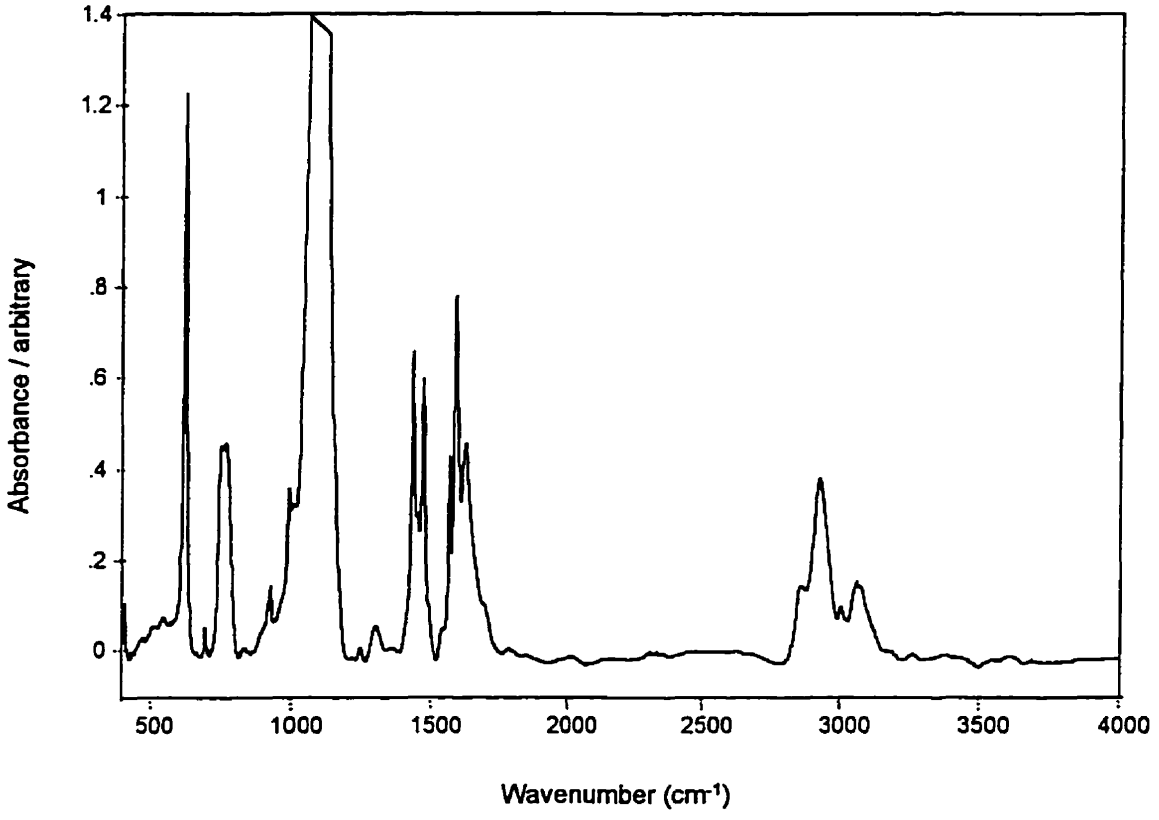

Fig. 8.2. FT-IR spectrum of poly(2-vinylpyridine) formed by electropolymerization with NH_4ClO_4 as supporting electrolyte. The conditions of the electropolymerization are same as described in the title of Fig. 8.1.

8.1.3. ^{1}H NMR Spectroscopy Characterization

The poly(2-vinylpyridine) coating formed by electropolymerization as described previously was dissolved completely in $DMSO_{-d6}$ for ^{1}H NMR spectroscopic analysis. The spectrum is shown in Fig. 8.3 and has been compared with the standard poly(2-vinylpyridine) ^{1}H NMR spectrum published in "The Aldrich Library of ^{13}C and ^{1}H FT NMR Spectra" (Pouchert and Behnke, 1993) and a good agreement is found. The characteristic absorbances of the methine protons of the ortho-substituted pyridine ring clearly appear at 7.3, 7.7 and 8.5 ppm. The characteristic absorbances of the aliphatic methine and methylene protons are also present at 1.8 and 3.0 ppm, respectively. The strong peak at 2.6 ppm is due to the $DMSO_{-d6}$ solvent and the absorbance at 3.5 ppm is from moisture in the polymer sample. There is no evidence of the methine proton associated with the C=C bond in the monomer, which otherwise should appear in the range of ~5 to 6 ppm. This confirms that all the vinyl double-bonds have been opened and the polymerization process is completed. A group of absorbance peaks that is usually assigned to aliphatic methyl protons are also found in the range from 1.3 to 1.5 ppm. This may be evidence of a hydrogen termination, which will also be discussed later.

8.1.4. Polymer Molecular Weight Measurement

Attempts to measure the molecular weight of the polymer coating formed using gel permeation chromatography met with little success. The basic problem in applying this technique to measure the molecular weight of the polymer coating formed is that the coating is not soluble in the commonly used organic solvents, such as tetrahydrofuran or

trichlorobenzene. It is likely that the polymer is somehow crosslinked. A mechanism for this possible crosslinking will be proposed later in Chapter 10.

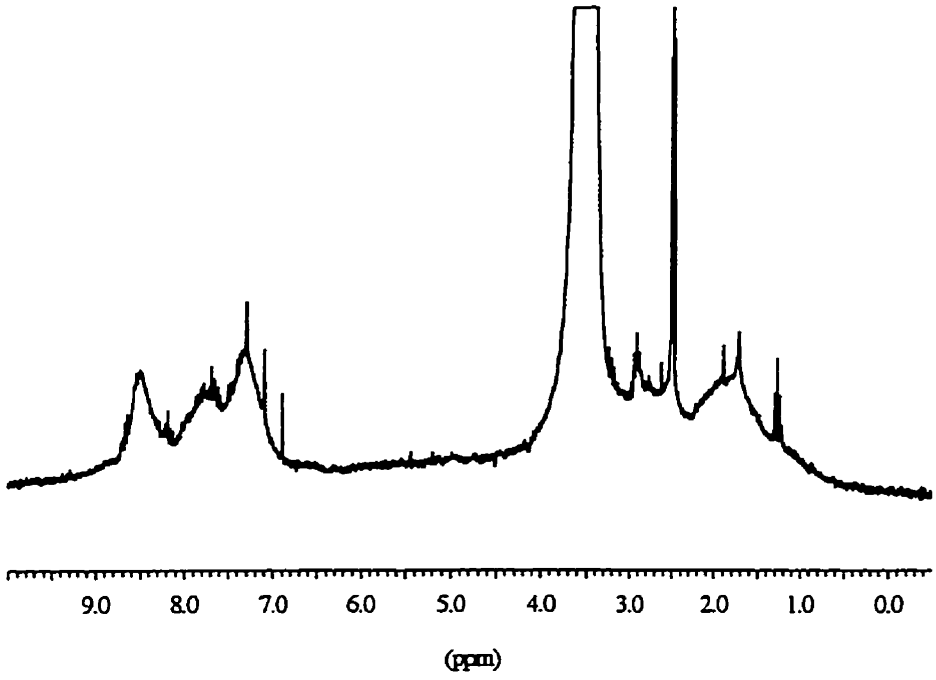

Fig. 8.3. ^{1}H NMR spectrum of poly(2-vinylpyridine) formed by electropolymerization as described in the caption for Fig. 8.1 and dissolved in $DMSO_{-d6}$.

8.2. Coating Property Measurement

8.2.1. Chemical Composition Measurement

The chemical composition of the polymer coating has been measured by isotope ratio mass-spectroscopy to yield the results given in Table 8.1. The coating is formed under the same conditions as described in the caption for Fig. 8.1. The elemental ratio of carbon to nitrogen (7.03:1) is very close to the stoichiometric value of 7:1 for poly(2-

vinylpyridine) $(C_7H_7N)_n$. However, the amount of hydrogen in the coating is somewhat higher than that expected from the poly(2-vinylpyridine) stoichiometry. Same as the ^1H NMR results, this may indicate that hydrogen ions or hydrogen radicals, formed by H^+ reduction at the cathode, play an important role in the electropolymerization process. Alternatively, very low molecular weight polymer could be being formed. A detailed discussion of this issue will be presented later.

Table 8.1. Elemental analysis of the formed polymer coating compositions. The coating is formed under the same conditions as described in the caption for Fig. 8.1.

	Elemental ratio (molar)		
	C : N	C : H	H : N
Experimental	7.03 : 1	1 : 1.06	7.42 : 1
Theoretical	7:1	1:1	7:1

8.2.2. Inorganic Impurity Measurement

Because of the yellow colour of both the poly(2-vinylpyridine) coating and the associated electrolytic solution, it was suspected that ionic iron species might also be formed as a result of a redox couple on the mild steel substrates. Iron could become trapped in the polymer coating and leak into the solution, causing them both to become yellow. Therefore, the polymer sample was examined by direct current plasma (DCP) spectroscopy in organic and aqueous solutions to detect the presence of iron and manganese species. The electrolyte was also examined for the same purpose. The coating is formed under the same conditions as described in the caption for Fig. 8.1. In either case, no iron or manganese species was detected above a detection limit of 50 ppb. This result

was not unexpected since all the electrochemical process was carried out entirely at electrode potentials below the system open circuit potential (E_{opc}). These DCP results, together with the previous results from the polymer characterization, indicate that the electrochemically produced poly(2-vinylpyridine) coatings are reasonably pure.

8.2.3. Glass Transition Temperature Measurement

The glass transition temperature (T_g) of the poly(2-vinylpyridine) coating polymer has been measured with a differential scanning calorimeter (DSC). The coating is formed under the same conditions as described in the caption for Fig. 8.1. The DSC diagram is shown in Fig. 8.4. The glass transition region covers a wide range of temperatures, indicating that there may be a broad distribution of the polymer molecular weights. However, the T_g is found to be quite high (105°C), indicating a high average molecular weight of the polymer. In the literature (Fell et al., 1993), it has been reported that poly(2-vinylpyridine) formed by bulk polymerization with a M_w of 300,000-400,000 has a T_g of 104°C.

8.2.4. Porosity Measurement

The coating porosity has been measured using the copper cementation experiments described by De Bruyne et al., (1995). After immersing a coated sample in a 0.1 M $CuSO_4$ solution for 30 seconds, the sample was rinsed with deionized water and air dried for the microscopic examination (with CSML). The coating is formed under the same conditions as described in the caption for Fig. 8.1, no trace of copper deposit was found on the coating surface, which otherwise would be distinguished from the polymer coating due to

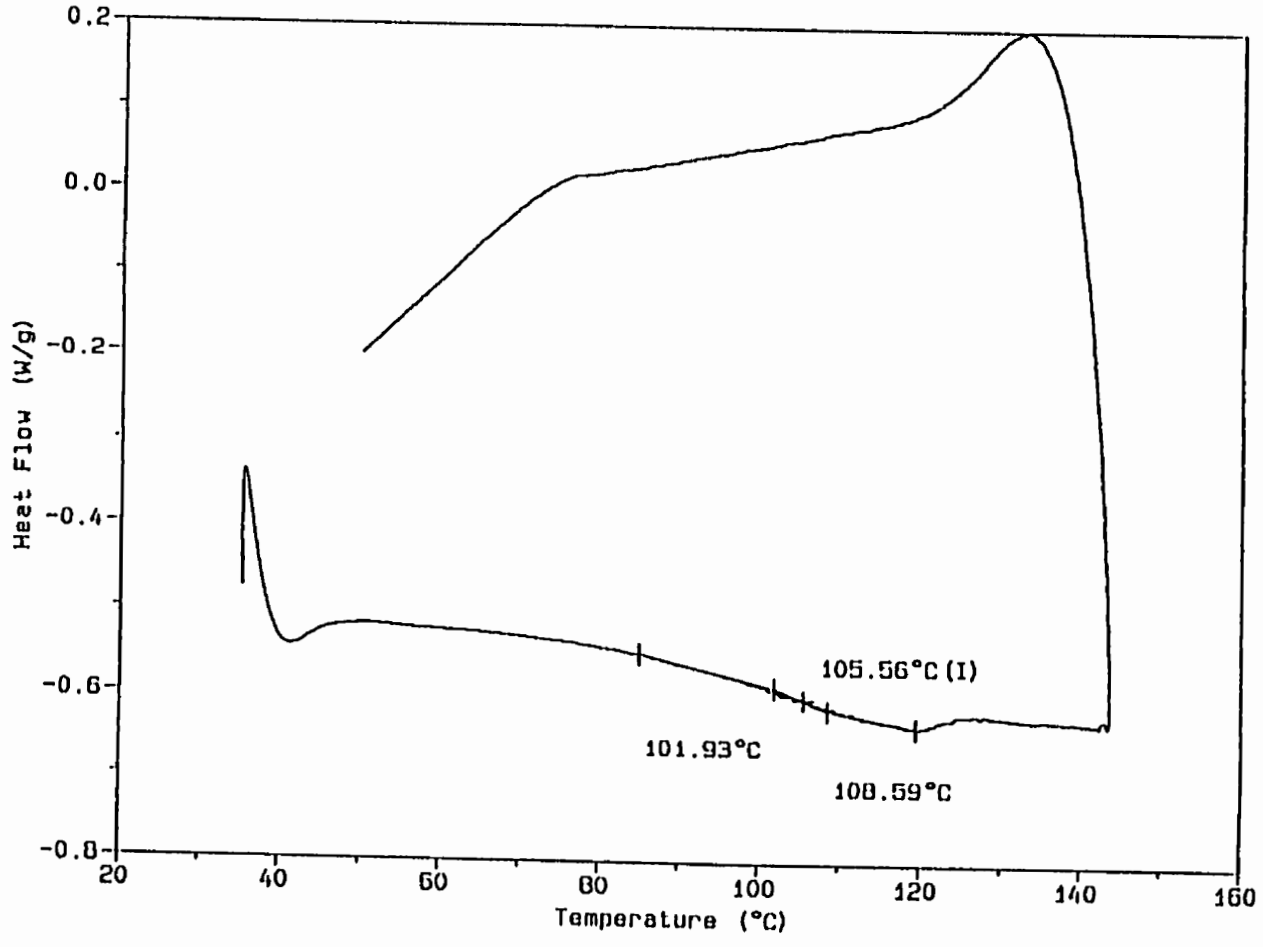

Fig. 8.4. Glass transition temperature measurement with DSC. The conditions of the electropolymerization is same as described in the title of Fig. 8.1.

the much higher intensity of reflected light for copper deposits. This suggests that the coating is non-porous, at least down to the resolution of the CSLM analysis (–0.5 μm).

8.2.5. Conductivity Measurement

The electrical conductivity of the coated samples (rather than of the coatings themselves) has been measured. The coating is formed under the same conditions as described in the caption for Fig. 8.1. Despite the variety of coating thicknesses, the coated samples have always been found to have infinite electrical resistance. In other words, the formed poly(2-vinylpyridine) coating is insulating. This result is consistent with that reported in the literature (Sekine et al., 1992; De Bruyne et al., 1995).

Questions arise as to how a thick insulating coating can be formed electrochemically and how it can be used in a polymer-modified electrode to support electrochemical reactions. Although some tentative explanations have been suggested in the literature, apparently no firm understanding or reasonable explanation has been presently available. Later in this thesis, an explanation will be given based on the experimental results and proposed mechanism.

8.2.6. Adhesion Measurement

The characteristics of the polymer coating adhesion on a mild steel substrate have been examined by the surface cross-hatching technique. The coating is formed under the same conditions as described in the caption for Fig. 8.1. Excellent surface adhesion of the poly(2-vinylpyridine) coating on the mild steel substrate has been confirmed qualitatively regardless of the coating thickness.

8.2.7. Corrosion Resistance Measurement

Polarization curves of coated metal samples before and after thermal curing were obtained to evaluate the corrosion resistance of the poly(2-vinylpyridine) coatings. The coating is formed under the same conditions as described in the caption for Fig. 8.1. Since very similar results were obtained from the coatings before and after the thermal curing, only a polarization curve from a coating before the thermal curing is shown in Fig. 8.5. For the purpose of comparison, a polarization curve of a bare mild steel coupon has also been obtained and presented in Fig. 8.5. It is found that after the metal sample is coated with poly(2-vinylpyridine), the system open circuit potential is shifted negatively and the corrosion current is diminished significantly. These results indicate that the corrosion resistance of a coated sample is increased. This finding is consistent with that obtained by Sekine et al. (1992) using the ac impedance technique and by De Bruyne et al. (1995) using the polarization technique. In addition, it was found that there was no significant difference in the corrosion resistance of the coated samples before and after thermal curing. This results agree with the report of De Bruyne et al. (1995), but differ from that reported by Sekine et al. (1992). De Bruyne's coating however was formed at elevated temperature (50~70 °C) on zinc substrates, while our coatings are formed at 20°C on mild steel, which is similar to Sekine's procedure. The reason for this disagreement may be due to the crosslinking of our polymer sample. More details about the polymer sample crosslinking will be discussed later in the process mechanism section.

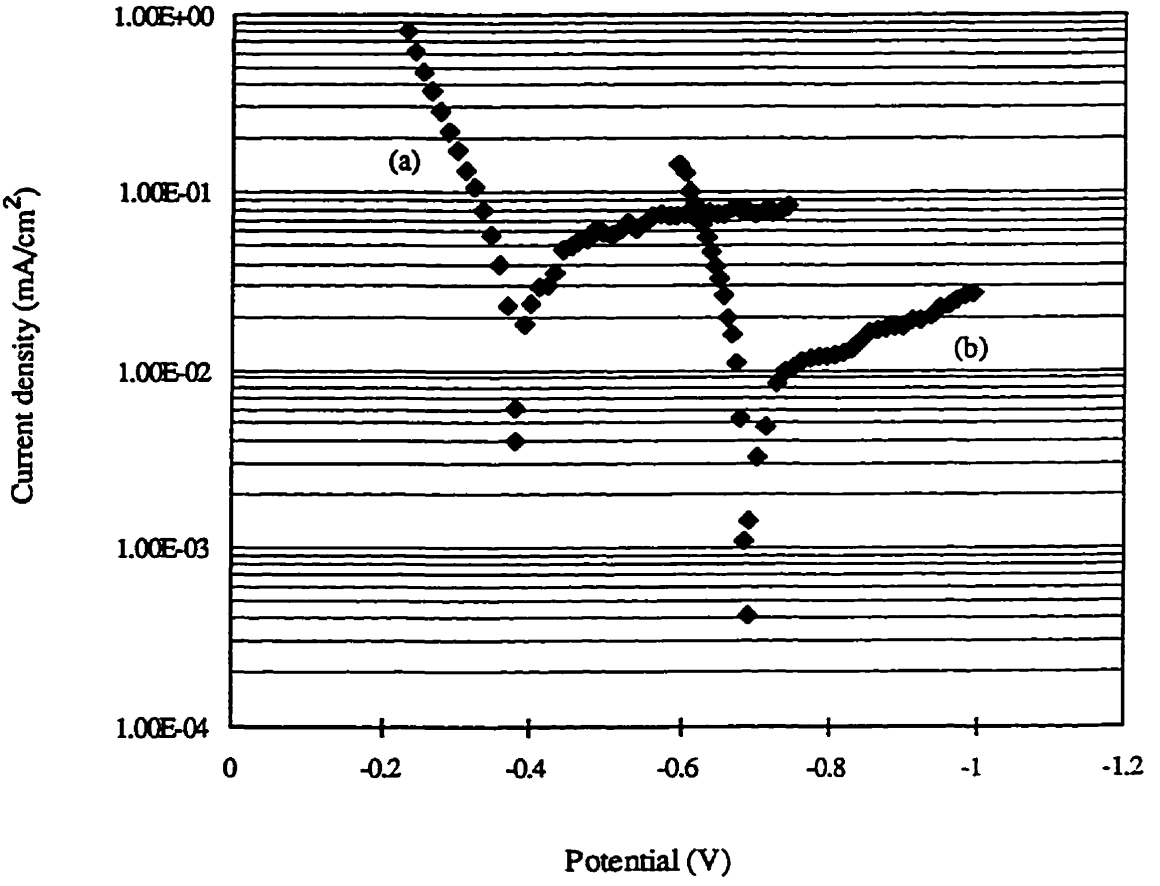

Fig. 8.5. Comparison of polarization curves for (a) bare mild steel and (b) mild steel coated with poly(2-vinylpyridine) formed by electropolymerization. The coating formation follows the same procedure as described in Fig. 8.1. The samples are immersed in 3% NaCl solution for 3 hours under ambient conditions before the polarization curves are taking.

8.3. Coating Morphology Analysis

Coating morphology evaluation has been carried out using confocal scanning laser microscopy (CSLM). The surface scanning and image processing follow the procedure described in Section 5.6. The images shown in Fig. 8.6 represent a 200 μm × 200 μm area of a coating formed under the same conditions described in the caption for Fig. 8.1. Figs. 8.6a to 8.6d are the 2nd, 14th, 26th and 38th slice (intensity) image, respectively, taken from the entire set of 40 images. Focused parts of the surface are clearly shown in each image, while all other parts of the surface are out of focus. The big advantage of CSLM is that out-of-focus planes are totally eliminated. Fig. 8.7a is the maximum intensity image of the top surface of the coating, obtained by combining the entire set of intensity images. Similarly, the maximum intensity image of the steel substrate directly underneath the coating imaged in Fig. 8.6 has been obtained and is shown in Fig. 8.7b. The 3-D reconstructed surface topographic images of the coating and substrate in Figs. 8.6 and 8.7 are presented in Figs. 8.8a and 8.8b, respectively. By combining Figs. 8.8a and 8.8b, a volumetric portion of the polymer coating layer can be imaged, as shown in Fig. 8.9. This volumetric portion of the polymer coating layer has the advantage of providing a good stereoscopic expression of the specific coating. It should be noted that the coating thickness is more uniform than what would be expected based only on the morphology of the top surface of the coating in Fig. 8.8a. Some of the relief in the top surface is caused by the topography of the substrate. The topography of the polymer coating conforms reasonably to the topography of the metal substrate, although it is somewhat smoother. On the whole, the coating is smooth and so distinct features do not appear in the images.

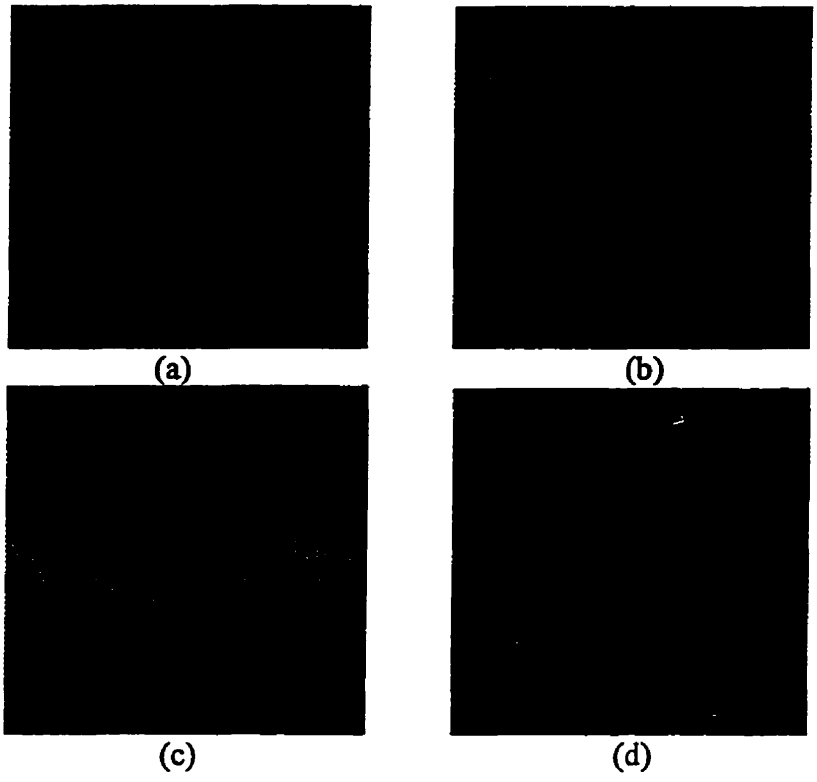

Fig. 8.6 CSLM images of a poly(2-vinylpyridine) coating (200 μm × 200 μm) formed by electropolymerization. (a), (b), (c) and (d) are the 2nd, 14th, 26th, and 38th image, respectively, of the entire set of 40 images. The coating formation follows the same procedure mentioned in Fig. 8.1. The surface scanning and image processing follow the procedure described in Section 5.6.

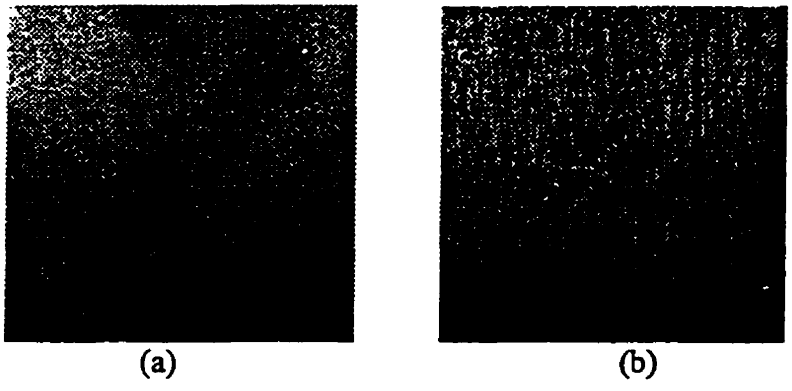

Fig. 8.7 CSLM images of a poly(2-vinylpyridine) coating formed by electropolymerization (200 μm × 200 μm). Maximum intensity image of (a) the coating surface, and (b) the metal substrate which locates at the same surface area as image (a).

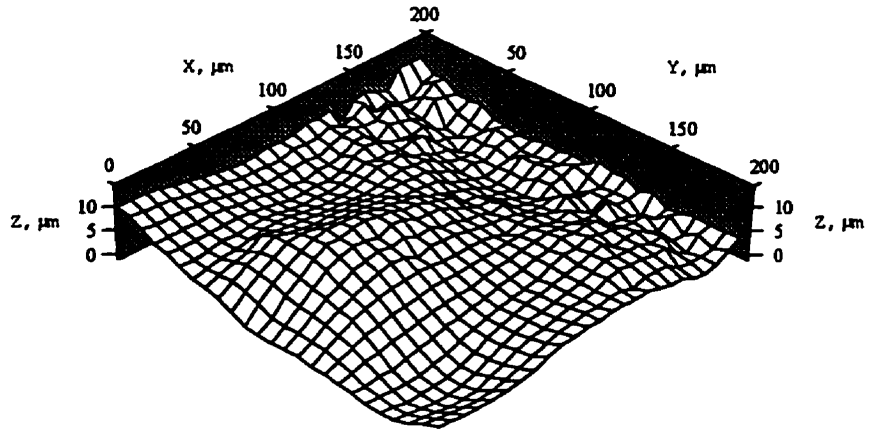

(a)

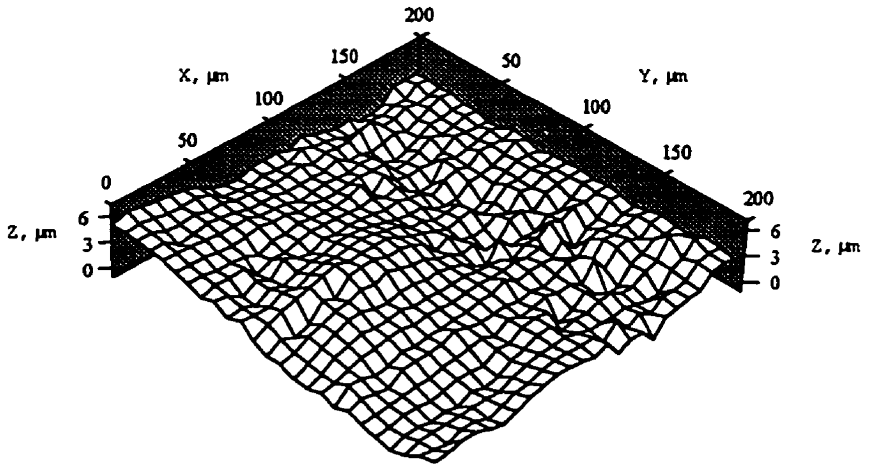

(b)

Fig. 8.8. 3-D reconstructed surface topography of (a) the polymer coating and (b) the metal substrate in Figs. 8.7a and 8.7b. The coating formation and image processing follow the same procedures mentioned in the text.

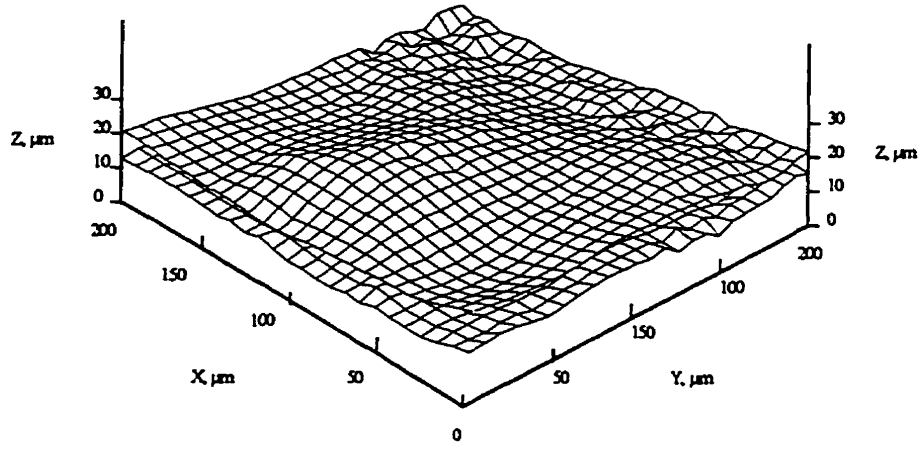

Fig. 8.9. The volumetric portion of the scanned polymer coating: a combination of the images in Figs. 8.8a and 8.8b. The polymer coating surface is shown above the metal substrate surface. The coating formation and image processing follow the same procedures as in Fig. 8.8.

A side profile of the coating obtained by a cross-sectioning laser beam scan over an arbitrarily chosen direction within the scan area of the previous figures is presented in Fig. 8.10a. Such a figure is very useful since it provides direct visualization of the thickness and uniformity of the coating. Two bright bands appear across the entire scan length in Fig. 8.10a. The upper band corresponds to the coating/air interface, while the lower band corresponds to the coating/steel interface. It is interesting to note that the lower band is brighter than the upper one despite the fact that it is below the outer surface. This is due to the larger change in the refractive index across this interface than across the coating/air interface.

Fig. 8.10b shows how the intensity of the reflected light varies along the vertical direction at a particular point along the scan line. Two sharp peaks appear at depths of 6.1

μm and 13.3 μm (measured from an upper reference point) and correspond to the top points of the coating and substrate, respectively. The coating thickness at this particular location which is given by the spacing between the maxima of these peaks is found to be 7.2 μm. Such a thickness is typical of that obtained for poly(2-vinylpyridine) in this study and is much smaller than that reported by others using gravimetric methods (De Bruyne et al., 1995). By repeating this process at a number of points along the line, the variation of thickness along the line can be determined. This allows flaws in the coating, as small as the image resolution (e.g., 0.4 μm in Fig. 8.10b), to be detected, which is difficult to achieve with a standard microscope.

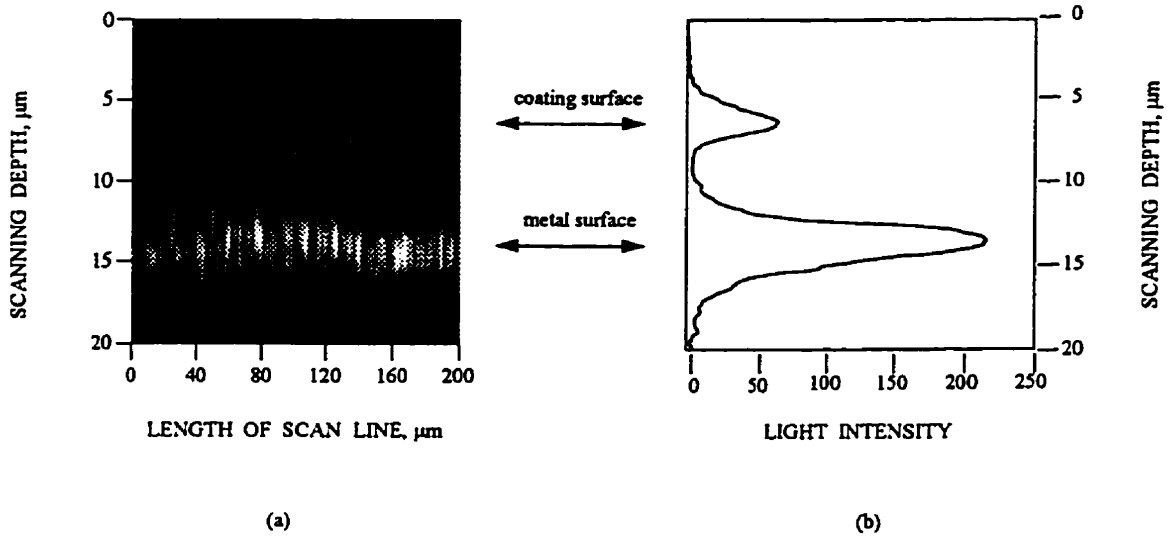

Fig. 8.10. A line scan image of the sectional coating thickness profile. The line was randomly selected from the same surface as Fig. 8.6. The two bright bands in (a) highlight the top outlines of the polymer coating and metal substrate (20 μm × 200 μm). The plot shows the variation of reflected light intensity with depth into the specimen.

The coating density can be estimated by combining the average coating thickness obtained above with the sample weight increase before and after electropolymerization. For example, for the coating in Figs. 8.6 to 8.10 (i.e., 7.9 mg coating on 5.5 cm^2 substrate with an average thickness of 7.2 μm), a density of 1.99 g/cm^3 is obtained. This value differs significantly from the value of 0.9985 g/cm^3 for the 2-vinylpyridine monomer (Weast and Astle, 1992) and the value of 1.153 g/cm^3 for poly(2-vinylpyridine) formed by bulk polymerization (Miller, 1983).

To test the reliability of the density determination, the density value of 1.99 g/cm^3 has been used to estimate the coating thickness for another poly(2-vinylpyridine) film produced by the same process as mentioned above after 1.5 hours of CPS electrolysis. The sample shows a weight increase of 5.6 mg, which is calculated to have a coating thickness of 5.1 μm based on the above density. This result compares favourably to a value of 5.2 μm obtained by direct graphic analysis of the light intensities from the CSLM images. This close agreement also indicates that the densities of both coatings are very similar. If the density of the polymer formed by bulk polymerization were used for above calculation, a large error would have been introduced in estimating the coating thickness; an even larger error would have been introduced if the density of the monomer were used. The results of the sample calculations are summarized in Table 8.2. These results suggest that the values of coating thickness reported in the recent publication (De Bruyne et al., 1995) overestimate the true values considerably, where the values of coating thickness were calculated from a hypothetical specific gravity of coating of 1 kg/dm^3.

Table 8.2. Coating thickness estimated by different methods

Methods	Coating thickness (μm)
Thickness by direct measurement using CSLM.	5.2
Thickness calculated from coating weight (5.6 mg) and area (5.5 cm^2), using the measured polymer coating density of 1.99 g/cm^3.	5.1
Thickness calculated from same coating weight and area using the density of 1.153 g/cm^3 for polymer formed by bulk polymerization	8.8
Thickness calculated from same coating weight and area using the monomer density of 0.9985 g/cm^3.	10.2
Thickness calculated from same coating weight and area using the hypothetical density of 1 kg/dm^3 as used by De Bruyne et al. (1995).	10.2

It is important to point out that the measured coating density is abnormally higher than that of a polymer product from a bulk polymerization. Although it is not unusual for the polymer to have a higher density (up to 30%) from a polymerization process with branching and crosslinking involved, it is abnormal to have a density of about 100% higher than that from the bulk polymerization. A possible resource of this error may be from the fact that the refractive indexes of the coating and the testing environment (e.g., the air) are different. A more detailed discussion of this aspect will be presented later.

Another important application of CSLM in coating morphology analysis is to measure quantitatively the coating surface roughness distribution. It is obvious that a uniform surface should show a narrow roughness distribution, while a very irregular surface will have a wide roughness distribution. Fig. 8. 11 shows a finely polished metal substrate surface (1 mm × 1 mm). Fig. 8.11a is the maximum intensity image of the surface. Fig. 8.11b depicts the surface roughness distribution diagram obtained from Fig.

8.11a with necessary image processing. The regular nature of the coating is clearly shown in this distribution diagram. The surface height gives the distance of a point on the surface to some reference point. An elevation of 0 μm corresponds to the highest surface point, while a height of 9 μm corresponds to the lowest point on the surface. Fig. 8.11c is the 3D reconstructed surface topography. Fig. 8.12 shows an image of a larger area (4 mm × 4 mm) of a poly(2-vinylpyridine) coating obtained under similar experimental conditions as mentioned previously but at a pH of 7.5. Only a patchy coating is formed at this pH, as can be observed from the relevant maximum intensity image (Fig. 8.12a). The irregular nature of such a coating is clearly shown in the distribution diagram of surface height presented in Fig. 8.12b. The irregular nature of the coating is further illustrated in the sectional scan (20 μm × 200 μm) in Fig. 8.12c. Although this scan shows that coating is present everywhere along the arbitrary direction chosen, the thickness varies from 4.5 μm at point *a* to 8 μm at point *b*. This variation is very large considering that the coating is less than 10μm everywhere. It should be noted that over other portions of the substrate, no coating has formed whatsoever. Obviously, the determination of an average thickness based on the gravimetric method is meaningless for the purpose of characterizing coatings such as the one shown in Fig. 8.12.

The above results on the coating morphological analysis with CSLM have also been published recently (Ling et al., 1998b).

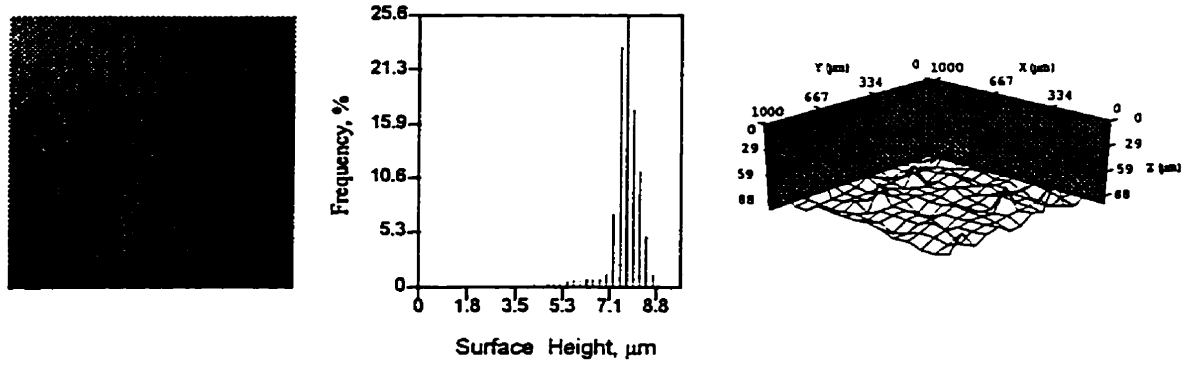

(a) (b) (c)

Fig. 8.11a: An maximum intensity image (1 mm × 1 mm) of a finely polished metal substrate. Fig. 8.11b: Surface roughness distribution diagram of the metal substrate. The smooth surface leads to a narrow distributed surface roughness. Fig. 8.11c: A 3D reconstructed surface topography of the metal substrate.

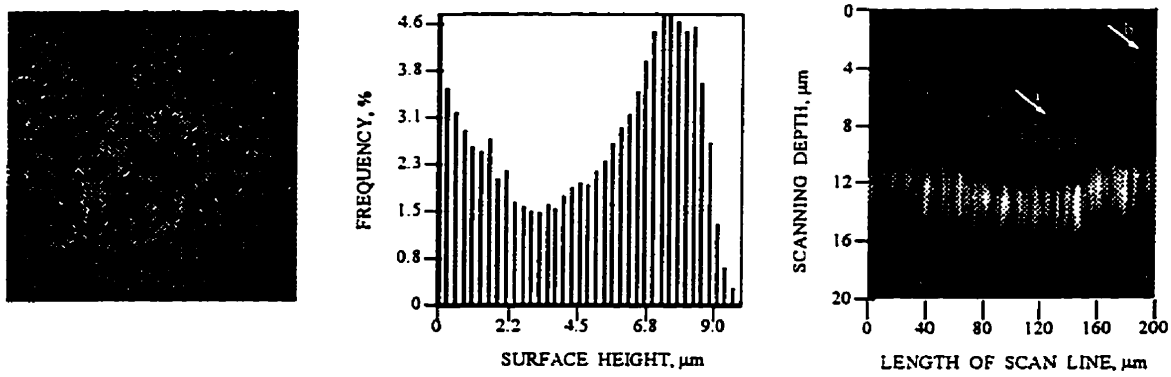

(a) (b) (c)

Fig. 8.12a: An maximum intensity image (4 mm × 4 mm) of an irregular coating obtained with similar experimental conditions to those in Fig. 8.10, but at a pH of 7.5. Fig. 8.12b: Surface roughness distribution diagram of the polymer deposit in Fig. 8.12a. Fig. 8.12c: A sectional scan of the surface along an arbitrary direction chosen direction (20 μm × 200 μm).

CHAPTER 9

RESULTS AND DISCUSSION — PART FOUR: MECHANISM STUDIES OF POLY(2-VINYLPYRIDINE) COATING FORMATION BY ELECTROPOLYMERIZATION

9.1. Inhibition Study

Previous investigators have suggested that poly(2-vinylpyridine) coating formation by electropolymerization might occur by either an anionic polymerization mechanism or a combination of anionic and free radical polymerization (Sekine et al., 1992; De Bruyne et al., 1995). However, in view of the reaction conditions, it does not seem likely that an anionic aqueous mechanism would be possible since the polymerization is carried out in an acidic medium with methanol as a co-solvent. Anionic processes prefer an aprotic medium and require exclusion of proton-donating materials during the course of reaction. Methanol and acidic aqueous solutions are normally used as terminators for an anionic process (Morton, 1983). Consequently, it would be difficult for any anionic-polymerization-based mechanism to occur under the condition used in this project.

To test for a free radical mechanism, free radical inhibitors and scavengers such as *p*-benzoquinone and DPPH (10^{-3} M) were added to the electrolyte prior to electropolymerization. The other solution components were left unchanged, as described

in the caption for Fig. 8.1. The two-hour process was carried out either by CPS (between −0.7 and −2.5 V at 30 mV/s) or chronoamperometric electrolysis (at −1.3 V).

For the chronoamperometric electrolysis with *p*-benzoquinone, intense hydrogen evolution was observed at the cathodic surface throughout the process. The electrolysis current remained at a high level, although it decreased slowly during the electrolysis (Fig. 9.1). The appearance of the solution was altered noticeably during the electrolysis, starting from the green colour of benzoquinone to dark brown and eventually black. After a two-hour electrolysis, some black deposit was found on the cathode surface. The deposit did not cling to the substrate well and was easily flushed away by a stream of water.

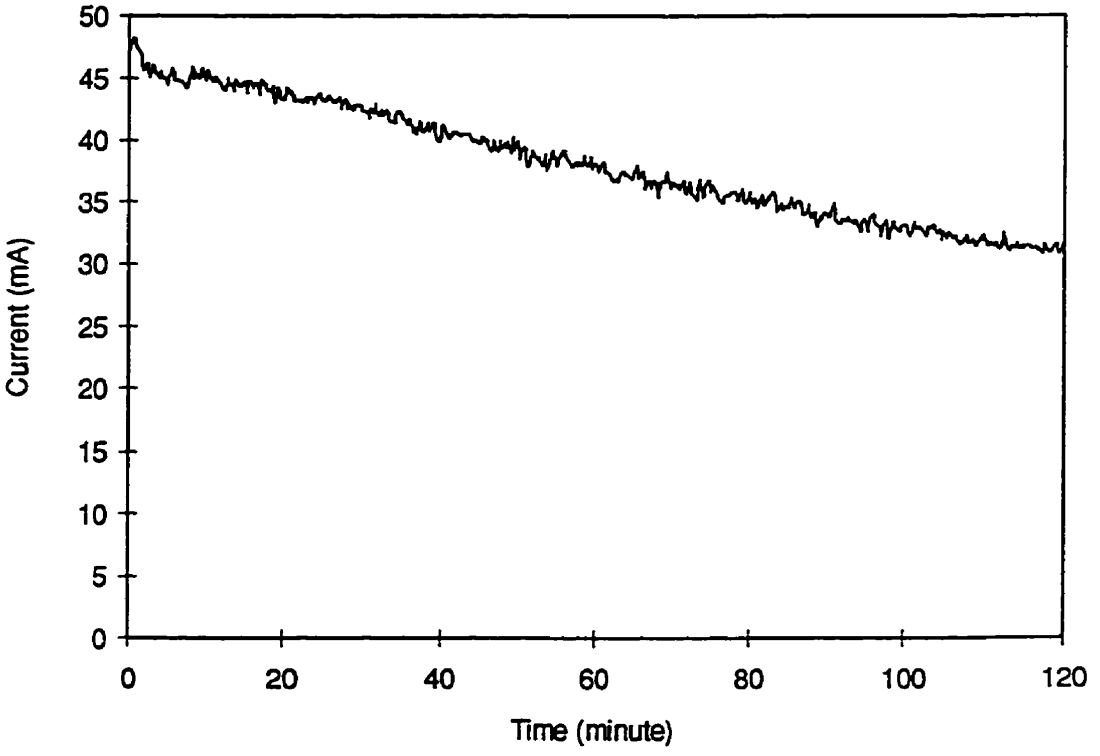

Fig. 9.1. The effect of *p*-benzoquinone (10^{-3} M) on the electropolymerization process. The i-t diagram of a two-hour chronoamperometric electrolysis at −1.3 V. The electrolyte and operating conditions are the same as described in Fig. 8.1.

A similar phenomenon was observed during the CPS electrolysis. The peak current of the process remained high and intense hydrogen evolution was observed throughout the process (Fig. 9.2a). A slightly more black deposit was collected from the cathode surface than that during the chronoamperometric process. The deposit was washed and dried and dissolved in methanol for u.v.-visible spectroscopic examination. No characteristic band of 2-vinylpyridine or poly(2-vinylpyridine) was observed in the spectrum, indicating no polymer coating was formed in the presence of *p*-benzoquinone inhibitor.

Although no polymer has been formed during the electrolysis in the presence of *p*-benzoquinone, monomer reduction could still occur at the cathode surface. This is confirmed by the appearance of a series of reduction waves for 2-vinylpyridine in the i~t curves for the CPS electrolysis (Fig. 9.2b). No such information could be obtained from the i~t curve of the chronoamperometric process. The CPS technique is therefore useful for diagnostic purposes in addition to being an effective method for producing coatings.

When DPPH was used, no visible coating was observed on the substrate at the end of a two-hour CPS electrolysis. Intense hydrogen evolution was observed at the cathodic surface throughout the process. Similar to the observation when *p*-benzoquinone was used, the electrolysis current remained high throughout the processes of both the chronoamperometric and the CPS electrolysis. The corresponding i-t diagrams are similar to Fig. 9.1 and 9.2, respectively. During the electrolysis, the solution colour changed from deep violet to light yellow. This colour change, together with that in the case of *p*-benzoquinone, indicates that some redox reactions involving the inhibitors likely occur. Some possible reactions have been suggested in the literature (Odian, 1983). Detailed studies of these reactions are beyond the scope of this project.

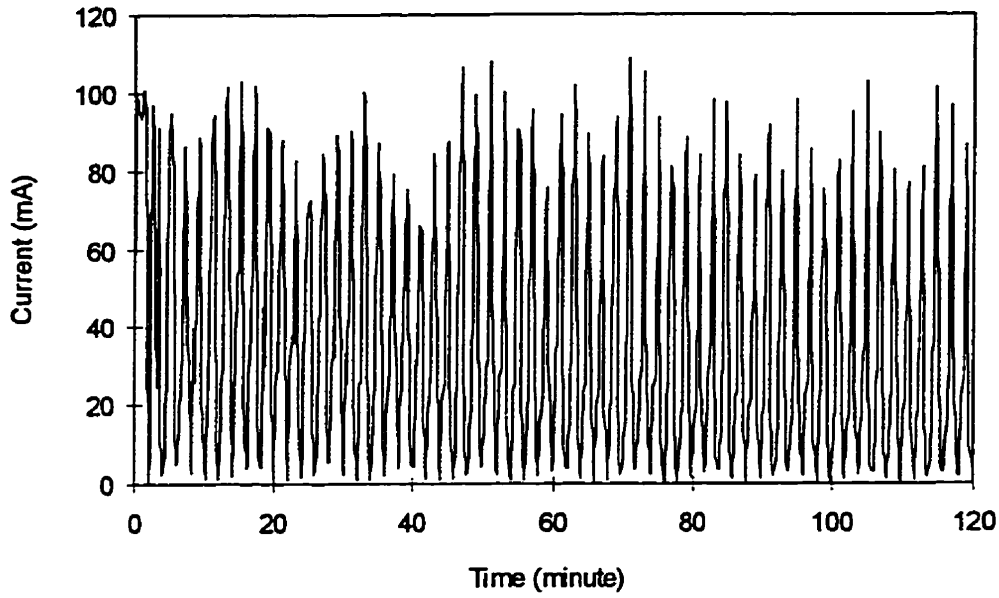

(a)

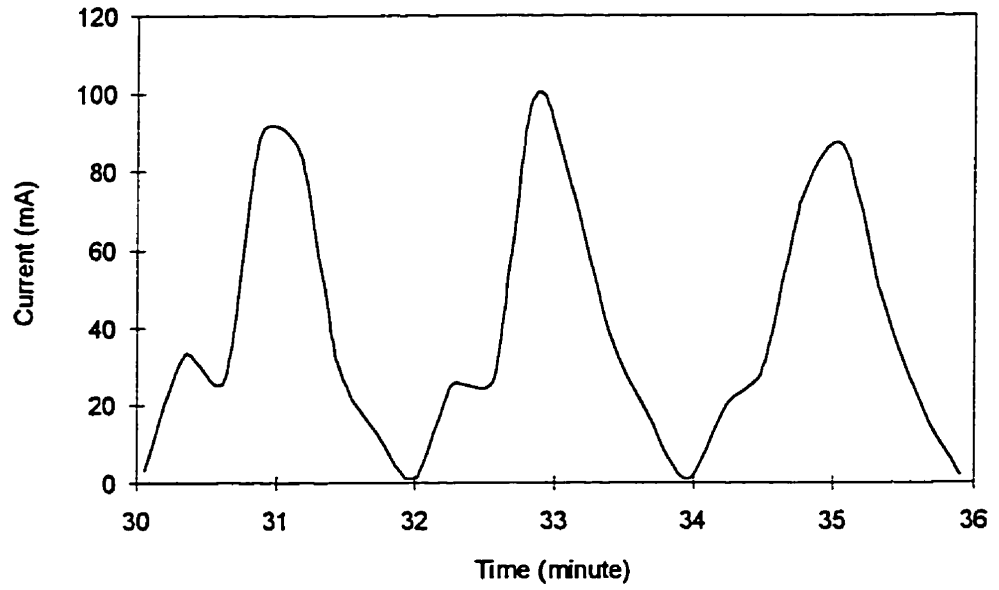

(b)

Fig. 9.2. The effect of *p*-benzoquinone (10^{-3} M) on the electropolymerization process. The i-t diagram of a two-hour CPS electrolysis between –0.7 and –2.5 V at 30 mV/s. The other operating conditions are the same as described in Fig. 9.1. Fig. 9.2b is an enlarged portion of the i-t diagram of Fig. 9.2a.

Although it is still difficult to determine if any anion is generated at the cathode during the electropolymerization, it is certain that no anion contributes to the formation of the polymer coating due to the strong proton-donating environment of the system. Therefore, it can be concluded that poly(2-vinylpyridine) coating formation by electropolymerization is a free radical process.

Table 9.1. Summary of the experimental results from the inhibition study of the mechanism of poly(2-vinylpyridine) coating formation in acidic aqueous media by electropolymerization. The experimental conditions are described in Fig. 9.1.

Inhibitor and its concentration	**Coating weight ± 0.3 (mg)**	**Comments**
p-benzoquinone (10^{-3} M) †	0.7	Scattered black deposit
p-benzoquinone (10^{-3} M) ‡	1.5	Scattered black deposit
DPPH (10^{-3} M) †	—	No visible coating formed
DPPH (10^{-3} M) ‡	—	No visible coating formed. Violet solution changes to yellow.
no inhibitor ‡	7.9	Thick and uniform coating with yellow colour

†: Chronoamperometric electrolysis at −1.3 V for 2 hours.

‡: CPS electrolysis between −0.7 and −2.5 V at 30 mV/s for 2 hours.

9.2. Surface Enhanced Raman Scattering Spectroscopic Study

9.2.1. Ordinary Raman Scattering of the Bulk Solution

An ordinary Raman spectrum of neat 2-vinylpyridine was obtained to serve as a reference (Fig. 9.3). The spectrum has been compared with a standard Raman spectrum of 2-vinylpyridine in the literature (Lin-Vien et al., 1991) and good agreement is found.

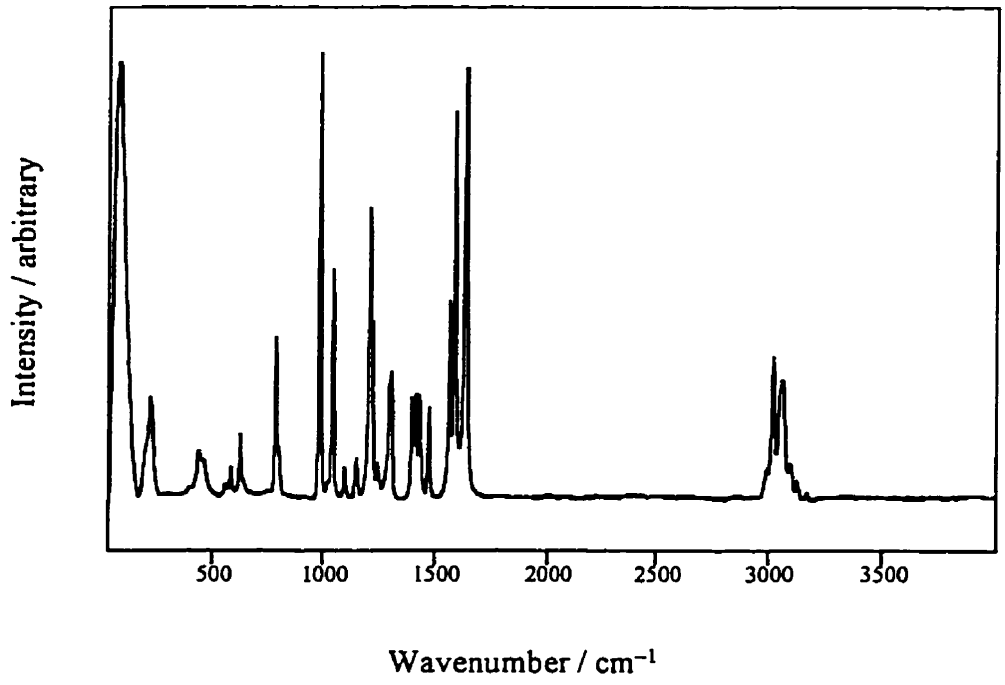

Fig. 9.3. Ordinary Raman spectrum of neat 2-vinylpyridine at 20°C.

Spectra of 0.25 M 2-vinylpyridine aqueous solutions containing 20% methanol were then obtained at different values of solution pH (Fig. 9.4). Results are shown for electrolytes at pH 10.0, 7.4, 4.8 and 1.0 in which NH_4OH or $HClO_4$ was used for pH adjustment (initial pH = 7.4). Comparison of Fig. 9.3 with Fig. 9.4 shows that the spectrum for pure 2-vinylpyridine does not contain the strong water absorbance peak at

high wavenumber (> 3100 cm^{-1}) nor the absorbances at 2848, 2952 and 1453 cm^{-1}, both of which are present in the spectra of the aqueous-methanol solution. The characteristic band for ClO_4^- at 932 cm^{-1} appears in the solution spectra in Fig. 9.4 as well as changes in intensity due to the variation of the ClO_4^- concentration in the solutions. No ClO_4^- absorbance appears in the pure 2-vinylpyridine spectrum. There is no distinct band observed in either figure in the range of 1700 to 2800 cm^{-1}, indicating that no pyridine-chlorine bond exists in the system (Lin-Vien et al., 1991).

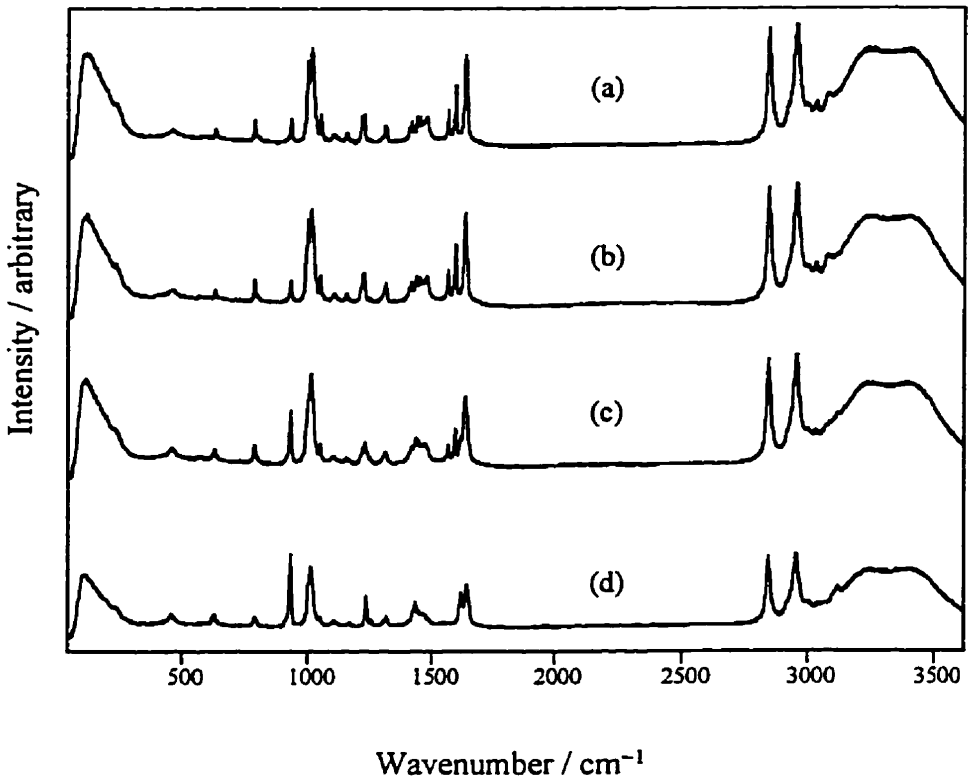

Fig. 9.4. Ordinary Raman spectra from a 0.25 M 2-vinylpyridine aqueous solution (with 20% methanol) at 20 °C and at different solution pH, adjusted with concentrated $HClO_4$ or NH_4OH. (a) pH = 10.0; (b) pH = 7.4; (c) pH = 4.8; (d) pH = 1.0.

In Fig. 9.4, the effect of pH on the extent of protonation of 2-vinylpyridine in aqueous medium can be seen. The most striking differences in these spectra are in the 1550-1650 cm^{-1} double-bond stretching region that is shown in more detail in Fig. 9.5. The spectrum from a low pH solution (Fig. 9.5d) has a distinct band at 1619 cm^{-1}, which has been reported previously (Putterman et al., 1979) and assigned to the ν_{8a} ring mode of the pyridinium ion on the basis of similar bands in substituted (Clements and Wood, 1973a) and unsubstituted (Clements and Wood, 1973b) salts. This band becomes weaker as the solution pH increases to 4.8 (Fig. 9.5c) and totally vanishes at pH 7.4 (Fig. 9.5b) and 10 (Fig. 9.5a). The bands at 1565 and 1595 cm^{-1} in pure 2-vinylpyridine are normally assigned to ν_{8a} and ν_{8b} modes of the neutral pyridine ring. It is observed that these bands appear in the spectrum for pure 2-vinylpyridine in Fig. 9.3 and the solution spectra at pH 7.4 and 10.0 (Figs. 9.5a and 9.5b). These bands become weaker as solution pH decreases (Fig. 9.5c) and totally vanish at very low pH (Fig. 9.5d). Only at pH 4.8 do the peaks for both the neutral and protonated forms of the monomer co-exist. Comparison of Figs 9.5a and 9.5b shows that the spectra above pH 7.4 are identical. This indicates that the protonation of 2-vinylpyridine is no longer changing and that 2-vinylpyridine is likely completely neutral once a pH of 7.4 is reached. It is also noticed that the band at 1630 to 1640 cm^{-1} from the spectra of both pure 2-vinylpyridine and the higher pH solutions (down to pH 4.8) is shifted to 1640 to 1650 cm^{-1} at pH 1.0. The reason for this shift is not clear.

These spectra are consistent with the pH dependence of 2-vinylpyridine protonation in aqueous solution and its effect on electropolymerization postulated previously. At high pH (e.g., pH > 7.4), most of the 2-vinylpyridine molecules exist in

their neutral form in the solution and so a further increase in pH has no effect on 2-vinylpyridine protonation. At low solution pH (e.g., pH = 1), most of the 2-vinylpyridine molecules exist in their protonated form. When the solution pH has an intermediate value (e.g., pH = 4.8), both neutral and protonated 2-vinylpyridine species co-exist in the solution and consequently, the corresponding spectrum has the characteristics of both forms. These results are also consistent with the reported *p*Ka value for the protonation of 2-vinylpyridine (Perrin, 1965). As shown in Chapter 6, only at this intermediate pH when both neutral and protonated forms of 2-vinylpyridine are present in solution can good quality polymer films be formed via electropolymerization.

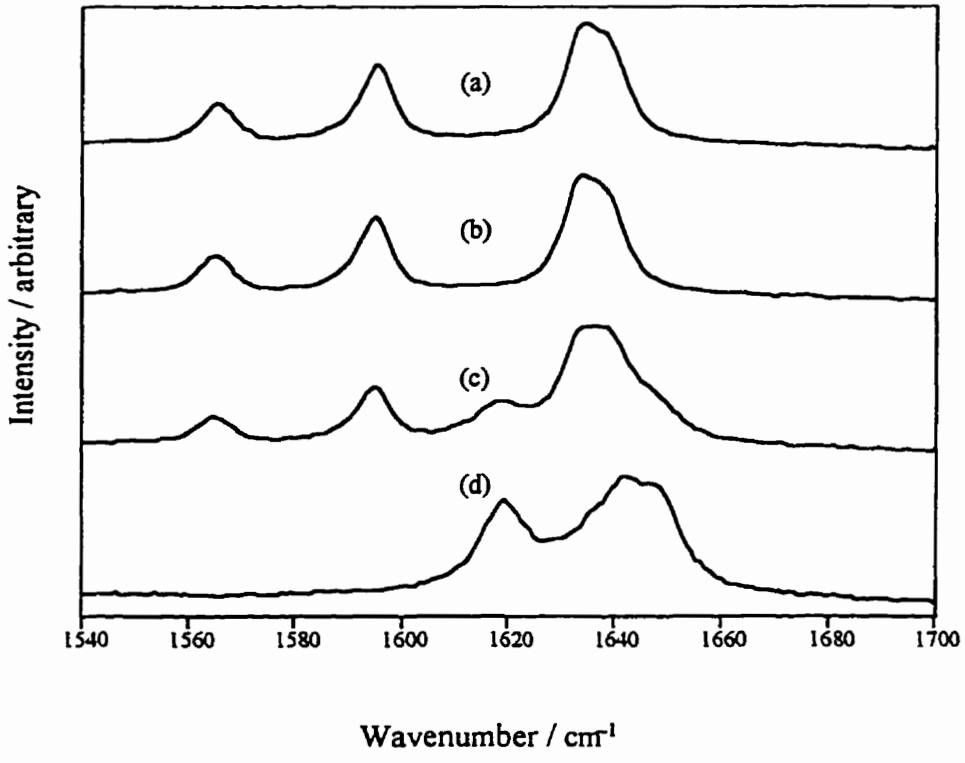

Fig. 9.5. Detailed view of the range from 1540 to 1700 cm^{-1} of the Raman spectra in Fig. 9.4. (a) pH 10.0; (b) pH 7.4; (c) pH 4.8; (d) pH 1.0.

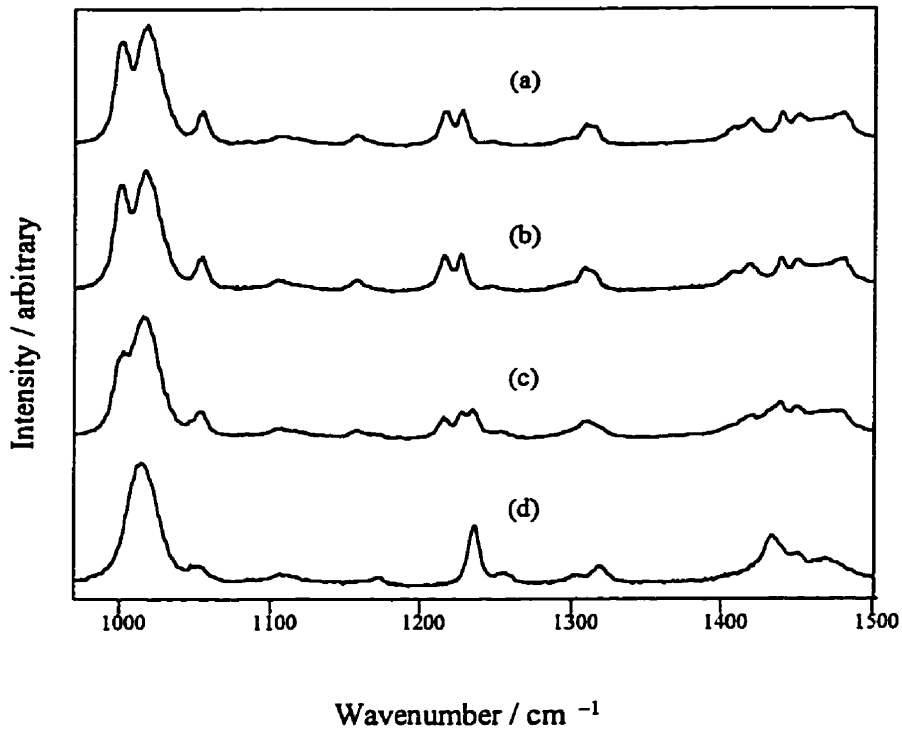

Fig. 9.6. Detailed view of the range from 970 to 1500 cm^{-1} of the Raman spectrum in Fig. 9.4. (a) pH 10.0; (b) pH 7.4; (c) pH 4.8; (d) pH 1.0.

Other changes are also evident in other bands shown in Fig. 9.6, although not all these bands have been definitively assigned. A double-peaked band at 1215 and 1228 cm^{-1} is converted to a single-peaked band at 1236 cm^{-1} when solution pH decreases from 7.4 to 1.0. Meanwhile, the spectrum at pH 4.8 shows a triple-peaked band, containing the characteristic bands from both high and low pH solutions. This 1236 cm^{-1} band is normally assigned to N-H in-plane wag (Lin-Vien et al., 1991). Another double-peaked band appears at 1001 and 1016 cm^{-1} at high pH (Figs. 9.6a and 9.6b). When the solution pH decreases, the peak at 1001 cm^{-1} first diminishes to a shoulder at pH 4.7 (Fig. 9.6c) and then totally disappears at pH 1.0 (Fig. 9.6d). Meanwhile the band at 1016 cm^{-1} does

not change. Similarly, a multi-peaked band in the range from 1400 to 1500 cm^{-1} shows similar changes as the solution pH is altered.

On the other hand, it is also observed that some bands do not shift during the change of solution pH. Among them are the bands at 1016 and 1450 cm^{-1}. Although the band at 1054 cm^{-1} does not shift in position, it is found to decrease in size as the solution pH decreases. Since no assignments for these bands are available, it is not possible to attribute these changes definitively to protonation of 2-vinylpyridine. However, their similarity to the trends observed for the peaks in the vicinity of 1600 cm^{-1} suggests that they may be related to 2-vinylpyridine protonation.

The characteristic bands of pure and dissolved 2-vinylpyridine obtained above, together with other Raman spectra in the literature (Lin-Vien et al., 1991), are used in the next sub-section for comparison with SERS spectra obtained from electropolymerization on copper electrodes.

9.2.2. SERS at Copper Electrode Surfaces

When the electrolytic cell is operated at its open circuit potential (E_{opc}) of –0.18 V in a solution of pH 4.8, the SERS spectrum obtained for the surface of a copper electrode immersed in a 0.25 M 2-vinylpyridine solution (Fig. 9.7a) is similar to the ordinary Raman spectrum in Fig. 9.4 for the bulk solutions, but without the characteristic bands of water and methanol. This indicates that the monomer is preferentially adsorbed and no significant adsorption of water or methanol occurs at the electrode surface. When the potential of the working electrode (E_w) was increased in the positive direction (i.e., $E_w > E_{opc} = -0.18$ V), changes in the spectra are observed. At E_w of –0.1 and 0 V (Figs. 9.7b

and 9.7c, respectively), the characteristic band for the pyridinium ion at 1619 cm^{-1} disappears from the spectra, while the characteristic band for the neutral pyridine ring at 1565 cm^{-1} remains unchanged and the band at 1595 cm^{-1} shifts to 1601 cm^{-1}. (It may be worthwhile to point out that the peak at 1630-40 appears at all potentials.) This suggests that only the neutral form of vinylpyridine molecule is now adsorbed on the copper surface and the pyridinium ions have been repelled from the working electrode which is now anodic. It is also observed that a new band at 1538 cm^{-1} appears and a band at 1449 cm^{-1} disappears when the working electrode becomes anodic. No explanation has been made for these changes. Other changes in the spectrum are also observed, such as the changes to the multi-peaked band at 1215 to 1236 cm^{-1}. The band at 1236 cm^{-1}, which is normally assigned to N-H in-plane wag, disappears when the working electrode becomes anodic, while the peak at 1228 cm^{-1} remains the same and the peak at 1215 cm^{-1} diminishes to a shoulder. Although the band at 788 cm^{-1} and the shoulder at 1001 cm^{-1} do not shift in position, they decrease in intensity. Another noteworthy finding from Fig. 9.7 is that the spectrum for −0.1 V is virtually identical to that for 0 V, suggesting that the desorption of pyridinium ions at the copper surface is essentially complete and independent of the magnitude of the anodic electrode potential.

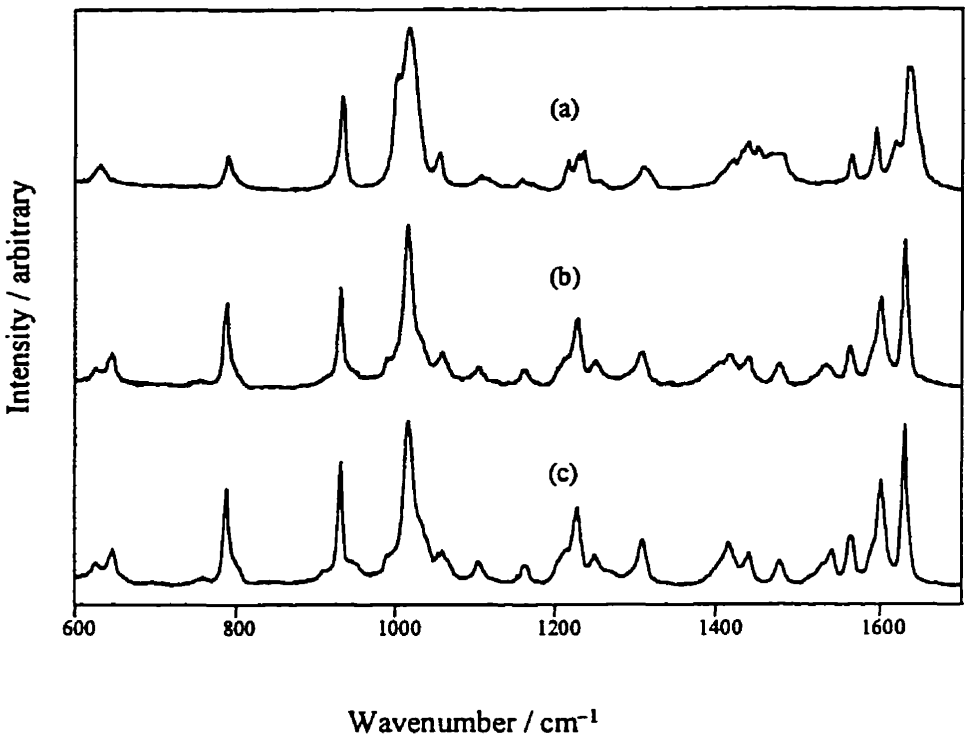

Fig. 9.7. SERS spectra of a copper electrode surface immersed in a solution at pH 4.8 containing 0.25 M 2-vinylpyridine. (a) at open circuit potential (E_{opc} = –0.18 V) when no current flows; (b) working electrode at –0.1 V with anodic current flowing; (c) working electrode at 0 V with anodic current flowing.

Some opposite findings had been reported by Lippert and Brandt (1988) in their SERS studies of poly(2-vinylpyridine) adsorption from a chloride solution. They found that when the electrode was anodic (i.e., $E_w > E_{opc}$), the species on the electrode surface was predominantly the pyridinium ion. When the working electrode potential was near E_{opc}, the species on the electrode surface were predominantly neutral pyridine molecules. The discrepancy in these results may be due to the differences in the anions used in the two studies. Lippert and Brandt interpreted their results by the formation of an anionic poly(2-vinylpyridine)-H-Cl complex and its adsorption to the anodic surface. However, in

our case, no characteristic band for the analogous poly(2-vinylpyridine)-H-ClO_4 complex between 1700 to 2800 cm^{-1} has been observed. Consequently, no monomer or polymer anions that adsorb onto the electrode likely exist. This result is consistent with the FT-IR spectra for the polymer coatings and indicates that although there are perchlorate ions present in the formed coatings, they are in physically trapped in the polymer network rather than present in an anionic polymer complex (Nakamoto, 1963).

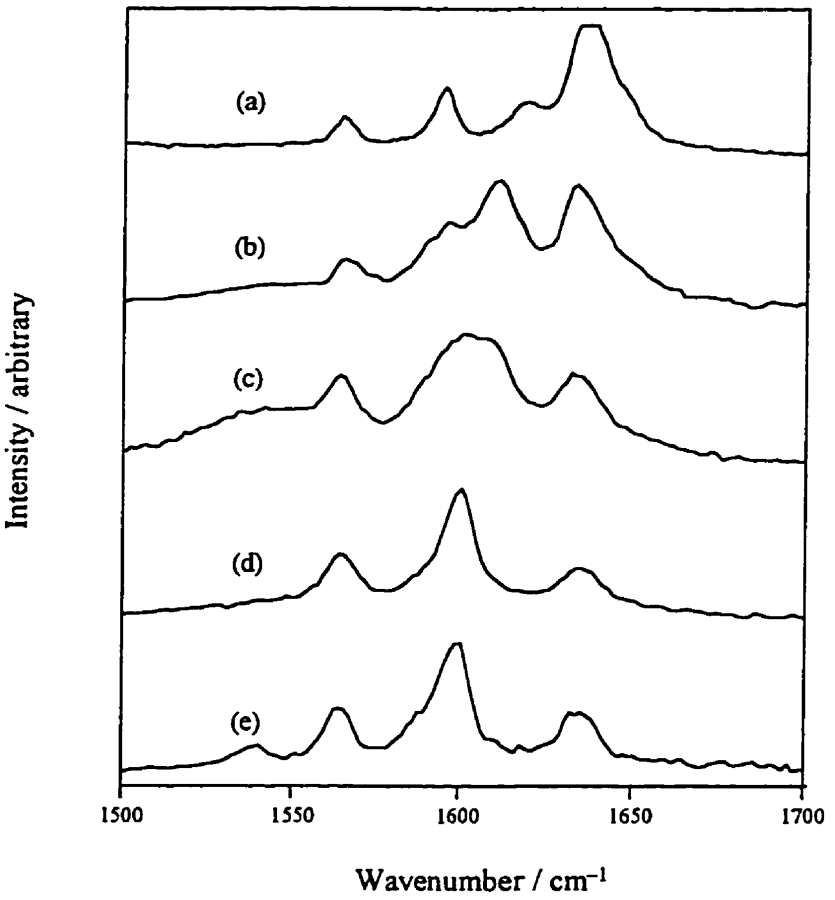

Fig. 9.8. SERS spectra in the 1500–1700 cm^{-1} region at a copper electrode surface immersed in a solution at pH 4.8 containing 0.25 M 2-vinylpyridine. (a) at open circuit potential (E_{opc} = –0.18 V); (b) at –0.3 V; (c) at –0.6 V; (d) at –1.0 V; (e) at –1.3 V.

When the potential of the working electrode is decreased below E_{opc}, the spectra in Figs. 9.8, 9.9 and 9.10 are obtained. Significant changes in the spectra are found as the electrode potential was made progressively more negative. While one characteristic band for the pyridinium ion at 1632 cm^{-1} shows no position shift but only a intensity decrease as the working electrode potential changes to more negative values, the other characteristic band at 1619 cm^{-1} shifts to 1611 cm^{-1} at –0.3 V (Fig. 9.8b), to 1608 cm^{-1} at –0.6 V (Fig. 9.8c) and eventually to 1600 cm^{-1} at –1.0 V and below, where it overlaps with one of the fingerprint bands of the neutral pyridine ring (Figs. 9.8d and 9.8e). While one of the characteristic bands for a neutral pyridine ring at 1565 cm^{-1} appears at all potentials, the other one at 1595 cm^{-1} starts to shift to a higher wavenumber soon after the cathodic current begins to flow (Fig. 9.8b) and reaches 1600 cm^{-1} and overlaps with the shifted pyridinium band at –0.6 V (Fig. 9.8c), remaining at this wavenumber as the potential becomes more negative (Figs. 9.8d and 9.8e).

At more negative potentials (e.g., $E_w < -1.0$ V), more changes can be observed in the spectra. For example, a new band appears at 1537 cm^{-1} at –1.3 V (Fig. 9.8e). As shown in Fig. 9.9d, the band at 1476 cm^{-1} begins to split into a double-peaked band at –1.0 V. While the peak at 1437 cm^{-1} remains unchanged, the peak at 1449 cm^{-1} diminishes and disappears (Figs. 9.9d and 9.9e). The band at 1420 cm^{-1} also shifts when the working electrode becomes cathodic and disappears when E_w reaches –1.0 V (Figs. 9.9c, 9.9d and 9.9e). Bands at 1318 to 1305 cm^{-1} and at 1236 and 1216 cm^{-1} are found to shift in the direction of smaller wavenumbers. Some of the bands also diminish after shifting (Figs. 9.9d and 9.9e). While the band at 1016 cm^{-1} remains unchanged, the shoulder at 1001 cm^{-}

^{1} disappears, and a new band at 970 cm^{-1} appears when electrode potentials are more negative than –0.6 V (Figs. 9.10c, 9.10d and 9.10e).

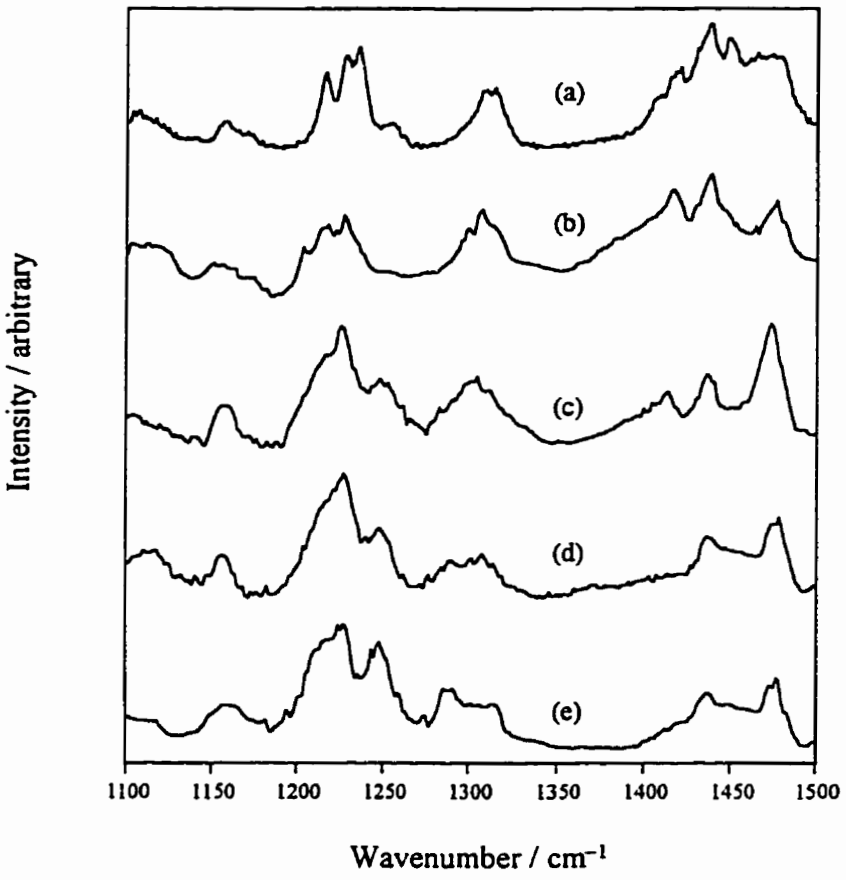

Fig. 9.9. SERS spectra in the 1100–1500 cm^{-1} region from a copper electrode surface immersed in a solution at pH 4.8 containing 0.25 M 2-vinylpyridine. (a) at open circuit potential (E_{opc} = –0.18 V); (b) at –0.3 V; (c) at –0.6 V; (d) at –1.0 V; (e) at –1.3 V.

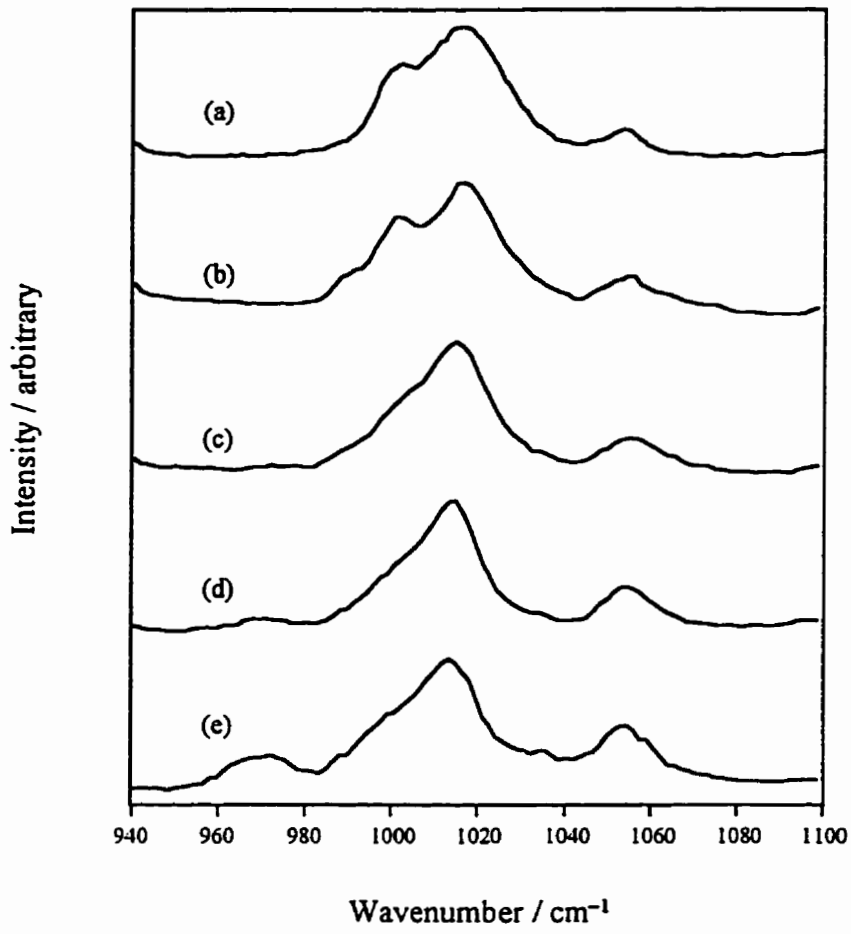

Fig. 9.10. SERS spectra in the 940–1100 cm^{-1} region from a copper electrode surface immersed in a solution at pH 4.8 containing 0.25 M 2-vinylpyridine. (a) at open circuit potential (E_{opc} = –0.18 V); (b) at –0.3 V; (c) at –0.6 V; (d) at –1.0 V; (e) at –1.3 V.

It should be pointed out here that since Raman scattering can be affected by electric fields, the peak position in a Raman spectrum for a given bond may shift when the electrode potential changes. This sometimes makes it more complicated to interpret the spectral results. Nevertheless, it is still possible to make the following conclusions from the above Raman and SERS experiments:

1). 2-vinylpyridine can be protonated in acidic aqueous solutions. At a high solution pH (> 7.4), most 2-vinylpyridine species exist in their neutral form; at a low solution pH (< 1.0), most 2-vinylpyridine species are in their protonated form; at an intermediate solution pH (~ 4.8), 2-vinylpyridine species exist in both neutral and protonated forms (Figs. 9.4 to 9.6).

2). Neutral form of 2-vinylpyridine adsorbs on an anodic electrode surface, while protonated 2-vinylpyridine is not be adsorbed (Fig. 9.7).

3). Both neutral and protonated forms of 2-vinylpyridine species are adsorbed on an cathodic electrode surface. However, once the electrode potential is sufficiently cathodic, neutral 2-vinylpyridine is the predominant form adsorbed at the cathode of pre-coated electrodes (Figs. 9.8-9.10).

9.3. Extended Voltammetry

A series of voltammetry experiments have been carried out on mild steel electrodes pre-coated with poly(2-vinylpyridine) via the usual electropolymerization process described in the caption for Fig. 8.1. It is found that the cathodic potential scan can be extended to potentials more negative than –5 V without intense hydrogen evolution. During a wide range cathodic potential scan, three current peaks appear in the voltammogram (Fig. 9.11) at half-wave potentials of –0.95, –1.30 and –1.91 V, respectively, indicating that more than one electron transfer reaction is occurring in the process. We have found a similar phenomenon with other electrode materials such as

copper, brass, zinc and lead and with various supporting electrolytes (e.g., SO_4^{2-}, NO_3^-, Cl^-, etc.).

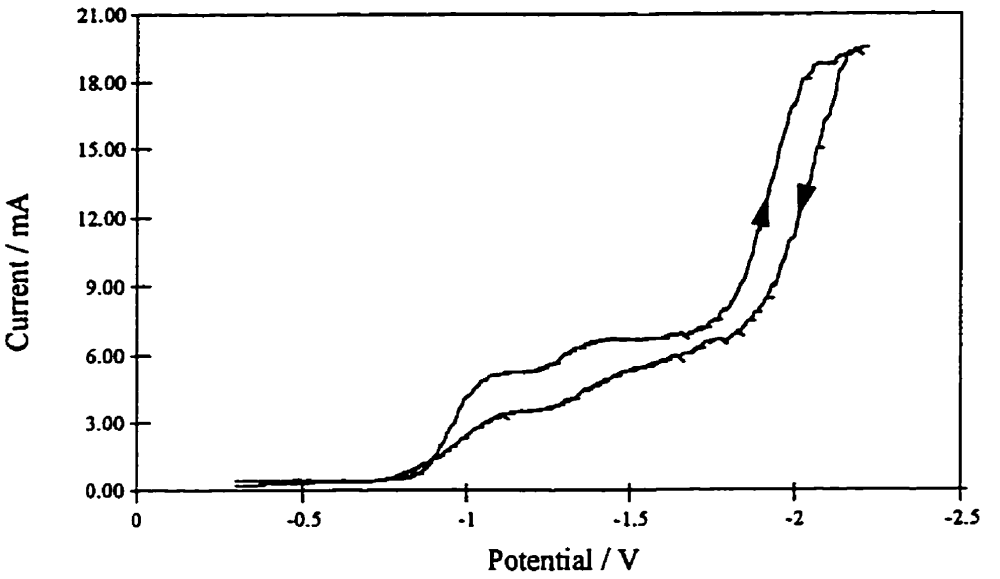

Fig. 9.11. Voltammogram on a pre-coated steel electrode immersed in a 0.25 M 2-vinylpyridine aqueous solution. Potential scan rate is 30 mV/s. The three observed $E_{1/2}$ are –0.95, –1.30 and –1.91 V, respectively. The arrows indicate the direction of the scan.

A mechanism involving more than one electron transfer process is more complex than the conventional single reaction process proposed for electropolymerization (Gaylord, 1970, 1974). Similar phenomena have been reported recently for the electropolymerizations of maleic anhydride in an acetonitrile-dimethylformamide mixture (Akbulut and Hacioglu, 1991) and of allylphenylether in acetonitrile (Sen et al., 1995). However, no process mechanism has been proposed to interpret the observation reasonably. A mechanism based on the reduction of the formed poly(2-vinylpyridine) at the cathode surface that involves multiple electron transfer processes will be proposed in the next chapter.

Further voltammetric experiments have been carried out to test the hypothesis of the formed polymer reduction mechanism on the cathode surface. Poly(2-vinylpyridine) formed by the free radical bulk polymerization process was dissolved in an acid solution to form a 0.1 *wt. %* polyelectrolyte solution. No monomer was added to the electrolyte. The other components of the solution (i.e., the methanol content, the nature and concentration of supporting electrolyte, etc.) and the experimental operating conditions were the same as used for a standard electropolymerization process described in the caption for Fig. 8.1. However, the solution pH could only be adjusted to lower than 2.9 or higher than 9.2 since any intermediate value was found to be very unstable. An mild steel electrode pre-coated with poly(2-vinylpyridine) was used as the working electrode. At pH 2.9, the voltammogram (Fig. 9.12a) clearly shows two current waves at $E_{1/2}$ of −1.24 and −1.88 V, while the voltammogram from the pH 9.2 electrolyte shows only the hydrogen evolution rise (Fig. 9.12b).

Comparison of the above results shows that the wave with a $E_{1/2}$ of −0.95 V in Fig. 9.11 does not appear in Fig. 9.12, while the other two waves are very close to those in Fig. 9.12. Since the voltammogram in Fig. 9.12 is obtained from a electrolyte containing no monomer, it is clear that the wave with a $E_{1/2}$ of −0.95 V in Fig. 9.11 may likely be associated with reduction of 2-vinylpyridine monomer. The other two waves in Fig. 9.11 can be attributed to the reduction of poly(2-vinylpyridine) at the cathode surface. Further discussion of the polymer reduction reaction and its significance to electropolymerization coating formation will be presented in the next chapter.

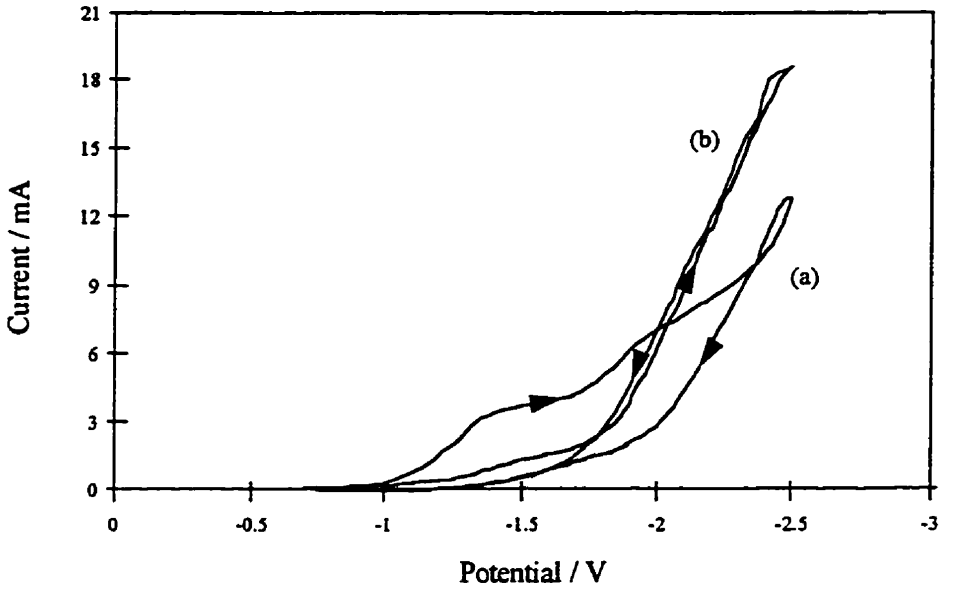

Fig. 9.12. Voltammogram of a pre-coated electrode immersed in a 0.1 *wt.* % poly(2-vinylpyridine) electrolyte. (a) Solution pH = 2.9, adjusted with concentrated $HClO_4$ and (b) solution pH = 9.2, adjusted with concentrated NH_4OH. Potential scan rate = 30 mV/s. The poly(2-vinylpyridine) is formed by bulk polymerization, with benzoyl peroxide as initiator. The two observed $E_{1/2}$ are −1.24 and −1.88 V, respectively. The arrows indicate the direction of the scans.

CHAPTER 10

PROCESS MECHANISM IDENTIFICATION OF POLYMER COATING FORMATION BY ELECTROPOLYMERIZATION IN AQUEOUS MEDIUM

In this chapter, the process mechanism of poly(2-vinylpyridine) coating formation by electropolymerization on mild steel substrates in an aqueous solution will be proposed based on the accomplished experimental results. Previous experimental results and conclusions will be reviewed and reinterpreted in terms of the process mechanism. Experimental results for electropolymerization using other substrates and monomers will also be presented to assess the proposed mechanism.

10.1. Process Mechanism Identification

Structurally, 2-vinylpyridine is similar to styrene but with a nitrogen atom in the *ortho*-position of the pyridine ring

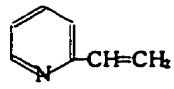

(I)

Due to the presence of the electronegative nitrogen atom in the pyridine ring, 2-vinylpyridine is weakly basic with an *e* value of –0.42 in the *Q-e* scheme (Greenley, 1984). The nitrogen atom can attract cations in electrolyte (e.g., hydrogen ion in an acidic aqueous medium) and enable the 2-vinylpyridine molecule to be protonated:

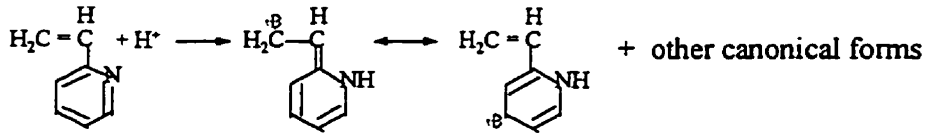

(I) (II) (IIa) (10.1)

The protonation of 2-vinylpyridine has been confirmed by the results of our ordinary Raman scattering spectroscopic study of the bulk solutions. In an aqueous solution, the following equilibrium exists between the 2-vinylpyridinium ions and neutral 2-vinylpyridine molecules:

$$M\text{–}H^{+} \overset{Ka}{\rightleftharpoons} M + H^{+} \tag{10.2}$$

where *M* and *M–H*$^{+}$ represent the neutral and protonated forms of 2-vinylpyridine, respectively, and *p*Ka = 4.92 (Perrin, 1965). Therefore, we have

$$4.92 = \mathrm{pH} - \log\frac{[M]}{[M\text{–}H^{+}]} \tag{10.3}$$

We can solve Equation (10.3) to obtain the concentration distribution curves for neutral and protonated 2-vinylpyridine species as a function of electrolyte pH (Fig. 10.1).

It is clear that nearly all 2-vinylpyridine molecules exist in their neutral form at the original electrolyte pH of 7.5, while 2-vinylpyridinium ions represent only 0.2% of the total 2-vinylpyridine mass. When the solution pH increases further, the extent of 2-vinylpyridine protonation has virtually no change. When the electrolyte pH is reduced to a

value close to the *p*Ka value for 2-vinylpyridine, there is an abundance of both 2-vinylpyridinium ions and neutral 2-vinylpyridine molecules in the electrolyte. When the electrolyte pH is reduced further (e.g., < 3), most of the 2-vinylpyridine molecules in the electrolyte exist in their protonated form, while only a very small amount remains in the neutral form. Below this pH value, no further change of the extent of 2-vinylpyridine protonation occurs in the electrolyte. This analysis is consistent with the previous results of the Raman scattering spectroscopic studies reported in Chapter 9.

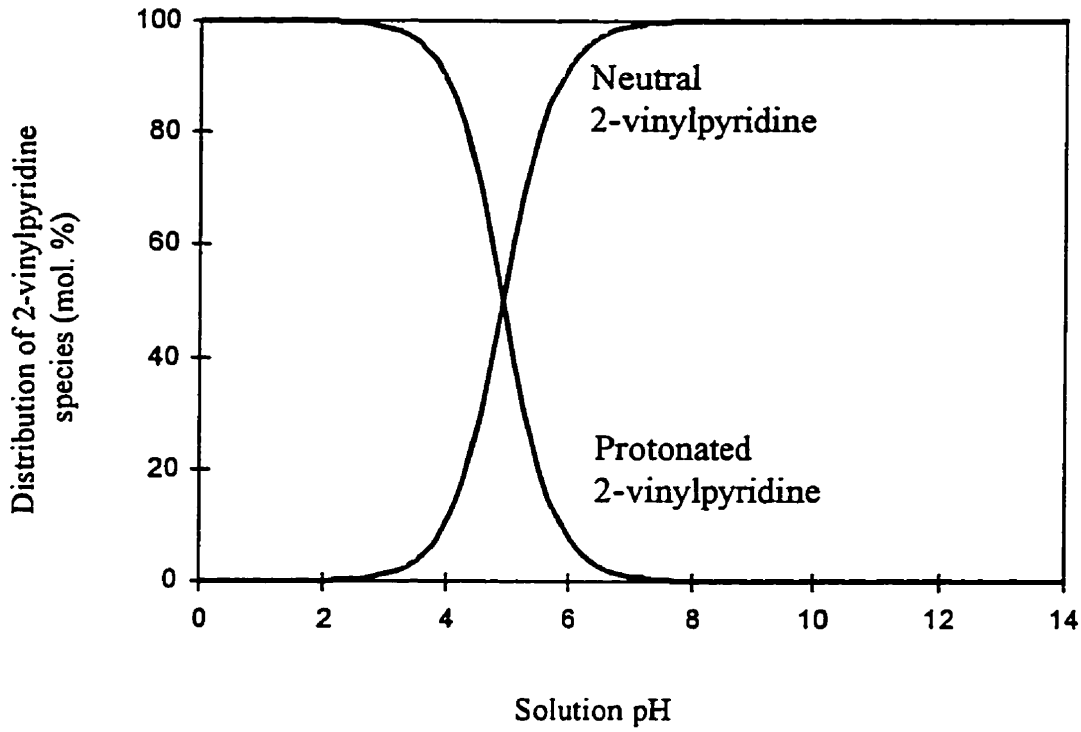

Fig. 10.1. The concentration distribution curves of neutral and protonated 2-vinylpyridine in aqueous solution at different pH.

The 2-vinylpyridinium ions are then attracted by the electric field to the cathode where they migrate and adsorb:

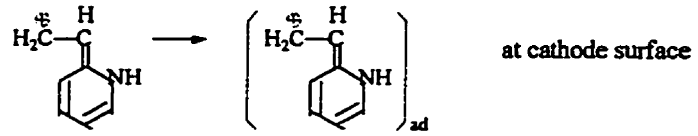

(II) (III) (10.4)

The adsorption of the ions is indicated by the surface enhanced Raman scattering (SERS) spectroscopic studies (Fig. 9.6 to 9.8). SERS spectra show that neutral 2-vinylpyridine is also present on the cathodic surface.

The adsorbed pyridinium ions (III), which are more easily reduced than a neutral molecule, would then be converted to a free radical (IV) at a $E_{1/2}$ about −1 V :

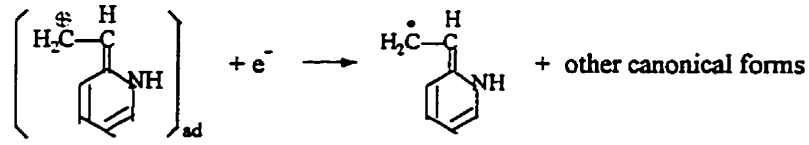

(III) (IV) (10.5)

However, the generated free radical (IV) is unstable and would combine with a neutral 2-vinylpyridine molecule (I) to form an energetically more favoured secondary radical (IVa), which would likely tautomerize back to the aromatic pyridine (IVb):

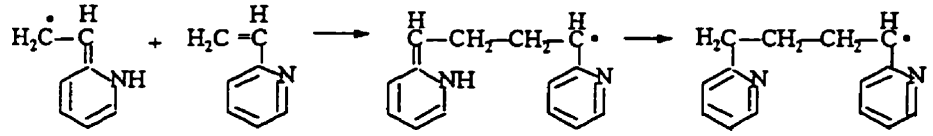

(IV) (I) (IVa) (IVb) (10.6)

The free radicals (IVb) would then combine with more neutral 2-vinylpyridine molecules (I) to initiate and propagate the polymerization.

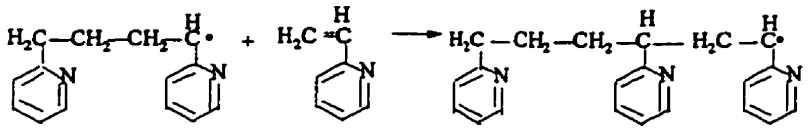

(IVb) (I) (V) (10.7)

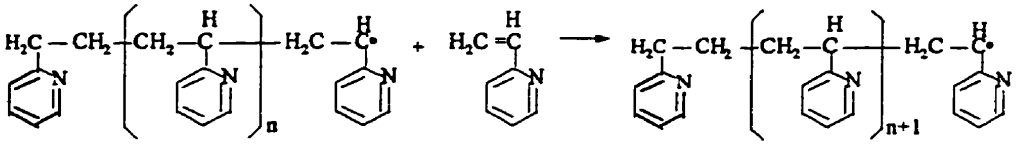

(VIa) (I) (VIb) (10.8)

The propagation process may eventually be terminated by another radical, such as the hydrogen radical generated at the cathode surface by H^+ reduction:

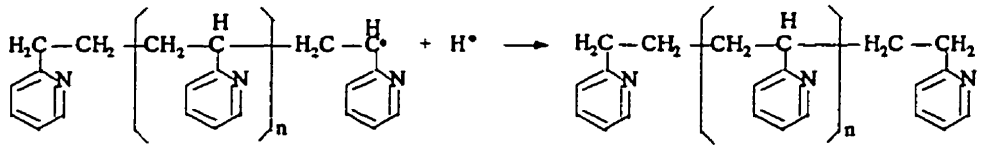

(VIa) (VII) (10.9)

or by combination or disproportionation. The free-radical mechanism for the electropolymerization is supported by the results of the inhibition studies. The formation of poly(2-vinylpyridine) coatings has been confirmed by u.v.-visible, FT-IR and proton NMR spectroscopy.

From the above analysis, it is clear that both neutral and protonated 2-vinylpyridine species play important roles in the electropolymerization process. It is essential to have enough 2-vinylpyridinium ions in the electrolyte to adsorb on the cathode and be reduced to form radicals. It is also crucial that a sufficient amount of neutral 2-vinylpyridine molecules be present in the electrolyte to stabilize the generated radicals and carry out the polymerization. The feasibility of the reduction of the 2-vinylpyridinium ions at the

cathode and the opening up of the vinyl double-bond in a neutral 2-vinylpyridine molecule is necessary for electropolymerization. Due to the high polarity of the vinyl double-bond in the 2-vinylpyridinium ions, it is difficult for them to open up for the propagation reaction (Odian, 1991).

When the solution pH is 7.5 or above (Fig. 7.1), no 2-vinylpyridine reduction peak appears on the corresponding voltammogram due to the deficiency of 2-vinylpyridinium ions in the solution. Therefore, a good quality polymer coating cannot be formed on the electrode surface. Instead, intense hydrogen evolution is observed. When the electrolyte pH is reduced, the 2-vinylpyridinium ion reduction peak appears in the voltammograms and hydrogen evolution is diminished and inhibited significantly. However, when the electrolyte pH is too low (below 3.5), this does not favour efficient coating formation although a sufficient amount of free radicals is generated from the reduction of 2-vinylpyridinium ions. This is due to the lack of neutral 2-vinylpyridine molecules in the electrolyte to stabilize the generated radicals and initiate and propagate polymerization. Only when the solution pH has a medium value (i.e., close to the *p*Ka value of the monomer) where there is an abundance of both neutral and protonated 2-vinylpyridine species in the electrolyte, can efficient radical generation, stabilization, and polymer chain initiation and propagation reactions occur. This is the fundamental requirement for the formation of good polymer coatings.

Soon after the formation of the polymer film on the electrode surface, the electrolysis current decreases markedly due to the high resistance of the formed polymer films. However, the current does not drop to zero, but remains at a certain (very low) value throughout the rest of the process. The source of this so-called *residual current* may

partially be the continuous hydrogen evolution, and may also be electron transfer processes directly related to the electropolymerization.

The formed poly(2-vinylpyridine) coating still has many features of the monomer. For example, it is a weak base due to the presence of the electronegative nitrogen atom in its structure with a *p*Ka value of ~ 4 (Satoh et al., 1989). Therefore, the polymer can also attract hydrogen ions and be protonated in an acidic electrolyte (Wall, et al., 1951; Lippert and Brandt, 1988; Garrell and K. D. Beer, 1988):

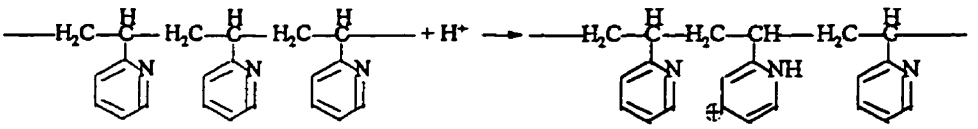

(10.10)

(VII) (VIII)

The protonated polymer (VIII) may then undergo reduction at the cathode surface and be converted to a polymeric radical (IX) (*dead polymer revivification* is the phrase used in this thesis):

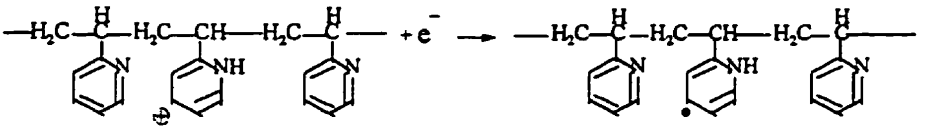

(10.11)

(VIII) (IX)

Since the active site of the polymeric radical (IX) is likely to be in the middle of the chain, a branched polymer would then be produced when it combines with neutral 2-vinylpyridine molecules:

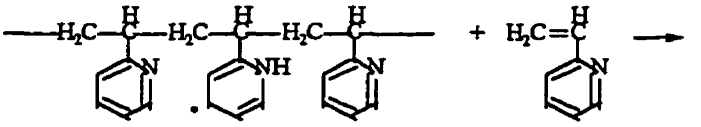

(IX) (I)

(10.12)

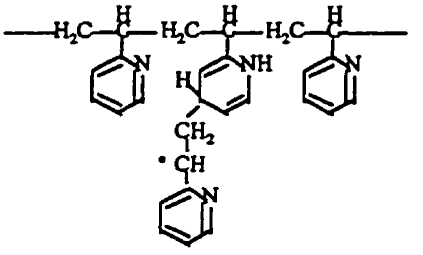

(X)

If the polymer radical reacts with another polymer molecule containing a double-bond (formed by e.g., disproportionation termination, hydrogen abstraction or some chain transfer reactions) or with another polymer radical, a crosslinked polymer would be produced. These branched and crosslinked polymer molecules could be further protonated and reduced at the cathode surface and make the polymer even more highly branched or crosslinked.

Thus, when poly(2-vinylpyridine) films form on the cathode surfaces, reduction of not only the monomer, but also the formed polymer occurs. Both processes contribute to the process current. The appearance of more than one wave in the corresponding voltammogram (Fig. 9.10) presumably reflects the fact that reduction occurs at different types of sites during this branching and cross-linking process. The formation of highly branched and crosslinked polymers explains the fact that these poly(2-vinylpyridine) films are relatively insoluble in organic solvents. It also explains the fact that only when the cathodic-limit electrode potential is negative enough (e.g., < -1.5 V) during CPS electrolysis can good quality (thick and uniform) coatings be formed. The electrode

potential must be negative enough for polymer reduction and consequently branching and cross-linking to occur.

Another *unusual* phenomenon observed in the electropolymerization process is that the colour of the formed poly(2-vinylpyridine) coating is yellow (Sekine et al., 1992; De Bruyne et al., 1995) rather than colourless as in the case of bulk polymerization. A similar phenomenon has been observed by other researchers in the formation of other polymer coatings by electropolymerization. For example, Akbulut and Hacioglu (1991) obtained a brown polymer coating on a platinum cathode surface from the colorless maleic anhydride. In this project, yellow-coloured poly(2-vinylpyridine) films have been consistently observed on different electrode materials. Therefore, the colour of the coating is considered not to be caused by the nature of the electrode material but to be directly related to the mechanism of electropolymerization.

During the poly(2-vinylpyridine) coating formation, hydrogen evolution occurs on the cathode surface throughout the process. The generated hydrogen radicals can combine with the active polymer chains and terminate the polymerization process. This hydrogen termination process may occur at an early stage, causing the formed polymer to have relatively short chains. However, these short-chain polymers soon become revived and start to become branched and crosslinked. As this hydrogen-termination/short-polymer-revivification process continues, the ultimate polymer chains would be linearly short but highly branched and crosslinked. Considering the fact that a 2-vinylpyridine oligomer has a yellow colour (Jenkins et al., 1979; Mathis and Hogen-Esch, 1982; Meverden and Hogen-Esch, 1983; Sekine et al., 1992; De Bruyne et al., 1995), it seems reasonable to suggest that the formed poly(2-vinylpyridine) coatings adopt the same colour as the structurally

similar (i.e., linearly-short chain) 2-vinylpyridine oligomer. In order for this explanation to be correct, the yellow colour of the coating would be due to the presence of linearly short chains, but not to its molecular weight. Although it was not practically possible to measure the molecular weight of the electrochemically formed 2-vinylpyridine polymer due to its low solubility in the solvents, the measured T_g indicated that the average molecular weight is quite high. The frequent occurrence of hydrogen termination may be the reason, at least partially, of the higher hydrogen ratio in the elemental analysis results (Section 8.2.1.).

Although the reduction of 2-vinylpyridinium ions is considered to be the primary source of free radicals which initiate the polymerization, it is also possible, at least theoretically, to reduce neutral 2-vinylpyridine to generate anionic radicals

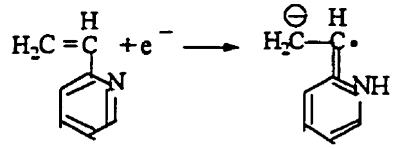

(I) (XI) (10.13)

Such a reduction reaction should occur at a more negative cathodic potential than that of the 2-vinylpyridinium ion. The relevant current peak may be covered by that of hydrogen evolution and therefore cannot be monitored on the voltammogram. However, although anionic radicals would be generated at cathode surfaces, it would be difficult for the generated 2-vinylpyridine anionic radicals (XI) to linger at the electrode surfaces. They are likely to be repelled into the bulk solution by the cathode and make no contribution to coating formation. Moreover, anionic radicals in environments such as those of this project will be consumed immediately by the proton-donating species (e.g., hydrogen ions, methanol and water) in the media. Hence, anionic polymerization is not expected to

contribute to coating formation no matter if neutral form 2-vinylpyridine reduction occurs at the electrode surface.

No electropolymerization occurs at potentials above –0.8 V when no monomer reduction occurs and only H_2 evolution takes place. Thus, it would be reasonable to conclude that 2-vinylpyridine radical formation (Reactions (10.6) to (10.8)) is necessary to initiate the electropolymerization rather than hydrogen radical initiation (reaction (10.14)) or translation (reaction (10.15)):

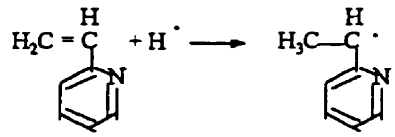

(10.14)

(I) (XII)

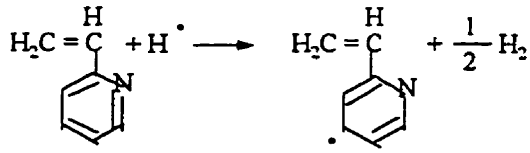

(10.15)

(I) (XIII)

Furthermore, even if the hydrogen radical initiation occurred, it would have to take place between hydrogen radicals and neutral 2-vinylpyridine molecules since it is difficult to open the highly polarized double-bond in 2-vinylpyridinium ions. Then, polymer coating formation would preferentially occur in an electrolyte with a high pH value, such as 7.5 or higher. However, this contradicts our experimental results on the impact of the electrolyte pH on the electropolymerization process (Section 7.1). Considering all these experimental results together, it is reasonable to conclude that the electropolymerization is initiated by

monomer radicals produced from 2-vinylpyridinium ion reduction rather than by hydrogen radicals from hydrogen ion reduction.

Since the formed poly(2-vinylpyridine) can be protonated in acidic aqueous solutions (reaction 10.10), there is an equilibrium between the protonated and neutral form poly(2-vinylpyridine) species. From the poly(2-vinylpyridine) *p*Ka value (~ 4 from Satoh, et al., 1989) and the following mass balance equation,

$$\mathrm{pKa} = \mathrm{pH} - \log\frac{[P]}{[P\text{–}H^{+}]} \qquad (10.16)$$

where P and $P\text{–}H^{+}$ present the neutral and protonated forms of poly(2-vinylpyridine) species, respectively, it is readily seen that 13.7 % of poly(2-vinylpyridine) is protonated at pH 4.8. This might provide enough charged sites for the coating to be electrically conducting in an acidic aqueous solution and to support electrochemical reactions after the working electrode is completely covered by the polymer coating. This may also explain why a pre-coated electrode could be used as a polymer-modified electrode for the extended linear sweep voltammetry studies presented in Chapter 9. Upon drying or curing, these charged sites are neutralized and the coating becomes insulating. It should be noted that the coating is always in a dry state when its conductivity has been measured. In fact, this phenomenon is quite similar to the electrode doping process, in which an insulating polymer becomes conducting after being immersed in a strong electrolyte (Murray, 1984a and 1984b). On the other hand, at a solution pH of 6.5 (typical for drinking water and the salt spray test for corrosion protection in 3% NaCl solution), 99.7 % of the polymer is in its neutral form and the coating is basically insulating. Although it has been reported that polyvinylpyridine formed by bulk, solution, emulsion or suspension polymerization swells

in water (Luskin, 1974), no evidence of swelling is found for the poly(2-vinylpyridine) formed by electropolymerization. This may be one of the consequences of the highly branched and crosslinked structure of the polymer.

10.2. Process Mechanism Verification

10.2.1. Coating Formation on Different Substrates

Besides mild steel, other materials such as copper (> 99.99%), brass (C3600, with 60-63% Cu, 33-37% Zn, 2.5-37% Pb and 0.35% Fe), lead (> 99.9%), zinc (> 99.9%), graphite, stainless steel (SS 316), platinum (> 99.99%) and aluminum (> 99.9%) have been used as substrates for 2-vinylpyridine electropolymerization. Most of the electrodes have the same shape as that of the mild steel coupon with a 5.5 cm^2 area, except for the graphite and platinum electrodes. The graphite electrode is a 5 mm (diameter) rod of 3.4 cm in length with an active area of 5.5 cm^2, while the platinum electrode is a section of coil of 1 mm in diameter and 40 cm in length (i.e., an active electrode area of 12.6 cm^2). In each case, the electropolymerization processes is carried out by CPS electrolysis for 2 hours. While the solution composition is the same as before (i.e., 0.25 M 2-vinylpyridine in 20% methanol aqueous solution with 0.05 M NH_4ClO_4 as supporting electrolyte and solution pH of 4.8, adjusted with $HClO_4$), some electrochemical parameters (e.g., the range of potential sweep) are different from those in operation for mild steel substrates. The ranges of potential sweep for different electrode systems have been summarized in Table 10.1.

Table 10.1. Results of poly(2-vinylpyridine) coating formation on different substrates by two-hour CPS electrolysis. The electrolyte is 0.25 M 2-vinylpyridine in 20% methanol aqueous solution with 0.05 M NH_4ClO_4 as supporting electrolyte and solution pH of 4.8, adjusted with $HClO_4$. Potential scan rate is 30 mV/s. Unless specifically mentioned, all electrodes are in the shape of coupon with an active electrode area of 5.5 cm^2.

Type of Substrate	Potential Range for CPS Electrolysis (V)	Coating Weight (mg)	Comment
Mild steel	–0.7 to –2.5	7.9	Thick and uniform coating
Copper	–0.7 to –2.2	7.9	Thick and uniform coating
Brass	–0.7 to –2.2	8.1	Thick and uniform coating
Lead	–0.7 to –2.5	12.4	Thick and uniform coating
Zinc	–0.9 to –2.5	14.7	Thick and uniform coating
Graphite †	–0.7 to –2.5	6.5	Thick and uniform coating
Platinum ‡	–0.3 to –2.3	—	No visible coating formed
Stainless Steel	–0.3 to –2.3	0.8	Small amount scattered deposits
Aluminum	–0.6 to –2.5	—	No visible coating formed

† in the shape of a rod.

‡ in the shape of a coil, with an active electrode area of 12.6 cm^2.

For the copper and brass substrates, the CPS electrolysis is carried out in the potential range of –0.7 V to –2.2 V. As in the case of mild steel electrodes, hydrogen bubbles are observed on the electrode surfaces during the electropolymerization. The coating formed are uniform and hard and adhere very well to the substrates. The thickness of the obtained coatings is close to those formed on mild steel substrates. The I-t diagrams for copper and brass electrodes are very similar to that of the mild steel electrodes. As an example, the I-t diagram for the brass electrode (very similar to that of the copper

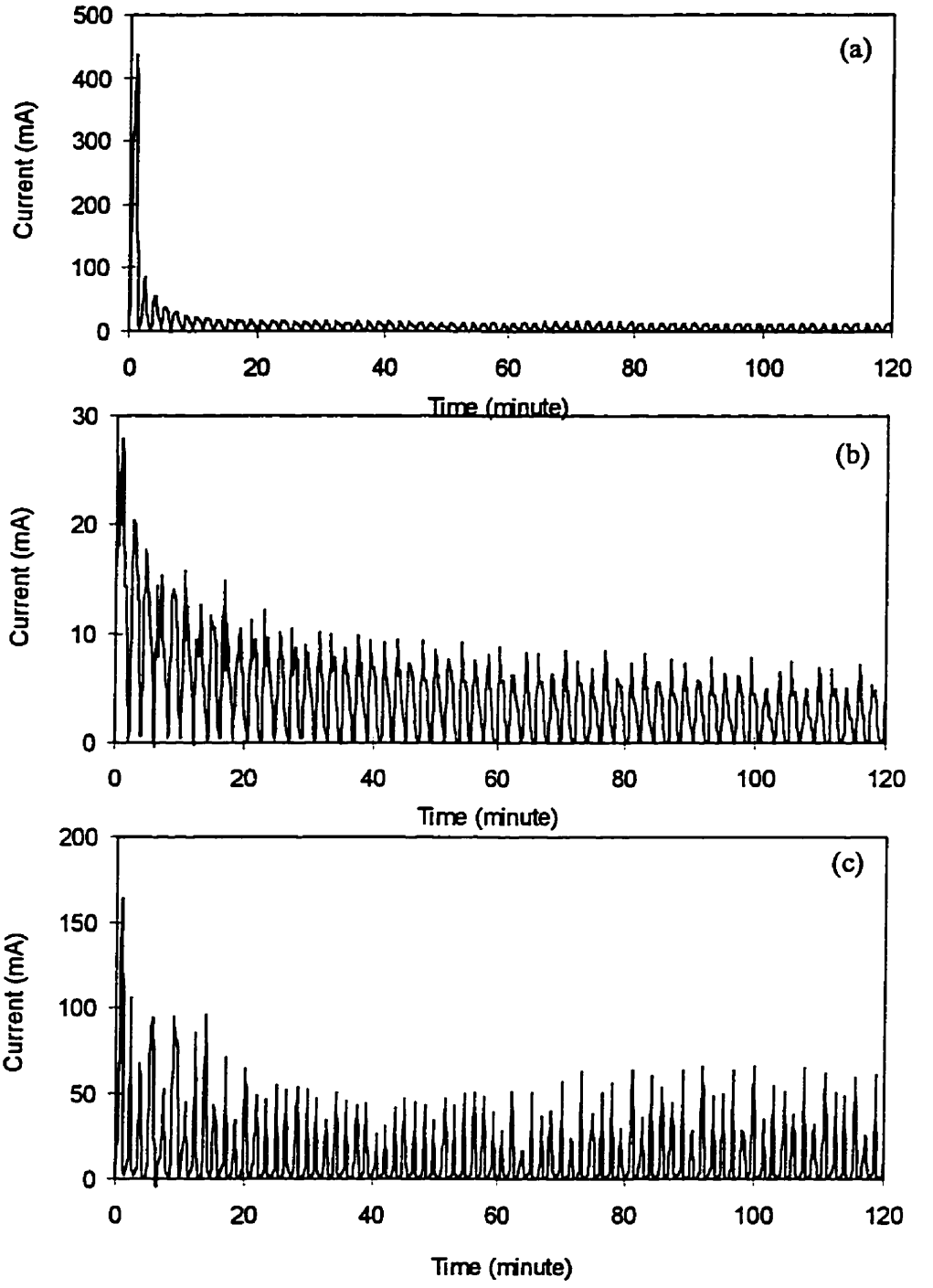

Fig. 10.2. I-t diagrams of CPS electrolysis of 2-vinylpyridine on different electrodes. The working electrodes are (a) brass; (b) lead; (c) stainless steel. The detailed electrolyte composition, experimental conditions and the dimension of the electrodes are described in Table 10.1.

electrode) is shown in Fig. 10.2a. The diagram for brass is very similar to that for copper. For zinc and lead substrates, the CPS electrolysis is carried in the potential range of –0.9 to –2.5 V and –0.7 to –2.5 V, respectively. Only small amounts of hydrogen are observed at the beginning of the electrolysis and no hydrogen is observed during the rest of the electrolysis period. The formed coatings are very smooth and uniform and thicker than in the case of mild steel. The I-t diagrams, very similar to each other, appear different from the one for brass (therefore, mild steel as well) electrode. As an example, the I-t diagram for the lead electrode is shown in Fig. 10.2b. Because of the less intense hydrogen evolution, the current is much lower than that for the brass electrode. For example, the first current peak for the brass electrode is about 430 mA, while only about 28 mA in the case of the lead electrode. The difference in hydrogen evolution is not unexpected since it correlates well with the hydrogen overpotential of the various substrates. The higher the hydrogen overpotential of a particular substrate, the less intense is hydrogen evolution during electrolysis, and the thicker and more uniform is the coating. The results also indicate that hydrogen evolution is an important source of the electrolysis current during the electropolymerization.

The poly(2-vinylpyridine) coatings formed on the above metal substrates are all yellow, which is consistent with the previous conclusion that the colour of the coatings is not related to the nature of the substrates but to intrinsic properties of the polymer itself. The reaction electrolytes after the electrolysis are yellow in the cases of copper and brass substrates, as with mild steel. However, for the cases of zinc and lead electrodes the yellow colour of the electrolyte is much lighter although the coatings have the same yellow colour as with copper and brass. This may again reflect the effects of hydrogen evolution

on the coating formation process. Intense hydrogen evolution blows polymer formed on the electrode into solution and causes the electrolyte to become yellow. It also would decrease the uniformity of the coating and could have adverse effects on the coating adhesion. Since virtually no hydrogen evolves on lead or zinc during the electrolysis, very little polymer would detach from the coating to make the solution turn yellow. This result suggests that another important aspect of coating formation by electropolymerization (but which has not received much attention) is the detachment of formed polymer. A contributing factor for the thicker coatings being formed on lead and zinc electrodes may be the minimal removal of polymer from these substrates during electropolymerization.

The adverse effects of hydrogen evolution are observed most clearly in the coating formation processes on stainless steel or platinum substrates. In the case of a stainless steel substrate, intense hydrogen evolution is observed during the electrolysis at a rather positive electrode potential (~ –0.45 V). During the electrolysis, the current remains high (~ 70 mA) instead of dropping quickly after the onset of the electrolysis as it does in the case of some other metal substrates (e.g., mild steel, lead and zinc). The relevant I-t diagram is shown in Fig. 10.2c. Because of the intense hydrogen evolution, the current response looks noisy and irregular. The electrolyte colour turns yellow quickly during the electrolysis. After 2 hours of CPS electrolysis between –0.3 to –2.3 V, only a small amount of a yellow coating forms in a scattered manner on the electrode surface. Nevertheless, the deposit is very hard and strongly adherent to the substrate surface. The reason for the low hydrogen overpotential of the stainless steel electrode is presumably due to the presence of chromium in the stainless steel samples. Platinum is well known for its low hydrogen overpotential and therefore it is not surprising to observe intense

hydrogen evolution at a very positive electrode potential (~ –0.35 V). After two hours of CPS electrolysis in the potential range of –0.3 to –2.3 V, no visible coating formation can be observed on the electrode surface. The electrolysis current also remains high during the electrolysis and the associated I-t diagram is quite similar to that of a stainless steel electrode. The solution colour also turns yellow quickly during the electrolysis.

Electropolymerization of 2-vinylpyridine on aluminum electrode shows unique results. Unlike the case of any other electrode material, the voltammogram on an aluminum electrode shows no current wave for 2-vinylpyridine reduction. The electrolysis current remains at a very low level (< 0.18 mA/cm^2) up to –1.87 V. However, when the cathodic potential becomes more negative than –1.87 V, intense hydrogen evolution occurs. After a two-hour CPS electrolysis between –0.6 and –2.3 V at 30 mV/s, no visible coating forms on the aluminum electrode. No current drop has been observed during the electrolysis. The current response is irregular. The reason for this behaviour is not clear. It may be related to the formation of an extremely thin but highly dense aluminum oxide film on the substrate surface, which not only has a very high hydrogen overpotential, but also prevents 2-vinylpyridine species (specifically protonated 2-vinylpyridine ions) from adsorbing on the electrode surface. The entire I-t diagram of the two-hour process is shown in Fig. 10.3a and an enlarged portion of the I-t diagram is shown Fig. 10.3b, which shows clearly that no monomer reduction occurs during the potential sweep.

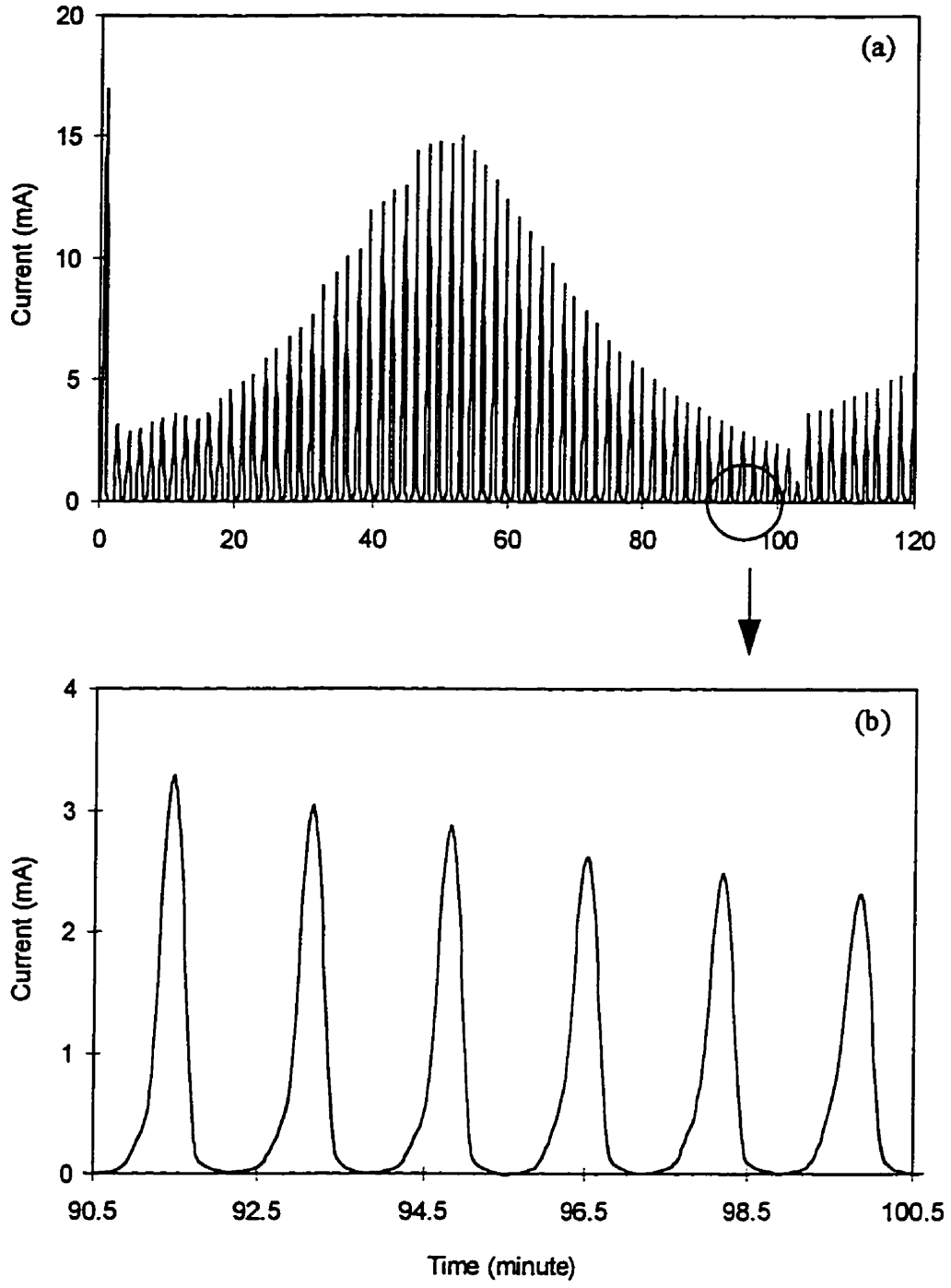

Fig. 10.3. I-t diagrams of CPS electrolysis of 2-vinylpyridine on an aluminum electrode. The current response is random and irregular, and no monomer reduction wave can be observed during the potential sweep. The detailed electrolyte composition, experimental conditions and the dimension of the electrodes are described in Table 10.1.

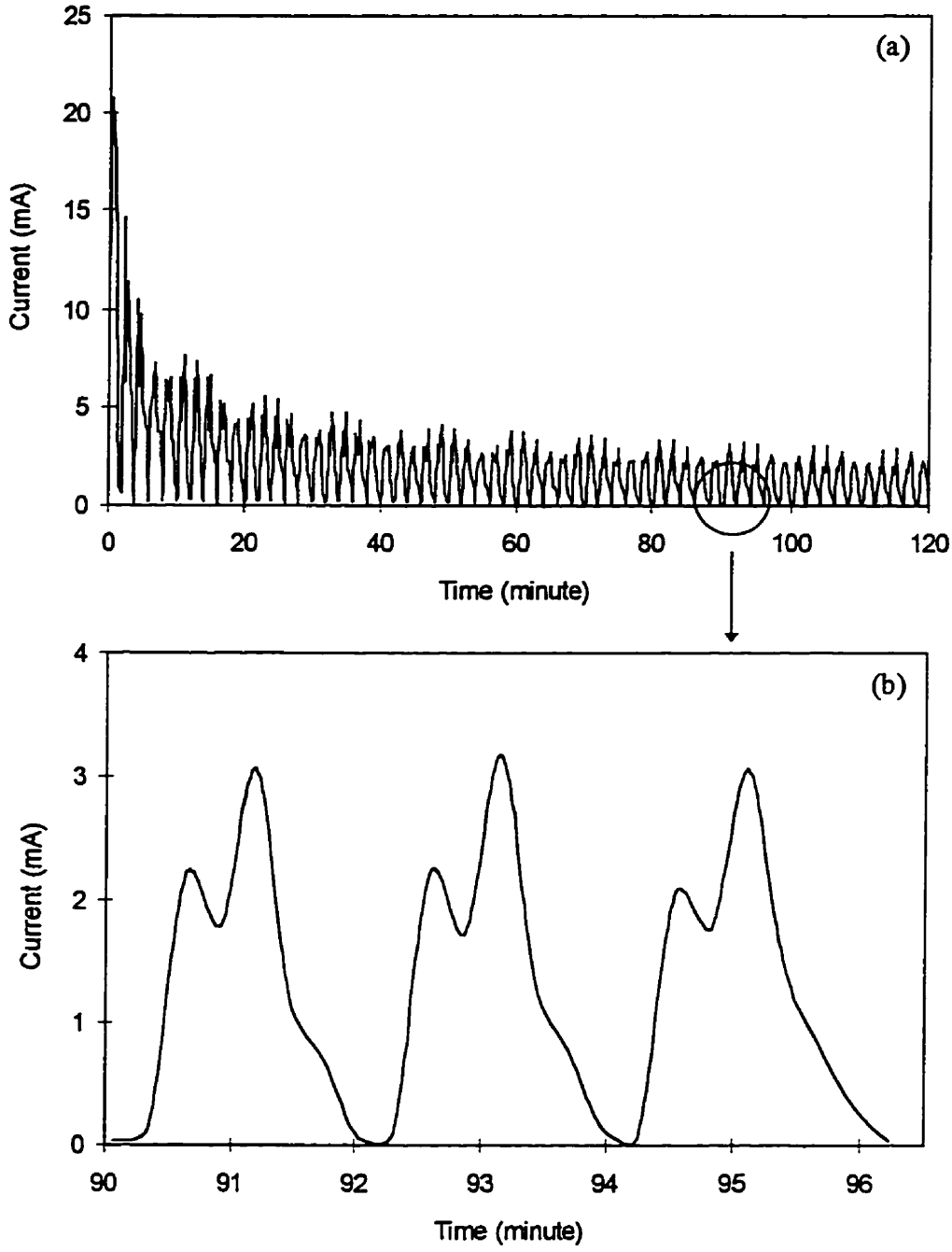

Fig. 10.4. I-t diagrams of CPS electrolysis of 2-vinylpyridine on a graphite electrode. The electrolysis current starts low (only 20 mA) due to the less intense of hydrogen evolution. Fig. 10.4b shows clearly the feature of monomer reduction reaction during the potential sweep. The detailed electrolyte composition, experimental conditions and the dimension of the electrodes are described in Table 10.1.

Electropolymerization of 2-vinylpyridine on a graphite electrode shows very interesting results. Graphite also has a high hydrogen overpotential and therefore, the corresponding cathodic linear sweep can be extended to –3 V without severe interference from hydrogen evolution. After two hours of CPS electrolysis between –0.7 and –2.5 V, the experimental results obtained are rather similar to those from zinc and lead electrodes. The I-t diagram is shown in Fig. 10.4. The electrolysis current starts low (only 20 mA) due to the less intense of hydrogen evolution. The enlarged I-t diagram shows clearly the feature of monomer reduction reaction during the potential sweep. The coating is yellow, while the electrolytic solution is still clear after the two-hour CPS electrolysis. The coating is hard and tightly adherent to the graphite rod. This suggests a potential application of poly(2-vinylpyridine) coatings for protecting graphite materials from scratching and abrasion during material handling processes. Abundant research has been done for similar applications using different monomers via electropolymerization (Subramanian and Jakubowski, 1978; MacCallum and MacKerron, 1982; Chang et al., 1987; Iroh et al., 1990 and 1991; Wimolkiatisak and Bell, 1992; Iroh et al., 1993a and 1993b; Liang et al., 1993c; Iroh et al., 1994).

Another important observation from the above experiments on electropolymerizing 2-vinylpyridine coating on various substrates is that the criterion that determined the optimum solution pH value for a mild steel substrate apparently can also be applied to other electrode systems. This indicates that the effect of solution pH on the electropolymerization process is dictated by the *p*Ka value of the monomer and independent of the nature of the electrode materials. More discussion of this issue will be present in the next section. The experimental conditions and results are summarized in

Table 10.1. For comparison, the experimental conditions for a system with mild steel substrate and the corresponding results are also listed in the table.

10.2.2. Electropolymerization of Coatings with Various Monomers

The most important aim in forming polymer coatings from other monomers in this study is to critically assess the proposed mechanism for electropolymerization of 2-vinylpyridine. To facilitate coating formation as much as possible, zinc and lead working electrodes (active area of 5.5 cm^2) are used. Based on the proposed mechanism, the following three criteria are key to successful electropolymerization: 1) the monomer should have an unsaturated molecular structure (e.g., C=C or C=N bond), which is active enough for polymerization. Such information can be inferred from the Q values in the Q-e scheme; 2) the monomer should have enough basicity that it can be protonated, adsorb on an electrode surface and undergo cathodic reduction. Such information can be obtained from the pKa values of the monomer; 3) the polymer formed should also have sufficient basicity that it can be protonated and cathodically reduced and consequently undergo revivification. A multi-waved voltammogram will then be a good indication for such a process. A number of the monomers have been selected for electropolymerization since they fulfill these requirements. To further evaluate the proposed mechanism, several monomers that do not meet the above criteria have also been tested. Nevertheless, the same electrochemical approach that was successful for 2-vinylpyridine has been applied to all of the monomers.

The following monomers have been selected for electropolymerization: 4-vinylpyridine (Aldrich, inhibited with 100 ppm hydroquinone), 1-vinylimidazole (BDH),

aniline (AnalaR), arylamide (J. T. Baker), acrylonitrile (Aldrich, inhibited with 35-45 ppm hydroquinone monomethyl ether), methacrylonitrile (Aldrich, inhibited with 50 ppm hydroquinone monomethyl ether) and methyl methacrylate (BDH, inhibited with 10 ppm hydroquinone monomethyl ether). The monomers are purified by passing through the inhibitor remover columns (Aldrich, column 30,631-2). Some properties (such as *p*Ka and *Q-e* scheme) of the selected monomers are listed in Table 10.2. The purified monomers are then dissolved in an aqueous solution containing 10 *vol.* % methanol to make 0.25 M monomer solutions. Supporting electrolyte is added to each solution to bring its concentration to 0.05 M and the corresponding acid or base is used to adjust the solution pH. For a monomer with a known *p*Ka value (Perrin, 1965), the solution pH is then directly adjusted close to this value. Otherwise, exploratory tests are carried out to determine a proper electrolyte pH. Voltammograms are obtained for every monomer system with a zinc or lead working electrode to decide the potential range for the CPS electrolysis. The detailed experimental conditions and results are summarized in Table 10.2. For comparison, the results for a poly(2-vinylpyridine) coating are also listed in the table.

4-Vinylpyridine readily dissolves in a 10% methanol aqueous solution to give an initial pH of 7.65. NH_4ClO_4-$HClO_4$ solution is first used as the supporting electrolyte and also to adjust the solution pH to 5.5. Surprisingly, the solution becomes turbid a few minutes after the mixing and then a large amount of white precipitate forms. No distinct changes in solution temperature and pH are observed during this precipitation process. However, if the solution pH is reduced quickly after the mixing of the solution to lower than 1.5, the precipitation can be prevented. However, once the precipitate has formed,

Table 10.2. Electropolymerization of various monomers via CPS electrolysis for 2 hours[⊗]

Type of Monomer	$Q^{\dagger}$ Value	$e^{\dagger}$ Value	$pKa^{\ddagger}$ Value of Monomer	Solution pH	Half-Wave Potential (V)	CPS Range (V)	Coating Weight (mg)	Coating Description
2-Vinylpyridine	1.41	−0.42	4.92	4.8	−0.95; −1.30; −1.91	−0.9 to −2.3	14.7	Thick and uniform coating,
4-Vinylpyridine	2.47	0.84	5.62	5.5[•]	−1.0; −1.85	−0.7 to −2.3	8.0	Thick and uniform coating
1-Vinylimidazole	0.11	−0.68	7.5	7.5	−1.2; −1.6; −2.3	−0.7 to −2.5	2.1	Thin and uniform film
Acrylonitrile	0.48	1.23	—	2.0	−1.1	−1.0 to −2.2	1.6	Thin and uniform coating
Methacrylonitrile	0.86	0.68	—	2.5	−1.1	−1.0 to −2.1	1.4	Thin and uniform coating
Methyl methacrylate[ξ]	0.78	0.40	—	1.8	−0.65	−0.48 to −1.8	1.1[Γ]	Powdery coating
Acrylamide[ξ]	0.23	0.54	—	2.5	−1.1	−0.7 to −2.3	1.3	Thin and non-uniform film
Aniline	—	—	4.6	4.5	—	—	—	Anodic coating formation

[⊗] Each monomer has a concentration of 0.25 M and is dissolved in a 10 *vol* % methanol aqueous solution. Except where mentioned specifically, the supporting electrolyte is NH_4ClO_4, the solution pH is adjusted by $HClO_4$ and the working electrode is zinc (5.5 cm^2).

[•] Supporting electrolyte is 0.05 NH_4NO_3 and solution pH is adjusted by HNO_3.

[†] From Greenley, 1984.

[ξ] On lead electrodes

[Γ] Some precipitate also accumulates at the bottom of the electrolytic cell.

[‡] From Perrin, 1965.

adjustment to a low solution pH cannot make the precipitant disappear. Precipitation always occurs when the solution has a high pH (> 5.5).

The reason for the above precipitation is not clear. A possible cause may be the formation of a carbonium radical, $M^{+\bullet}$, by the strong oxidant ClO_4^- (Shapoval and Gorodyskii, 1973)

$$ClO_4^- + 2M + H_2O \longrightarrow ClO_3^- + M^{+\bullet} + OH^- \qquad (10.17)$$

The carbonium radical $M^{+\bullet}$ would then begin cationic polymerization

$$M^{+\bullet} + M \longrightarrow M\text{-}M^{+\bullet} \qquad (10.18)$$

where M is the 4-vinylpyridine monomer and $M^{+\bullet}$ represents the relevant carbonium radical. The ability of 4-vinylpyridine to undergo such a reaction may be due to its high Q value in the Q-e scheme (Table 10.2).

NH_4NO_3-HNO_3 solution is then used as the supporting electrolyte (0.05 M NH_4NO_3) and also to adjust the solution pH to 5.5. In this case, the solution remains clear and no precipitation occurs up to 3 days. Linear sweep voltammetry is carried out between –0.7 and –2.5 V at 30 mV/s. The obtained voltammogram is shown in Fig. 10. 5.

It is seen that at least two reduction current waves appear in the voltammogram. The two reduction waves have $E_{1/2}$ of –1.0 V and –1.85 V, respectively, followed by the large wave for hydrogen evolution. An anodic linear sweep voltammogram that has also been obtained shows no current wave other than one for oxygen evolution. The effects of the solution pH on the shape of the voltammograms and on the rate of the current decreases during a one-hour chronoamperometric electrolysis are shown in Figs. 10.6 and 10.7, respectively. The results are found to be quite similar to that for 2-vinylpyridine electropolymerization, as shown in Figs. 7.1 and 7.3, respectively.

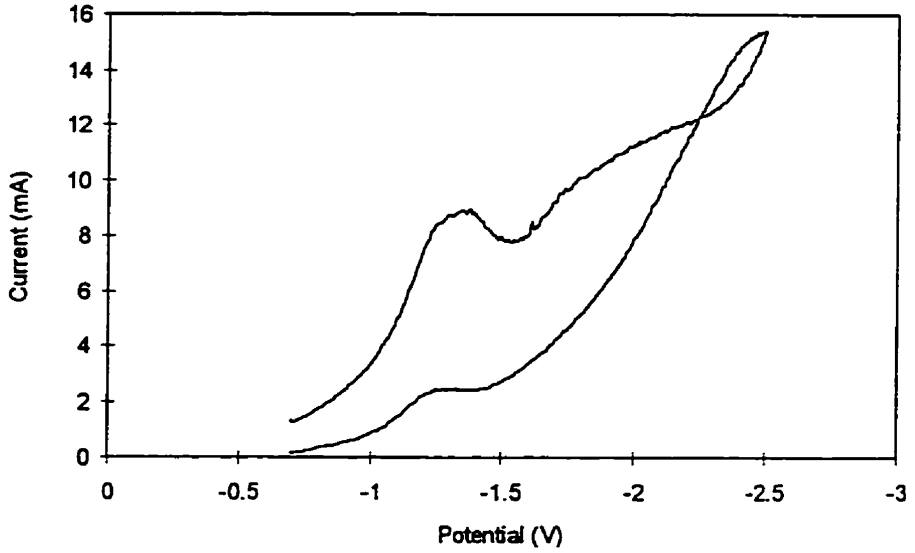

Fig. 10.5. Cathodic linear sweep voltammogram of 4-vinylpyridine (0.25 M) in 10% methanol aqueous solution, with 0.05 M NH_4NO_3 as supporting electrolyte. Solution pH is 5.5 adjusted with HNO_3. Potential scan is between –0.7 to –2.5 V at 30 mV/s. Working electrode is zinc (5.5 cm^2).

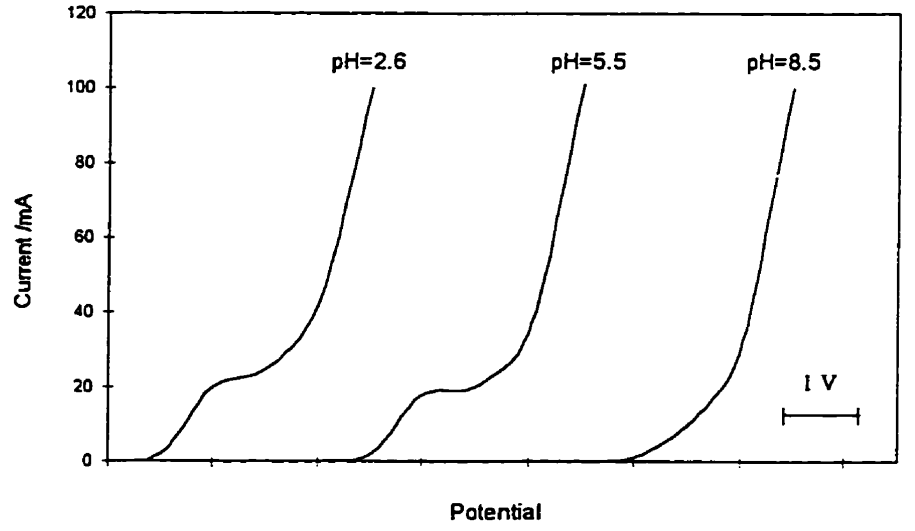

Fig. 10.6. The effect of solution pH on the shape of the linear sweep voltammograms of 0.25 M 4-vinylpyridine. Solution pH is adjusted with concentrated HNO_3. Potential scan is between –0.7 V and –2.5 V at 30 mV/s. The curves have been shifted along the potential axis deliberately to avoid any overlap.

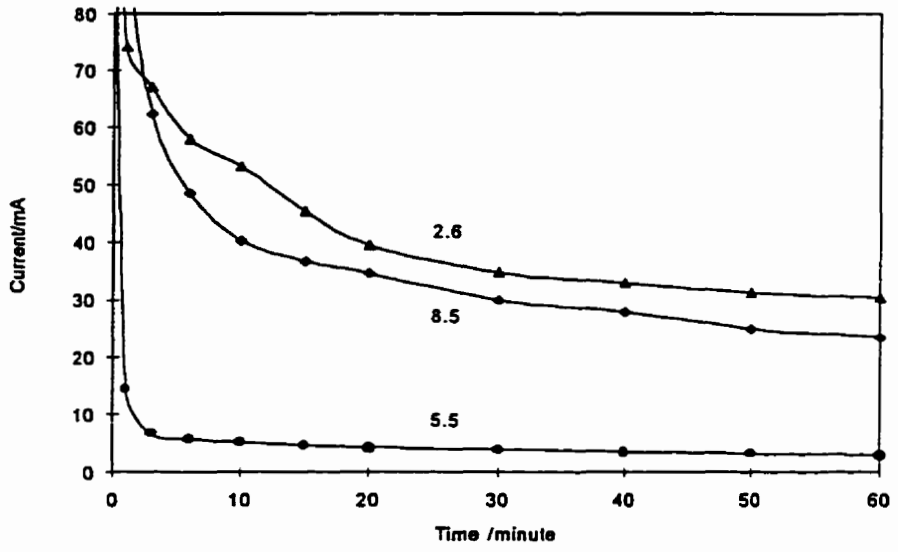

Fig. 10.7. The effect of solution pH on electrolytic current during chronoamperometric electrolysis of 4-vinylpyridine at a constant potential of −1.5 V. Solution pH are 2.6 (—▲—), 5.5 (—●—) and 8.5 (—◆—), adjusted with HNO_3.

Chronoamperometric electrolysis has been carried out for poly(4-vinylpyridine) coating formation at cathodic potentials of −1.0, −1.2 and −1.5 V, at pH 5.5. No visible coating is found on the electrode surface after 1 hour of chronoamperometric electrolysis at a potential of −1.0 V, whereas only very thin coatings are obtained at −1.2 and −1.5 V. Hydrogen evolution is observed during the above processes, and is likely partially responsible for the thinness and poor uniformity of the coatings. CPS electrolysis between −0.7 V and various cathodic limits has also been carried out for poly(4-vinylpyridine) coating formation. When the cathodic limit of the scan is not low enough (i.e., −1.5 V), only a very thin coating forms after a two-hour electrolysis. When the cathodic limit is decreased to −2.3 V, a thick and uniform poly(4-vinylpyridine) coating forms on the electrode surface. The relevant I-t diagram is shown in Fig. 10.8. The coating is also

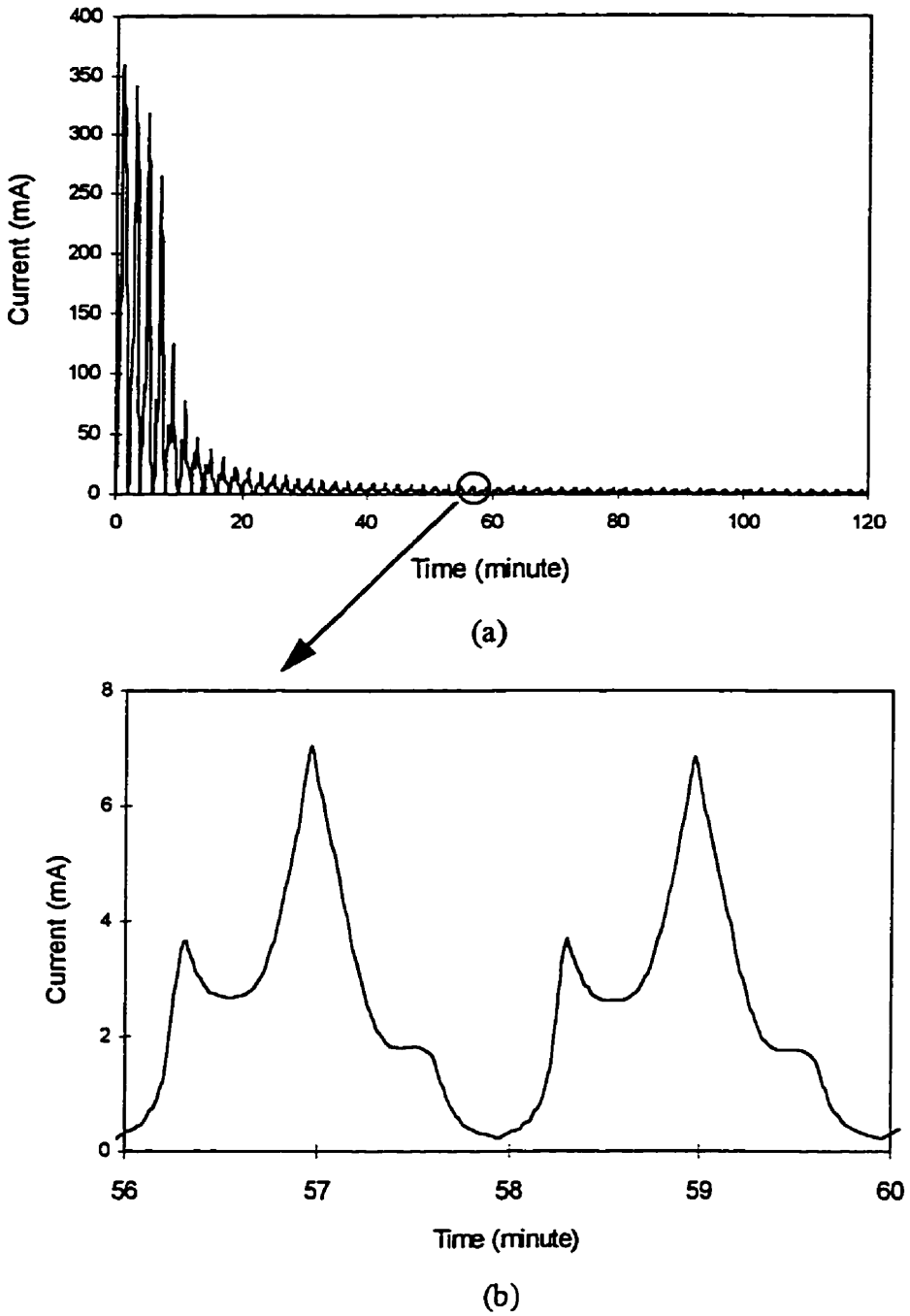

Fig. 10.8. The I-t diagram of a two-hour CPS electrolysis of 0.25 M 4-vinylpyridine in 10% methanol aqueous solution. The supporting electrolyte is NH_4NO_3, and the solution pH is 5.5, adjusted with HNO_3. The cathodic potential sweep range is between –0.7 and –2.3 V at 30 mV/s.

yellow, but with a slightly green tint. The coating is somewhat powdery and the adhesion to the electrode surface is not as good as in the case of the poly(2-vinylpyridine) coating with NH_4ClO_4 as supporting electrolyte. The coating is relatively uniform with an average thickness of 9.4 μm based on CSLM analysis. Combined with a coating weight of 8.0 mg, the poly(4-vinylpyridine) coating is found to have a density of 1.55 g/cm^3. The coating is also electrically insulating and cannot be dissolved in common organic solvents (e.g., THF, TCB or chloroform, etc.). The results are summarized in Table 10.2.

The above experiments on poly(4-vinylpyridine) coating formation by electropolymerization have been carried out under the guidance of the previous experience with 2-vinylpyridine and the proposed mechanism for polymer coating formation. This includes, for example, the selection of the solution pH (close to the monomer *p*Ka value), the type of electrochemical technique (CPS electrolysis) and the potential range for the CPS electrolysis (from the multi-waved voltammogram), etc. The results with 4-vinylpyridine confirm that the proposed process mechanism incorporates the intrinsic characteristics of the electropolymerization coating formation. It can be applied not only to 2-vinylpyridine system, but to other organic systems as well. More applications of the proposed process mechanism to other monomer systems are discussed below in a less detailed manner.

The electropolymerization of 1-vinylimidazole has been carried out in a similar way as for the vinylpyridines, and the experimental results are similar as well. Since 1-vinylimidazole has a much smaller Q value (0.11) in the Q-e scheme, its relative reactivity is much smaller than that of the vinylpyridines. The higher *p*Ka value (7.5) indicates its stronger basicity, and so the corresponding electrolyte (0.25 M 1-vinylimidazole in 10%

methanol aqueous solution with 0.05 M NH_4ClO_4 as supporting electrolyte) has an initial pH of 8.7. The solution pH is then decreased to 7.5 with $HClO_4$. Several reduction waves appear on the voltammogram from the above electrolyte on a zinc working electrode, with $E_{1/2}$ of −1.2, −1.6 and −2.3 V (Fig. 10.9). Hydrogen evolution is relatively intense during the voltammetry measurement and the obtained voltammogram is relative noisy, especially near the cathodic limit. Chronoamperometric and CPS electrolysis have also been carried out for poly(1-vinylimidazole) coating formation on zinc substrates. Some yellow coating (2.1 mg) forms after a two-hour CPS electrolysis between −0.7 and −2.5 V at 30 mV/s. During the electropolymerization, the colour of the electrolytic solution changes to light yellow. The coating is rather thin, but quite uniform, hard and tightly adherent to the electrode surface. It is also electrically insulating and cannot be dissolved in THF and TCB. The relevant results are also summarized in Table 10.2.

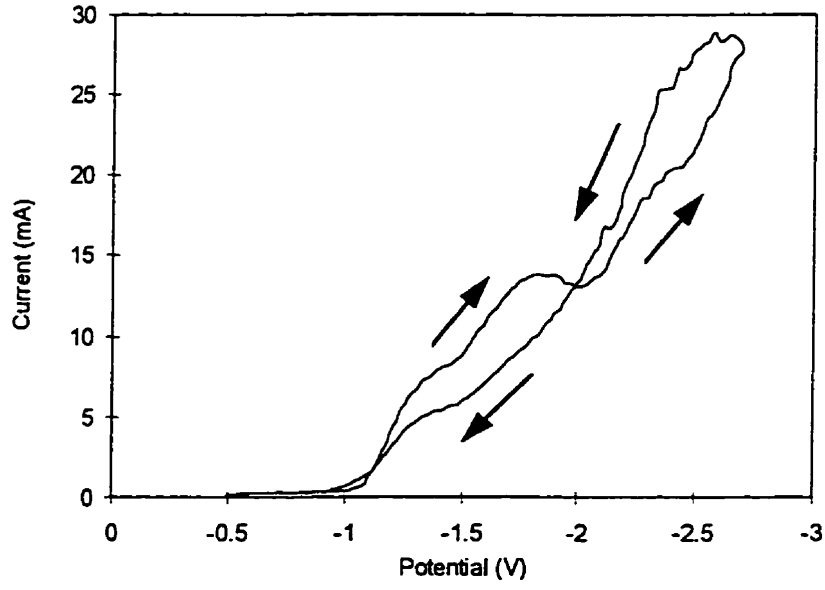

Fig. 10.9. The linear sweep voltammogram of 0.25 M 1-vinylimidazole in 10% methanol aqueous solution on a zinc electrode. The supporting electrolyte is 0.05 M NH_4ClO_4, and the solution pH is 7.5, adjusted with $HClO_4$. The cathodic potential scan rate is 30 mV/s.

The reason for the formation of a very thin poly(1-vinylimidazole) coating on the electrode surface may be related to its relative low reactivity. Although 1-vinylimidazole can be protonated in aqueous solutions, its reduction potential is more negative than that of the vinylpyridines due to the low reactivity. Therefore, hydrogen evolution becomes a more competitive reaction on the cathode surface. This causes the formed coating to be rather thin and the voltammogram to be relatively noisy.

Electropolymerization of acrylonitrile is carried out in a similar way as for the 2-vinylpyridine. The organic dissolves in the solvent readily and no precipitation occurs. Unlike vinylpyridines, acrylonitrile is not basic and its addition to the electrolyte does not change the electrolyte pH significantly. The pH changes only from 5.6 to 5.2 (compared to a change from 5.6 to 7.5 in 2-vinylpyridine solutions). However, the solution pH is not stable. A small amount of acid (e.g., $HClO_4$) or base (e.g., NH_4OH) added to the solution can change the solution pH below 2.0 or above 8.5, respectively, from the original pH value of 5.2. Linear sweep voltammetry has been carried out between the potentials of –1.06 and –2.15 V at 30 mV/s at solution pH of 2.0 on a zinc electrode. A small but consistent current wave ($E_{1/2}$ of –1.1 V) is observed before the large hydrogen evolution wave (Fig. 10.10). However, no second reduction wave associated with the organic appears, even in the voltammogram on a pre-coated electrode (not shown here). At high solution pH (e.g., 8.5), no monomer reduction wave can be observed from the relevant voltammogram. Chronoamperometric electrolysis has been carried out at –1.25 V and no coating can be found after a one hour electrolysis. The decline in electrolysis current is more gradual than that in the vinylpyridine situation. CPS electrolysis has also been carried out over a potential range from –1.0 to –2.2 V at 30 mV/sec at a solution pH of 2.0 on a

zinc electrode. The coating is thin but uniform, hard and tightly adherent to the electrode surface. It is also electrically insulating but can be partially dissolved in THF and methanol. The relevant results are also summarized in Table 10.2.

The reason for the formation of only a thin polyacrylonitrile coating by electropolymerization may be due to significant differences with the previously proposed mechanism for 2-vinylpyridine. The nitrogen atom in an acrylonitrile molecule is in the form of C≡N, so that it is not electronegative as it is in vinylpyridine. Consequently, acrylonitrile is not a weak base and does not become protonated in acidic aqueous medium. Although it may still be reduced at the cathode and form coatings by some other mechanism (which is not clear yet), the formed polymer is not readily reducible, as in the cases of polyvinylpyridines and poly(1-vinylimidazole). Thus, the corresponding voltammogram (Fig. 10.10) is not multi-waved, like those of 1-vinylimidazole and vinylpyridines. Good quality coatings (i.e., thick, uniform and relatively insoluble in organic solvents) cannot be formed using the same approach that works for vinylpyridines. Instead, hydrogen evolution becomes intense and dominant.

The electropolymerization of methylacrylonitrile is carried out in a similar way as for acrylonitrile, and the experimental results are quite similar as well. The solution pH is initially 4.7, but very sensitive between pH 2.5 and 9.0. A reduction wave ($E_{1/2}$ of −1.1 V) appears in the voltammogram of the solution of pH 2.5, but no such wave was observed of the solution of pH 9.0. Chronoamperometric (at −1.2 V) and CPS (between −1.0 and −2.1 V) electrolysis have been carried out for polymethylacrylonitrile coating formation on zinc substrates. Some thin, but uniform coating forms after a two-hour CPS electrolysis.

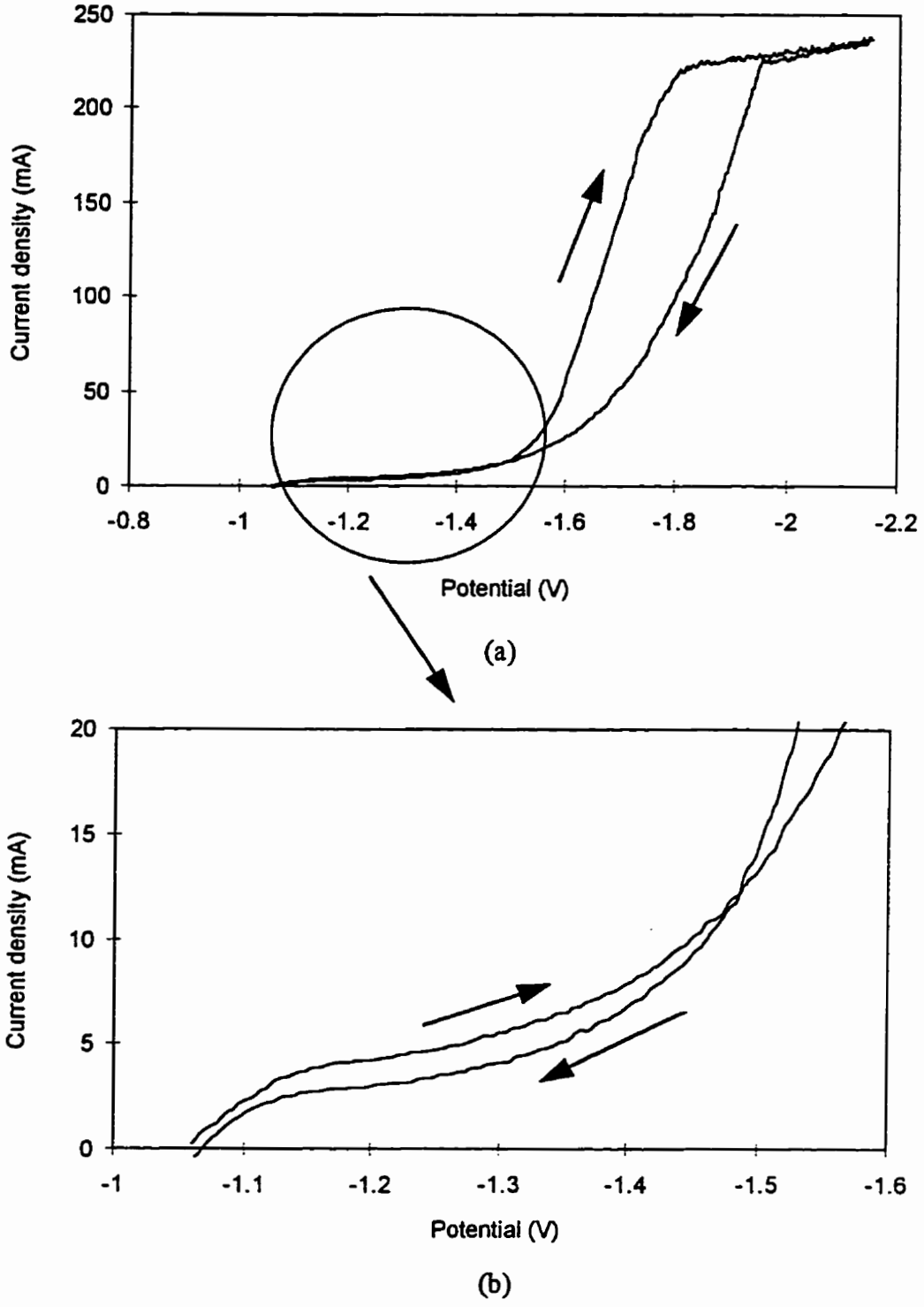

Fig. 10.10. The linear sweep voltammogram for a 0.25 M acrylonitrile in 10% methanol aqueous solution on a zinc electrode. The supporting electrolyte is NH_4ClO_4, and the solution pH is 2.0, adjusted with $HClO_4$. The cathodic potential scan rate is 30 mV/s.

The coating is hard and tightly adherent to the substrate. It is also electrically insulating and can be partially dissolved in THF and methanol. The relevant results are summarized in Table 10.2.

The electropolymerization of methyl methacrylate is carried out in a similar manner. The pH of a 0.25 M methyl methacrylate aqueous solution (with 10% methanol) is initially 6.9, but is unstable and varies between 1.8 and 8.4. A reduction current wave ($E_{1/2}$ of –0.65 V) appears in the voltammogram (on a lead working electrode) of solution pH 1.8 (Fig. 10.11). No monomer reduction wave was observed in high pH solution (e.g., pH 8.5). Chronoamperometric (at –0.6 V) and CPS electrolysis (between –0.48 and –1.8 V) are carried out for poly(methyl methacrylate) coating formation on lead substrates. During the electrolysis, the current decreases quickly (Fig. 10.12). Some white particles form in the solution and accumulate at the bottom of the cell, while other particles adhere to the cathode and form a coating. The coating poorly adheres to the substrate surface and can be easily wiped off. The relevant results are also summarized in Table 10.2.

The reason for the poor coating by the electropolymerization approach used for vinylpyridines may also be due to the fact that a different mechanism is operating. Similar to acrylonitrile and methacrylonitrile, methyl methacrylate is not an organic base and therefore does not become protonated in an acidic aqueous solution. Although it can still be reduced at the cathode surface and form a polymer following some unknown mechanism, the formed polymer does not adhere on the electrode surface and cannot be reduced to form good quality coatings. Instead, hydrogen coverage is dominating on the cathode surface and intense hydrogen evolution occurs. The formed polymer products slough off into the bulk solution, either by hydrogen gas evolution or by electrode

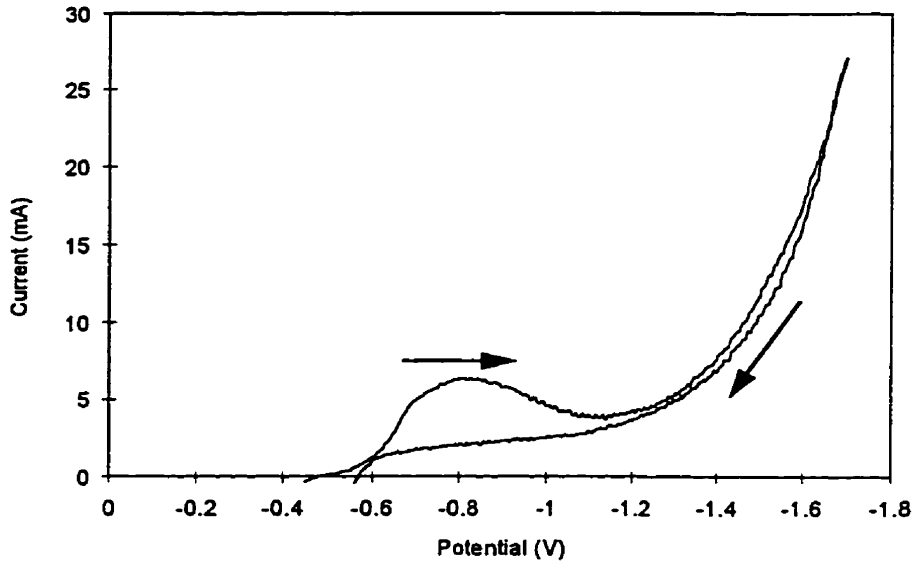

Fig. 10.11. The linear sweep voltammogram for a 0.25 M methyl methacrylate aqueous solution in 10% methanol on a lead electrode. The supporting electrolyte is NH_4ClO_4, and the solution pH is 1.8, adjusted with $HClO_4$. The cathodic potential scan rate is 30 mV/s.

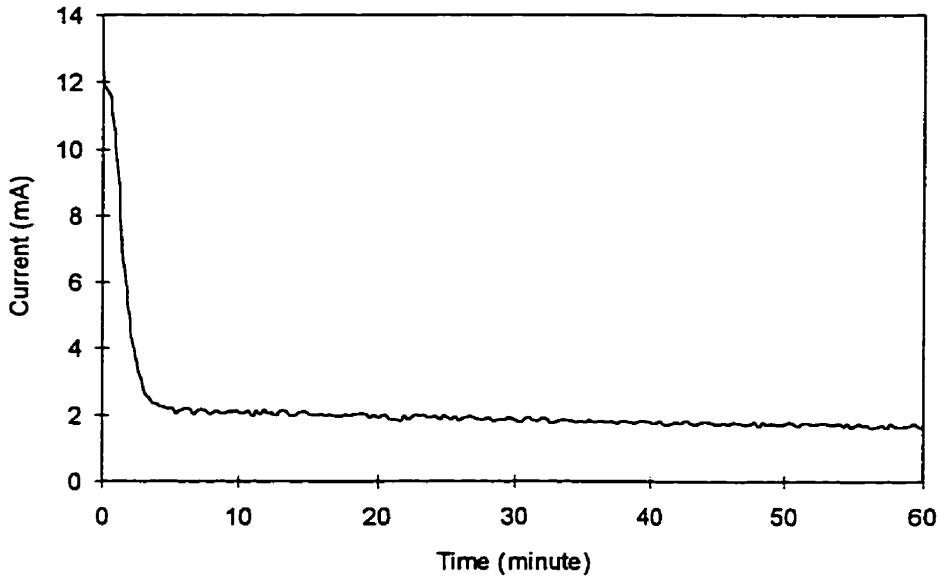

Fig. 10.12. The I-t diagram of chronoamperometric electrolysis for a 0.25 M methyl methacrylate in 10% methanol aqueous solution at –0.6 V . The supporting electrolyte is NH_4ClO_4, and the solution pH is 1.8, adjusted with $HClO_4$.

repulsion. The experimental results are summarized in Table 10.2. Detailed study of the mechanism is out of the scope of this project.

The electropolymerization of acrylamide is carried out in a similar manner as above. The pH of a 0.25 M acrylamide aqueous solution (with 10% methanol) is initially 5.6, but is not stable and varies between pH 2.5 and 8.5. In a solution of pH 2.5, a reduction current wave appears in the voltammogram on a lead working electrode with a half-wave potential of −1.1 V. Chronoamperometric (at −1.2 V) and CPS (between −0.7 to −2.3 V at 30 mV/s) electrolyses have been carried out for polyacrylamide coating formation on lead substrates. During the electrolyses, the current also decreases, but the hydrogen evolution is strong and the current decrease is not as rapid as that in vinylpyridine electropolymerization. Some coating (1.3 mg) is found after two-hour CPS electrolysis. The coating is thin and white in colour, but not distributed evenly on the substrates. The experimental conditions and results are also summarized in Table 10.2.

The results from electropolymerization of aniline are initially surprising. It was carried out in a similar manner as described above. The 0.25 M aniline aqueous solution (with 10% methanol) had an initial pH of 7.1 due to the weak basicity of the aniline. The *p*Ka value of aniline in aqueous solution is 4.6 (Perrin, 1965). Therefore, the solution pH was adjusted to 4.5 with $HClO_4$. A linear sweep voltammogram was then measured on a zinc working electrode. Although a multi-waved voltammogram (similar to Fig. 10.9) was expected, no reduction wave was actually observed. Intense hydrogen evolution occurred on the cathode surface. Nevertheless, a dark colour coating was formed on the platinum anode after a few seconds. The coating was uniform and insoluble in organic solvents. It even had a strong resistance to strong acid solutions (e.g., the Electrode-Cleaner® from

Fisher Scientific). The reason for the organic oxidation reaction on the anode instead of a reduction reaction on the cathode is not clear. It has been suggested (Venugopal et al., 1995) that the protonated aniline molecules might form a complex with the anions of the supporting electrolytes. This complex could migrate to the anode and undergo polymerization. Study of the detailed mechanism is beyond the scope of this thesis.

The above studies show that the electropolymerization mechanism identified from poly(2-vinylpyridine) coating formation successfully reflects some intrinsic characteristics of the process. It has been successfully applied to several other monomers, such as 4-vinylpyridine and 1-vinylimidazole. In addition to the usual properties required for polymerization, these monomers have sufficient basicity that they can be protonated in an acidic solution, adsorb at the cathode and undergo cathodic reduction to generate free radicals. For best results, the formed polymers should also be sufficiently basic that they can undergo protonation, reduction and revivification to produce branching and crosslinking polymer coatings. Solution pH always plays an important role regardless of the electrodes or the monomers, indicating the fundamental relationship between the *p*Ka value of the monomers and the electropolymerization process. Electropolymerization of those monomer/polymer systems, such as methyl methacrylate, acrylonitrile and acrylamide, etc. that do not fulfill all of the above requirements was unsuccessful.

CHAPTER 11

CONCLUSIONS AND RECOMMENDATIONS

11.1. Conclusions

Polymer coating formation by electropolymerization on electrically conducting substrates has been studied in aqueous solutions. Starting with the 2-vinylpyridine monomer, various aspects of the electropolymerization process were investigated in a laboratory-scale electrolytic cell. The effects of operating parameters were studied individually and via orthogonal- fractional-factorial-designed experiments. The relative importance of the operating parameters and an optimum combination of some important operating parameters were determined. The formed polymer coatings were characterized via UV-visible, FT-IR and ^{1}H NMR spectroscopy. Coating morphology and topology were studied quantitatively using confocal scanning laser microscopy. In addition, the mechanism of the electropolymerization process was investigated employing inhibition, surface enhanced Raman scattering (SERS) spectroscopy and linear sweep voltammetry on electrodes pre-coated with poly(2-vinylpyridine). Based on the experimental results, a detailed mechanism of the electropolymerization process was proposed and related to experimental results obtained using other electrode substrates and monomers. The major conclusions are summarized below:

1). Various electrochemical techniques were investigated for the electropolymerization. Cyclic potential sweep (CPS) electrolysis was found to be the most suitable method for coating formation by electropolymerization. A cathodic potential scan range from –0.7 to –2.5 V at a

scan rate of 30 mV/s was found suitable for 2-vinylpyridine electropolymerization on mild steel substrates. CPS has also been proven to be a powerful technique to study the mechanism of the electropolymerization process.

2). 2-Vinylpyridine can be protonated in an acidic aqueous medium to form 2-vinylpyridinium ions that adsorb on the cathode and can be reduced to free radicals. The generated radicals, after stabilization by a neutral 2-vinylpyridine molecule, initiated the polymerization. Propagation of the polymer chain involved the repeated combination of the ever-growing polymer radical with neutral 2-vinylpyridine molecules. Therefore, solution pH value was critical for the electropolymerization process. Only when solution pH was in a narrow range of 4.5 to 5.5 (close to the *p*Ka value of the monomer) could electropolymerization be initiated and propagated successfully.

3). Higher monomer concentration was found to favour coating formation. It provided effective competition with the hydrogen evolution on the cathode surface and led to the formation of thick and uniform polymer coatings. However, excessively high monomer concentration made monomer dissolution difficult and resulted in a polymer coating that was not completely solidified. Methanol content in the electrolyte was another important factor in electropolymerization. A suitable methanol content in the electrolyte was found to be between 10 to 25 *vol* %. A low methanol content did not allow sufficient monomer dissolution and a high methanol content led to a thin coating. An operating temperature between 20 and 40 °C was found to be most favourable for coating formation. A high operating temperature (> 40°C) tended to generate a low molecular weight polymer and increase the solubility of the coating polymer in the electrolyte, consequently leading to a thin coating. A low operating temperature (i.e., 10°C) sometimes was suitable for coating formation due to the benefit of the formation of

a higher molecular weight polymer. The relative importance of the above operating parameters decreased in the following order: monomer concentration > solution pH > methanol content in the solvent > operating temperature.

4). The effects of other operating parameters on the electropolymerization have also been examined. The electrolysis duration was found to affect the coating thickness proportionally before the first two hours. After two hours had elapsed, electrolysis duration was observed to have only a minimum effect. NH_4ClO_4 was found to be the best supporting electrolyte for the coating formation, although its concentration did not affect the process significantly. The presence of the anion ClO_4^- appeared to play an important role in the electropolymerization coating formation process, however, the research provided no clear explanation for this observation.

5). The mechanism of the electropolymerization has been confirmed as a free radical polymerization by inhibition studies. This initiation mechanism appears to occur as the consequence of 2-vinylpyridinium reduction reaction on the cathode rather than hydrogen radical initiation or transfer process. The conclusion is based on the experimental results of voltammetric studies and the impact of electrolyte pH on the electropolymerization process. Surface enhanced Raman scattering (SERS) spectroscopy was applied to investigate the organic monomer protonation and adsorption behaviour in the bulk solution and on electrode surfaces. Further evidence for 2-vinylpyridine protonation, adsorption and reduction on the cathodic surfaces was obtained. The voltammetry study on electrodes pre-coated with poly(2-vinylpyridine) suggested that the formed coating could be further protonated in an acidic medium and undergo revivification at a more negative electrode potential.

6). The formed coating polymer has been characterized via various spectroscopic techniques, such as UV-visible, FT-IR and ^{1}H NMR. These investigations confirmed that polymerization had occurred and that no significant organic by-product was being formed in the coating. The isotope elemental analysis of the formed polymer coating showed a chemical composition close to that expected from the stoichiometry of 2-vinylpyridine. The DCP analysis confirmed the absence of metal ions, such as iron, in the coating polymer. DSC analysis was used to determine the T_g of the coating polymer which indicated a rather high average molecular weight with a somewhat broad distribution.

7). Various coating properties have also been investigated. Coating adhesion on a mild steel substrate was studied using the cross hatching technique and good adhesion was found. Coating porosity was studied using a copper cementation method which confirmed a very dense coating. The conductivity of the coating was examined with an electrometer equipped with a four-point resistance probe. Infinite resistance was measured. The coating corrosion protection was investigated by a polarization technique. A significant improvement in corrosion resistance was confirmed.

8). Coating morphology and topology was evaluated quantitatively using confocal scanning laser microscopy. Under appropriate conditions, a typical coating thickness of 7.2 μm was produced within two hours of CPS electrolysis between –0.7 and –2.5 V at 30 mV/s. Coating roughness was also evaluated with the same technique. Coating density was estimated from the coating thickness measurements and the measured coating weights.

9). Poly(2-vinylpyridine) coatings were also formed on various substrates by the electropolymerization technique. The results indicated that the proposed process mechanism is independent of the properties of the electrode materials. Hydrogen evolution was found to play

a role in the process by decreasing the uniformity and thickness of the coating. On the other hand, its formation on the electrode surface during the electrolysis tended to make the coatings more dense and compact.

10). Various other polymer coatings were formed by the electropolymerization technique. These results confirmed some of the requirements for applying the proposed mechanism to electropolymerization coating formation. They include monomer protonation in a proper pH range; adsorption of the monomer species on the cathodic surface; monomer reduction and radical generation on the electrode surface; radical stabilization and polymerization. The polymer chains so formed can be further protonated and undergo revivification on the cathode, leading to a linearly short, but highly branched and cross-linked structure. This might enable further thermal curing to be omitted. The formed polymer coating, therefore, can be thick and uniform and insoluble in the solvents.

11). Electropolymerization has been shown to produce good quality polymer coatings from simple organic compounds in a single step. Surface enhanced Raman scattering (SERS) spectroscopy has been successfully applied in studying the mechanism of electropolymerization coating formation. Confocal scanning laser microscopy has been successfully applied in quantitative evaluation of polymer coating thickness and coating roughness distribution. Results obtained in this work should contribute significantly to the understanding and development of the technique of electropolymerization.

11.2. Recommendations

1). The detailed role of NH_4ClO_4 as the supporting electrolyte in the electropolymerization is an unsolved aspect of this research. It appears that the most intensive hydrogen evolution occurred in the presence of NH_4ClO_4, but it is also the electrolyte which produced the best coatings. It also makes the formed coating compact instead of powdery. It is not clear how the ClO_4^- ions improve the quality of the formed coatings. Additional research should be carried out on this topic. It is believed that a good understanding of this effect will enable further improvement of the electropolymerization technique.

2). The measured density of the poly(2-vinylpyridine) coating of 1.99 g/cm^3 is surprising since it is much higher than that expected for a polymer coating. However, most data of polymer densities reported are for polymers formed by bulk methods. No data of a polymer density from a coating has been reported due to the technical difficulties in coating thickness measurement. The arrangement of polymer chains and the degree of ordering for a polymer from bulk polymerization are likely to be considerably different for a polymer that is formed on and adheres to an electrode. The presence of polymer chains within the electric field at a cathode may also cause the polymer structure to be much more compressed than that otherwise possible. Although the highly branching and cross-linking of the formed polymer cannot entirely explain the density of 1.99 g/cm^3, it may partly contribute to the high value. Since no metal has been detected in the polymer coating, the high density cannot be attributed to this factor. Last but not least, there may be errors associated with the coating thickness measurement by CSLM. As has recently been pointed out by Dr. Kevin Ellis, the polymer coating refractive index might be different from that of the air in the experimental environment

6). Pulse plating is a relatively new and very promising electrochemical technique for various coating formation processes. Nevertheless, no application of this technique has ever been reported for electropolymerization. Since the nature of the pulse plating technique, i.e., the periodical alternation of the current density seems to fit the characteristics of the electropolymerization process, it would be worthwhile to investigate the possibility of applying this technique to electropolymerization. An appropriate combination of the electrochemical parameters of the pulse plating technique may bring further improvements to the electropolymerization process.

7). So far, the research in polymer coating formation by electropolymerization is very fundamental. Some modeling work should be done in the area to simulate the electropolymerization process. This will be helpful in understanding the process mechanism from another point of view and instructive for potential industrial practice.

8). Other monomers and monomer combinations should be investigated for formation of polymer coatings. This will be helpful for a more sophisticated understanding of the process mechanism and expand the application of the technique. Electrochemical copolymerization is certainly an interesting research area warranting more attention.

REFERENCES

Abruna, H. D., P. Denisevich, M. Umana, T. J. Meuyer and R. W. Murray, *J. Amer. Chem. Soc.*, **103** (1981) 1.

Adamcova, Z. and L. Dempirova, *Progr. Org. Coatings*, **16** (1989) 295.

Akbulut, U., J. E. Fernandez and R. L. Birke, *J. Polym. Sci. Polym. Chem.*, **13** (1975) 133.

Akbulut, U. and B. Hacioglu, *J. Polym. Sci., Part A, Polym. Chem.*, **29** (1991) 219.

Albrecht M. G. and J. A. Creighton, *J. Am. Chem. Soc.*, **99** (1977) 5215.

Anderson, J. D., M. M. Baizer and E. J. Prill, *J. Org. Chem.*, **30** (1965) 1645.

Arapapavinasam, S. S., *J. Polym. Sci., Polym. Chem.*, **31** (1993) 1105.

ASTM, in "Annual Book of ASTM Standards", ASTM, Philadelphia, PA, 1993, Vol. 06.01, Designation: D 522 - 92, p. 85.

Bard, A. J. and L. R. Faulkner, "Electrochemical Methods", John Wiley & Sons, Inc., New York, 1980, p. 218.

Bartlett, P. D. and H. Kwart, *J. Am. Chem. Soc.*, **72**(3) (1950) 1051.

Beer, K. D. W. Tanner and R. L. Garrell, *J. Electroanal. Chem.*, **258** (1989) 313.

Belanger, D. and M. S. Wrighton, *Anal. Chem.*, **59** (1987) 1426.

Bhadani, S. N. and G. Parravano, Electrochemical Anionic Polymerization of 4-Vinylpyridine in Pyridine, J. of Polymer Science, Part A-1, Vol. 8, 225-235 (1970).

Bhadani, S. N. and S. Kundu, *J. Polym. Mater.*, **1** (31) 1984.

Bhanu, V. A. and K. Kishore, *Chem. Rev.*, **91** (2) (1991) 99.

Billingham, N. C. and P. D. Calvert, *Adv. Polym. Sci.*, **90** (1989) 104.

Bockris, J. O'M and A. K. N. Reddy, "Modern Electrochemistry", Plenum Press, New York, 1970.

Borman, W. H. F., U. S. Pat. 3,335,075 (1967).

Brandt, E. S., *Anal. Chem.*, **57** (1985) 1276.Breitenbach, J. W. and C. Srna, *Pure Appl. Chem.*, **4** (1962) 245.

Brewer, G. E. F., in "Advances in Chemistry" series 119, American Chemistry Society, Washington, D. C., 1973.

Brolo, A. G., D. E. Irish and B. D. Smith, *J. Mol. Struct.*, **405** (1997) 29.

Chandler, G. K. and D. Pletcher, *J. Appl. Electrochem.*, **16** (1986) 62.

Chang, R. K. and T. E. Furtak, "Surface Enhanced Raman Scattering", Plenum Press, New York, 1982.

Chang, J., P. Bell and S. Shkolnik, Electro-copolymerization of Acrylonitrile and Methyl Acrylate onto Graphite Fibers, *J. Appl. Polym. Sci.*, **34** 2105 (1987).

Chohan, M. H., M. Asghar, M. Mazhar and U. Rafique, *Mod. Phys. Lett.*, B, **6**(27) (1992) 1755.

Clements, R. and J. L. Wood, *J. Mol. Struct.*, **17**, 283 (1973).

Clements, R. and J. L. Wood, *J. Mol. Struct.*, **17**, 265 (1973).

Cooke, B. A., N. B. Ness and A. L. L. Palluel, in "Industrial Electrochemical Processes", A. T. Kuhn, Ed., Elsevire, New York, 1971.

Crescenti, L., G. B. Gechele and M. Pizzoli, *Eur. Polym. J.*, **1** (1965), 293.

Davidovits P. and D. M. Egger, *Nature*, **223**, 831 (1969).

De Bruyne, A., J. L. Delplancke and R. Winand, *J. Appl. Electrochem.*, **25** (1995) 284.

Denisevich, P., H. D. Abruna, C. R. Leidner, T. J. Meyer, and R. W. Murray, *Inorg. Chem.*, **21** (1982) 2153.

Desbene-Monvernay, A., J. E. Dubois and P. C. Lacaze, *J. Electroanal. Chem.*, **89** (1978) 149.

Devaraj, G., S. Guruviah and S. K. Seshadri, *Mat. Chem. Phys.*, **25** (1990) 439.

Dey, A. N. and E. J. Rudd, J. *Electrochem. Soc.*, **121** (1974) 1294.

Dey, A. "Orthogonal Fractional Factorial Designs", Wiley Eastern Limited, New Delhi, 1985.

Diaz, A. F., K. K. Kanazawa and G. P. Gardini, *Chem. Soc., Chem. Commun.* (1979), 635.

Diaz, A. F. and K. K. Kanazawa, in "Extended Linear Chain Compounds", J. S. Miller, Ed., Vol. 3, Plenum Press, New York, 1983.

Diaz, A. F., Chemically Modfied Electrodes and Conducting Polymers, in "Organic Electrochemistry", H. Lund and M. M. Baizer, Eds., 3rd editions, Marcel Dekker, Inc., New York, 1991, p. 1363.

DiNardo, N. J., "Nanoscale Characterization of Surfaces and Interfaces", VCH, Weinheim, Germany, 1994.

Dineen, E., T. S. Schwan and C. Z. Wilson, *Trans. Electrochem. Soc.*, **96** (1949) 266.

Dixon, A. E., S. Damaskinos, M. R. Atkinson and L. H. Cao, *SPIE*, **1556,** (1991a) 144.

Dixon, A. E., S. Damaskinos and M. R. Atkinson, *Nature*, **351** (1991b) 551.

Dorfner, K., "Ion Exchangers Properties and Applications", Ann Arbor Science, Ann Arbor, 1972.

Dujardin, S., R. Lazzaroni, L. Riggo, J. Riga and J. J. Verbist, *J. Mater. Sci.*, **21** (4342) 1986.

Durney, L. J., "Electroplating Engineering Handbook", 4th edition, Van Nostrand Reinhold Company, New York, 1984.

Edneral, N. V., A. V. Ivanov, G. N. Kosyak and E. I. Fomicheva, *Russ. J. Nondestruc. Test.*, **29** (1993) 674.

Everson, M. P. and J. H. Helms, *Synth. Met.*, **40** (1991) 97.

Federation of Societies for Coating Technology, "Federation Series on Paint Technology, Unit 26, Corrosion and the Preparation of Metallic Surfaces for Painting", Federation of Societies for Coatings Technology, Philadelphia, PA, 1978.

Fell, N. F., Jr. and P. W. Bohn, *Anal. Chem.*, **65** (1993) 3382.

Fetters, L. J., in "Advances in Polymer Science", Vol. 38, Springer-Verlag, New York, 1984.

Fettes, E. M., "Chemical Reactions of Polymers", Mir, Moscow, 1967.

Fleischmann, M., P. J. Hendra and A. McQuillan, *J. Chem. Phys. Lett.*, **26** (1974) 123.

Fleischmann, M., I. R. Hill, G. Mengoli and M. M. Musiani, *Electrochim. Acta*, **28**(11) (1983) 1545.

Foster, R., "Organic Charge-Transfer Complexes", Academic Press, London, 1969, p. 296.

Fowkes, F. W., C. Y. Sun and S. T. Joslin, in "Corrosion Control by Organic Coatings", Henry Leidheiser, Jr., Ed., National Association of Corrosion Engineers, Houston, Texas, 1981, 1.

Funke, W., in " Surface Coatings-2", A. D. Wilson, J. W. Nicholson and H. J. Prosser, Eds., Elsevier Applied Science, Essex, England, 1987, p. 107.

Funt, B. L., *Macromol. Rev.*, **1** (1968) 35.

Funt, B. L., E. M. Peters and J. D. Van Dyke, *J. Polym. Sci., Part A: Polym. Chem.*, **24** (1529) 1986.

Funt, B. L., Electrochemical Polymerization, in "Organic Electrochemistry", H. Lund and M. M. Baizer, Eds., 3rd editions, Marcel Dekker, New York, 1991, p. 1337.

Garcia-Camarero, E., F. Arjona, C. Gullen, E. Fatas, C. Montemayor, *J. Mater. Sci.*, **25** (4914), 1990.

Garg, B. K., R. A. V. Raff and R. V. Subramanian, *J. Appl. Polym. Sci.*, **22** (1978) 65.

Garrell, R. L. and K. D. Beer, *Spectrochim. Acta*, **43B**(4/5) (1988) 617.

Garrell, R. L. and K. D. Beer, *Langumir*, **51** (989) 452.

Gaylord, N. G., *J. Polym. Sci., Macromol. Rev.*, **4** (1970) 183.

Gaylord, N. G. and S. S. Dixt, *J. Polym. Sci., Macromol. Rev.*, **8** (1974) 51.

Giam, C. S., in "Pyridine and its Derivatives", R. A. Abramovitch, Ed., Interscience Publishers, New York, 1961, Supplement Part 3, p. 112.

Gouveia, V. J. P., I. G. Guta and J. C. Rubin, *J. Electroanal. Chem.*, **371** (1994) 37.

Grace, W. R. et al., Br. Pat. 1,134,387 (1967).

Grace, W. R. et al., Br. Pat. 1,179,543 (1969).

Greenley, R. Z., in "Polymer Handbook", 3rd edition, J. Brandrup and E. H. Immergut, Eds., John Wiley & Sons, New York, 1984, II-267.

Gui, J. and T. Devine, *Corr. Sci.*, **36** (1994) 441.

Guntherodt H. J. and R. Wiesendanger, "Scanning Tunneling Microscopy", Springer-Verlag, New York, 1992.

Hacioglu, B., U. Akbulut and L. Toppare, *J. Polym. Sci., Polym. Chem.*, **27**(11) (1989) 3875.

Harsanyi, G., "Polymer Films in Sensor Applications", Technomic Publishing, Lancaster, Pennsylvania, 1995.

Haworth, B. and T. M. Robinson, *Polym. Test.*, **10** (1991), 205.

Heben, M. J., R. M. Penner, N. S. Lewis, M. M. Dovek and C. F. Quate, *Appl. Phys. Lett.*, **54,** (1989) 1421.

Hillman, A. R. in "Electrochemical Science and Technology of Polymers", R. G. Linford, Ed., Elsevier Applied Science, London, 1987, Vol. 1, Chapter 5, p. 103.

Hogen-Esch, T. E. and W. L. Jenkins, *J. Am. Chem. Soc.*, **103** (1981) 3666.

Hogen-Esch, T. E., Q. Jin and D. Dimov, *J. Phys. Org. Chem.*, **8** (1995) 222.

Hong, H., D. Davidov and R. Neumann, *Adv. Mat.*, **7** (1995) 846.

Huang, S. S., J. Lin, H. G. Lin and R. Q. Yu, *Mikrochim. Acta*, **117** (1995) 145.

Hummel, D. O., "Atlas der Polymer - und Kunststoffanalyse", Band 1, Polymere: Struktur und Spektrum, Carl Hanser Verlag, Verlag Chemie, 1978. p. 132.

Iroh, J., J. P. Bell and D. A. Scola, Thermoplastic Matrix Composites by Aqueous Electrocopolymerization onto Graphite Fibers, *J. Appl. Polym. Sci.*, **41** 735 (1990).

Iroh, J. O., J. P. Bell and D. A. Scola, Aqueous Electropolymerization of Polyacrylamide onto AS-4 Graphite Fibers, *J. Appl. Polym. Sci.*, **43** 2237 (1991).

Iroh J. O. and M. M. Labes, Pulsed-Current Electropolymerization and Postelectropolymerization of Acrylamide in Sulfuric Acid, *Macromolecules*, **25** (5178) 1992.

Iroh, J., J. P. Bell and D. A. Scola, Mechanism of the Electrocopolymerization of Styrene and N-(3carboxyphenyl) maleimide onto Graphite Fibers in Aqueous Solution, *J. Appl. Polym. Sci.*, **47** 93 (1993a).

Iroh, J., J. P. Bell and D. A. Scola, Rate of Electropolymerization of N,N'Dimethy Acrylamide in Aqueous Sulfuric Acid Solution, *J. Appl. Polym. Sci.*, **49** 583 (1993b).

Iroh, J., J. P. Bell, D. A. Scola and J. P. Wesson, Electrochemical Process for Preparing Continuous Graphite Fibre-Thermoplastic Composites, *Polymer*, **35** 1306 (1994).

Jeanmaire D. L. and R. P. Van Duyne, *J. Electroanal. Chem.*, **84** (1977) 1.

Jenkins, W. L., C. F. Tien and T. E. Hogen-Esch, *Pure and Appl. Chem.*, **51** (1979)139.

Kamachi, M., J. Satoh and S. I. Nozakura, *Polym. J.*, **9**(3) (1977) 301.

Kamachi, M., J. Satoh and S. I. Nozakura, *J. Polym. Sci., Polym. Chem.*, **16** (1978) 1789.

Kamachi, M., D. J. Lian and S. I. Nozakura, *Polym. J.*, **11**(12) (1979a) 921.

Kamachi, M., J. Satoh and S. I. Nozakura, *Polym. Prepr.* **20** (1979b) 567.

Kaneko, M., Polymer-Coated Electrodes: New Materials for Science and Industry, in "Advances in Polymer Science", Vol. 84, Springer-Verlag, Berlin, Heidelberg, 1988, p. 149.

Kaneto, K., Y. Kohno, K. Yoshino and Y. Inuishi, *Chem., Soc., Chem. Commun.*, 1983 382.

Katchalsky, A. and I. R. Miller, *J. Polym. Sci.*, **13** (1954) 57.

Katchalsky, A., K. Rosenheck and B. Altmann, *J. Polym. Sci.*, **23**(1957) 955.

Khan, I. M. and T. E. Hogen-Esch, *Makromol. Chem., Rapid Commun.*, **4** (1983) 569.

Khan, I. M., in "Encyclopedia of Polymer Science and Engineering", H. G. Mark, N. M. Bikales, C. G. Overberger, G. Enges and J. I. Kroschwitz, Eds., John Wiley & Sons, Inc., New York (1989), p. 567.

Klein, L. C., "Sol-Gel Optics: Processing and Applications", Kluwer Academic Publishers, Boston, 1994.

Kobayashi, M. and M. Imai, *Surf. Sci.*, **158** (1985) 275.

Koenig, J. L., in "Advances in Polymer Science", Vol. 54, Springer-Verlag, Berlin, 1994, p. 87.

Kunimura, S., T. Ohsaka and N. Oyama, *Macromol.*, **21** (1988) 894.

Lippert, J. L. and E. S. Brandt, *Langmuir*, **4** (1988) 127.

Luskin, L. S., in "Functional Monomers, Their Preparation, Polymerization and Application", Vol. 2, R. H. Yocum and E. B. Nyquist, Eds., Marcel Dekker, Inc., New York, 1974.

MacCallum, J. R. and D. H. MacKerron, The Electropolymerisation of Acrylamide on Carbon Fibers, Brit. *Polym. J.*, **14** 14 (1982).

Mano, E. B. and B. L. Calafate, *J. Polym. Sci., Polym. Chem. Ed.*, **21** (829) 1983.

Martin, T. J., K. Prochazka, P. Munk and S. E. Webber, *Macromol.*, **29** (1996) 6071.

Mathis, C. and T. E. Hogen-Esch, *J. Am. Chem. Soc.*, **104** (1982) 634.

Matsuzaki, K. and T. Sugimoto, *J. Polym. Sci.*, A-2, **5** (1967) 1320.

Matsuzaki, K., T. Matsubara and T. Kanai, *J. Polym. Sci. Polym. Chem.*, **14** (1976) 1475.

Matsuzaki, K., T. Matsubara and T. Kanai, *J. Polym. Sci. Polym. Chem.*, **15** (1977) 1573.

Matsuda, N., T. Sawaguchi, M. Osawa and I. Uchida, *Chem. Lett.*, (1995) 145.

McCarley, R. L., *J. Electrochem. Soc.*, **137** (1990) 218C.

McKinney, D. S. and J. P. Fugassi, US Pat. 2,961,384 (1960).
McLean, R. A. and V. L. Anderson, "Applied Factorial and Fractional Designs", Marcel Dekker, Inc., New York, 1984.

Mengoli, G. and B. M. Tidswell, *Polym.*, **16** (1975) 881.

Mengoli, G., in "Advances in Polymer Science", Vol. 33, Springer-Verlag, New York, 1979.

Mengoli, G., S. Daolio, U. Giulio and C. Folonari, *J. Appl. Electrochem.*, **9** (1979a), 483.

Mengoli, G., S. Daolio, U. Giulio and C. Folonari, *J. Appl. Polym., Sci.*, **23** (1979b) 2117.

Mengoli, G., P. B. Bianco, S. Daolio and M. M. Musiani, *J. Appl. Electrochem.*, **10** (1980) 459.

Mengoli, G., P. Bianco, S. Daolio and M. T. Munari, *J. Electrochem. Soc.*, **128** (1981) 2276,.

Mengoli, G., M. M. Musiani and B. Pelli, *Electrochimi. Acta*, **28**(12) (1983) 1733.

Mengoli, G. and M. M. Musiani, *Electrochimi. Acta*, **31**(2) (1986a) 201.

Mengoli, G., and M. M. Musiani, Abstract L12, in "Proceedings of Electrochemistry of Polymer Layers", Duisburg, Germany, Sept. 15-17, 1986b.

Mengoli, G and M. M. Musiani, *J. Electrochem. Soc.*, **134**(12) (1987) C643.

Mengoli, G., M. M. Musiani and F. Furlanetto, *J. Electrochem. Soc.*, **137** (1990) 162.

Mengoli, G., M. M. Musiani, C. Pagura and F. Paolucci, *Corro. Sci.*, **32(7)** (1991) 743.

Mengoli, G and M. M. Musiani, *Progr. Org. Coatings*, **24** (1994) 237.

Meverden, C. C. and T. E. Hogen-Esch, *Makromol. Chem., Rapid Commun.*, **4** (1983) 563.

Miller, R. L., in "Polymer Handbook", J. Brandrup and E. H. Immergut, Eds., 3rd edition, John Wiley & Sons, New York, 1984, Chapter 6.

Minsky, M., U. S. Patent 3,013,346, *Microscope Apparatus*, Dec. 19, 1961.

Missono, Y., M. Nagase and K. Itoh, *Spectrochim. Acta*, **50A** (1994) 1539.

Montgomery, J., *Mat. Evalu.*, **52** (1994) 1354.

Morton, M., "Anionic Polymerization: Principles and Practice", Academic Press, Toronto, 1983.

Mostefai, M., M. Pham, J. Marsault, J. Aubard and P. Lacaze, *J. Electrochem. Soc.*, **143** (1996) 2116.

Murray, R. W., in "Electroanalytical Chemistry", A. J. Bard, Ed., Vol. 13, Marcel Dekker, New York, 1984, p. 191.

Murray, R. W., *Ann. Rev. Mater. Sci.*, R. A. Huggins, J. A. Giordmaine and J. B. Wachtman, Eds., Vol. 14, 1984, p. 145.

Musiani, M. M., F. Furlanetto, P. Guerriero and J. Heitbaum, *J. Appl. Electrochem.*, **23** (1993) 1069.

Nabiev, I., I. Chourpa and M. Manfait, *J. Raman Spectrosc.*, **25** (1994) 13.

Nakamoto, K., "Infrared Spectra of Inorganic and Coordination Compounds", John Wiley & Sons, New York, 1963.

Narmann, H., P. Simak and G. Koehler, Ger. Offen., 3,223,544 (1983).

Natta, G., G. Mazzanti, P. Longi, G. Dall'asta and Bernardini, *J. Polym. Sci.*, **51** (1961) 487.

Newman, J. S., "Electrochemical Systems", 2nd edition, Prentice Hall, Englewood Cliffs, NJ, 1991.

Nishihara, H., M. Noguchi and K. Aramaki, *Inorg. Chem.*, **26** (1987) 2862.

Ngo, T., L. Brandt, R. S. Eilliams and H. D. Daesz, *Surf. Sci.*, **291** (1993) 411.

Noel, M. and K. I. Vasu, "Cyclic Voltammetry and the Frontiers of Electrochemistry", Aspect Publications Ltd., London, 1990.

Nuyken, O., in "Handbook of Polymer Synthesis", Part A, H. R. Kricheldorf Ed., Marcel Dekker, Inc., New York, 1992, p. 126.

Odian, G., "Principles of Polymerization", 3rd edition, McGraw-Hill Inc., New York, 1991.

Odziemkowski, M., J. Flis and D. E. Irish, *Electrochim. Acta*, **39** (1994) 2225.

Ogumi, Z., Z. Tekehara, S. Yoshizawa, *Bull. Chem. Soc. Jpn.*, **49** (2883) 1976.

Ohno, H., H. Nishihara and K. Aramaki, *Corr. Sci.*, **30**(6/7) (1990) 603.

Ohsaka, T., T. Hirokawa, H. Miyamoto, and N. Oyama, *Anal. Chem.*, **59** (1987) 1758.

Oyama, N. and F. C. Anson, *J. Electrochem. Soc.*, **127**(1) (1980) 247.

Parravano. G., *J. Am. Chem. Soc.*, **73** (1951) 628.

Pemberton, J. E., in "Electrochemical Interfaces: Modern Techniques for in site Interface Characterization", H. D. Abruna, Ed., VCH, New York, 1991, Chapter 5, p. 193.

Perrin, D. D., "Dissociation Constants of Organic Bases in Aqueous Solution", Butterworths, London, 1965, p. 176.

Petro, A. J. and C. P. Smyth, *J. Amer. Chem. Soc.*, **79** (1957) 6142.

Pettinger, B., in "Adsorption of Molecules at Metal Electrodes", J. Lipkowski and P. N. Ross, Ed., VCH, New York, 1992, Chapter 6, p. 285.

Phillips, J. P., L. D. Freedman and J. C. Craig, Eds., in "Organic Electronic Spectral Data", Vol. 6, Wiley-Interscience, New York, 1970, p. 110.

Pistoia, G., A. Ricci and M. A. Voso, *J. Polym. Sci., Polym. Chem.*, **14** (1976) 1811.

Pistoia, G., A. Ricci and M. A. Voso, *J. Appl. Polym. Sci.*, **20** (1978) 2441.

Pouchert, C. J. "The Aldrich Library of Infrared Spectra", Ed. 3, Aldrich Chemical Co., Milwaukee, 1981.

Pouchert, C. J., "The Aldrich Library of NMR Spectra", Ed. 2, Aldrich Chemical Co., Milwaukee, 1983.

Pouchert, C. J. and J. Behnke, "The Aldrich Library of 13C and 1H FT NMR Spectra", Vol. 3, Aldrich Chemical Co., Milwaukee, 1993.

Putterman, M., J. Koenig and J. B. Lando, *J. Macromol. Sci., Phys.*, **B16** (1979) 89.

Rafique, U., M. Mazhar and F. A. Khwaja, *Synth. Met.*, **78** (1996) 73.

Reilly, F. C., *Met. Finish.*, **92**(1) (1994) 49.

Rodger, W. E. S., G. Dent and M. Edmondson, *J. Chem., Soc., Dalton Trans.*, (1996) 791.

Roessiger, V. and P. Raffelsberger, *Met. Finish.*, **90** (1992) 9.

Rosen, S. L., "Fundamental Principles of Polymeric Materials", 2nd edition, John Wiley & Sons, New York, 1993.

Ruckenstein, E. and J. S. Park, *J. Appl. Polym. Sci.*, **42** (925) 1992.

Salamone, J. C., A. W. Wisniewsky and E. J. Ellis, *Polym. Prepr. Am. Soc. Div. Polym. Chem.*, **16** (1975) 727.

Satas, D., "Coatings Technology Handbook", Marcel Dekker, Inc., New York, 1991.

Satoh, M., E. Yoda, T. Hayashi, and J. Komiyama, *Macromol.*, **22** (1989) 1808.

Seery T. A. P. and E. J. Amis, *Macromol.*, **24** (1991) 5463.

Seki, H., *J. Electron Spectrosc. Relat. Phenom.*, **39** (1986) 289.

Sekine, I., K. Kohara, T. Sugiyama and M. Yuasa, *J. Electrochem. Soc.*, **139** (1992) 3090.

Sen, S., A. Usanmaz and A. M. Onal, *J. Polym. Sci., Polym. Chem.*, **33** (1995) 1817.

Shapoval G. S. and A. V. Gorodyskii, *Russ. Chem. Rev.*, **42** (5) (1973) 370.

Sharp, M., D. D. Montgomery and F. C. Anson, *J. Electroanal. Chem.*, **194** (1985) 247.

Sheard, S. J. and M. G. Somekh, *Appl. Phys. Lett.*, **53**(26) (1988) 2715.

Shelepin, I. V. and A. I. Fedorova, *Russ. J. Phys. Chem.*, **38**(11) (1964) 1452.

Shugar, G. J. and J. A. Dean, "The Chemist's Ready Reference Handbook", McGraw-Hill, New York, 1989.

Silkin, V. Y. and A. E. Ponomarev, *Meas. Techn.*, **36**(9) (1993) 997.

Silverstein, R. M., G. C. Bassler and T. C. Morrill, "Spectrometric Identification of Compounds", fourth edition, John Wiley & Sons, New York, 1981.

Smid, J., in "Structure and Mechanism in Vinyl Polymerization", T. Tsuruta and K. F. O'Driscoll, Eds., Marcel Dekker, New York, 1969, p. 419.

Snogren, R. C., "Handbook of Surface Preparation", Palmerton Publishing, 1974.

Sobiesky, J. F. and M. C. Zerner, U. S. Pat. 3,464,960 (1969).

Solov'ev, S. M., *Meas. Tech.*, **34**(11) (1991) 1122.

Soum, A. and M. Foutanille, *Polym. Prepr. Am. Chem. Soc. Div. Polym. Chem.*, **21** (1980) 23.

Subramanian, R. V. and J. J. Jakubowski, Electropolymerization on Graphite Fibers, *Polym. Eng. Sci.*, **18** 590 (1978).

Subramanian, R. V., in "Advances in Polymer Science", Vol. 33, Springer-Verlag, New York, 1979.

Taj, S., M. F. Ahmed, S. Sankarapapavinasam, *J. Appl. Electrochem.*, **23** (1993) 247.

Tashiro, K., K. Matsushima and M. Kobayashi, *J. Phys. Chem.*, **94** (1990) 3197.

Tang, L. C. and B. Francois, *Eur. Polym. J.*, **19** (1983) 715.

Tenenbaum, L. E., in "Pyridine and its Derivatives", E. Klingsberg, Ed., Interscience Publishers, Inc., New York, 1961, Part Two, p. 212.

Teng, F. S., R. Mahalingam, R. V. Subramanian and R. A. V. Raff., *J. Electrochem. Soc.*, **124** (1977) 995.

Tidswell, B. M. and D. A. Mortimer, *Eur. Polym. J.*, **17** (1981a) 735

Tidswell, B. M. and D. A. Mortimer, *Eur. Polym. J.*, **17** (1981b) 745.

Tien, C. F. and T. E. Hogen-Esch, *Macromol.*, **9**(5) (1976) 871.

Tomcufcik, A. S. and L. N. Starker, in "Pyridine and its Derivatives", E. Klingsberg, Ed., Interscience Publishers, New York, 1961, Part 3, Chapter 9, p. 74.

Tomilov, A. P., in "Electrochemistry of Organic Compouinds", Naukova Dumka, Kiev, 1968, pp. 525-526.

Toomey, J. Jr., in "Advances in Heterocyclic Chemistry", Vol. 37, Academic Press, Inc., Orlando, Florida, 1984.

Troch-Nagels, G., R. Winand, A. Weymeersch and L. Renard, *J. Appl. Electrochem.*, **22** (1992) 756.

Vakula, V. L. and L. M. Pritykin, "Polymer Adhesion: Physico-Chemical Principles", New York, 1991.

Venugopal, G., X. Quan, G. E. Johnson, F. M. Houlihan, E. Chin and O. Nalamasu, *Chem. Mater.*, 7(2) (1995) 271.

Vork, F. T., L. J. J. Jansen and E. Barendrecht, *Electrochim. Acta*, **32** (1987) 1187.

Wall, F. T., J. J. Ondre and M. Pikramenou, *J. Am. Chem. Soc.*, **73** (1951) 2821.

Walter, G. W., *Corr. Sci.*, **26**(1) (1986a) 27.

Walter, G. W., *Corr. Sci.*, **26**(1) (1986b) 39.

Wang, J., S. P. Chen, and M. S. Lin, *J. Electroanal. Chem.*, **273** (1989) 231.

Weast, R. C. and M. J. Astle, Eds., "CRC Handbook of Chemistry and Physics", 72nd edition, CRC Press, Inc., Boca Raton, Florida, 1992.

Weill, G. and G. Hermann, *J. Polym. Sci, A-2*, **5** (1967) 1293.

Wicks, Z. W. Jr., F. N. Jones and S. P. Pappas, "Organic Coatings: Science and Technology", Volume I: Film Formation, Components, and Appearance Volume II: Applications, Properties, and Performance, John Wiley & Sons, New York, 1992.

Wiesendanger R. and H. J. Guntherodt, "Scanning Tunneling Microscopy II", Springer-Verlag, New York, 1992.

Wiesendanger R. and H. J. Guntherodt, "Scanning Tunneling Microscopy III", Springer-Verlag, New York, 1993.

Wilson, C. Z., *Trans. Electrochem. Soc.*, **75** (1939) 353.

Wilson, C. Z., Rec. *Chem. Progr.*, **10** (1949) 25.

Wilson, T. and C. Sheppard, "Theory and Practice of Scanning Optical Microscopy", Academic Press, New York, 1984.

Wilson, T., "Confocal Microscopy", Academic Press, New York, 1990.

Wimolkiatisak, A. S. and J. P. Bell, Toughening of Graphite-Epoxy Composites with an Electrocopolymerized-Temperature Thermoplastic Interphase, *J. Appl. Polym. Sci.*, **46** 1899 (1992).

Yamazaki, N., I. Tanaka and S. Nakahama, *J. Macromol. Sci. Chem.*, **A2** (1968) 1121.

Yang, S. K., V. V. Varadan and V. K. Varadan, *Materials Evaluations*, **48** (1988) 471.

Yassin, A. A. and N. A. Rizk, *J. Polym. Sci., Polym. Chem.*, **16** (1978a) 1475.

Yassin, A. A. and N. A. Rizk, *Polym.*, **19** (1978b) 57.

Yin, R. and T. E. Hogen-Esch, *J. Polym. Sci., Polym. Chem.*, **32** (1994) 363.

Young, J. Z. and F. Roberts, *Nature*, **231** (1951) 167.

Yoshida, M., Kogyo Kagaku Zasshi, **63** (1960) 893.

Yoshida, M., N. Sakamoto, K. Ikemi and S. Arichi, *Bull. Chem. Soc. Jan.*, **66**(6) (1993) 1598.

Zhang, X., J. P. Bell and M. Narkis, The Electropolymerization of Poly(styrene-co-4-carboxyphenyl maleimide) Coatings onto Steel, *J. Appl. Polym. Sci.*, **62** (1996) 1303.

Zhang, X. and J. P. Bell, The *In-Situ* Synthesis of Protective Coatings on Steel Through a Surface Spontaneous Polymerization Process, *J. Appl. Polym. Sci.*, **66** (1997) 1667.

IMAGE EVALUATION
TEST TARGET (QA-3)

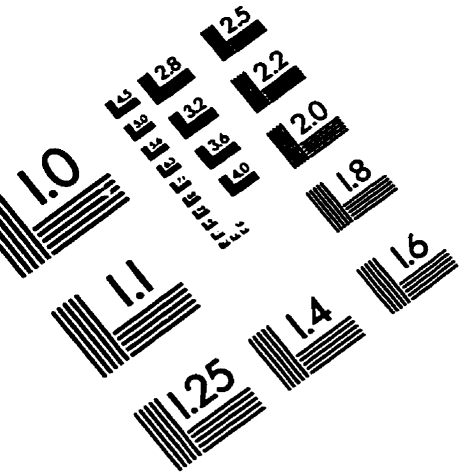

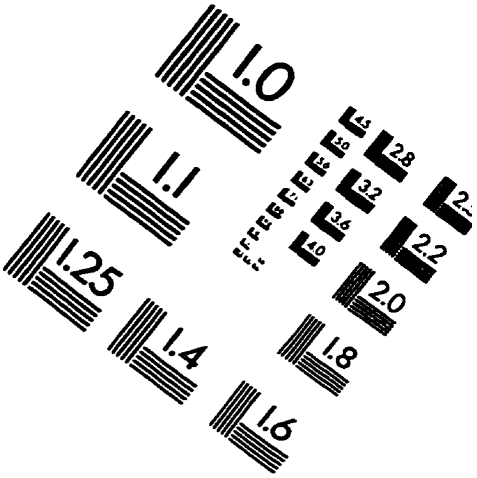

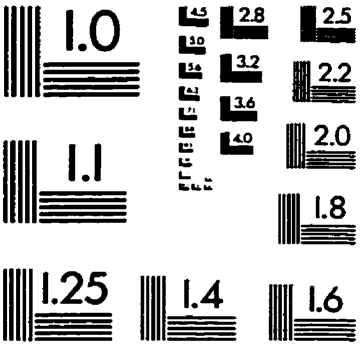

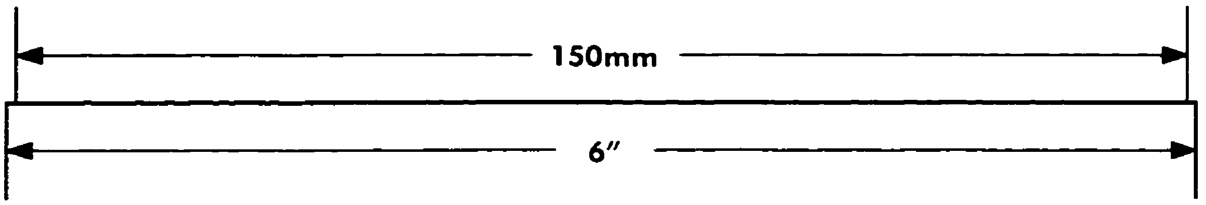

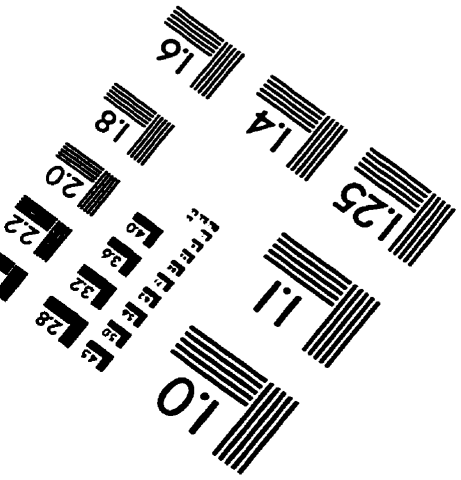

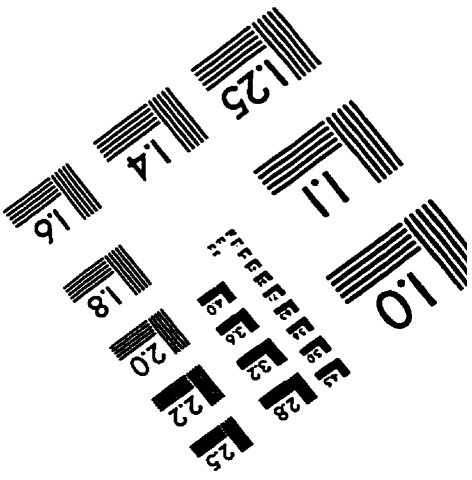

APPLIED IMAGE, Inc
1653 East Main Street
Rochester, NY 14609 USA
Phone: 716/482-0300
Fax: 716/288-5989